eman ta zabal zazu

Universidad del País Vasco
Euskal Herriko Unibertsitatea
Departamento de Neurociencias

Therapeutic potential of the endocannabinoid system in multiple sclerosis: novel clues from oligodendrocyte CB_1 receptors and ABHD6

DOCTORAL THESIS

Andrea Manterola Juaristi

2019

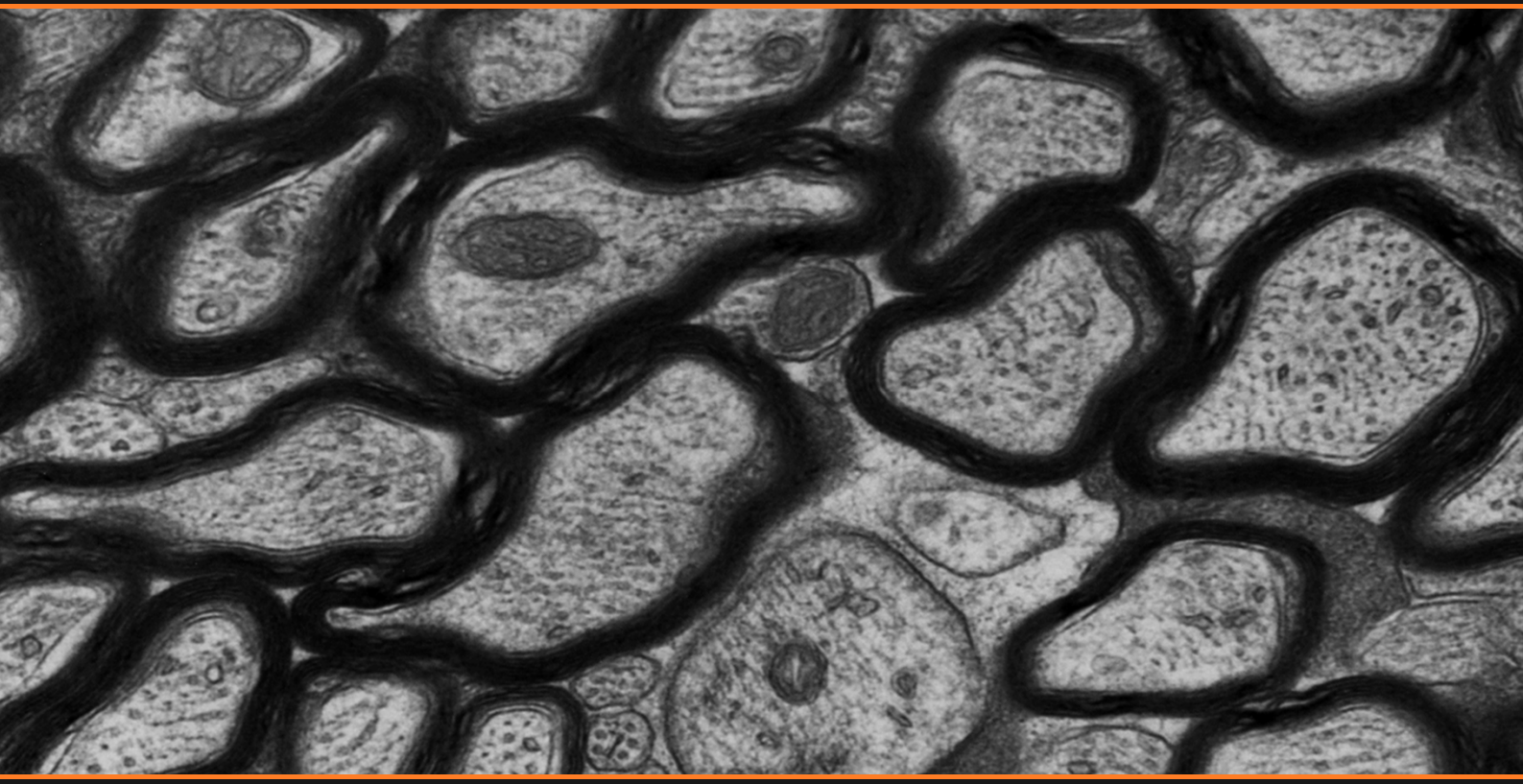

Achucarro
BASQUE CENTER FOR NEUROSCIENCE

eman ta zabal zazu

Universidad del País Vasco
Euskal Herriko Unibertsitatea

Therapeutic potential of the endocannabinoid system in multiple sclerosis: novel clues from oligodendrocyte CB_1 receptors and ABHD6

DOCTORAL THESIS

Andrea Manterola Juaristi
Graduate in Biology
Thesis supervisors: Susana Mato Santos and Carlos Matute Almau
Department of Neurosciences
University of the Basque Country UPV/EHU - Achucarro Basque Center for Neuroscience
Leioa, 2019

The data presented here have been published in part in:

1. **Manterola A**, Bernal-Chico A, Cipriani R, Ruiz A, Pérez-Samartín A, Moreno-Rodríguez M, Hsu K-L, Cravatt B, Brown JM, Rodríguez-Puertas R, Matute C*, Mato S* (2018). Re-examining the potential of targeting ABHD6 in multiple sclerosis: efficacy of systemic and peripherally restricted inhibitors in experimental autoimmune encephalomyelitis. *Neuropharmacology* 18: 181-191.
2. **Manterola A**, Bernal-Chico A, Cipriani R, Canedo-Antelo M, Moreno-García Á, Martín-Fontecha M, Pérez-Cerdá F, Sánchez-Gómez MV, Ortega-Gutiérrez S, Brown JM, Hsu KL, Cravatt B, Matute C, Mato S (2018) Deregulation of the endocannabinoid system and therapeutic potential of ABHD6 blockade in the cuprizone model of demyelination. *Biochem Pharmacol* 141: 189-201.

Andrea Manterola was recipient of a predoctoral fellowship from the Basque Government (PRE_2014_1_32). This research was supported by the Ministry of Economy and Competitiveness (Grants SAF2013-45084-R and SAF2016-75292-R), the Basque Government (Grant IT702-13), CIBERNED (Grant PRY-15-404), ARSEP Foundation and WOP Foundation.

Summary

Multiple sclerosis (MS) is the most common inflammatory disorder of the human central nervous system (CNS) and the leading cause of disability in young and middle-aged people in the developed world. Of unknown aetiology, the disease has for many years been explained by a coincidence of environmental and genetic factors leading to the appearance of focal inflammatory lesions associated with oligodendrocyte destruction and axonal degeneration. The composition of established inflammatory infiltrates varies between patients and/or lesion stages but commonly includes T-lymphocytes and macrophages. Furthermore, activated astrocytes and microglial cells participate in lesion development, progression and resolution by the secretion of cytokines and other inflammatory mediators as well as neural growth factors. Acute MS symptoms are often reversible during the initial relapsing-remitting course of the disease, although most of the patients enter a secondary progressive stage in which irreversible axonal degeneration causes persistent disability. Remission in MS is largely dependent on the generation of **mature oligodendrocytes** capable of myelin repair from a proliferating **oligodendrocyte precursor cell** (OPC) population that normally resides in the adult CNS. Notably, inhibition of OPC differentiation takes place at sites of chronically demyelinated MS lesions and likely contributes to disease progression. As such, the identification of novel molecules that promote OPC lineage progression and myelin repair in lesion areas is a current state of art strategy aimed at the development of novel, regenerative treatments for MS.

Decades of research have demonstrated that the **endocannabinoid system** offers the potential to relieve symptomatology in MS. It is a consistent finding that cannabinoid agonists present in the hemp plant (*Cannabis sativa* L.) exert symptom control in mouse models of MS, associated to neuroprotective, anti-inflammatory and regenerative mechanisms. These beneficial effects of cannabinoids normally involve **cannabinoid CB_1 receptors** expressed at high levels in neuron terminals, as well as CB_2 receptors mainly localized in hematopoietic cells. Of particular interest in the context of MS, oligodendrocyte lineage cells express low levels of CB_1 receptors that would participate to the beneficial effects of cannabinoids in this disease condition, according to *in vitro* studies. However, assessment of the biological and therapeutic relevance of this receptor population in MS is hampered, at least in part, by the lack of bona fide demonstration that oligodendroglial cells *in situ* express CB_1 receptors. On the other hand, the utility of cannabis-based medicines in MS patients seems to be limited by the appearance of dose-related toxic effects, associated to the stimulation of the bulk cannabinoid receptor populations in the CNS. Current research in the field aims thus at establishing the cellular specificity of cannabinoid mediated effects while searching for pharmacological strategies that improve the benefit-to-risk ratio of cannabinoid modulating drugs in this disease condition.

Among endogenously produced cannabinoids or endocannabinoids, **2-araquidonoylglycerol** (2-AG) is regarded as an important mediator of neuroprotection in neuroinflammatory conditions. Within the CNS, 2-AG is primarily inactivated through enzymatic hydrolysis by monoacylglycerol lipase (MAGL) and, to a lesser extent, by **α/β-hydrolase domain-containing 6** (ABHD6). Administration of MAGL inhibitors mimics the protective efficacy of exogenous cannabinoid agonists in MS animal models and targeting this enzyme has been recently postulated a novel strategy for the treatment of this and other neuroinflammatory conditions. Unfortunately, chronic MAGL inactivation also engages unwanted effects, such as **desensitization of brain CB_1 receptors and functional tolerance**, which put into question the utility of drugs targeting this enzyme in the clinical practice. On the other hand, there is preliminary evidence suggesting that ABHD6 blockade might exert symptom control in MS without major side effects. However, the biological actions of ABHD6 inhibitors in oligodendrocytes and white matter tracts are ill defined.

In the above mentioned context, the **Global Aim** of this Doctoral Thesis is to broaden current knowledge on the role of the endocannabinoid system in myelin biology and pathology, with a particular emphasis in MS.

Our **Specific Aims** were as follows:

Objective 1. To investigate the ultrastructural localization of CB_1 receptors in OPCs and mature OLs of the adult mouse brain, as well as the presence of abnormalities affecting myelin ultrastructure in CB_1 receptor knockout mice at the peak of myelination.

Objective 2. To examine the utility of targeting ABHD6 as novel therapeutic strategy in MS using selective inhibitors and complementary *in vivo* and *in vitro* models that mimic different aspects of the disease.

The **Results** of this Doctoral Thesis are thus divided in 2 independent sections:

In the **first block of Results**, by applying electron microscopy techniques to the analysis of wild-type and NG2-EYFP transgenic mice, we show that at least 6% of OPCs in the hippocampus and 27% of myelinating oligodendrocytes in the corpus callosum express CB_1 receptors. Comparative analysis of receptor density showed that, in the adult hippocampal formation, grey matter OPCs exhibit lower levels of CB_1 receptors than synaptic profiles. On the other hand, ultrastructural analysis of myelin allows concluding that CB_1 receptor knockout mice do not reveal gross abnormalities affecting myelin thickness at the peak of myelination.

In the **second block of Results**, by using pharmacological approaches and complementary mouse models mimicking different aspects of MS pathology, we show that targeting ABHD6 elicits only mild protective effects against white matter injury. Preventive administration of the systemically active ABHD6 inhibitor KT182 engages only a modest attenuation of neurological disability during the progression of experimental autoimmune encephalomyelitis (EAE). However, this subtle therapeutic effect is not mimicked by administration of the brain impermeant inhibitor KT203, pointing to the requirement of early ABHD6 inactivation in nervous tissue for therapeutic benefit in the EAE model. None of the inhibitors attenuates inflammation in the chronic phase of the disease. Conversely, ABHD6 inhibition prevents myelin destruction and demyelination-driven microglia and astroglia inflammatory reaction in the cuprizone model. However, blockade of the enzyme in an established demyelinating context is unable to accelerate myelin repair in this toxic model of immune-independent myelin damage. Inhibition of ABHD6 activity does not attenuate excitotoxicity in oligodendrocyte cultures nor promote the differentiation of precursor cells as possible mechanisms of myelin protection and repair. By contrast, experiments in neuron cultures have unveiled an off-target activity of the ABHD6 inhibitor KT182 leading to attenuation of NMDA induced mitochondrial damage and excitotoxicity. With regard to the long-term consequences of ABHD6 blockade, our results indicate that administration of ABHD6 inhibitors results in a partial loss of CB_1 receptor functionality in selected brain areas.

In conclusion, these results indicate that targeting ABHD6 offers only a limited potential for MS therapy. On the other hand, we provide conclusive evidence that CB_1 receptors are expressed and quantifiable in brain oligodendroglia, including both myelinating oligodendrocytes and OPCs. These results support the hypothesis that these receptor populations contribute to fine-tune the myelination process *in vivo* and strengthen the possibility that currently available cannabinoid modulating drugs regulate MS progression, at least in part, through the activation of CB_1 receptors expressed in oligodendrocyte populations. Collectively, these data broaden current knowledge on the role and therapeutic potential of targeting the endocannabinoid system in MS.

Introduction

1. Oligodendrocytes and myelin

Oligodendrocytes (**OLs**), first described by Pío del Río-Hortega in 1921, are the glial cells responsible for producing central nervous system (CNS) **myelin**, which can be defined as a highly specialized multilamellar lipid structure enabling rapid conduction of action potentials. In addition to electrically insulating axons by ensheathing nerve fibres with myelin, oligodendrocytes provide essential metabolic support for axon function and neuron survival (Nave and Werner 2014).

Oligodendroglial cells originate from multipotential neural progenitor cells during the late stages of embryonic development, which under specific signals, start to express oligodendrocyte transcription factor 2 (Olig2) triggering the first embryonic wave of specification of **oligodendrocyte progenitors cells** (**OPCs**) (Naruse et al. 2017). The expression of a set of markers including platelet derived growth factor receptor alpha (PDGFRα) and the neuron-glial antigen 2 (NG2) proteoglycan (Richardson et al. 2011) characterize these precursor cells. The majority of myelinating oligodendrocytes (OLs) develop from OPCs in an early postnatal period corresponding to 10 weeks in mice and 5-10 years in humans. Nevertheless, a significant population of OPCs remain in a precursor state in the adult brain (Simons and Nave 2015) and retain the ability to generate oligodendrocytes and myelin in response to neuronal activity changes once developmental myelination is terminated. Recent research proposes that this process contributes not only to myelin maintenance and repair, but also to improving the conduction of new circuits thus participating in CNS plasticity and learning (McKenzie et al. 2014; Xiao et al. 2016).

1.1. Myelin formation and remodeling

1.1.1. Oligodendrocyte differentiation

The differentiation of OPCs towards mature OLs follows several stages of cell maturation defined by morphological aspects and by the expression of specific-marker proteins (Baumann and Pham-Dinh 2001). Hence, in the first step of differentiation into late progenitor cells or pre-oligodendrocytes, PDGFRα and NG2 expressing OPCs acquire the marker O4 and develop a more complex shape. At this stage, cells lose their motility but maintain their ability to proliferate. Following oligodendrocyte lineage progression, these late progenitors give rise to pre-myelinating, immature cells that express the earliest myelin-related marker 2',3'-cyclic nucleotide-3'-phosphodiesterase (CNPase). Finally, these cells differentiate into mature oligodendrocytes characterized by the expression of myelin related genes as myelin proteolipid protein (PLP) and myelin basic protein (MBP) (**Figure 1**).

The generation of myelin forming oligodendrocytes follows an intrinsic program of OPC proliferation, migration and differentiation, which is controlled by **intracellular factors** and **exogenous signals** (Almeida et al. 2011). The fact that oligodendrocytes *in vitro* are able to produce myelin and wrap chemically fixed axons and carbon nanofibers above a minimum caliber (> 0.3 µm) (Lee et al. 2012; Rosenberg et al. 2008) suggest that only limited bidirectional signaling is required. Thereby, oligodendrocytes would be stimulated to myelinate by default but locally restricted by inhibitory signals (Nave and Ehrenreich 2014).

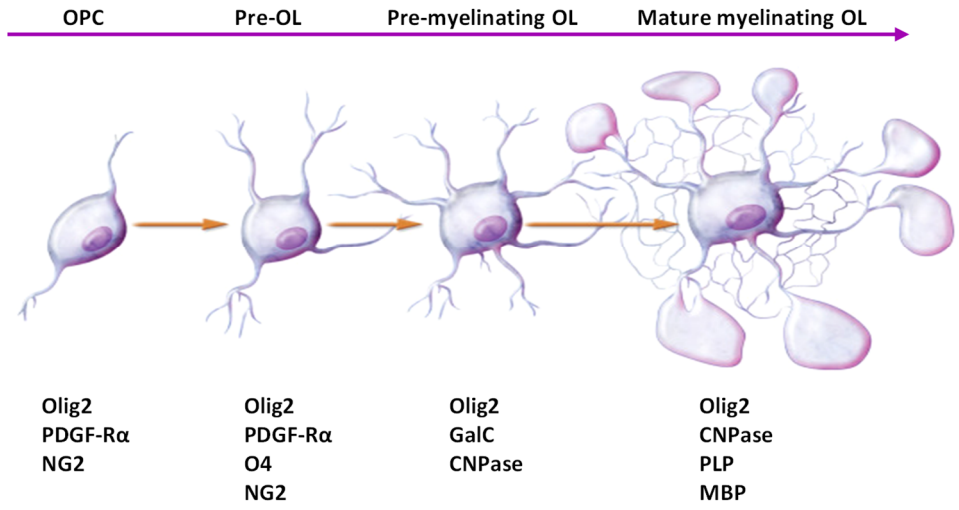

Figure 1. Markers of oligodendrocyte lineage specification and maturation. The image shows oligodendrocyte lineage progression from precursor cells (OPCs) to myelinating oligodendrocytes (OL). Adapted from Kinney and Volpe, 2018.

The **intracellular network** that regulates oligodendrocyte differentiation and maturation compresses a complex variety of transcriptional regulators mediating chromatin remodeling, histone modification and DNA methylation in these cells (Hernandez and Casaccia 2015). OPCs are highly proliferative bipolar cells in a transcriptionally active chromatin state characterized by high expression of cell cycle genes and transcriptional inhibitors of genes associated to the differentiated state (*Hes5*, *Tcf7l2*, *Id2/Id4*, *Sox5*, *Sox6*, *Sox11*…). Thus, the maturation of OPCs is under the control of transcription factors able to repress the expression of myelin gene inhibitors, such as *E2f4* and *Yy1*, and to positively regulate the expression of myelin related genes, including *Myrf* and *Sox 10*. Importantly, the transcriptional rate of a myelin-related gene and the abundance of its protein product may not necessarily be correlated, as regulatory microRNAs affect the stability of messenger RNAs during oligodendrocyte lineage progression (Barca-Mayo and Lu 2012).

Extracellular signals controlling oligodendrocyte maturation and myelination during development include juxtacrine signals from axons, elements from the extracellular matrix (ECM) and soluble factors produced by astrocytes and microglia/macrophages (Nave and Werner 2014). Stimulatory cues that drive active myelination include axonal neuregulin/ErbB receptor signaling (Lundgaard et al. 2013), activation of integrin and dystroglycan receptors in oligodendroglia by ECM laminin (Colognato and Tzvetanova 2011), signaling mediated by astroglia leukemia inhibitory factor (LIF) (Ishibashi et al. 2006), epidermal growth factor (EGF) (Aguirre et al. 2007), insulin growth factor I (IGF-I) (Ye et al. 1995), fibroblast growth factor (FGF) (Furusho et al. 2012), ciliary neurotrophic factor (CNTF) (Stankoff et al. 2002), brain derived neurotrophic factor (BDNF) (Xiao et al. 2010) and neurotrophin-3 (NT-3) (Kahn et al. 1999), among others. On the other hand, inhibitory control of myelination is exerted by a series of cell-adhesion molecules and secreted factors such as polysialylated neural cell adhesion molecule (PSA-NCAM) (Charles et al. 2000), Jagged1/Notch-1 signaling (Wang et al. 1998), LINGO-1/RhoA signaling (Mi et al. 2005) and wingless/int (Wnt) ligands (Fancy et al. 2009).

There is consistent evidence that **G-protein coupled receptors** (GPCRs) regulate several aspects of the multistep process that characterizes myelination (Mogha et al. 2016). For instance, during early developmental stages, Wnt ligands negatively regulate OPC maturation through the action of GPCRs, which mediate β-catenin translocation with the consequent activation of Tcf/Lef transcription (Kim et al. 2008). At the same time, Wnt signaling, together with Cxcl12 signaling through GPCR Cxcr4, also regulates OPCs migration (Tsai et al. 2016). Moreover, the adhesion-type protein Gpr56/Adgrg1 keeps OPCs in a proliferative state due to its interactions with $G\alpha_{12/13}$ and activation of RhoA, a protein implicated in the inhibition of differentiation process. Thus, the expression of this GPCR is downregulated in premyelinating oligodendrocytes and inexistent in mature oligodendrocytes (Giera et al. 2015). On the other hand, rhodopsin family members Gpr17 and Gpr37 are considered key regulators of the maturation. Whereas Gpr17 is expressed during the formation of premyelinating cells and lost in mature oligodendrocytes, Gpr37 expression begins in premyelinating cells and maintained in mature oligodendrocytes. Both proteins mediate inhibition of oligodendrocyte differentiation by the activation of $G\alpha_{i/o}$ signaling pathway, which promotes a reduction in cAMP levels and the activation of Raf-MAPH-ERK cascade. This pathway results in the inhibition of ERK1/2 translocation to the nucleus, which in turn triggers an attenuation of promyelinating transcription factor *Myrf* and an increase in inhibitory Hes56 protein levels (Shin et al. 2013).

Finally, it is important to highlight that myelination is modulated by neuronal activity via **axon-derived neurotransmitters** including adenosine (Stevens et al. 2002), glutamate (Mangin et al. 2012) and GABA (Zonouzi et al. 2015). Up to date, most of the research concerning neurotransmitter-mediated regulation of myelination has focused in glutamate signaling, probably due to the fact that the majority of myelinated projection neurons are glutamatergic. In this regard, the prevailing view is that ionotropic AMPA/kainate receptors inhibit OPC proliferation while NMDA receptors and metabotropic glutamate receptors belonging to the GPCR superfamily promote cell maturation and differentiation (Spitzer et al. 2016).

Apart from integrating all these signals to achieve an appropriate differentiation stage, oligodendrocytes have to terminate active myelination precisely and switch into a state of myelin maintenance at an appropriate time-point. These processes are regulated by a variety of molecules including kinases Fyn and FAK. Moreover, Ca^{2+}, as second messenger, has been proposed as a relevant regulator of myelination acting through PKC, ERKs, CREB and Ca^{2+}/calmodulin kinases II and IV (Soliven 2001).

Fyn is a member of the Src non-receptor tyrosine kinase family whose expression is predominant during oligodendrocyte differentiation and which is necessary for myelination and MBP translation (White et al. 2012). In fact, Fyn- deficient mice present severe hypomyelination and oligodendrocyte loss in CNS white matter (Sperber and McMorris 2001). Similarly, FAK integrates signals from ECM to produce changes in cytoskeletal dynamics leading to differentiation and myelination. It has been observed that FAK knockout mice show a reduction in the oligodendrocyte process outgrowth (Forrest et al. 2009).

The mitogen activated protein kinase (MAPK)/extracellular related kinase (ERK) pathway is a point of convergence of many extracellular signals in oligodendrocytes including neuregulin 1, BDNF, IGF-1 and FGF (Ahrendsen and Macklin 2013). Double mutants lacking FGFR1/2 have reduced ERK activation which results in normal oligodendrocyte differentiation and initial myelin wrapping but significant myelination deficits (Furusho et al. 2012). Conversely, conditional ablation of ERK1/2 or the upstream activator B-Raf in oligodendrocytes results in defective differentiation and

dysmyelination (Galabova-Kovacs et al. 2008; Ishii et al. 2012). In addition, the p38 MAPK pathway positively regulates oligodendrocyte differentiation through crosstalk with the ERK and c-Jun N-terminal kinase (JNK) pathways that blocks c-Jun mediated inhibition of myelin gene expression (Chew et al. 2010). Finally, inducible conditional ablation of ERK1/2 in oligodendrocytes of the adult CNS results in reduced myelin gene expression and late onset axonal degeneration, accompanied by astrogliosis, microglial activation, partial loss of oligodendrocytes, and functional impairment illustrating the critical role for ERK1/2 MAPK signaling in myelin maintenance and axonal integrity (Ishii et al. 2014).

The phosphatidylinositol-3-kinase (PI3K)/Akt and the mammalian target of rapamycin (mTOR) signaling pathways are additional major integrators of multiple extracellular signals that influence oligodendrocyte development including neuregulins, integrins, IGF-1, NT-3 and LIF (Ahrendsen and Macklin 2013). Akt signaling in oligodendrocytes is activated upstream by lipid second messengers generated by PI3K and downstream by Fyn and FAK (Colognato and Tzvetanova 2011). Using a variety of molecular strategies, several laboratories have shown that Akt/mTOR signaling is a master regulator of myelination in the CNS. The expression of constitutively active Akt in oligodendrocytes causes CNS hypermyelination during development and aging without affecting OPC number, proliferation or survival (Flores et al. 2008). Increased myelin production per oligodendrocyte is driven by Akt signaling through mTOR and is reversible upon treatment with rapamycin (Narayanan et al. 2009). Finally, conditional knockout of the phosphatase and tensin homolog (PTEN) which normally reduces the production of upstream PIP3 that activates Akt results in dramatic hypermyelination in the CNS (Harrington et al. 2010). Nevertheless, over-activation of the Akt/mTOR pathway by PTEN deletion results in late axon degeneration, likely related to dystrophic myelination, and does not promote detectable benefits in a demyelination repair setting. In all, these data suggest that although Akt signaling through mTOR is both necessary and sufficient to regulate myelination in the CNS, quantitative fine-tuning of this intracellular pathway may be required for clinical benefit.

1.1.2. Myelin biogenesis and compaction

OPCs are multipolar cells with processes that extend and retract like filopodia (Kirby et al. 2006). When the first contact with an axonal membrane occurs, the tip of the OPC process is either retracted or stabilized. If stabilized, a specialized membrane domain for continued axoglial communication is formed giving rise to all the signals described above (**Figure 2**).

During postnatal development, oligodendrocyte myelin membranes may grow as much as 5,000 μm^2 per day (Pfeiffer et al. 1993). Mature myelin comprise of up to 160 membrane layers, and myelin segments or internodes expand up to 1.7 mm (Nave and Werner 2014). Electron microscopy analyses have revealed that this structure is a single extension of oligodendrocyte membrane, which has a triangular shape. Thus, the outer layer is in direct contact with the oligodendrocyte cell body, while the innermost layer, also known as inner tongue, contacts with the axon. The myelination process involves two coordinated movements of the oligodendrocyte membrane towards the axon. The first one consists on the wrapping, where oligodendrocyte makes contact with the axon and the inner tongue expands the membrane underneath the previously generated layers. Secondly, a lateral extension of all layers occurs towards the node of Ranvier to increase myelin length. The correct progression of myelin development also involves a complex system of cytoplasmic-rich channels containing microtubules and vesicular carriers, which allows the transport of newly synthesized myelin components from the oligodendrocyte somata to the growing areas (**Figure 2**).

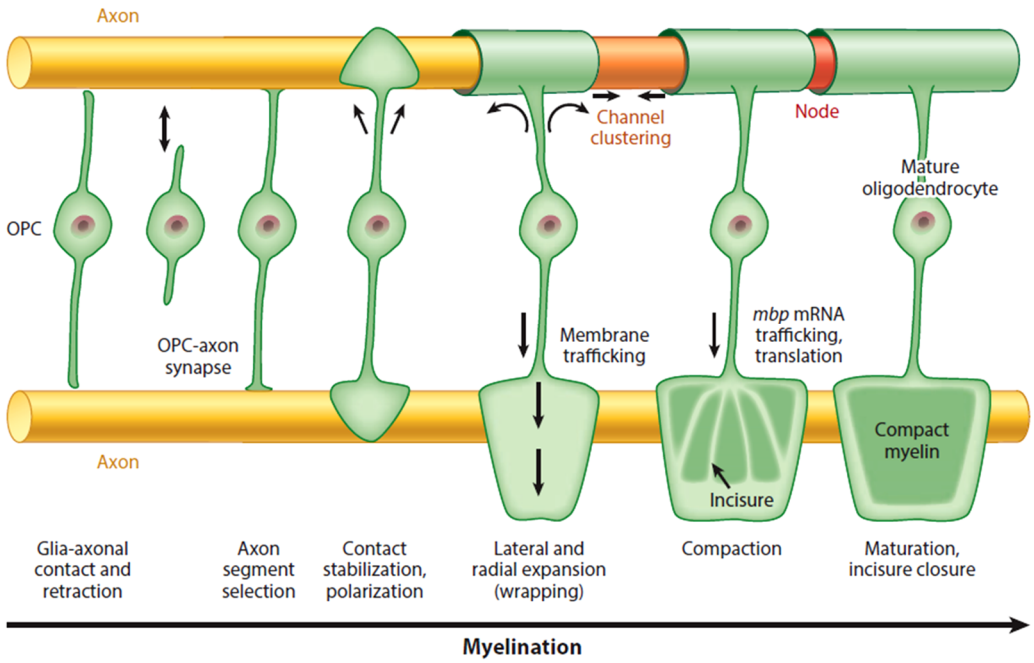

Figure 2. Schematic model of the differentiation of a committed oligodendrocyte progenitor cell (OPC) into a mature myelinating oligodendrocyte. OPCs extend and retract cellular processes until initial contacts are stabilized. In the lower half of the figure, the myelin sheath is depicted as unrolled. From Nave and Werner, 2014.

Although these cytoplasmic channels are largely present in myelin sheaths, their number is notably decreased when developmental myelination is completed (Snaidero and Simons 2014). This communication pathway between oligodendrocyte and axon makes myelin a dynamic structure, allowing active and plastic design of myelin sheath.

Finally, the compaction of the myelin sheath starts in the outermost layers and progresses both radially and longitudinally at early developmental stages. It is well documented that MBP and CNPase play a key role in this process (Snaidero and Simons 2014). MBP mRNA is transported from the nucleus to the innermost layers where is translated to protein and subsequently transported to the outer layers, where initiation of compaction takes place. Conversely, CNPase acts as spacer between two adjacent cytoplasmic membranes, preventing a premature compaction of this area so that, in absence of CNPase, myelin compaction extends to inner tongue and eliminates its capacity to continue wrapping.

1.1.3. Myelin plasticity and remodeling

Myelin is a dynamic structure since several studies have demonstrated its adaptive capacity in response to changes in neuronal activity. Noteworthy, oligodendrocytes responsible for myelin synthesis are produced continuously in the healthy adult brain from OPCs that are able to divide and differentiate (Rivers et al. 2008) in response to several signals, including environmental stimuli. The differentiation of adult OPCs to myelinating oligodendrocytes enables improving the conduction of new circuits by synthesizing myelin, inducing sodium channels to cluster at 'pre-nodes' (Freeman et al. 2015) or by transferring substrates for energy production (Fünfschilling et

al. 2012). Magnetic resonance imaging (MRI) has allowed the detection of changes in human white matter structure after being trained in complex sensory motor tasks (Bengtsson et al. 2005; Scholz et al. 2009) and also in rats during motor training (Sampaio-Baptista et al. 2013). Finally, inhibition of new oligodendrocyte generation results in the blockade of *de novo* myelination and leads to failure in motor task learning (McKenzie et al. 2014). Collectively, these observations show that myelin remodeling plays an active role in learning and memory.

1.2. Multiple sclerosis

Myelin breakdown is the major pathological hallmark of demyelinating diseases affecting the central and peripheral nervous system. These myelin diseases comprise a heterogeneous group of genetic disorders, known as leukodystrophies, and the clinically more relevant acquired demyelinating diseases, which present during adolescence and early adult life.

Multiple sclerosis (MS) is a chronic inflammatory disease of the CNS characterized by widespread areas of focal demyelination, which was first clinically described by Jean-Martin Charcot in the mid-nineteenth century (Murray 2009). Regarded as the most prevalent non-traumatic neurological disease among young adults, MS affects 2.3 million people worldwide according to the Atlas of MS data base (2013) and has a great socio-economic impact in developed countries. Despite some exceptions, the global distribution of the disease increases with increasing distance from the equator. It is also classically accepted that the prevalence of MS affects more women than men, a difference that has increased markedly during the last decades. Both genetic and environmental factors are thought to be enhancing female-to-male incidence ratio for MS (Browne et al. 2014).

MS is recognized as a complex disease with different clinical and pathological phenotypes that reflect different pathways leading to tissue injury, being **demyelination**, **inflammation** and **neuronal/axonal degeneration** the major hallmarks of the disease (Compston and Coles 2008). Although the etiology of MS remains unclear, it is generally accepted that the disease process starts with the migration of autoreactive lymphocytes across the blood-brain barrier continued by glial activation and chronic neurodegeneration (Weiner 2004). During the last decades, primary death of oligodendrocytes and early axonal impairments have gained importance as alternative etiopathogenic mechanisms contributing to MS initiation and progression.

1.2.1. Multiple sclerosis phenotypic classification

MS diagnostic criteria have changed over time, thanks to the evolution of research and incorporation of technology to aid the diagnostic process. Based on clinical relapse rate, MRI and disease progression, MS is classified into different subtypes, as re-defined by Lublin in 2014 (Lublin 2014) and described in the revision of 2017 of McDonald criteria (Thompson et al. 2018).

Relapsing-remitting MS (RRMS). It is the most common form of MS, characterized by defined acute exacerbations with complete or incomplete recovery. During periods between relapses, patients show relative clinical stability with no disease progression (**Figure 3**). A relapse or attack, is defined by the International Panel on the Diagnosis of MS as 'patient-reported symptoms or objectively observed signs typical of an acute inflammatory demyelinating event in the CNS, current or historical, with duration of at least 24 hours, in the absence of fever or infection' (Polman et al. 2011). Approximately 85% of people with MS are initially diagnosed with RRMS. However, numerous patients diagnosed with this form of MS eventually develop a secondary progressive disease phase. Recently, it has been described that sometimes patients can present only a single attack. This type of event has been named as "Clinically Isolated Syndrome" (CIS) and is now considered part of the relapsing-remitting MS disease spectrum (Lublin 2014) (**Figure 3**).

Secondary Progressive MS (SPMS). Characterized by gradual progression after a relapsing course (Pasquali et al. 2015) (**Figure 3**). Around 40% of patients develop this form of MS within 20 years of the initial event. In most of the cases, SPMS involves a gradual decline in neurologic functioning and affects areas previously involved in the relapsing course of the disease (Katz Sand 2015).

Primary Progressive MS (PPMS). Patients with primary-progressive MS (PPMS) experience a progressive decline in neurological functions from disease onset and never have acute attacks (**Figure 3**). This form represents about 10% of MS cases (Koch et al. 2009), usually patients tend to have a later age onset and the prognosis is worse compared to RRMS patients.

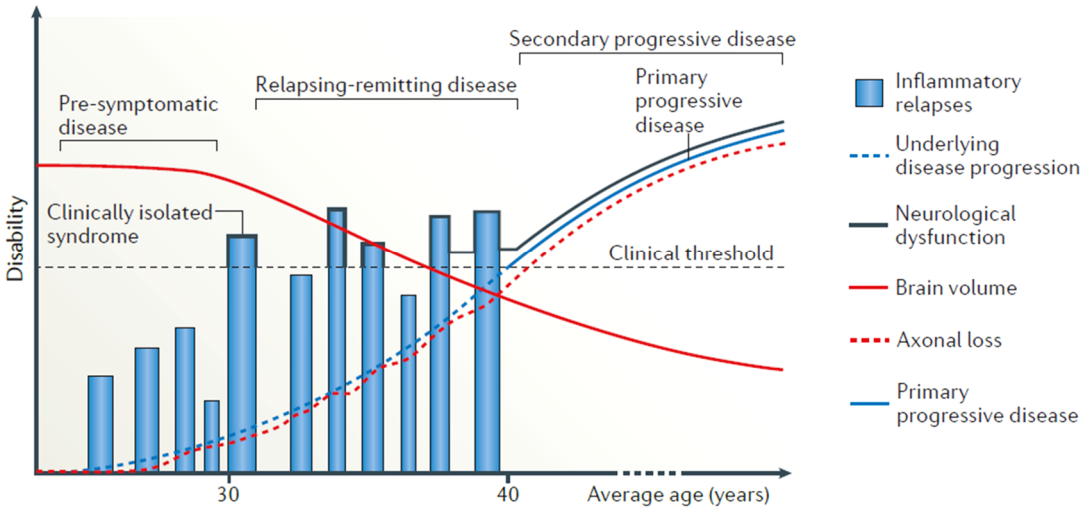

Figure 3. Representation of MS subtypes depicting the characteristic neurological dysfunction, brain atrophy and axonal loss associated to each subtype. From Dendrou et al., 2015.

1.2.2. Etiology and pathophysiology of multiple sclerosis

MS has been associated to a variety of environmental factors, including vitamin D deficiency, obesity or cigarette smoking, but also to genetic and epigenetic modifications affecting the human leukocyte antigen (HLA) or major histocompatibility complex (MHC) gene family, among other genes (Thompson et al. 2018). Detailed histopathological analysis has revealed a marked heterogeneity between MS lesions, which suggest that disease initiation and progression are driven by complex pathogenic mechanisms (Lucchinetti et al. 2000). Over the years, a variety of MS models mimicking specific aspects of MS pathology have been developed (**Box 1**).

Immune dysregulation leading to altered 'crosstalk' between the innate and adaptive immune systems is considered a key event mediating CNS damage in MS (Grigoriadis et al. 2015). This process appears to involve dendritic cells, which migrate across de blood brain barrier and secrete a variety of cytokines inducing T cell differentiation. In this regard, the secretion of IL-12 mediates $CD4^+$ T cell differentiation into IFNγ-secreting Th11 helper cells. On the other hand, in the predominant presence of IL-23, $CD4^+$ T cells differentiate into IL-17 secreting Th17 cells (Serafini et al. 2006). Pathogenicity triggered by these activated T cells consists in many events. On one hand, they induce an increase in blood brain barrier permeability by producing matrix metalloproteinases

and radical oxygen species. Secondly, they promote the recruitment of monocytes from the bone marrow and produce cytokines that induce macrophage, microglial and astrocyte activation, which in turn release pro-inflammatory mediators, oxygen and nitric oxide radicals that participate to myelin breakdown and axonal degeneration (Strachan-Whaley et al. 2014). Besides that, $CD8^+$ T cells also release pro-inflammatory mediators such as IL-17 and lymphotoxin, and their presence in CNS has been associated to axonal damage (Bitsch et al. 2000). Moreover, other cell types such as natural killer cells -by stimulating APC maturation and cytokine production- and B cells -by antibody and auto-antibody production- have also been implicated in the immunopathogenesis of MS.

Although the predominant view has been that acute demyelinating lesions start with deregulation of the immune system, newly forming lesions of certain MS patients exhibit profuse oligodendrocyte apoptosis with early microglial activation, in the virtual absence of infiltrating lymphocytes or myelin phagocytes. By contrast, 'older' lesions in the same patients exhibited positive expression of these immune cells (Barnett and Prineas 2004; Lucchinetti et al. 2000). These observations suggest that, at least in a subset of MS patients, autoimmunity might be a secondary response to massive **primary oligodendrocyte apoptosis**. According to the above mentioned histological findings, MS active lesions in white matter are classified in three groups. The most common types include patterns I and II, which are characterized by the presence of mononuclear phagocytes and perivascular T cell infiltration, and also by immunoglobulin and complement deposition in the case of type II lesions. By contrast, oligodendrocyte apoptosis and/or dying-back oligodendropathy starting at the innermost myelin tongue are considered the main features of pattern III lesions (Reich et al. 2018) (**Figure 4**). In PPMS and SMPS patients, active demyelinating plaques are less frequent and inactive lesions are dominant. These inactive lesions are characterized by well-defined demyelination, decreased axonal density, variable activation of microglial cells in the area around the plaque and macrophage absence (**Figure 4**).

In the last years, **neurodegeneration** has been highlighted as a primary cause of long-term neurological disability in MS. Indeed, synaptic alterations, axonal injury and neuronal loss have been consistently described in the context of MS (Centonze et al. 2009; Seehusen and Baumgärtner 2010; Vercellino et al. 2009). Furthermore, neurodegeneration might occur early in the disease course and not only because of myelin loss (Seehusen and Baumgärtner 2010). In this regard, converging lines of evidence support the hypothesis that **glutamate-mediated excitotoxicity** is a key etiopathogenic mechanisms of neurodegeneration, as well as of demyelination, in MS. Both neurons and oligodendrocytes are vulnerable to the excessive activation of ionotropic AMPA/kainate and NMDA glutamate receptors (Choi 1988; Matute et al. 2001). This overactivation results in a massive entry of extracellular calcium, which triggers a depolarization of the mitochondrial membrane and a production of reactive oxygen species that culminate with the initiation of death cascades. Glutamate concentration in cerebrospinal fluid is higher in acute compared with silent MS patients and controls subjects and is associated to the severity and course of the disease (Stover et al. 1997). Moreover, impaired glutamate clearance and beneficial effects resulting from AMPA/kainate and NMDA receptor antagonists have been reported in mouse MS models (Bolton and Paul 1997; Pitt et al. 2000).

Box 1. Modeling MS in mice

Animal modeling has been critical for addressing MS pathogeny and as a testing tool for therapeutic approaches. Although the complexity and heterogeneity of human MS cannot be fully replicated, a number of complementary animal models resembling the disease have been developed.

Experimental autoimmune encephalomyelitis (EAE) (Procaccini et al. 2015)

- *Induction*: immunization with self-antigens derived from myelin proteins. Freund´s adjuvant and pertussis toxin are often administered to potentiate humoral immune responses.
- *Mechanism*: autoreactive inflammatory T cells infiltrate into the CNS, drive the activation of resident microglia and astrocytes, and the subsequent recruitment of macrophages and monocytes from circulating blood.
- *Characteristics*: demyelination of spinal cord and brain associated to neurological dysfunction. First symptoms appear 9-12 days after immunization and consist in tail and hind limb weakness, followed by paralysis and forelimb affection.
- *Applications and translational value*: study of immune system activation, neuroinflammation and therapeutic utility of immunomodulatory agents.
- *EAE variants*:
  - *Relapsing-remitting EAE in Biozzi ABH or SJL/J mice:* immunization with MBP_{84-104} or $PLP_{139-151}$ triggers RR disease allowing for the study of relapse frequency.
  - *Chronic EAE in C57BL/6J mice:* immunization with $MOG_{35–55}$ induces acute disease followed by partial recovery during a chronic phase. Reminiscent of primary and secondary progressive MS.
  - *EAE in non-obese diabetic (NOD) mice:* display a RR course upon immunization with MOG_{35-55} followed by a chronic, non-remitting stage.
  - *EAE in transgenic mice:* MOG_{35-55} specific T cell transgenic (2D2) and B cell knock in mice (IgH MOG). Suitable for *in vitro* study of immune cell activation and function.

Toxic models of demyelination

1. <u>*Demyelination by cuprizone feeding*</u> (Kipp et al. 2017)

- *Induction:* administration of cuprizone (bis-cyclohexanone-oxaldihydrazone) in the diet.
- *Mechanism:* cuprizone is a copper chelator that causes primary and selective death of mature OLs with subsequent demyelination. This process takes place with a marked activation of astrocytes and microglia without major involvement of T cells. OL apoptosis relies on mitochondrial disruption, which makes these cells enable to fulfil the extensive metabolic demand.
- *Characteristics*: cuprizone feeding induces a highly reproducible demyelination pattern affecting several brain regions. Almost complete demyelination takes place following 5-6 weeks of cuprizone treatment and is followed by spontaneous remyelination when mice are fed normal chow.
- *Applications and translational value*: study of the mechanisms driving primary de- and remyelination and testing of therapeutic strategies designed to modulate these processes.

2. <u>*Demyelination by lysolecithin*</u> (Keough et al. 2015)

- *Induction:* lysolecithin (LPC) injection in the brain or spinal cord.
- *Mechanism:* this activator of phospholipase A2 induces focal demyelination due to its detergent action on myelin sheaths, rather than to direct effects on OLs. Even though it is not immune-mediated demyelination, lesion sites are infiltrated with T cells, B cells, macrophages and neutrophils, which seem to be involved in CNS repair. Complete remyelination occurs at 5-6 weeks after toxin injection.
- *Applications and translational value*: study of the mechanisms driving primary de- and remyelination and assessment of therapeutic strategies designed to suppress myelin damage and to promote the repair process.

Theiler´s murine encephalomyelitis virus (TMEV) (DePaula-Silva et al. 2017)

- *Induction:* infection with picornavirus such as TMEV.
- *Mechanism:* macrophages/microglia activated by cytokines produced by TMEV-specific $CD4^+$ T cells are the first effectors of demyelination. Axonal damage precedes demyelination, suggesting that axonal degeneration might trigger recruitment of T cells and macrophages into the CNS. Suitable model to study PPMS.
- *Characteristics*: symptoms appear around 30-60 days post-infection and consist in impaired motor coordination, incontinence, axonal loss-mediated paralysis and spinal cord atrophy.
- *Applications and translational value*: study of the mechanisms leading to axonal degeneration and testing of neuroprotective agents and therapeutic approaches targeting adhesion molecules.

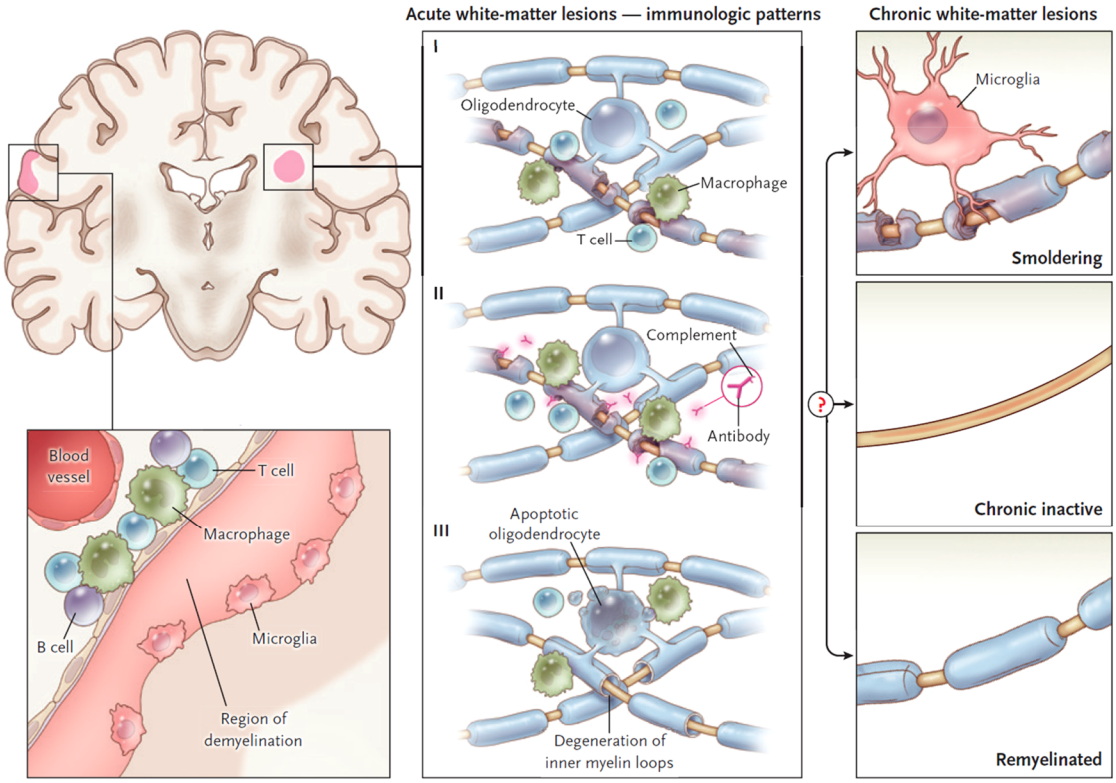

Figure 4. Lesion types in MS. Early active white matter demyelination falls into three major categories. The most common patterns I and II types are mediated by immune system dysregulation, while pattern III lesions, are characterized by primary oligodendrocyte apoptosis. After the acute phase, factors that remain poorly understood determine whether surviving axons in a lesion are remyelinated by a thin myelin sheath, whether inflammation resolves without remyelination and evolves to a chronic inactive state, or whether inflammation and slow myelin degeneration persist in a smoldering lesion. From Reich et al., 2018.

Despite the fact that most of MS lesions remain permanently demyelinated, myelin repair occurs spontaneously in some of them, named "shadow plaques" (Chang et al. 2012). **Remyelination**, which is considered a physiological response, is defined as a regenerative process whereby myelin sheaths are restored. This process occurs through the activity of OPCs, which are recruited into MS lesions and differentiate into myelinating oligodendrocytes (Franklin and Ffrench-Constant 2017; Kremer et al. 2018) giving rise to shorter and thinner myelin sheaths than the original ones (**Figure 5**). The mechanisms responsible for OPC activation and recruitment are still poorly defined, but it is speculated that may be related to tissue injury-mediated innate immune responses. This hypothesis proposes that changes in tissue integrity are first detected by **microglia**. Activated microglial cells secrete a battery of signaling molecules promoting the activation of resident **astrocytes**, which in turn release OPC modulating factors (Franklin and Ffrench-Constant 2017).

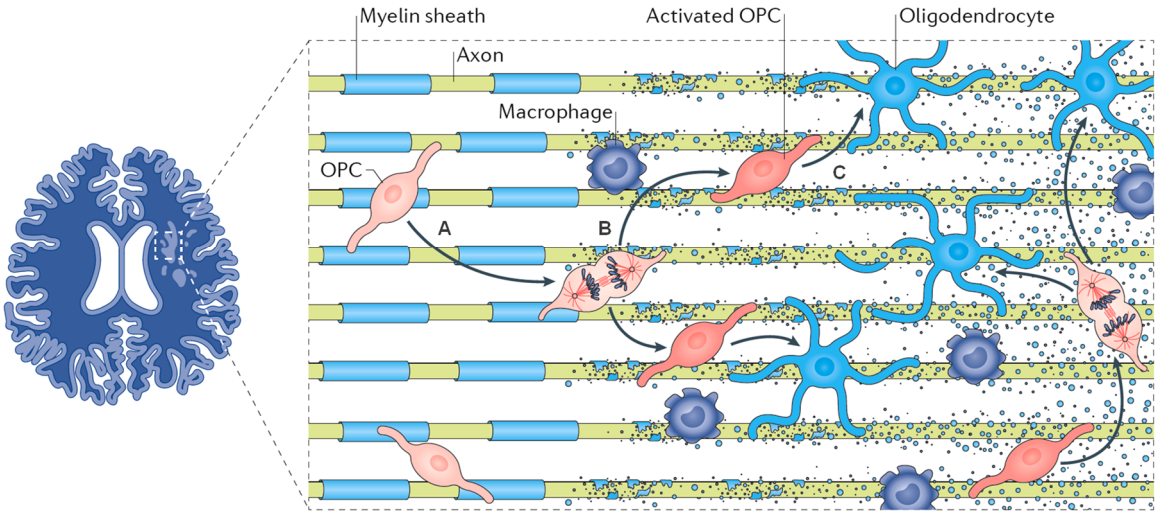

Figure 5. Schematic model of remyelination in MS. Successful remyelination requires the recruitment (**A**), proliferation (**B**) and differentiation (**C**) of oligodendrocyte precursor cells (OPCs) into myelinating oligodendrocytes at lesion sites. From Franklin and Ffrench-Constant, 2017.

Although remyelination is a consistent finding in MS, it is also well established that this process becomes inefficient and neurological disability increases during disease progression (Franklin 2002). Several studies suggest that this failure in the repair process occurs due to an inhibition of OPC differentiation at the site of injury, rather than as a consequence of deficient OPC migration or proliferation (Kremer et al. 2018). For this reason, differentiation promoting strategies that promote the generation of myelin-producing cells from existing OPCs in injured areas has become a major focus of MS research.

1.2.3. Current therapeutic strategies in multiple sclerosis

Current MS therapies consist mainly in disease-modifying agents (DMTs). These DMTs have been develop to intervene in different disease-mediator mechanisms, including antigen presentation, peripheral immune response or target tissue within the CNS itself (Weissert 2013). These type of therapies aim at reducing relapse rate and thus ameliorate the course of relapsing multiple sclerosis and the quality of life (Wingerchuk and Carter 2014). However, current DMTs fail to benefit the progressive phase of MS, in which neurodegenerative mechanisms gain clinical importance. Thus, new strategies focused on the protection of CNS from inflammatory injury or promoting neuronal and myelin regeneration need to be developed for the treatment during progressive stages.

2. The endocannabinoid System

Brain endocannabinoid system is a neuromodulatory system implicated in a wide variety of physiological functions, including movement, memory and cognition, mood, pain, temperature regulation and appetite, among others. The endocannabinoid system is comprised of cannabinoid receptors, their endogenous ligands, termed *endocannabinoids*, and the enzymes for the biosynthesis and degradation of these compounds (**Figure 6**). Cannabinoid receptors are the main molecular targets of **Δ^9-Tetrahydrocannabinol** (**Δ^9-THC**), a phytocannabinoid compound known to mediate the psychoactive effects of the marijuana plant (*Cannabis sativa* L), which has been used for over 5000 years as a recreational and medicinal drug.

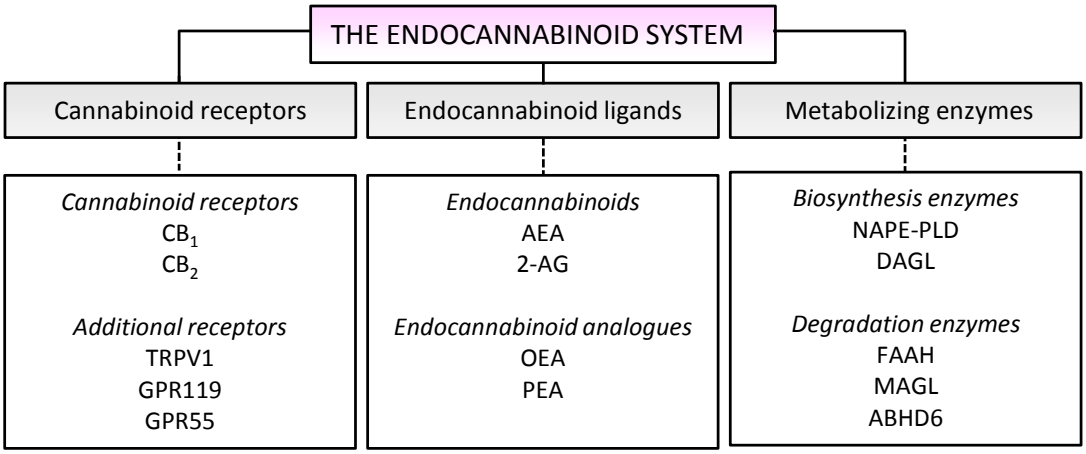

Figure 6. Over-view of molecular composition of endocannabinoid system. Adapted from André and Gonthier, 2010.

2.1. Brain cannabinoid receptors

The isolation of Δ^9-THC in 1964 from confiscated hashish (Mechoulam 1970) brought about the generation of a large amount of synthetic compounds with a similar structure to phytocannabinoids, which finally led to the identification of the first receptor for these molecules named **cannabinoid receptor 1** (**CB_1 receptor**). This receptor was successfully cloned from rat cerebral cortex (Matsuda et al. 1990), human testis and brain (Gérard et al. 1991) and mouse brain (Chakrabarti et al. 1995). Not long after, another cannabinoid receptor was identified in rat (Munro et al. 1993) and mouse (Shire et al. 1996) and was termed as **cannabinoid receptor 2** (**CB_2 receptor**).

Cannabinoid CB_1 and CB_2 receptors belong to the superfamily of GPCRs. These signaling proteins are composed by an N-terminal extracellular domain that possesses potential glycosylation sites, an intracellular C-terminal domain coupled to a G protein and 7 transmembrane domains. Initial studies showed that CB_1 receptors are predominantly expressed in the brain whereas CB_2 receptors are mainly localized in peripheral cells derived from immune system. Although each receptor is associated to specific signaling pathways, both share the ability to couple G_i proteins (Howlett 2002).

CB_1 receptor is one of the most abundant GPCRs in the mammalian brain responsible for mediating the psychoactive effects of cannabis (Herkenham et al. 1990). In humans, CB_1 receptor is encoded by the *Cnr1* gene and consists of 472 amino acids (473 in rat and mouse) (Zou and Kumar 2018). Recent studies have described the crystal structure of this protein (Hua et al. 2016; Shao et al. 2016) and unveiled the structural changes that occur upon agonist binding, thus offering a possibility for better understanding the biochemistry of these molecules.

Brain CB_1 receptor expression is widespread and heterogeneous. The regions that express highest levels of this protein include those which are involved in memory and learning processes (**hippocampus and cortex**), in the regulation of motor activity (**cerebellum and basal ganglia**), in the emotional behavior (**amygdala**) or sensory (**thalamus**) and pain (**hypothalamus**) perceptions, among others (Zou and Kumar 2018).

Concerning the cellular distribution of CB_1 receptors, these proteins are mainly localized in **mature neurons** within the CNS. In particular, CB_1 receptors are expressed at high levels in GABAergic neurons and in to a lower extent in glutamatergic cells of the forebrain (**Figure 7**) (Gutiérrez-Rodríguez et al. 2017; Kawamura et al. 2006; Marsicano and Lutz 1999). The majority of neuronal CB_1 receptors accumulate **presynaptically on axons terminals** and are centrally involved in the maintenance of synapse homeostasis by negatively regulating neurotransmitter release (**Figures 7** and **8**) (Katona and Freund 2012). A number of anatomical and functional studies have reported the existence of CB_1 receptors at postsynaptic sites where could participate in cell autonomous regulation processes (Marinelli et al. 2008; Maroso et al. 2016; Rodriguez et al. 2001). On the other hand, the presence of CB_1 receptor levels in **glial cells** has also been convincingly demonstrated during the last decade. In particular, **astrocytes** express detectable amounts of CB_1 as demonstrated by electron microscopy analysis (Gutiérrez-Rodríguez et al. 2018; Han et al. 2012). Despite being expressed at low levels, astroglial CB_1 receptors play a crucial role in neuron-astrocyte communication, memory and behavior (Metna-Laurent and Marsicano 2015; Oliveira da Cruz et al. 2016; Robin et al. 2018). A number of *in vitro* studies also supports the localization of CB_1 receptors in additional glial cells type, namely microglia (Stella 2010) and oligodendrocytes (Bernal-Chico et al. 2015; Gomez et al. 2010). However, both the *in vivo* distribution and the physiological role of CB_1 receptor populations the in microglia and oligodendroglia remain poorly investigated.

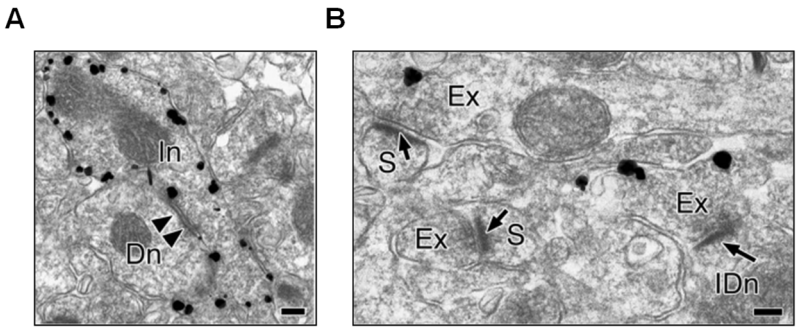

Figure 7. Immunoelectron microscopy showing presynaptic localization of CB_1 receptors in the mouse hippocampus. Micrographs show CB_1 receptor immunoparticles located ion inhibitory (In) (**A**) and excitatory (Ex) (**B**) terminals synapsing onto dendrites (Dn) and dentritic spines (S). From Kawamura et al., 2006.

Like many other GPCRs, CB_1 receptors are primarily localized in the **plasma membrane**. Nevertheless, recent outstanding studies have demonstrate that this receptor is also present in different intracellular compartments such as **endosomes** (Leterrier et al. 2004) and **mitochondria** (Bénard et al. 2012; Hebert-Chatelain et al. 2016). This last population seems to be crucially implicated in memory processes through the control of neuronal energy metabolism.

Cannabinoid **CB_2 receptors** are localized at highest levels in **peripheral immune cells and tissues** and regarded as the main substrate for cannabinoid immunomodulatory activity (Berdyshev 2000; Howlett 2002). Of specific immune cell types, the highest levels of CB_2 are found in macrophages, $CD4^+$ and $CD8^+$ T cells, B cells, natural killer cells, monocytes and polymorphonuclear neutrophils. Healthy CNS tissue contains only very low expression levels of CB_2 receptors and the neuronal expression of this protein remains controversial (Atwood and Mackie 2010). Pharmacological studies in cultured cells also support a marginal expression of CB_2 receptors in astrocytes and oligodendroglia (Gomez et al. 2011; Stella 2010). Conversely, it is well established that CB_2 receptors are localized in brain **microglia** during neuroinflammation and its expression levels vary depending on the activation state of the cell (Mecha et al. 2016). Notably, microglial CB_2 receptors regulate the migration and infiltration of these cells into brain areas during active neurodegeneration (Fernández-Ruiz et al. 2008; Navarro et al. 2016). Thus, CB_2 activation affects a myriad of innate and adaptive immune responses from inflammation to neuroprotection. The scarcity of neuronal CB_2 receptors together with the anti-inflammatory properties derived from the activation of this protein in microglia and peripheral immune cells makes CB_2 selective drugs attractive as therapeutics that would presumably lack psychoactivity.

In addition to their activity at CB_1 and CB_2 receptors, endocannabinoids can non-specifically activate many other receptors (Gorzkiewicz and Szemraj 2018). In particular, type-1 transient receptor potential vanilloid (TRPV1) ion channels that naturally respond to low pH and capsaicin, bind some *N*-arachidonoyldopamines an fatty acylethanolamides including the principal endocannabinoid ***N*-arachidonoyletanolamine** (**anandamide, AEA**) (Di Marzo and De Petrocellis 2010). Some other non-cannabinoid receptors that also respond to endocannabinoids include peroxisome proliferator-activated receptors (PPARs), non-selective cation channels such as TRPA1 or TRPM8, ligand-gated ion channels including 5-HT3, metabotropic receptors including GPR55 (with 14% of sequence similarity with CB_1 and CB_2 receptors), glycine and nicotinic acetylcholine receptors, voltage-gated ion channels including T-type calcium channels and the TASK potassium channels.

2.2. Endocannabinoid production and signaling machinery

Endocannabinoids can be defined as a group of lipid messengers synthesized from cellular membrane components. Although several molecules have been identified, **anandamide** (Devane et al. 1992) and **2-arachidonoylglycerol** (**2-AG**) (Sugiura et al. 1995) are the best-characterized endocannabinoids, both of which are **synthesized on demand** usually in response to elevations of intracellular calcium (Pertwee et al. 2010). Although both AEA and 2-AG are able to bind and activate CB_1 and CB_2 receptors, these compounds play differential roles in the regulation of biological responses (Busquets-Garcia et al. 2011). In this regard, it is worth mentioning that 2-AG is a full agonist of cannabinoid receptors, whereas AEA usually behaves as partial agonist of the receptor (Howlett 2002). Notably, 2-AG levels in the CNS are around 200-800 times higher than those for AEA (Sugiura et al. 2002) and it is increasingly accepted that the former is the main ligand for presynaptic CB_1 receptor mediated control of synaptic function (Katona and Freund 2008).

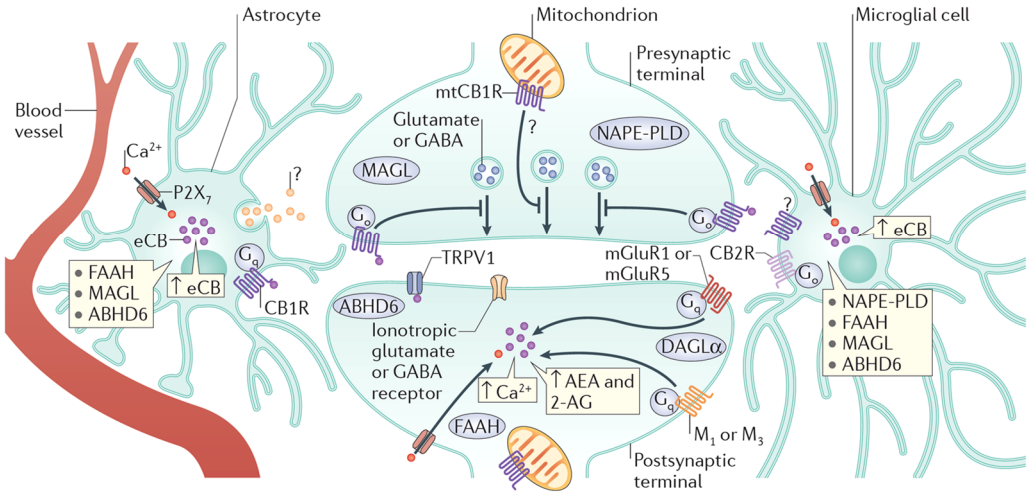

Figure 8. Architecture of neuronal and glial endocannabinoid system. Cannabinoid CB_1 receptors (CB_1R) are typically present at presynaptic terminal and coupled to $G_{i/o}$ proteins. Activation of neuronal CB_1R by 2-arachidonoylglycerol (2-AG) or *N*-arachidonoylethanolamine (AEA) triggers the suppression of neurotransmitter release. CB_1R are also expressed by mitochondria ($mtCB_1R$) at pre-and postsynaptic sites. Stimulation of $mtCB_1R$ leads to the inhibition of oxidative phosphorylation and ATP production in the mitochondria. AEA can also activate postsynaptic type-1 transient receptor potential vanilloid receptor channels (TRPV1), increasing the postsynaptic current while 2-AG can stimulate postsynaptic $GABA_A$ receptors. Postsynaptic depolarization following activation of several receptors, including group I metabotropic glutamate receptors ($mGluR_{1/5}$) and muscarinic M_1 and M_1 receptors, leads to on demand synthesis of 2-AG by the action of diacylglycerol lipase-α (DAGLα). Consecutively, 2-AG activates presynaptic CB_1R in a retrograde manner acting as a negative-feedback mechanism to suppress synaptic transmission. The major 2-AG degrading enzyme monoacylglycerol lipase (MAGL) is located at presynaptic terminals and in astrocytes. In contrast, α-β-hydrolase domain 6 (ABHD6) regulates 2-AG levels at the site of production. The major enzyme involved in AEA synthesis, N-acyl phosphatidyl ethanolamine-phospholipase D (NAPE-PLD), is predominantly located in the presynaptic terminal, although it may also be expressed postsynaptically. The enzyme responsible for AEA hydrolysis (FAAH) is present at the postsynaptic terminal. Microglial cells express CB_2 receptors, and possibly CB_1R, involved in the control of inflammatory reactions. Moreover, astrocytes show G_q-coupled CB_1R, that once stimulated lead to an increase in intracellular calcium concentration with the subsequent release of 'gliotransmitters'. Endocannabinoid biosynthesis in microglia and astrocytes can be stimulated by ATP through the activation of P_2X_7 purinoreceptors. From Lutz et al., 2015.

The synthesis and degradation of endocannabinoids are tightly regulated processes. The main pathway for AEA biosynthesis involves a calcium-dependent ***N*-acyltransferase** (**NAT**) that transfers **arachidonic acid** (**AA**) from phosphatidylcholine to phosphatidylethanolamine, thus generating ***N*-acylphosphatidylethanolamine** (**NAPE**) (Cadas et al. 1996). In a second step, AEA is cleaved from its membrane precursor NAPE through a reaction catalyzed by a phosphodiesterase of the phospholipase D-type (**NAPE-PLD**) (Okamoto et al. 2004). Alternatively, NAPE can be hydrolyzed, by phospholipase C (**PLC**), to phospho-AEA, which, in turn, is dephosphorylated by phosphatases (Liu et al. 2006). Although neural activity induces AEA release in a calcium-dependent manner, calcium entry into neurons is not an exclusive pathway for AEA generation, since the activation GPCRs like dopamine D_2 receptors, group I metabotropic glutamate ($mGlu_{1/5}$) receptors and muscarinic acetylcholine M_3 receptors can trigger AEA production (Piomelli 2003).

The most accepted pathway for 2-AG biosynthesis is the hydrolysis of membrane phosphatidylinositols by **PLC** leading to the production of **1,2-diacylglycerol** (**DAG**), which in turn is converted to 2-AG by the action of postsynaptic integral membrane protein **diacylglycerol lipase** (**DGLα/β**) (Bisogno 2008; Bisogno et al. 2003). Characterization studies using DGLα and DGLβ deficient mice have suggested that α form of the enzyme is the primary responsible of 2-AG synthesis in CNS, whereas the DGLβ isozyme plays primary role in the liver (Gao et al. 2010; Tanimura et al. 2010). Neuronal 2-AG biosynthesis can be induced by membrane depolarization or by activation of G_q coupled GPCRs, such as $mGlu_{1/5}$ receptors and M_1/M_3 (Hashimotodani et al. 2005; Kano et al. 2009).

Regarding endocannabinoid production in glial cells, 2-AG biosynthesis by cultured microglia and astrocytes is coupled to the activation of P_2X_7 ionotropic receptors, which triggers a sustained rise in intracellular calcium (Walter et al. 2004; Witting et al. 2004). OPCs and OLs *in vitro* also exhibit constitutive 2-AG production (Bernal-Chico et al. 2015; Gomez et al. 2010), but the extracellular signals regulating endocannabinoid biosynthesis in oligodendroglia remain uncertain. Concerning metabolic routes, endocannabinoids are normally degraded through hydrolysis by specific **serine hydrolases** although **oxidative pathways** have also been pointed out (**Figure 9**).

The metabolism of AEA and 2-AG and the subsequent termination of their signaling activity takes place intracellularly. However, cannabinoid specific transporters have not been characterized and how released endocannabinoids access their metabolic enzymes remains unclear. **Fatty acid amide hydrolase** (**FAAH**) is regarded as the main enzyme responsible for the hydrolysis of AEA (Cravatt et al. 1996) into free AA and ethanolamine (**Figures 8** and **9**). As an alternative to FAAH, AEA can be hydrolyzed by **N-acylethanolamine-hydrolyzing acid amidase** (**NAAA**). The most important difference between FAAH and NAAA is pH dependency of their catalytic activities, as FAAH is active in a wide range of pH while NAAA shows a pH optimum at 4.5-5, consistent with its localization in lysosomes. On the other hand, 2-AG is preferentially metabolized by **monoacylglycerol lipase** (**MAGL**) (Dinh et al. 2002). MAGL is widely expressed through the nervous system and mediates approximately 85% of 2-AG metabolism into arachidonic acid and glycerol (Savinainen et al. 2012). These hydrolytic enzymes exhibit a differentially localization in the synaptic cleft, with FAAH being present mainly at the postsynaptic compartment and MAGL localized in the vicinity of CB_1 receptors at the presynaptic site (**Figure 9**) (Gulyas et al. 2004). In addition to their expression in neurons, FAAH and MAGL are also present in glial cells (Lutz et al. 2015). Astrocyte MAGL, in particular, has been crucially involved in the termination of neuronal 2-AG signaling as well as in the production of pro-inflammatory prostaglandins from this endocannabinoid ligand (Chen et al. 2016; Viader et al. 2015).

Apart from MAGL, two other serine hydrolases that break down 2-AG have been more recently identified, namely **α/β-hydrolase domain containing 6** and **12** (**ABHD6** and **ABHD12**) (Blankman et al. 2007) (**Figure 10**). Both enzymes hydrolyze 2-AG to a similar extent despite sharing less than 20% sequence homology. ABHD6 is a 30 KDa integral membrane enzyme where the active site is predicted to face the cell interior and includes a catalytic triad determined by aminoacids S148-D278 and H306 (Blankman et al. 2007; Navia-Paldanius et al. 2012). This serine hydrolase is highly expressed in the immune system and the small intestine, followed by the brain (The Human Protein Atlas). At the cellular level, ABHD6 is primarily expressed at the postsynaptic compartment of principal glutamatergic neurons, with some expression on GABAergic cells, astrocytes and microglia (Marrs et al. 2010). The highest ABHD6 enzymatic activity in nervous tissue has been measured in the frontal cortex, hippocampus, striatum and cerebellum (Baggelaar et al. 2017). In physiological

conditions, this enzyme accounts only for approximately 4% of brain 2-AG hydrolysis and there are several alternative substrates that can be hydrolyzed by ABHD6 (Navia-Paldanius et al. 2012). However, several studies have pointed out the importance of ABHD6 in the regulation of 2-AG metabolism during neuroinflammation, based on increased expression levels of this enzyme and the beneficial effects of its blockade in rodent models of CNS damage (Poursharifi et al. 2017).

ABHD12 is an integral membrane protein with the active site facing the lumen that accounts for approximately 9% of total 2-AG hydrolysis (Blankman et al. 2007). Pointing to an essential role of this serine hydrolase in brain physiology, mutations in the *Abhd12* gene that severely compromise its expression and/or function underlie a neurodegenerative disease called PHARC (polyneuropathy, hearing loss, ataxia, retinitis pigmentosa and cataract) (Blankman et al. 2013; Chen et al. 2013; Fiskerstrand et al. 2010). This piece of evidence has discouraged the evaluation of ABHD12 inhibitors for therapeutic benefit in neuroinflammatory conditions.

During the last decade, a number of studies have demonstrated the relevance of 2-AG enzymatic hydrolysis in the generation of the AA pool available for cycloxygenase-2 (COX-2) mediated prostaglandin (PGs) biosynthesis (**Figure 9**). In particular, MAGL-dependent hydrolysis of 2-AG has been put forward as the major source of AA for the synthesis of pro-inflammatory PGs in certain neurodegenerative, inflammatory conditions (Nomura et al. 2011). In this scenario, the anti-inflammatory benefits of MAGL and ABHD6 inhibitors in rodent models of neuroinflammation may depend on a reduced PG production rather than on enhanced endocannabinoid signaling (Nomura et al. 2011; Piro et al. 2012).

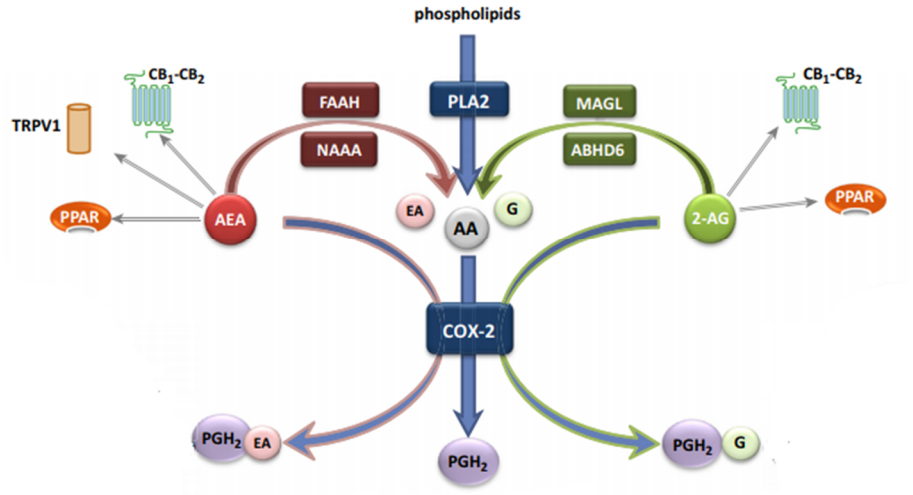

Figure 9. Endocannabinoid degradation pathways. Monoacylglycerol lipase (MAGL) and α/β hydrolase domain 6 (ABHD6) hydrolyze 2-arachidonoylglycerol (2-AG) into arachidonic acid (AA) and glycerol (G). Fatty acid amide hydrolase (FAAH) and *N*-acylethanolamine hydrolyzing acid amidase (NAAA) degrade *N*-arachidonoylethanolamine (AEA) into AA and ethanolamine (EA). MAGL and possibly other endocannabinoid hydrolytic enzymes contribute to the AA pool. AA is oxidized by cyclooxygenase-2 (COX-2) to give PGH2, which in turn is taken up by specific prostaglandin synthases to generate prostaglandins (PGs). As an alternative to hydrolysis, 2-AG and AEA can be oxidized by COX-2, to render PG-glycerol esters (PG-Gs) and PG-ethanolamides (PG-EAs). Adapted from Alhouayek et al., 2014.

On the other hand, the activity of 2-AG and AEA can also be terminated by oxidative metabolism via COX-2, leading to the formation of PG glycerol esters (PG-Gs) and PG glycerol ethanolamides (PG-EAs), respectively (Kozak et al. 2004) (**Figure 9**). Although the biological relevance of this novel pathway is only beginning to be understood, the bioactive lipid prostaglandin D2-glycerol ester has been implicated in the control of macrophage activation and inflammation by ABHD6 (Alhouayek et al. 2013). Furthermore, based on the above mentioned observations it is hypothesized that the anti-inflammatory effects of COX-2 inhibitors could be more complex than the inhibition of PG synthesis by a reduction in AA availability, and may involve increased endocannabinoid levels acting through canonical or non-canonical cannabinoid receptors (Alhouayek et al. 2014).

2.3. CB_1 receptor signaling

Activation of CB_1 receptors is associated to a variety of cellular responses that depending on cellular type, ligand and ligand-receptor interaction. Agonist binding to the receptor can trigger signaling cascades via G protein-dependent and -independent pathways. Canonical CB_1 receptor activation involves the activation of **$G_{i/o}$ proteins** and the subsequent exchange of GDP with GTP, which triggers the release of the α-subunit from the βγ dimer. In this scenario, each partner has de ability of interact with different effectors. Activation of the α_i subunit induces the inhibition **adenylyl cyclase** (**AC**) with a consequent reduction in cyclic adenosine monophosphate (cAMP) and decrease in **protein kinase A** (**PKA**) dependent signaling cascades, effects that are shared by CB_2 receptors (Howlett 2002). At the same time, released βγ dimers activate other signaling pathways including extracellular regulated kinases or **mitogen-activated protein kinase** (**MAPK**) such as **ERK**, **c-Jun** and **p38** (Bouaboula et al. 1995; Galve-Roperh et al. 2002; Rueda et al. 2000). CB_1 receptor mediated inhibition of transmitter release involves the inhibitor of **voltage-gated calcium channels** (**VGCCs**) at the presynaptic site and the activation of **inwardly rectifying K^+ channels** (**GIRK**) (Howlett 2002). Additionally, CB_1 receptors can also activate a number of different signal transduction pathways involved in cell survival and differentiation, such as the **phosphatidylinositol 3-kinase cascade** (**PI3K/Akt**) (Gómez del Pulgar et al. 2000) and **ceramide biosynthesis** (Galve-Roperh et al. 2000) and the **mTOR** pathway (Puighermanal et al. 2009). Non-canonical signaling of CB_1 receptors involves the activation of alternative G proteins depending on the ligand or the cell type. Of particular relevance for the regulation of synaptic function, **astroglial CB_1 receptors** trigger calcium release from intracellular stores through their coupling to **$G_{q/11}$ proteins** in certain conditions (Navarrete and Araque 2008). Finally, several studies have demonstrated that CB_1 receptors are able to form CB_1/CB_1 oligomers and CB_1 heterodimers with other GPCRs (Morales and Reggio 2017) whose activation triggers complex pharmacological effects that cannot be solely attributed to CB_1 receptor signaling.

2.4. CB_1 receptor regulation of central nervous system function

Neuronal CB_1 receptors are coupled to the inhibition of glutamate and GABA release from presynaptic terminals, which confers this protein the ability to modulate neurotransmission. This ability of CB_1 receptors to limit excitatory transmission has been proposed as underlying mechanism of CB_1 receptor-mediated neuroprotection against excitotoxicity, which is known to be a key pathological process of many neurological and neurodegenerative disorders (Chiarlone et al. 2014; Katona and Freund 2008). CB_1 receptor mediated-inhibition of transmitter release underlies particular forms of short-term plasticity known as **depolarization-induced suppression of inhibition** and **excitation** (**DSI**, **DSE**) (Katona and Freund 2012). In addition, CB_1 receptors are crucial mediators of **long-term depression** (**LTD**) of GABA or glutamate release after sustained synaptic activity through the brain (Castillo et al. 2012). Notably, astrocyte CB_1 receptors has also been

implicated in the control of synaptic function through the regulation of **gliotransmitter release** (Martin-Fernandez et al. 2017; Navarrete and Araque 2010). Highlighting the importance of this mechanism in brain physiology, astroglial CB_1 receptors mediate the memory disrupting effects of cannabinoids through the induction of hippocampal LTD (Han et al. 2012).

The modulation of synaptic transmission through the activation of CB_1 receptors underlie most of the biological actions of endogenous and exogenous cannabinoids in the CNS. In addition to regulating **memory and learning** (Marsicano and Lafenêtre 2009), CB_1 receptors participate in **nociception** (Woodhams et al. 2017), **motor behavior** (Fernández-Ruiz 2009), **anxiety** and **stress responses** (Lutz et al. 2015), **appetite** and **feeding behavior** (Lau et al. 2017), among other physiological processes. As such, deregulation of CB_1 receptor signaling has been implicated in a variety of a CNS disease conditions (Fernández-Ruiz et al. 2010). The capability of endocannabinoids to normalize glutamate homeostasis, reduce **excitotoxicity** and decrease **oxidative injury** and **inflammation** has prompted active research on the utility of the endocannabinoid system as a source of novel therapeutic targets in neurodegenerative diseases.

3. Role of the endocannabinoid system in multiple sclerosis

3.1. Dysregulation of the endocannabinoid system in multiple sclerosis

The involvement of the endocannabinoid system in MS control is supported by a number of studies showing alterations in the levels of endocannabinoids and cannabinoid receptors in the mouse models of the disease.

Decreased CB_1 receptor levels have been reported in EAE model (Berrendero et al. 2001; Cabranes et al. 2006; Palazuelos et al. 2008), while demyelination by cuprizone feeding is associated to increased levels of the protein (Manterola et al. 2018). This apparent discrepancy might reflect, at least in part, the different degree of neurodegeneration in the EAE and cuprizone models. Indeed, neuronal damage and synaptic loss are prominent features in the EAE model, whereas demyelination-associated degeneration of axons is only marginal during cuprizone-feeding (Skripuletz et al. 2011). On the other hand, increased CB_2 receptor mRNA and/or protein expression is a consistent finding in rodent models of MS (Loría et al. 2008; Maresz et al. 2007; Palazuelos et al. 2008), in good agreement with the proposed relevance of this cannabinoid receptor in the control inflammation.

MS is associated to increased concentrations of AEA as determined in brain tissue, cerebrospinal fluid and plasma from MS patients (Centonze et al. 2007; Eljaschewitsch et al. 2006; Jean-Gilles et al. 2009). Nevertheless, lower levels of AEA have also been reported in patients with MS (Di Filippo et al. 2008). On the other hand, findings in animal models are equally controversial, since reduced (Cabranes et al. 2005; Manterola et al. 2018), increased (Baker et al. 2001; Centonze et al. 2007) and unaltered (Witting et al. 2006) concentrations of AEA have been described. Elevated concentrations of this cannabinoid have been related to increased NAPE-PLD and reduced FAAH expression or activities in EAE mice and MS patients (Baker et al. 2001; Centonze et al. 2007).

Concerning 2-AG, most studies report unaltered concentrations of this endocannabinoid compound both in animal models (Manterola et al. 2018; Maresz et al. 2007) and in cerebrospinal fluid from MS patients (Centonze et al. 2007), although higher 2-AG levels have also been proposed in EAE mice (Baker et al. 2001). Concerning 2-AG metabolism, increased levels of MAGL (Manterola et al. 2018) and ABHD6 (Wen et al. 2015) have been postulated in rodent models of the disease.

3.2. Therapeutic potential of the endocannabinoid system in multiple sclerosis

The therapeutic potential of cannabinoids in the in MS has been studied for many years based on early reports on the beneficial effects of cannabinoids in the control of relapse frequency, spasticity or tremor by self-medicating MS patients (Consroe et al. 1997). Consistently, exogenously administered cannabinoid agonists exert a variety of therapeutic benefits in MS animal models, which include **attenuated neurodegeneration**, **demyelination** and **inflammatory responses** as well as **remyelination promoting effects** (Arévalo-Martín et al. 2003; Cabranes et al. 2005; Maresz et al. 2007; Palazuelos et al. 2008).

Most of anti-inflammatory effects of cannabinoids in MS models are ascribed to CB_2 receptors regulating microglial and T cell function (Eljaschewitsch et al. 2006; Maresz et al. 2007). However, it is well known that activation of CB_1 receptors is crucial for cannabinoid-mediated control of MS progression. In particular, neuronal CB_1 receptors modulate EAE disease severity thanks to their ability to control inflammatory and excitotoxic neurodegeneration (Croxford et al. 2008; Maresz et al. 2007; Pryce et al. 2003). From a mechanistic perspective, CB_1 receptor mediated neuroprotective effects in an MS context most likely rely on the ability of these proteins to limit synaptic excitation and to activate pro-survival pathways (Marsicano et al. 2003; Monory et al. 2006).

Research on the therapeutic potential of cannabinoids in MS has successfully culminated in the commercialization of Sativex®, an oromucosal spray containing a 1:1 combination of the phytocannabinoids Δ^9-THC and cannabidiol, for the treatment of spasticity in patients with MS (Kmietowicz 2010). However, clinical experience with cannabis-based medicines in MS has demonstrated that the use of these compounds is usually accompanied by the appearance of unwanted effects including psychoactivity or memory impairments, associated to the stimulation of bulk CB_1 receptor populations in the CNS. Indeed, the therapeutic efficacy of the phytocannabinoid Δ^9-THC in animal models and MS patients is restricted to their administration at high doses, which activate the complex array of biological actions mediated by CB_1 receptors at different cellular locations (Baker et al. 2012). Current research on the therapeutic potential of the endocannabinoid system in MS aims thus at developing strategies allowing CB_1 and CB_2 mediated beneficial effects, whilst limiting adverse responses. In this context, enhancing the concentration of the endocannabinoids AEA and/or 2-AG by decreasing their enzymatic metabolism has been postulated as a potential alternative to the use of exogenous cannabinoids for MS control.

Pharmacological or genetic inactivation of FAAH results in substantial elevations of AEA in brain tissue (Cravatt et al. 2001). With regard to MS, several studies have suggested that **FAAH inhibitors** ameliorate spasticity in animal models of the disease (Baker et al. 2001; Ligresti et al. 2006; Pryce et al. 2013). However, the effects of FAAH on MS progression have been poorly investigated using chronic models of the disease. In this regard, mice lacking FAAH experience an initial inflammatory phase of EAE similar in severity to wild type controls, and exhibit only a modest protective phenotype during clinical remission (Webb et al. 2008).

Concerning 2-AG metabolism, a number of recent studies have consistently demonstrated that administration of **MAGL inhibitors** decreases neurological deficits and inflammation and promote remyelination in MS animal models (Bernal-Chico et al. 2015; Feliú et al. 2017; Hernández-Torres et al. 2014; Mecha et al. 2018). Unfortunately, chronic MAGL inactivation also engages unwanted effects, such as desensitization of brain CB_1 receptors and functional tolerance (Schlosburg et al. 2010), that put into question the utility of drugs targeting this enzyme in the clinical practice.

On the other hand, there is substantial evidence suggesting that **ABHD6 blockade** allows for fine-tuning of 2-AG levels both in the CNS and in the periphery, with potential therapeutic implications in MS. In particular, pharmacological ABHD6 inactivation exerts antiepileptic and anti-inflammatory activities in living mice that have been attributed to the elevation of 2-AG levels at **synapses** and in **peripheral macrophages**, respectively (Alhouayek et al. 2013; Naydenov et al. 2014). Importantly, these protective effects of ABHD6 inhibitors are maintained over a chronic dosage and are achieved without the broad spectrum of psychomotor and cognitive side effects associated to the administration CB_1 receptor agonists and high doses of MAGL blockers (Long et al. 2009). The potential of ABHD6 as novel treatment option in MS has been recently put forward based on the observation that the systemic inhibitor WWL70 exhibits potent anti-inflammatory and protective effects in the EAE mouse model (Wen et al. 2015). However, an important caveat to the interpretation of the results is that WWL70 exhibits potent anti-inflammatory effects in microglia independent of its ABHD6 blockade activity (Tanaka et al. 2017). In addition, the contribution of **central and peripheral ABHD6** to the control of autoimmune inflammation remain to be investigated.

3.3. Role of oligodendrocyte CB_1 receptors in multiple sclerosis control

The myelin protective and remyelination promoting effects of cannabinoids in MS animal models point to the possibility that **OPCs** and **OLs** might be direct targets of these compounds, despite the marginal expression of cannabinoid receptors in these cells. Indeed, early autoradiography studies showed almost virtually absent expression of CB_1 receptor in adult white matter tracts (Herkenham et al. 1991). Notably, *postmortem* analysis using immunohistochemical techniques in MS patients has suggested the expression of CB_1 receptors in lesion associated OPCs and OLs (Benito et al. 2007). However, extensive characterization of CB_1 receptor distribution in the CNS has failed to convincingly demonstrate the expression of these proteins in oligodendrocyte populations of the rodent or human brain.

The idea that oligodendroglia express CB_1 receptor has gained momentum with the recent work based in single cell RNA sequencing on cells of the oligodendrocyte lineage (Marques et al. 2016). This data demonstrate the presence of *Cnr1* transcripts in almost all populations identified, from OPCs to mature myelinating oligodendrocytes, pointing to a regulatory role of this protein at multiple stages of oligodendrocyte lineage (**Figure 10**). Importantly, *Cnr1* transcripts have also been detected in $A2B5^+$ OPCs resident in the adult human subcortical white matter (Sim et al. 2006). Interestingly, oligodendrocyte populations also express the enzymes responsible for endocannabinoid production/degradation, especially those corresponding to 2-AG (*Daglb* and *Mgll*). These observations put forward the hypothesis that oligodendrocytes may release 2-AG with the subsequent activation of CB_1 receptors exerting an autocrine regulation (Bernal-Chico et al. 2015; Gomez et al. 2010; Gomez et al. 2015).

Up to the date, the role of CB_1 receptors in regulating OPC and OL biology has been exclusively addressed using *in vitro* systems. In this regard, recent work suggests that CB_1 receptor activation by endogenous 2-AG is able to promote the OPC migration (Sanchez-Rodriguez et al. 2018). Additional studies in cultured cells suggest that CB_1 receptors promote the proliferation and differentiation of OPCs acting through ERK/MAPK and PI3K/Akt/mTOR signaling pathways (Gomez et al. 2010; Gomez et al. 2011; Gomez et al. 2015). Concerning cell survival, results from our laboratory suggest a role of CB_1 receptors in mediating OL from excitotoxicity (Bernal-Chico et al. 2015). Collectively, these *in vitro* observations suggest that CB_1 receptors expressed by OPCs and OLs might fine-tune developmental myelination as well as mediate protective and regenerating

effects in an MS context. However, our current understanding on the role of CB_1 receptors in oligodendrocyte biology and pathophysiology is hampered by the lack of *bona fide* demonstration of receptor expression in these cellular populations.

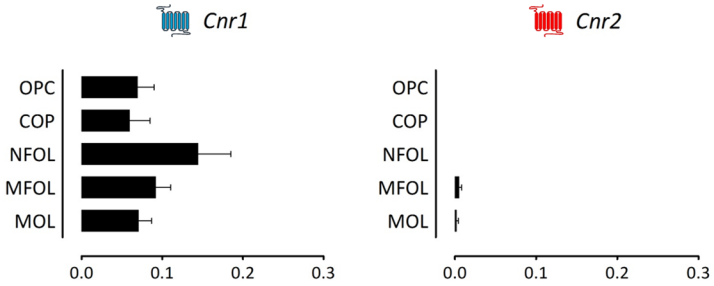

Figure 10. Average expression levels of *Cnr1* and *Cnr2* along the oligodendrocyte lineage. Single-cell RNA-seq data from the juvenile and adult mouse CNS adapted from http://linnarssonlab.org/oligodendrocytes/. The highest *Cnr1* expression levels within the oligodendrocyte lineage correspond to NFOLs. *Cnr1* expression was undetectable in MOL6 (excluded from the analysis). *Cnr2* expression was undetectable in OPC, COP, NFOL (not presented) as well as in MOL2, MOL3, MOL4 and MOL6 (excluded from the analysis). Note that *Cnr2* transcripts are expressed at lower levels than *Cnr1* transcripts through the oligodendrocyte lineage. OPC, oligodendrocyte precursor cells; COP, differentiation-committed oligodendrocyte precursors; NFOL, newly formed oligodendrocytes; MFOL, myelin forming oligodendrocytes; MOL, mature oligodendrocytes.

Objectives

The therapeutic potential of cannabis based medicines in MS is well established. Transcriptional analyses and *in vitro* pharmacological studies support the expression of low cannabinoid CB_1 receptor levels in OPCs and OL. Based on these studies, it is hypothesised that the protective and regenerative effects of cannabinoid compounds in MS would rely, at least in part, on the activation of CB_1 receptors expressed by oligodendroglia. However, the analysis of CB_1 receptor distribution in oligodendrocyte populations of the rodent and primate brain has been neglected due to the difficulties associated to the detection of the low protein levels expressed by these cells *in vivo*. Nowadays, *bona fide* demonstration of CB_1 receptor expression in oligodendrocyte lineage cells is a pending issue in the field and the role of these receptor populations in regulating myelination is controversial. On the other hand, it is well established that exogenous cannabinoid agonists exhibit unwanted side effects in the clinical management of MS patients that are associated to the activation of bulk CB_1 receptor populations in nervous tissue. Current research proposes that targeting the enzymatic hydrolysis of the major endocannabinoid 2-AG could offer the positive therapeutic potential resulting from cannabinoid receptor activation whilst limiting adverse effects. In brain tissue, 2-AG is primarily inactivated by monoacylglycerol lipase (MAGL) and to a lesser extent by α/β-hydrolase domain-containing 6 (ABHD6). Administration of MAGL inhibitors decreases neurological deficits and inflammation in MS animal models but also engages unwanted effects, namely such as desensitization of brain CB_1 receptors and functional tolerance, that put into question the utility of drugs targeting this enzyme in the clinical practice. On the other hand, there is substantial evidence suggesting that ABHD6 blockade allows for fine-tuning of 2-AG levels both in the CNS and in the periphery, with potential therapeutic implications in MS.

In the above mentioned context, the **Global Aim** of this Doctoral Thesis is to broaden current knowledge on the role of the endocannabinoid system in myelin biology and pathology, with a particular emphasis in MS.

Our **Specific Aims** were as follows:

Objective 1. To investigate the ultrastructural localization of CB_1 receptors in OPCs and mature OLs of the adult mouse brain, as well as the presence of abnormalities affecting myelin ultrastructure in CB_1 receptor knockout mice at the peak of myelination.

Objective 2. To examine the utility of targeting ABHD6 as novel therapeutic strategy in MS using selective inhibitors and complementary *in vivo* and *in vitro* models that mimic different aspects of the disease.

Material and Methods

1. Animals

For electron microscopy analyses we used mutant mice deficient in the cannabinoid CB_1 receptor (Marsicano et al. 2002) and their corresponding wild-type littermates, herein referred to as $CB_1^{-/-}$ and $CB_1^{+/+}$, respectively (colony founders kindly provided by Dr. Beat Lutz, Institute of Molecular Biology, Mainz, Germany). In addition, we used mice expressing enhanced yellow fluorescent protein (EYFP) under the control of the *NG2* gene promoter (colony founders kindly provided by Dr. Jacqueline Trotter, Institute of Molecular Biology, Mainz, Germany) (Karram et al. 2008). These mice were crossed with CB_1 deficient mice to obtain double mutant lines heterozygous for EYFP expression and wild type or knockout for CB_1 receptor expression (herein referred to as NG2-EYFP$^{+/-}$-$CB_1^{+/+}$ and NG2-EYFP$^{+/-}$-$CB1^{-/-}$, respectively). Demyelination by cuprizone feeding and EAE were induced in C57BL/6 wild type purchased from Charles River (Barcelona, Spain). Primary cultures of oligodendrocyte and neurons were obtained from Sprague Dawley rats bred at the Animal Facility of the University of the Basque Country UPV/EHU. Animals were housed under standard conditions (12 h light/dark cycles) with access to food and water *ad libitum*. All experiments were conducted under the supervision and with the approval of the Animal Welfare Committee of the University of the Basque Country UPV/EHU. All efforts were made to minimize animal suffering and to reduce the number of mice used, in compliance with the European Communities Council Directive of 22 September 2010 on the protection of animals used for scientific purposes (Directive 2010/63/EU).

2. Ultrastructural localization of CB_1 receptors in oligodendrocyte populations

2.1. Mice sacrifice and tissue processing

Mice were intraperitoneally (i.p.) anesthetized with ketamine/xylazine (80/10 mg/Kg; Imalgene®, Mérial, France/Rompun®, Bayer, Germany) and transcardially perfused with saline solution (0.9% NaCl; pH 7.4) to clear blood vessels followed by fixative solution containing 4% paraformaldehyde, 0.1% glutaraldehyde and 0.2% picric acid in 0.1 M phosphate buffer (PB; pH 7.4), using a peristaltic pump. After extraction, brains were postfixed overnight in 4% paraformaldehyde at 4˚C. Coronal sections (40 µm-thick) containing corpus callosum and hippocampus were obtained on a vibratome (VT1000S, Leica, Wetzlar, Germany) and stored in 0.1 M PB containing 0.02% sodium azide until use.

2.2. Preembedding immunogold method for electron microscopy

To study the ultrastructural localization of CB_1 receptors in myelinating oligodendrocytes we used a preembedding silver-intensified immunogold method applied to brain tissue from adult $CB_1^{-/-}$ and $CB_1^{+/+}$ mice (P60). Tissue sections were pre-incubated in a blocking solution containing 10% bovine serum albumin (BSA; Sigma-Aldrich, St. Louis, MO, USA), 0.1% sodium azide and 0.02% saponin in Tris-HCl buffered saline (TBS; pH 7.4) for 30 min at room temperature (RT). Subsequently, sections were incubated with a polyclonal rabbit anti-CB_1 receptor antibody (1:500; ImmunoGenes, Budapest, Hungary) prepared in blocking solution with 0.004% saponin for 2 days at 4˚C. After several washes in 1% BSA/TBS, tissue sections were incubated in a secondary 1.4 nm gold-labeled goat anti-rabbit IgG (1:200; Nanoprobes Inc., Yaphank, NY, USA) prepared in the washing solution with 0.1% sodium azide and 0.004% saponin for 4 hours at RT. Tissue was washed overnight in 1% BSA/TBS at 4˚C, postfixed in 1% glutaraldehyde in TBS for 10 min at RT and washed in double-distilled water (dd$H_2$0). Gold particles were silver-intensified with a HQ Silver kit (Nanoprobes) in the dark for 12 min and tissue was washed with ddH20 followed by 0.1 M PB. The day after, sections were osmicated (1% OsO_4 in 0.1 M PB; pH 7.4) for 30 min. After 3x10 min washes in 0.1 M PB, tissue

sections were dehydrated in graded ethanol concentrations (50-100%) to propylene oxide and embedded in epoxy resin (Sigma-Aldrich) by immersion in decreasing concentration of propylene oxide (1:3 for 30 min, 1:1 for 1 h and 3:1 for 2 h). Tissue was then embedded in fresh resin overnight and allowed to polymerize at 60˚C for 2 days. Following visualization at the light microscope, selected tissue portions were trimmed and glued onto epoxy resin capsules. Semi-thin sections (500 nm-thick) were cut from epoxy blocks using a Power Tome ultramicrotome (RMC Boeckeler, Tucson, AZ, USA) and stained with 1% toluidine blue. Ultrathin (50-60 nm-thick) sections were then cut with a diamond knife (Diatome, Hatfield PA, USA), collected on nickel mesh grids and stained with 4% uranyl acetate for 30 min and 2.5% lead citrate for electron microscope visualization.

2.3. Double pre-embedding immunogold and immunoperoxidase method for electron microscopy

The ultrastructural localization of CB_1 receptors in OPCs was studied using a double pre-embedding immunogold and immunoperoxidase method applied to brain tissue from NG2-EYFP $^{+/-}$-$CB_1^{+/+}$ and NG2-EYFP $^{+/-}$-$CB_1^{-/-}$ mice. Coronal sections containing the hippocampus were pre-incubated in 1% hydrogen peroxide (H_2O_2) for 15 min at RT. After several washes in TBS (pH 7.4) slices were blocked in 10% BSA, 0.1% sodium azide and 0.02% saponin in TBS for 30 min at RT. Subsequently, sections were incubated with primary polyclonal rabbit anti-CB_1 receptor antibody (1:500; ImmunoGenes) and monoclonal rat anti-GFP antibody (1:2000; Nacalai Tesque, Kyoto, Japan) prepared in blocking solution with 0.004% saponin for 2 days at 4˚C. Following several washes in 1% BSA/TBS, sections were incubated for 4 h at RT with biotinylated anti-rat IgG made in horse (1:200; Vector Laboratories, Burlingame, CA, USA) and 1.4 nm gold-labeled goat anti-rabbit IgG (1:200; Nanoprobes Inc.) prepared in 1% BSA/TBS with 0.004% saponin. Tissue slices were then washed in 1% BSA/TBS and treated with avidin-biotinylated-horseradish peroxidase complex (ABC; Elite, Vector laboratories). Sections were washed overnight in 1% BSA/TBS at 4˚C, postfixed in 1% glutaraldehyde in TBS for 10 min at RT and washed in ddH_20. Gold particles were silver-intensified and the immunoperoxidase reaction was developed using in 3´diaminobenzidine (DAB) as a chromogen (Roche Diagnostics, Mannheim, Germany). Sections were osmicated, dehydrated, embedded in epoxy resin and processed for electron microscopy visualization described above.

2.4. Semi-quantification of the CB_1 receptor immunogold and immunoperoxidase staining

The pre-embedding immunogold and immunoperoxidase methods were simultaneously applied to brain sections obtained from each of the individual $CB_1^{+/+}$, $CB_1^{-/-}$, NG2-EYFP$^{+/-}$-$CB_1^{+/+}$ and NG2-EYFP$^{+/-}$-$CB_1^{-/-}$animals (*n* = 3-5 each condition) studied. Immunogold and immunoperoxidase labeling were visualized on the tissue slices with a light microscope and portions of the corpus callosum and CA1 *stratum radiatum* with consistent immunolabeling of CB_1 receptors and NG2 cells were identified and trimmed down for ultrathin sectioning. To standardize conditions and avoid false negatives, only the first 20 ultrathin sections were collected onto the grids and photographed for analysis.

Ultrathin sections were examined with a Jeol JEM 1400 Plus electron microscope (Jeol, Tokio, Japan) at the Service of Analytical and High-Resolution Microscopy in Biomedicine of University of the Basque Country UPV/EHU. For the analysis of CB_1 receptor localization in mature oligodendrocytes and OPCs, the electron micrographs were taken with a digital sCMOS camera (Hamamatsu Photonics France, Cerdañola, Spain) at magnification 4,000-8,000 X and 8,000-15,000 X, respectively. Sampling was always carefully and accurately carried out in the same way for all the animals studied. Mature oligodendrocytes in the corpus callosum were identified by their distinctive morphological features, such as electron-dense nuclei with pronounced aggregates of

heterochromatin and the usual presence of thin rims of perinuclear cytoplasm (Peters and Folger 2013). Positive OPC processes in hippocampus *stratum radiatum* were identified by the presence of DAB immunodeposits. The density of CB_1 receptors in excitatory and inhibitory terminals was analyzed in 20 electron micrographs per animal (n = 3) taken in a systematic manner at magnification of 8,000 X. Image-J software (NIH, Bethesda, MD, USA) was used to measure the membrane length (perimeter) of oligodendrocyte somata, OPC processes and synaptic terminals. Positive labeling was considered if at least one immunoparticle was found within approximately 30 nm from the membrane. Percentages of CB_1 receptor positive somata and processes, as well as immunolabeling density (particles/µm membrane), were analyzed and displayed as mean ± SEM using a statistical software package. Results correspond to the analysis of 22-38 oligodendrocytes, 28-94 DAB positive OPC processes and 15-24 inhibitory and 97-107 excitatory synaptic terminals per animal.

3. Analysis of myelin ultrastructure

3.1. Mice sacrifice and tissue processing

Mice were anesthetized with tribromoethanol (Avertin, 0.2 mL per 10 g body weight; Sigma-Aldrich) and transcardially perfused with phosphate buffered saline (PBS; pH 7.4) followed by fixative solution containing 4% paraformaldehyde, 2.5% glutaraldehyde and 0.5% NaCl in 0.1 M PB, as described (Möbius et al., 2010). After extraction, brains were postfixed overnight at 4˚C in fixative solution and stored in 1% paraformaldehyde until use. Vibratome sections (40 µm-thick) cut in the sagittal plane were incubated in 1% OsO_4 for 30 min, dehydrated, embedded in epoxy resin and processed for electron microscopy visualization as described above. Tissue sections from $CB_1^{+/+}$ and $CB_1^{-/-}$ littermates (n = 3 each condition) were always processed in parallel to standardize analysis conditions.

3.2. Assessment of g-ratios

Electron microscopy images of the rostral and caudal corpus callosum were taken from randomly selected fields with a Jeol JEM 1400 Plus electron microscope at the Service of Analytical and High-Resolution Microscopy in Biomedicine of University of the Basque Country UPV/EHU. The *g*-ratios and the number of myelinated axons were analyzed in 20 electron micrographs per animal taken in a systematic manner at magnification of 4,000 X. To further ensure the analysis of randomly selected fibers in terms of *g*-ratio, a 1.2 mm grid was overlaid onto images and only axons whose cytoplasm was crossed by the grid junctions were analyzed. For *g*-ratio calculation, the areas corresponding to the unit integrated by 1) the axon plus the inner tongue and 2) to the whole fiber (**Figure 1A**) were measured using Image-J software. The diameters corresponding to the axon plus inner tongue (d_I) and the myelinated fiber as a whole (d_M) were then calculated from the corresponding area values and the *g*-ratios determined as the fraction d_I/d_M.

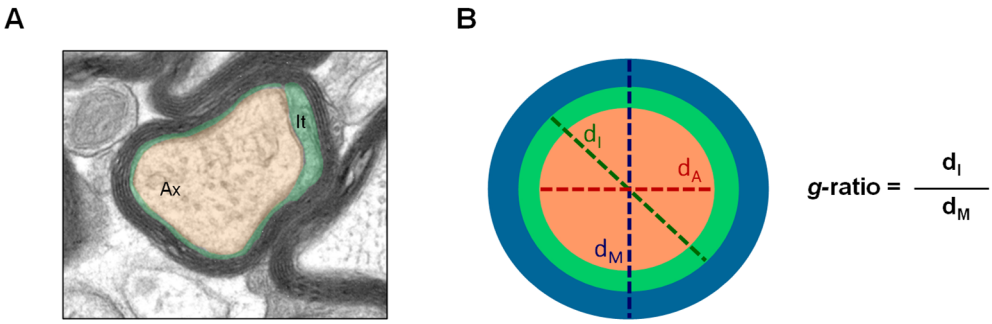

Figure 1. Quantification of *g*-ratios in electron microscope micrographs. (**A**) Representative electron microscope micrograph highlighting the area corresponding to the axon (Ax, orange) and to the inner tongue (It, green) in a myelinated fiber. (**B**) Schematic diagram depicting the parameters used for *g*-ratio analysis. The *g*-ratios of randomly selected fibers were calculated as the fraction of the diameters corresponding to the axon plus inner tongue (d_I) and to the whole fiber (d_M).

4. ABHD6 inhibitors

The selective ABHD6 inhibitors KT182 [4-[3'-(Hydroxymethyl)[1,1'-biphenyl]-4-yl]-1H-1,2,3-triazol-1-yl](2-phenyl-1-piperidinyl)-methanone] and KT203 4'-[1-[[2-(Phenylmethyl)-1-piperidinyl]carbonyl]-1H-1,2,3-triazol-4-yl]-[1,1'-biphenyl]-3-carboxylic acid] were synthesized in Benjamin F. Cravatt's laboratory at The Scripps Research Institute (La Jolla, CA, USA), as previously described (Hsu et al. 2013). The ABHD6 inhibitor WWL70 [N-Methyl-N-[[3-(4-pyridinyl) phenyl]methyl]-4'-(aminocarbonyl)[1,1'-biphenyl]-4-yl carbamic acid ester], and the FAAH inhibitors PF750 [N-phenyl-4-(quinolin-3-ylmethyl)piperidine-1-carboxamide] and URB597 [[3-(3-carbamoylphenyl)phenyl] *N*-cyclohexylcarbamate] were purchased from Tocris Bioscience (Bristol, UK). The ABHD6 inhibitor KT195 [4-(4'-Methoxy[1,1'-biphenyl]-4-yl)-1H-1,2,3-triazol-1-yl](2-phenyl-1-piperidinyl) methanone] was from Cayman Chemical (Ann Arbor, MI, USA).

5. *In vivo* models of MS

5.1. Demyelination by cuprizone feeding

Primary demyelination was induced by feeding 10 week-old male mice a diet containing 0.3% cuprizone (bis-cyclohexanone oxaldihydrazone; Sigma-Aldrich) mixed into milled chow (Altromin, Lemgo, Germany) for 3 or 6 weeks. Remyelination was studied in mice returned to normal chow for 2 weeks following a 6 weeks cuprizone challenge.

5.2. Experimental autoimmune encephalomyelitis (EAE)

EAE was induced in 10 week-old female mice by immunization with 300 µl of myelin oligodendrocyte glycoprotein 35-55 (MOG; 200 µg; CIPF, Valencia, Spain) in incomplete Freund's adjuvant supplemented with 8 mg/mL *Mycobacterium tuberculosis* H37Ra (8 mg/mL; DIFCO Laboratories, USA). Pertussis toxin (500 ng; Calbiochem, Merck Millipore, Burlington, MA, USA) was injected intraperitoneally both on the day of immunization and in the second day post-immunization (dpi). Body weight and motor deficits were recorded daily and symptoms were scored from 0 to 8 as follows: 0, no detectable changes in muscle tone and motor behavior; 1, flaccid tail; 2, paralyzed tail; 3, impairment or loss of muscle tone in hindlimbs; 4, hindlimb

hemiparalysis; 5, complete hindlimb paralysis; 6, complete hindlimb paralysis and loss of muscle tone in forelimbs; 7, tetraplegia; and 8, moribund. At the end of the experiment, animals were anesthetized with Avertin (240 mg/Kg i.p.; Sigma-Aldrich) and the conduction velocity of the corticospinal tract was assessed using stimulatory and recording electrodes placed in the primary motor cortex and in the vertebral canal at the L2 level respectively (Bernal-Chico et al. 2015).

5.3. In vivo administration of ABHD6 inhibitors

The ABHD6 inhibitors KT182 and KT203 were dissolved in 15% DMSO: 4.25% polyethylene glycol 400 (Sigma-Aldrich): 4.25% Tween-80 (Sigma-Aldrich): 76.5% saline immediately before use and administered (i.p.) at a 2 mg/Kg dose in a volume of 10 mL/Kg. To assess the effect of ABHD6 blockade during demyelination by cuprizone feeding, mice were daily treated with KT182 or vehicle for 21 days starting the first day of cuprizone administration. For remyelination studies, mice treated with cuprizone for 6 weeks were randomly assigned to experimental groups and received daily injections of KT182 or vehicle during 2 weeks starting at day 1 after toxin withdrawal. In the EAE model of demyelination, mice received daily injections of KT182 and KT203 or vehicle for 30 days using a prophylactic regimen that started at 1 dpi.

6. Gel-based competitive activity-based protein profiling (ABPP)

The *in vivo* ABPP profile of the ABHD6 inhibitors KT182 and KT203 was evaluated in brain proteomes from naive mice (*n* = 4) and randomly selected immunized mice scoring 3.5-4.5. Mice under isoflurane anesthesia (IsoVet®; B Braun, Melsungen, Germany) were killed by decapitation and their brains stored at -80°C until use. For the preparation of tissue proteomes, brains were homogenized with a glass-teflon douncer in a lysis buffer containing 20 mM HEPES, 250 mM sucrose and 2 mM DL-dithiothreitol (DTT) (pH 7.4) followed by a low-speed spin (3300 rpm, 5 min, 4°C) to remove debris. The supernatant was then centrifuged at 100,000 x g for 45 min to generate the cytosolic fraction in the supernatant and the membrane fraction as a pellet. The pellet was washed and resuspended in 20 mM HEPES (pH 7.4). The efficacy of the inhibitors to inactivate ABHD6 was also tested in cell proteomes prepared from primary rat cortical neurons, obtained and grown as described below. Cells were pre-treated with inhibitors KT182, KT203, WWL70 or KT195 for 30 min at 37 °C, washed twice with ice cold PBS and then scrapped and lysed in 500 µl of lysis buffer by sonication at 4°C. Proteomes were then isolated by centrifugation (100,000 x g, 45 min, 4°C) and resuspended in 20 mM HEPES (pH 7.4) by pipetting. Total protein concentration was determined using the Bradford Protein Assay (Bio-Rad, Hercules, CA, USA). Samples were stored at -80 °C until further use. Gel-based competitive ABPP experiments were performed as previously described (Hsu *et al*., 2013). Tissue proteomes were diluted to a 1-2 mg/mL final concentration and incubated with ABPP probes fluorophosphonate-rhodamine (FP-Rh) (Patricelli et al. 2001) or HT-01 (Hsu et al. 2013) (1 µM; kindly provided by Ku-Lung Hsu, University of Virginia, Charlottesville, VA, USA) for 30 min at 37°C. Probe-labelled reactions were denatured and loaded on 10% acrylamide SDS-PAGE gels. In-gel fluorescence was scanned with a ChemiDoc™ MP Imaging System (Bio-Rad) (**Figure 2**).

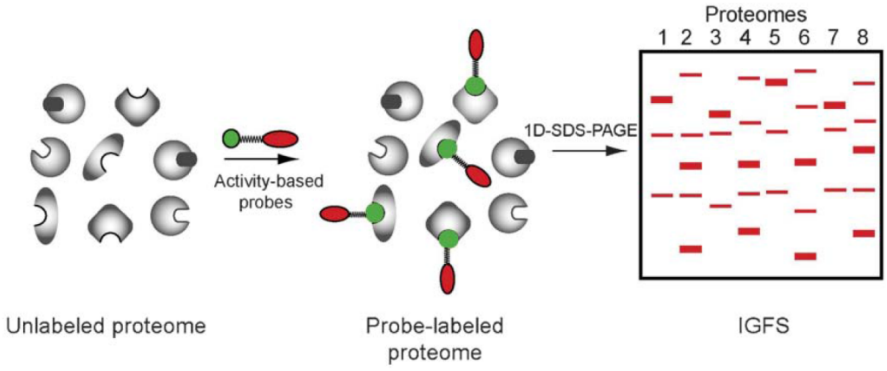

Figure 2. Activity-based protein profiling (ABPP) assays. ABPP probes label active, but not inactive (inhibitor-bound) enzymes in complex proteomes. Labeled enzymes are detected by in-gel fluorescence scanning and subsequently identified by their respective molecular weights (Sieber and Cravatt 2006).

7. Histology and immunohistochemistry analysis

7.1. Mice sacrifice and tissue processing

Mice were anesthetized with ketamine/xylazine (80/10 mg/Kg, i.p; Imalgene®/Rompun®) and transcardially perfused with saline solution followed by 4% paraformaldehyde in 0.1 M PB (pH 7.4). After extraction, brains and spinal cords were postfixed for 3 h in 4% paraformaldehyde, cryoprotected overnight in 20% sucrose at 4°C, embedded in Tissue-Tek OCT (Electron Microscopy Sciences, Hatfield, PA, USA) and stored at -80°C. Coronal or longitudinal sections (10 µm-thick) were obtained from brains and lumbar spinal cords, respectively, using a CM3050S cryostat (Leica) and stored at -20°C until use. Alternatively, postfixed brains were stored at 4°C in 0.1 M PB containing 0.02% sodium azide for vibratome slicing.

7.2. Histology

Coronal brain sections from cuprizone-treated mice (1 and -1 bregma; Paxinos and Franklin, 2012) and lumbar spinal cord longitudinal sections from EAE mice containing dorsal and lateral white matter were stained for myelin and inflammatory infiltrates using Luxol Fast Blue (LFB) and Nissl standard protocols. For LFB staining, brain sections were treated overnight in a solution containing ethanol at 95%, 0.5% glacial acetic acid and 0.1% LFB solvent 38 (Sigma-Aldrich) at 37-42°C, and then differentiated with a 0.01% lithium carbonate solution (Sigma-Aldrich). Tissues were dehydrated by passing them through a series of increasing alcohol concentrations (50%-100%) and mounted in DPX (Sigma-Aldrich). For Nissl staining, spinal cord sections were processed with xylene, rehydrated in series of decreasing ethanol concentrations and stained with a 1% toluidine blue solution in distilled water for 1 min. Samples were then washed with distilled water, dehydrated again in series of increasing alcohol concentrations and mounted in DPX.

7.3. Immunofluorescence and immunoperoxidase staining

Tissue sections were rinsed and blocked for 60 min in TBS (pH 7.4) supplemented with 5% NGS and 0.2% Triton X-100 following by overnight incubation at 4°C with mouse anti-MBP (1:1000; Covance, Princeton, NJ, USA), mouse anti-GFAP (1:40; Merck Millipore), rabbit anti-NG2 (1:200; Merck Millipore) or rat anti-CD11b (1:100; Merck Millipore). Following extensive washing, primary

antibodies were detected by incubation with Alexa Fluor 488 or 594 conjugated goat antibodies (1:400; Invitrogen, Carlsbad, CA, USA) for 1 h at RT. Hoechst 33258 (5 µg/mL; Sigma-Aldrich) was used for chromatin staining. Sections were mounted in Glycergel (Dako, Carpinteria, CA, USA) mounting medium.

For immunoperoxidase staining, brain sections were pre-incubated in 1% H_2O_2 for 10 min at RT. After several washes in TBS, slices were blocked for 30 min in 10% BSA, 0.1% sodium azide and 0.002% saponin in TBS, and subsequently incubated for 3 days at 4°C with rabbit anti-ABHD6 (1:250; kindly provided by J Mark Brown, Cleveland Clinic Lerner Research Institute, Cleveland, OH, USA). For primary antibody detection, tissue was incubated with biotinylated anti-rabbit IgG made in horse (1:200; Vector Laboratories, Burlingame, CA, USA) and treated with avidin biotinylated horseradish peroxidase complex (ABC; Elite, Vector Laboratories). Immunoperoxidase reaction was developed using DAB. Samples were washed with distilled water, dehydrated and mounted in DPX. Immunostaining controls were routinely performed with incubations in which primary antibodies were not included.

7.4. Image analysis

Optical images from tissue sections processed in parallel were acquired in the same session using a Zeiss Axioplan 2 microscope coupled to an Axiocam MRc5 digital camera (Zeiss, Oberkochen, Germany). Demyelination, glial reaction and ABHD6 expression in the cuprizone model were evaluated by examination of two digital 40X objective pictures from each coronal slice including the middle line of the corpus callosum. The extent of myelin damage was determined by scoring of LFB and MBP stained sections using a 4-point scale ranging from 4 (normal myelin) to 0 (complete demyelination). Analysis of the number of inflammatory infiltrates in spinal cord white matter was carried out by examination of 45-50 consecutive 20X objective optical sections per tissue section. $CD11b^+$ microglia/macrophages were quantified in lateral white matter by cell counting of 15-20 semiconsecutive optical sections per tissue slice obtained using a 40X objective.

Analysis of immunostained sections was carried out using microscope fluorescence intensity settings at which the control sections without primary antibody gave no signal. Immunoreactivity of glial cells was quantified using Image J Software. Threshold analysis of ABHD6 and GFAP immunostained area was carried out in 16-bit grey scale transformed pictures and the values were referred to the total corpus callosum area in each optical section. $CD11b^+$ cells were quantified by cell counting and data expressed as mean cell number per square millimetre (mm^2) of corpus callosum area. All histological analyses were carried out in at least 4 mice per group.

8. Gene expression analysis

Mice were anesthetized with ketamine/xylazine (80/10 mg/Kg, i.p; Imalgene®/Rompun®) and transcardially perfused with cold saline solution for 30 s. A single coronal slice was trimmed between levels +1 and -1 or levels +1.1 and +0.2 bregma (Paxinos and Franklin, 2012) from cuprizone-treated or EAE mice, respectively, using a David Kopf Instruments brain blocker (Tujunga, CA, USA). After extraction, brain and spinal cord tissue was protected in RNAlater solution (Qiagen, Hilden, Germany) and stored at -80°C until use.

Total RNA was extracted from tissue samples and cultures using RNeasy Protect Mini Kit (Qiagen) and Absolutely RNA Miniprep Kit (Agilent, Santa Clara, CA, USA), respectively. First strand cDNA synthesis was carried out with reverse transcriptase Superscript™ III (Invitrogen) using random primers. Specific primers targeted to exon junctions to avoid amplification of contaminating genomic DNA were designed with the Primer Express software (Applied Biosystems,

Foster City, CA, USA). Primer sequences were as follows: mouse and rat *Abhd6* forward 5′-ACC GGA AAT TGT TTT TGG AAA TC-3′ and reverse 5′-GCT AAT ATG TCT GCC CCC GA-3´; mouse *Iba1* forward 5′-GCA GGA AGA GAG GCT GGA GGG GAT C-3′ and reverse 5′-CTC TTA GCT CTA GGT GGG TCT TGG G-3; mouse *IL1β* forward 5′- GAG AGT GTG GAT CCC AAG CAA TAC- 3′and reverse 5′-GAC AAA CCG TTT TTC CAT CTT CTT-3´; mouse *TNFα* forward 5′-GCC TCT TCT CAT TCC TGC TTG TGG CAG-3′and reverse 5′- GAC GTG GGC TAC AGG CTT GTC ACT CG-3´; mouse *COX2* forward 5′-GGG AGT CTG GAA CAT TGT GAA-3′and reverse 5′- GCA CAT TGT AAG TAG GTG GAC TGT-3´; rat *Gapdh* forward 5′-GAA GGT CGG TGT CAA CGG ATT T-3′ and reverse 5′- CAA TGT CCA CTT TGT CAC AAG AGA A-3´; rat *Hprt1* forward 5′-ATG GAC TGA TTA TGG ACA GGA CTG A-3′ and reverse 5′-ACA CAG AGG GCC ACA ATG TG-3´; mouse *Gapdh* forward 5′-TGC AGT GCC AGC CTC GTC -3′and reverse 5′-GCC ACT GCA AAT GGC AGC-3´; mouse *Hprt1* forward 5′- TAC TGT AAT GAT CAG TCA ACG GGG-3′ and reverse 5′-GTT GAG AGA TCA TCT CCA CCA ATA AC- 3´. Real-time qPCR was performed using SsoFastTM EvaGreen Supermix which contains dNTPs, Sso7d fusion polymerase, $MgCl_2$, EvaGreen dye and stabilizers (Bio-Rad). Amplifications were run in a CFX96TM Real Time System (Bio-Rad). The target mRNA quantity in each sample was determined from the relative standard curve and expressed in arbitrary units corresponding to the dilution factors of the standard RNA preparation or using $2^{-\Delta\Delta Ct}$ algorithm. Values were adjusted to *Gapdh* and *Hprt1* levels as endogenous references.

9. Autoradiography

Anesthetized mice (IsoVet®) were killed by decapitation and the brains rapidly removed and stored at -80°C. Autoradiographic assays were carried out in 20 µm-thick sagittal sections cut in a CM3050S cryostat (Leica). For CB_1 receptor autoradiography slides were preincubated for 30 min at RT in a buffer containing 50 mM Tris-HCl with 1% BSA (pH 7.4) and subsequently incubated (2 h, 37°C) in the same buffer containing 3 nM [^{3}H](−)-cis-3-[2-Hydroxy-4-(1,1-dimethylheptyl) phenyl]-trans-4-(3-hydroxypropyl)cyclohexanol ([^{3}H]CP55,940; 150.2 Ci/mmol; ARC, San Louis, MA, USA). Nonspecific binding was determined in adjacent sections by co-incubation with 10 µM CP55,940. Unbound radioligand was removed by washing in 50 mM Tris-HCl containing 1% BSA (pH 7.4). After drying, autoradiograms were generated by apposing the tissues for 21 days at 4°C to ^{3}H-sensitive films (Kodak BioMax MR, Sigma-Aldrich). For cannabinoid agonist-stimulated [^{35}S]GTPγS autoradiography, sections were pre-incubated twice for 30 min at 30°C in a buffer containing 50 mM HEPES, 0.2 mM EGTA, 3 mM $MgCl_2$, 100 mM NaCl and 0.5% BSA (pH 7.4), to eliminate endogenous ligands. Sections were incubated for 120 min in the same buffer with 1 mM DTT, 2 mM GDP, 3 mU/mL adenosine deaminase and 0.04 nM [^{35}S]GTPγS (1250 Ci/mmol; Perkin Elmer, Waltham, MA, USA). Consecutive tissue sections were incubated with 1 µM of the cannabinoid receptor agonist WIN55,212-2. Nonspecific binding was determined in the presence of 10 µM guanosine- 5-O-(3-thio) triphosphate (GTPγS). Sections were then washed in 50 mM Tris-HCl (pH 7.4), rinsed, dried and exposed to ^{14}C-sensitive films (Amersham Systems, GE Healthcare Europe GmbH) with ^{14}C-polymer standards (Amersham Systems) for 2 days at 4°C. Autoradiograms were scanned and analyzed using Image J Software.

10. Western blot analysis

Mice were anesthetized with ketamine/xylazine (80/10 mg/Kg, i.p; Imalgene®/Rompun®) and transcardially perfused for 30 s with cold saline solution. Coronal brain slices between levels +1 and -1 or levels +1.1 and +0.2 bregma (Paxinos and Franklin, 2012) were trimmed using a David Kopf Instruments brain blocker and stored at -80˚C until use. Tissue was homogenized with a douncer and sonicated in 200 µl of RIPA containing a protease inhibitor cocktail (Complete, Mini EDTA-free tablets, Roche, Mannheim, Germany). Tissue homogenates were centrifuged at 4°C for 10 min at

12,000 rpm and protein content in the supernatant was quantified with the Bio-Rad Protein Assay (Bio-Rad). Tissue extracts (10 µg) were subjected to 10% SDS-PAGE and proteins were electroblotted to nitrocellulose membranes (Hybond ECL, GE Healthcare Europe GmbH, Barcelona, Spain). After blocking in 0.05% Tween/TBS (TBST) containing 5% BSA and 1% NGS for 1 h at RT, membranes were incubated overnight at 4˚C with rabbit anti-ABHD6 antibody (1:500; kindly provided by Dr J Mark Brown), rabbit anti-MBP (1:5000; Merck Millipore) and rabbit anti-β-actin (1:5000; Sigma-Aldrich) in blocking solution. After washing, membranes were incubated with horseradish peroxidase-conjugated secondary antibodies (1:5000; Sigma-Aldrich) and developed using enhanced chemiluminiscence according to the manufacturer's instructions (Super Signal West Dura, Pierce, Rockford, IL, USA). The protein bands were detected with a ChemiDoc™ XRS Imaging System (Bio-Rad). Signals were quantified using Image-J Software and values normalized to β-actin signal.

11. Oligodendrocyte cultures

Primary mixed glial cultures were prepared from newborn (P0-P2) Sprague-Dawley rats according to previously described procedures (McCarthy and de Vellis 1980). Briefly, forebrains were removed from the skulls and the cortices isolated and digested by incubation (15 min, 37°C) in HBSS 0.25% trypsin and 4% DNAse. Cells were dissociated by passage through needles (21 G and 23 G), centrifuged and resuspended in Iscove's modified Dulbecco's medium (Thermo Fisher Scientific) supplemented with 10% FBS (HyClone™, Thermo Fisher Scientific, Waltham, MA, USA) and antibiotic/antimycotic solution. Cells were seeded into poly-D-lysine- coated 75 cm^2 flasks, and maintained in culture at 37°C and 5% CO_2. After 10-15 days in culture, the flasks were shaken (400 rpm) for 2 h at 37°C to remove loosely adherent microglia. The remaining OPCs present on top of the confluent monolayer of astrocytes were dislodged by shaking overnight at 400 rpm. The cell suspension was then filtered through a 10 µm nylon mesh and preplated on bacterial grade Petri dishes for 2 h. The non-adherent OPCs that remained in suspension were recovered and plated again on bacterial grade Petri dishes for 1 h. The resulting OPC suspension was centrifuged and resuspended in a chemically defined Dulbecco's modified eagle's medium (Thermo Fisher Scientific) that contained 100 µg/mL transferrin, 60 ng/mL progesterone, 40 ng/ mL sodium selenite, 5 µg/mL insulin, 16 µg/mL putrescine and 100 µg/ mL BSA. For excitotoxicity experiments, cells were plated in poly-D-lysine-coated 48-well culture dishes at a density of 8×10^3 cells/well. Alternatively, OPCs were plated onto poly-D-lysine-coated glass coverslips in 24-well culture dishes at a density of 4×10^4 cells/well or 10^5 cells/well for western blot and qPCR analysis, respectively. Cells were cultured in the presence of the mitogenic factors PDGF-AA (5 ng/mL) and bFGF (5 ng/mL) for 2 days to expand their number and prevent their differentiation. The purity of the cultures was routinely assessed by examining cell morphologies under phase contrast microscopy and was confirmed by immunolabeling with cell-type specific antibodies against Olig-2 (1:1000; Merck Millipore); PDGFRα (1:200; Santa Cruz Bio technology); GFAP (1:80; Merck Millipore) or Iba-1 (1:2000; Wako, Richmond, VA, USA). After 2 days in culture Olig-2^+ cells represented 95 ± 0.2% of total cells, with the remaining cells being identified as $GFAP^+$ astrocytes or Iba-1^+ microglia (*n* = 7 cultures, 4 coverslips per culture; 15 microscopic fields per coverslip). In the same cultures, PDGFRα^+ oligodendrocyte progenitors represented 92.5 ± 0.5% of total cells. For excitotoxicity experiments, OPCs were allowed to differentiate for 1-2 days in fresh medium lacking mitogenic factors and supplemented with the differentiating factors triiodothyronine (T3; 30 ng/mL), ciliary neurotrophic factor (CNTF; 10 ng/mL) and neurotrophin-3 (NT-3; 1 ng/mL).

12. Oligodendrocyte toxicity assays

Oligodendrocytes were pre-incubated for 30 min with drugs or vehicle [DMSO 0.1-0.2% (v/v) final concentration] and exposed to AMPA plus cyclothiazide (10 µM: 100 µM; Abcam, Cambridge, UK) for 15 min. The medium was subsequently replaced and cells were incubated overnight in the presence of the ABHD6 inhibitor KT182 or the MAGL inhibitor JZL184 (Cayman Chemical). Oligodendrocyte viability was determined 24 h after the excitotoxic stimulus using 3-(4,5-dimethylthiazol-2-yl)-2,5-diphenyltetrazolium bromide (MTT; CellTiter 96® on-Radioactive Cell Proliferation Assay, Promega, Madison, WI, USA). Colored formazan product was determined photometrically at 570 nm in a Synergy-HT fluorimeter (Bio-Tek Instruments, Winooski, VT, USA). At least 3 independent experiments in triplicate were performed for each condition.

13. Oligodendrocyte differentiation assays

OPC differentiation was promoted switching the cultures to fresh medium lacking mitogenic factors and supplemented with the differentiating factors T3 (30 ng/mL), CNTF (10 ng/mL) and NT-3 (1 ng/mL), in the presence or absence of KT182 and JZL 184. Drugs were replenished in the cultures every day. Differentiation was assessed measuring expression levels of the oligodendrocyte differentiation marker MBP by western blot. Cells were harvested in 40 µL ice-cold electrophoresis sample buffer and were subjected to 10% SDS-PAGE as described above. Data are representative of at least 3 independent experiments.

14. Neuron cultures

Primary neuron cultures were obtained from Sprague-Dawley rat E18 embryos as described previously (Ruiz et al. 2014). Pregnant rats were anesthetized by isoflurane (IsoVet®) and killed by decapitation, embryos were extracted and placed in a Petri dish on ice containing HBSS (without Ca^{2+} and Mg^{2+} and supplemented by 10 mM glucose and 10 mM glycine). The brains were extracted and the cortex isolated carefully, ensuring elimination of blood vessels and meninges. Cortices were collected and incubated in the presence of 4% trypsin and 0.25% DNAse for 5 minutes at 37ºC and 5% CO_2. Enzymatic activity was stopped by addition of 4 mL Neurobasal medium (NB; Gibco-Thermo Fisher Scientific) supplemented with 0.02% B-27 (Gibco-Thermo Fisher Scientific), 0.01% Penicillin-streptomycin-fungizone (Sigma-Aldrich), 0.002% glutamine and 10% FBS (Gibco-Thermo Fisher Scientific). Following centrifugation (200 G, 5 min), the pellet was resuspended in 1 mL of NB+FBS and cells dissociated by passage through needles (21 G and 23 G). Cell suspension was passed through a 40 µm nylon filter (Millipore) and seeded onto poly-L-ornithine-coated 48-well plates at 1×10^5 cells per well. For confocal single-cell imaging experiments, cells were plated onto glassbottom m-dishes (Ibidi GmbH, Planegg/Martinsried, Germany). The medium was replaced by serum-free, B27-supplemented Neurobasal medium 24 h later. The cultures were essentially free of astrocytes and microglia and were maintained at 37°C and 5% CO_2. For mitochondrial calcium imaging, cells were transfected with a plasmid expressing the mitochondria-targeted 2mtD4cpv calcium probe kindly provided by Roger Tsien (University of California, La Jolla, CA, USA). For transfection 4×10^6 rat neurons were electroporated in suspension before plating with 3 µg of cDNA using Rat Neuron Nucleofector Kit (Lonza, Basel, Switzerland) according to the manufacturer instructions and plated and maintained as described above. Cultures were used at 8-9 days *in vitro*.

15. Neuronal toxicity assays

Neurons were exposed to N-methyl-D-aspartate (NMDA, 100 µM; Sigma-Aldrich) for 15 minutes at 37°C in Ca^{2+}- and Mg^{2+}-free HBSS containing 10 mM glucose, 2.6 mM $CaCl_2$ and 10 mM glycine. Drugs were present 30 min before and during the excitotoxic insult. The medium was subsequently replaced by B27-supplemented NB medium. Cell viability was assessed 24 h later using Citotox 96 colorimetric assay (Promega, Madison, WI, USA) which measures the activity of lactate dehydrogenase (LDH) and its capacity to convert tetrazolium salt into a red formazan product. This colorimetric reaction was measured at 490 nm using a Synergy-HT fluorimeter (Bio-Tek Instruments). All experiments were performed in triplicate and the values provided correspond to at least four independent assays.

16. Mitochondrial Ca^{2+} imaging

For the analysis of mitochondrial calcium responses, neurons transfected with the mitochondria targeted 2mtD4cpv calcium indicator (Palmer et al. 2006) were transferred to HBSS containing 20 mM HEPES, 10 mM glucose, 2.6 mM $CaCl_2$ and 10 mM glycine (pH 7.4) and imaged by a TCS SP8X confocal microscope (Leica). Cells were excited at 458 nm and cfp and yfp emission acquired for FRET ratio quantification at an acquisition rate of one frame/15 s for 5 min. For data analysis, a homogeneous population of 5-12 cells was selected in the field of view and neuronal somata selected as region of interest (ROI). Background values were always subtracted and data are expressed as $R/R_0 \pm$ S.E.M. (%) in which R represents the yfp/cpf fluorescence ratio for a given time point and R_0 represents the mean of the resting FRET ratio. Results for statistical comparison were calculated as area under the curve (AUC) of the response for each cell from the start of NMDA application.

17. Data analysis and statistics

Data are presented as mean ± standard error of mean (S.E.M.) and *n* represents the number of animals or cultures tested. Statistical analyses were performed using GraphPad Prism 6 for Windows, version 5.0 (GraphPad Software Inc. San Diego, CA, USA). Time courses of EAE scores were analyzed using the unpaired Mann-Whitney *U*-test. Non-time course score data, histological and biochemical results were analyzed by unpaired Student's *t*-tests or with Mann Whitney *U*-tests following application of normality tests. In all instances, p values < 0.05 were considered statistically significant.

Results - Objective 1

RESULTS - OBJECTIVE 1

1. Ultrastructural localization of CB_1 receptors in oligodendrocyte precursor cells

To study the localization of CB_1 receptors in OPCs we set up a double pre-embedding immunogold and immunoperoxidase method allowing for the simultaneous detection of NG2 positive profiles and CB_1 proteins at the EM level. To better identify NG2 positive structures by EM we took advantage of knockin mice expressing EYFP under the control of the *NG2* gene promoter (Karram et al. 2008). Characterization of these mice has demonstrated that almost all EYFP expressing cells in both grey and white matter express the transcription factors Olig2 and Sox10, as expected for immature oligodendrocyte lineage cells, but do not express proteins and transcription factors that exclusively mark mature oligodendrocytes. Mice heterozygous for NG2-EYFP were crossed with $CB_1^{+/-}$ mice to generate NG2-$EYFP^{+/-}$-$CB_1^{+/+}$ and NG2-$EYFP^{+/-}$-$CB_1^{-/-}$ double mutants. In these mice, OPC processes were identified by DAB immunodeposits of EYFP and the CB_1 receptor was detected by silver-intensified immunogold labelling (**Figure 1A**).

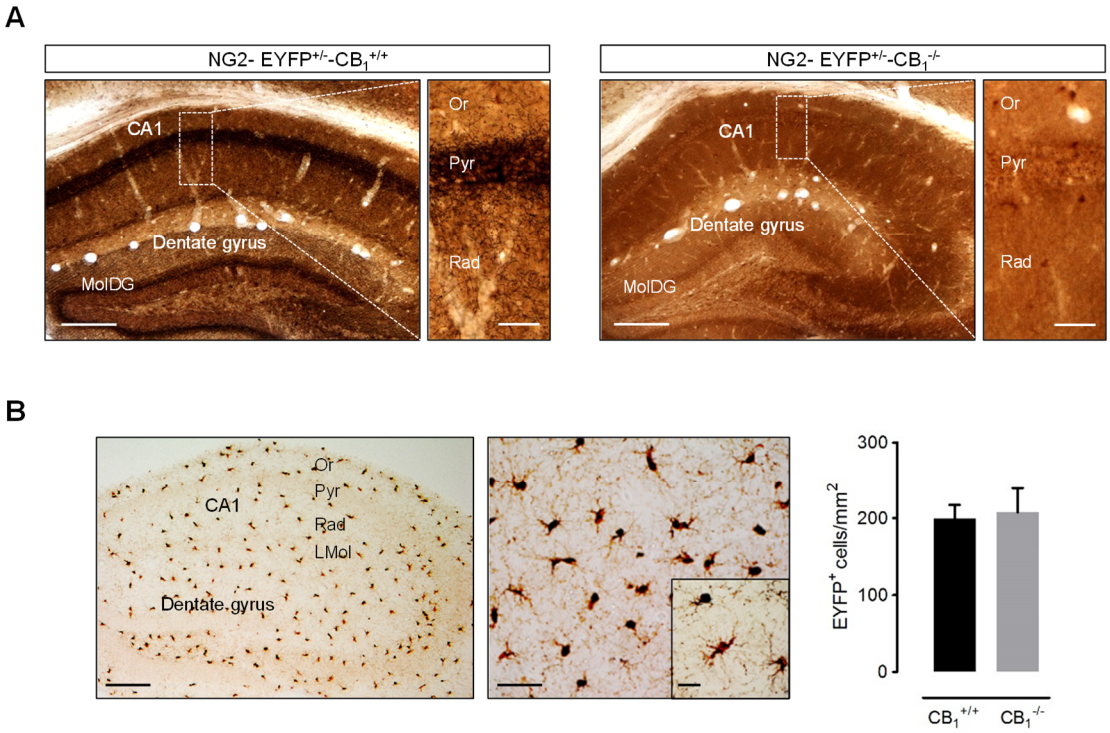

Figure 1. Localization of the CB_1 receptor protein in the hippocampus of NG2-$EYFP^{+/-}$-$CB_1^{+/+}$ mutant mice. (**A**) Representative images show pre-embedding silver intensified immunogold labeling of CB_1 receptors and immunoperoxidase labeling EYFP in coronal brain sections from NG2-$EYFP^{+/-}$-$CB_1^{+/+}$ and NG2-$EYFP^{+/-}$-$CB_1^{-/-}$ mice. Intense bands of CB_1 receptor immunostaining are observed in the stratum Pyr and MoDG. Detailed magnification images show dense CB_1 receptor neuropil labeling throughout CA1 Rad. The hippocampus of a NG2-$EYFP^{+/-}$-$CB_1^{-/-}$ mice shows no immunopositive profiles, demonstrating antibody specificity. (**B**) Immunoperoxidase labeling of EYFP in the hippocampus of NG2-$EYFP^{+/-}$-$CB_1^{+/+}$ mutant mice showing the typical distribution and morphology of NG2 cells in this brain area. Quantitative analysis of DAB immunostaining in CA1 *stratum radiatum* revealed no differences in the number of EYFP positive cells in NG2-$EYFP^{+/-}$ mice lacking CB_1 receptors (*n* = 3 mice per group). CA1, region 1 of *cornu ammonis*; Or, *stratum oriens*; Pyr, *stratum pyramidale*; Rad, *stratum radiatum*; MoDG, molecular dentate gyrus. Scale bars: 200 µm and 25 µm (**A**); 200 µm, 50 µm and 25 µm (**B**).

The pattern of CB_1 receptor immunostaining was first verified in adult NG2-EYFP$^{+/-}$-$CB_1^{+/+}$ mice (P60) by light microscopy evaluation of coronal sections containing the hippocampus. In good agreement to previous studies addressing the localization of CB_1 receptors in this brain area (Gutiérrez-Rodríguez et al. 2017; Hájos et al. 2000), we detected intense immunoreactivity for CB_1 receptors in a fibrous pattern throughout the hippocampal CA1 and CA3 subfields and the dentate gyrus (**Figure 1A**). The distribution of CB_1 receptor immunostaining followed the layered structure of the hippocampus, showing the highest density in the inner molecular layer of the dentate gyrus, the pyramidal cell layer and the *stratum radiatum* of the CA1 and CA3 subfields. The specificity of these signals was confirmed by their virtual disappearance in tissue sections from NG2-EYFP$^{+/-}$-$CB_1^{-/-}$ mice (**Figure 1A**). On the other hand, the overall DAB pattern in NG2-EYFP$^{+/-}$-$CB_1^{+/+}$ matched the known uniform distribution of NG2 cells in the rodent hippocampus (Karram et al. 2008). Importantly, NG2-EYFP$^{+/-}$-$CB_1^{-/-}$ mice lacking CB_1 receptor expression exhibited DAB positive cells in CA1 *stratum radiatum* similar in morphology and number to the cells in NG2-EYFP$^{+/-}$-$CB_1^{+/+}$ mice (**Figure 1A** and **B**).

At the ultrastructural level, presynaptic inhibitory terminals making symmetric synapses with postsynaptic dendrites within CA1 *stratum radiatum* of NG2-EYFP$^{+/-}$-$CB_1^{+/+}$ mice were decorated with high density of CB_1 receptor immunoparticles (Gutiérrez-Rodríguez et al. 2017; Hájos et al. 2000) (**Figure 2C**). As expected, much less labelling was observed in excitatory terminals identified by their typical ultrastructural features, namely, axon boutons with abundant synaptic vesicles forming asymmetric synapses with postsynaptic dendritic spines (**Figure 2C**). Once again, this CB_1 receptor distribution profile disappeared in NG2-EYFP$^{+/-}$-$CB_1^{-/-}$ mice, corroborating the specificity of the CB_1 receptor antibody used.

OPCs and their processes were identified at the EM level by the presence of electron dense DAB precipitates in their cytoplasm (**Figure 2A**). The percentage of CB_1 receptor immunopositive OPC processes in CA1 *stratum radiatum* of NG2-EYFP$^{+/-}$-$CB_1^{+/+}$ mice was 10.5 ± 0.72% (**Figure 2B**). This proportion decreased to 4.4 ± 0.40% in NG2-EYFP$^{+/-}$-$CB_1^{-/-}$ mice (***$p < 0.0001$; **Figure 2B**). Comparison between both genotypes suggested that, at least, 6% of OPCs from the hippocampal *stratum radiatum* of adult mice express CB_1 receptors.

The density of CB_1 receptor gold particles on DAB positive profiles was also analyzed and compared to values calculated for synaptic terminals of NG2-EYFP$^{+/-}$-$CB_1^{+/+}$ animals. CB_1 receptor immunopositive OPC profiles of the CA1 *stratum radiatum* exhibited CB_1 receptor metal particles at a density of 0.2 particles/µm on their plasma membranes (**Figure 2D**). Noteworthy, the density of CB_1 receptors was significantly lower in OPC processes than in excitatory terminals making asymmetric synapses within the same brain area (**$p < 0.01$) (**Figure 2D**). Altogether, these results suggest that, in the adult hippocampal formation, grey matter OPCs exhibit very low levels of CB_1 receptors as compared to synaptic profiles.

2. Ultrastructural localization of CB_1 receptors in myelinating oligodendrocytes

To study the localization of CB_1 receptors in mature oligodendrocytes we applied a silver intensified preembedding immunogold method to brain sections from $CB_1^{+/+}$ and $CB_1^{-/-}$ mice containing the corpus callosum and the hippocampal formation. As described above for NG2-EYFP$^{+/-}$-$CB_1^{+/+}$ mutants, the overall CB_1 receptor pattern in the hippocampal formation of wild-type animals matched the well-known distribution of the receptor protein in this brain area (**Figure 3A**). The CB_1 receptor immunostaining was absent in the CB_1 knockout hippocampus, confirming the specificity of the antibody used in these experiments (**Figure 3A**).

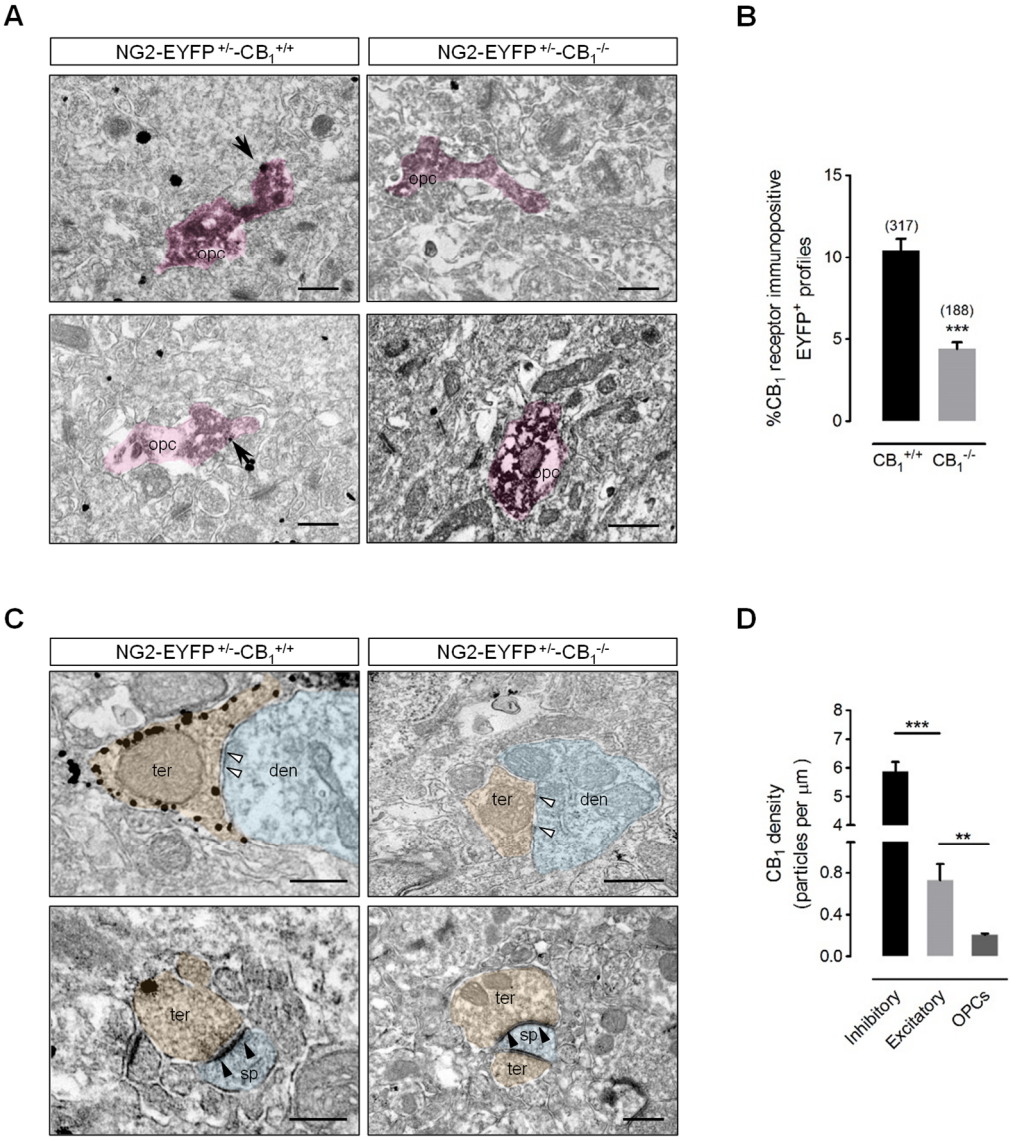

Figure 2. Localization of CB_1 receptors in oligodendrocyte precursor cells of the mouse hippocampus. (**A**) Representative electron micrographs showing pre-embedding silver intensified immunogold labeling of CB_1 receptors and immunoperoxidase labeling of EYFP in coronal brain sections from adult NG2-EYFP$^{+/-}$ mice. CB_1 receptor gold particles were localized on plasma membranes of OPC processes (black arrows). Scale bars: 500 nm. (**B**) Quantification of CB_1 receptor immunopositive OPC profiles in NG2-EYFP$^{+/-}$ mutant mice. The proportion of DAB positive profiles expressing CB_1 receptor metal particles was significantly lower in NG2-EYFP$^{+/-}$-$CB_1^{-/-}$ mice (n = 5 mice per group), demonstrating the specificity of receptor immunostaining. The numbers in parentheses on the top of each column indicate the number of OPC processes analyzed. (**C**) Distribution of CB_1 receptors in synaptic terminals of NG2-EYFP$^{+/-}$ mice. Scale bars: 500 nm. White arrowheads, inhibitory synapses; black arrowheads, excitatory synapses; den, dendrite (blue); opc, oligodendrocyte progenitor (pink); sp, dendritic spine (blue); ter, terminal (orange). (**D**) CB_1 receptor density (particles/µm plasma membrane) was quantified in receptor positive-OPC profiles, -inhibitory and -excitatory terminals in the *stratum radiatum* of NG2-EYFP$^{+/-}$-$CB_1^{+/+}$ mice (n = 3-5 mice per group). $^{**}p < 0.01$ and $^{***}p < 0.001$, Student´s *t*-tests.

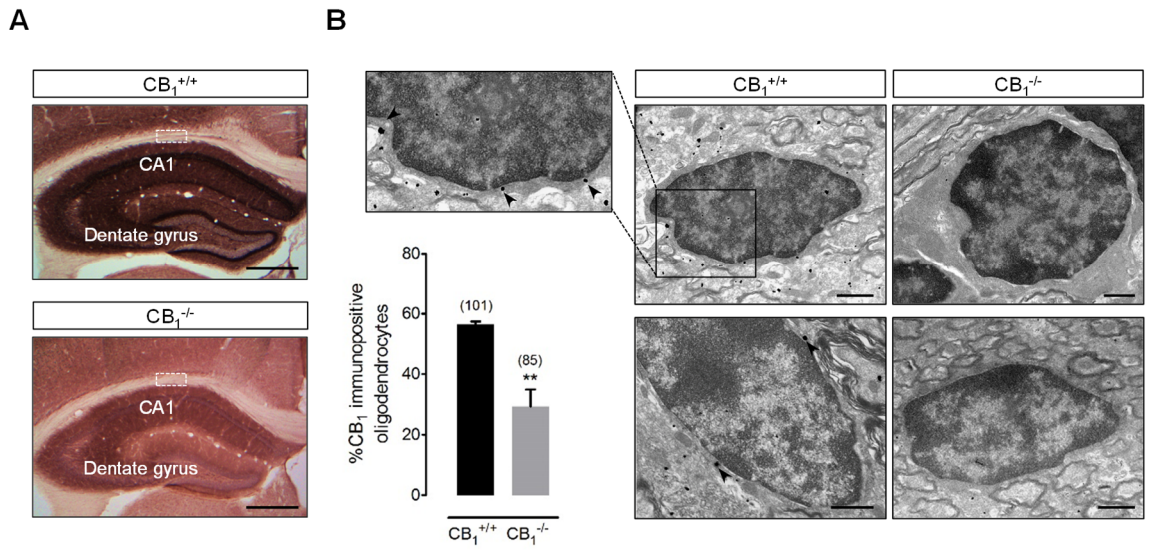

Figure 3. CB_1 receptor expression in myelinating oligodendrocytes of the mouse brain. (**A**) Specificity of CB_1 receptor immunostaining procedures for EM visualization of mature oligodendrocytes. A pre-embedding silver intensified immunogold method for the detection of CB_1 receptors was applied to coronal brain sections from wild-type ($CB_1^{+/+}$) and CB_1 receptor knockout ($CB_1^{-/-}$) mice at P60. Images depict the characteristic CB_1 receptor immunolabeling pattern in the mouse hippocampus that disappears in $CB_1^{-/-}$ mice. Dotted squares show the subcortical white matter area selected for EM analysis. Scale bars: 200 µm. (**B**) CB_1 receptor localization in identified oligodendrocytes within the subcortical white matter. CB_1 receptor gold particles were localized on plasma membranes of oligodendrocyte somata (black arrowheads). The proportion of CB_1 receptor gold particles in oligodendrocytes was significantly lower in $CB_1^{-/-}$ mice (n = 3 mice per group). The numbers of oligodendrocytes analyzed are indicated in parentheses on the top of each column. $^{**}p < 0.01$; Student´s t-test. Scale bars: 1 µm.

Following verification of CB_1 receptor immunostaining by light microscopy, we selected a defined area of the subcortical white matter adjacent to the hippocampal CA1 subfield for further ultrathin sectioning and quantitative EM analysis (**Figure 3A**). Mature oligodendrocytes within the subcortical white matter were identified by their distinctive morphological features, such as electron-dense nuclei with pronounced aggregates of heterochromatin and the usual presence of thin rims of perinuclear cytoplasm, and CB_1 receptor was detected by immunogold labelling. The proportion of oligodendrocytes exhibiting positive CB_1 receptor metal particles on their somatic membranes was 56.4 ± 0.9% in wild-type mice (**Figure 3B**). This proportion decreased to 29.3 ± 5.7% in CB_1 receptor null mice ($^{**}p < 0.01$). Comparison between both genotypes suggested that at least 27% of myelinating oligodendrocytes in the subcortical white matter of adult mice express CB_1 receptor on their somatic plasma membranes (**Figure 3B**).

3. Analysis of myelin ultrastructure in CB_1 receptor knockout mice

Mice lacking CB_1 receptors have been widely used for CNS studies and myelin abnormalities have not been reported. The fact that CB_1 receptor deficient mice do not exhibit severe myelin alterations suggest that this protein is not crucial for correct myelination *in vivo* or that there could be other compensatory factors for myelination that can counteract the loss of CB_1 receptors in adult mice. However, myelin ultrastructure has not been analyzed in detail in CB_1 receptor mutant mice.

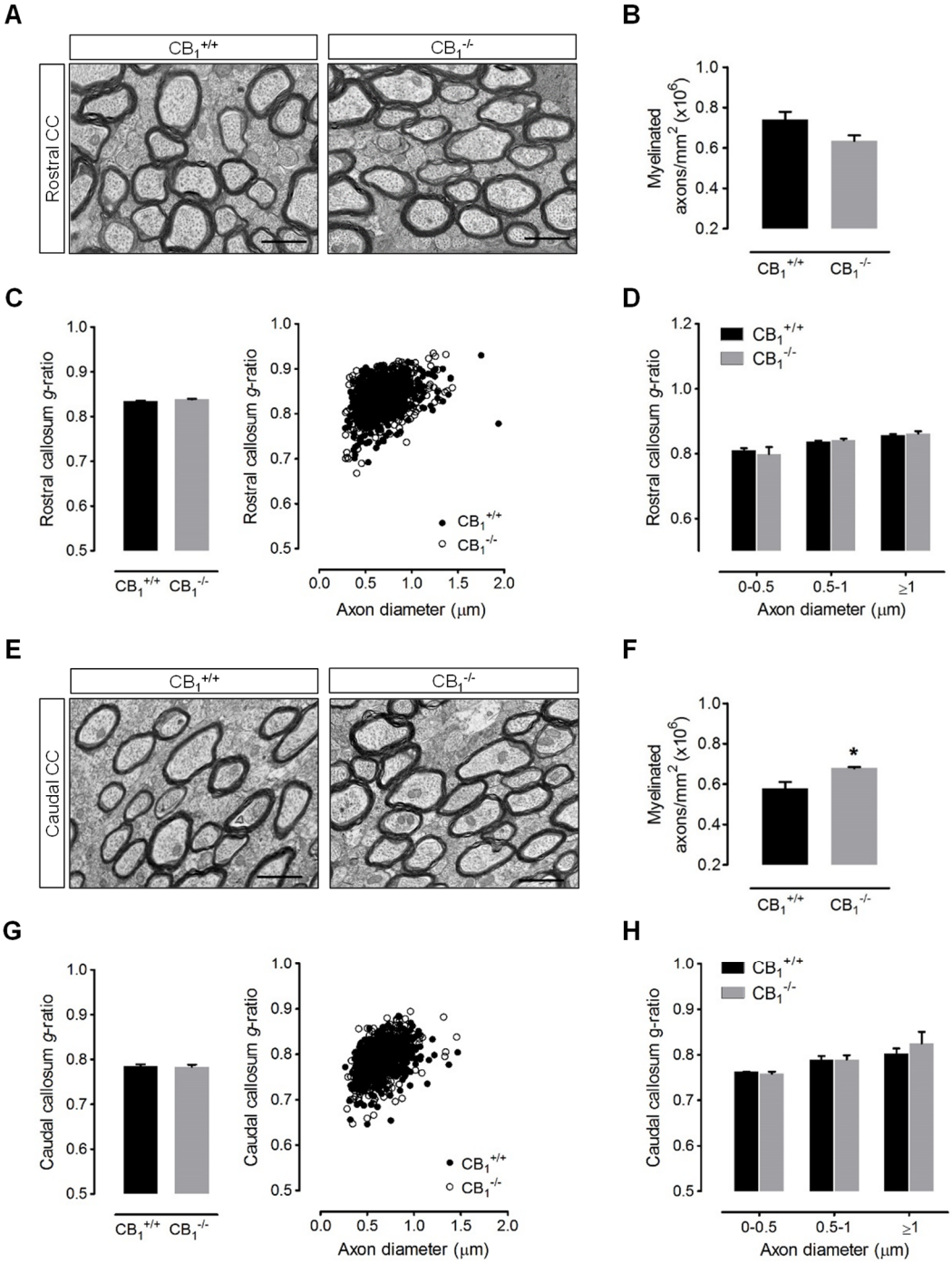

Figure 4. Electron microscopy analysis of corpus callosum myelin in CB_1 receptor knockout mice. (**A**, **E**) Representative electron micrographs show axon cross-sections in the wild-type and CB_1 knockout rostral and caudal corpus callosum at P30. Scale bars: 1 µm. (**B**, **F**) Density of myelinated axons in CB_1 knockout versus wild-type mice. Mice deficient in CB_1 receptors exhibited increased density of myelinated axons in caudal corpus callosum. (**C**, **G**) Mean *g*-ratios and plots showing the relation between *g*-ratio (y axis) and the corresponding diameter for all axons analyzed (x axis) in rostral and caudal corpus callosum. (**D**, **H**) Histograms of *g*-ratios classified as a function of axon diameter. CB_1 knockout mice did not exhibit changes in myelin caliber selectively affecting small or high caliber axons. A minimum of 827 and 103 axons per mouse were counted for assessing numbers of myelinated axons and *g*-ratios, respectively, in a total area of 1600 µm^2 (*n* = 3 mice per group). **p* < 0.05; Student´s *t*-test.

Therefore, the next aim of this work was to study possible abnormalities affecting myelin ultrastructure in $CB_1^{-/-}$ mice at the peak of myelination (P30). With this aim, we measured the myelin thickness (*g*-ratio) and the density of myelinated axons in randomly selected fields from rostral and caudal corpus callosum (**Figures 4A** and **E**). Myelinated axons in CB_1 receptor knockout brains exhibited *g*-ratio values similar to their wild-type littermates both in rostral (**Figures 4A** and **C**) and caudal (**Figures 4E** and **G**) corpus callosum. In the same sense, we did not observe significant alterations in *g*-ratio values between genotypes when binning axons by size to detect subtle alterations specifically affecting small or high caliber axons (**Figures 4D** and **H**). These results indicate that $CB_1^{-/-}$ mice do not show gross abnormalities affecting myelin thickness at this developmental stage. Finally, electron microscopy revealed that CB_1 knockout mice exhibit a subtle increase in the number of myelinated axons within caudal corpus callosum (**Figure 4F**). This observation supports the hypothesis that CB_1 receptors may regulate to some extent myelin formation and/or maintenance at the peak of myelination.

Results - Objective 2

RESULTS - OBJECTIVE 2

1. Effects of ABHD6 blockade in oligodendrocytes *in vitro*

1.1. ABHD6 blockade does not protect oligodendrocytes from excitotoxicity

Oligodendrocytes are highly vulnerable to excessive activation of glutamate receptors (Follett et al. 2000; Matute et al. 1997; McDonald et al. 1998) and converging lines of evidence suggest that glutamate-mediated excitotoxicity is a key etiopathogenic mechanism of demyelination in MS (Matute et al. 2001). Indeed, protection from oligodendrocyte excitotoxicity is a relevant mechanism for the beneficial effects associated to the inhibition of 2-AG hydrolytic enzyme MAGL in MS animal models (Bernal-Chico et al. 2015; Hernández-Torres et al. 2014). In this regard, previous results from our laboratory have shown that 2-AG engages CB_1 receptor mediated protective effects in cultured oligodendrocytes that are potentiated by pharmacological attenuation of MAGL activity (Bernal-Chico et al. 2015). Based on these results, we sought to investigate whether inhibition of an alternative 2-AG hydrolytic enzyme, namely ABHD6, modulates excitotoxicity to oligodendrocytes *in vitro*. We first corroborated the expression of ABHD6, among other 2-AG degrading enzymes, in cultured oligodendrocytes by qPCR analysis (**Figure 1A**). The ABHD6 inhibitor KT182 did not prevent oligodendrocyte death by activation of AMPA receptors at any of the concentrations tested (10 nM-1 μM) (**Figure 1B**). Confirming previous observations, MAGL inactivation with the selective inhibitor JZL184 effectively attenuated excitotoxicity in the same cultures (*$p < 0.05$ vs vehicle-treated cultures) (**Figure 1C**), thus corroborating the efficacy of 2-AG production and signaling machinery in our experimental conditions. These observations indicate that ABHD6 inactivation does not modulate excitotoxicity in oligodendrocytes *in vitro*.

1.2. ABHD6 inhibition does not promote oligodendrocyte maturation

Remyelination, which is usually a spontaneous endogenous process, is achieved when OPCs differentiate into myelin producing oligodendrocytes. Even though in MS brains OPCs are large in number, their differentiation capacity is limited in the context of this disease condition and enhancing the generation of myelin-producing cells has become major focus of MS research (Kremer et al. 2015). Noteworthy, blockade of MAGL accelerates differentiation of cultured OPCs by endogenously synthesized 2-AG (Gomez et al. 2010) and promotes remyelination *in vivo* (Feliú et al. 2017). Based on these studies, we next aimed at evaluating the efficacy of KT182 to induce differentiation of OPCs cultured from newborn rats. Basal differentiation of OPCs was induced by mitogen withdrawal and addition of thyroid hormone T3, CNTF and NT-3 for 48-96 h and confirmed by western blot analysis of the myelinating oligodendrocyte marker MBP (**Figure 1D**). Incubation with increasing concentrations of the ABHD6 inhibitor KT182 (10 nM-1 μM) failed to enhance the expression levels of MBP as determined by western blot analysis following 96 h of compound treatment (**Figure 1E**). In good agreement with previous reports (Gomez et al. 2010), the MAGL inhibitor JZL184 induced substantial differentiation of OPCs at this time point (*$p < 0.05$ vs vehicle-treated cultures) (**Figure 1E**). These results indicate that blockade of ABHD6 activity in OPCs is incapable of engaging maturation promoting mechanisms in these cells.

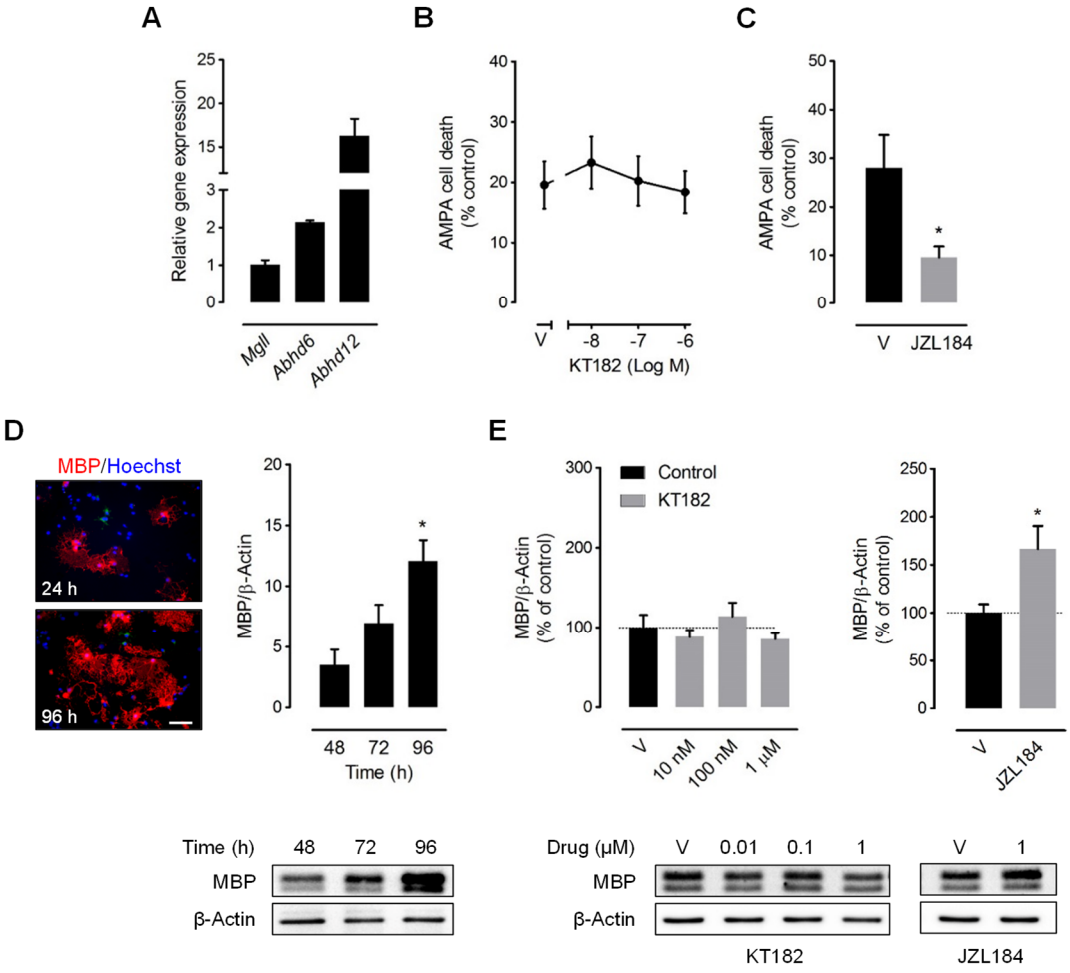

Figure 1. Effects of ABHD6 blockade in cultured oligodendrocytes. (**A**) *Abhd6*, *Abhd12* and *Mgll* expression levels in primary cultures of oligodendrocytes were determined by RT-qPCR (*n* = 3 cultures). Gene expression was normalized to *Gapdh* and presented relative to *Mgll.* (**B**, **C**) ABHD6 blockade did not prevent oligodendrocyte excitotoxicity. Graphs depict cell viability of oligodendrocytes exposed to AMPA plus cyclothiazide (10 µM:100 µM, 15 min) in the presence of the ABHD6 inhibitor KT182 (**B**) or the MAGL inhibitor JZL184 (**C**) (*n* = 4 cultures). (**D**, **E**) ABHD6 inactivation failed to promote OPC differentiation. (**D**) Western blot analysis of MBP expression in OPC cultures grown in the presence of T3,CNTF and NT-3 for 48-96 h (*n* = 3 cultures). Representative images of MBP immunolabeling in differentiating oligodendrocytes at different time points are shown. Scale bar: 50 µm. (**E**) Incubation of differentiating OPCs with the ABHD6 inhibitor KT182 did not increase the expression levels of MBP following 96 h of compound treatment at any of the concentrations tested (*n* = 3 cultures). Exposure to the MAGL inhibitor JZL184 for 96 h enhanced MBP expression in the same cultures. **p* < 0.05 versus OPC cultures differentiated for 48 h (**C**) or versus vehicle-treated (V) cells (**E**); Student's *t*-tests.

2. Effects of ABHD6 blockade in the cuprizone model of primary demyelination

2.1. ABHD6 inactivation attenuates demyelination and inflammation by cuprizone feeding

Previous results from our laboratory show that MAGL blockade attenuates demyelination and inflammatory responses associated to cuprizone administration (Bernal-Chico et al. 2015). In this study, we sought to examine the role of ABHD6 in the cuprizone model. To this end, we first

evaluated possible changes in the expression of ABHD6 during demyelination by cuprizone feeding. qRT-PCR analyses showed an upregulation of this serine-hydrolase at the transcriptional level during the time-course of cuprizone administration (*$p < 0.05$ vs control mice) (**Figure 2A**). Protein quantification showed a non-significant upregulation of ABHD6 expression (36 ± 25%) following 6 weeks of cuprizone feeding (**Figure 2B**). To further analyze possible changes in ABHD6 levels associated to cuprizone feeding we evaluated enzyme expression in damaged white matter by immunohistochemistry. Immunolabeling of ABHD6 in tissue sections evidenced a substantial increase in the expression levels of the enzyme in the demyelinated corpus callosum of mice treated with cuprizone for 6 weeks (**Figures 2C** and **D**). Collectively, these results suggest that primary demyelination of white matter tracts is associated to an enhanced expression of 2-AG hydrolytic enzyme ABHD6.

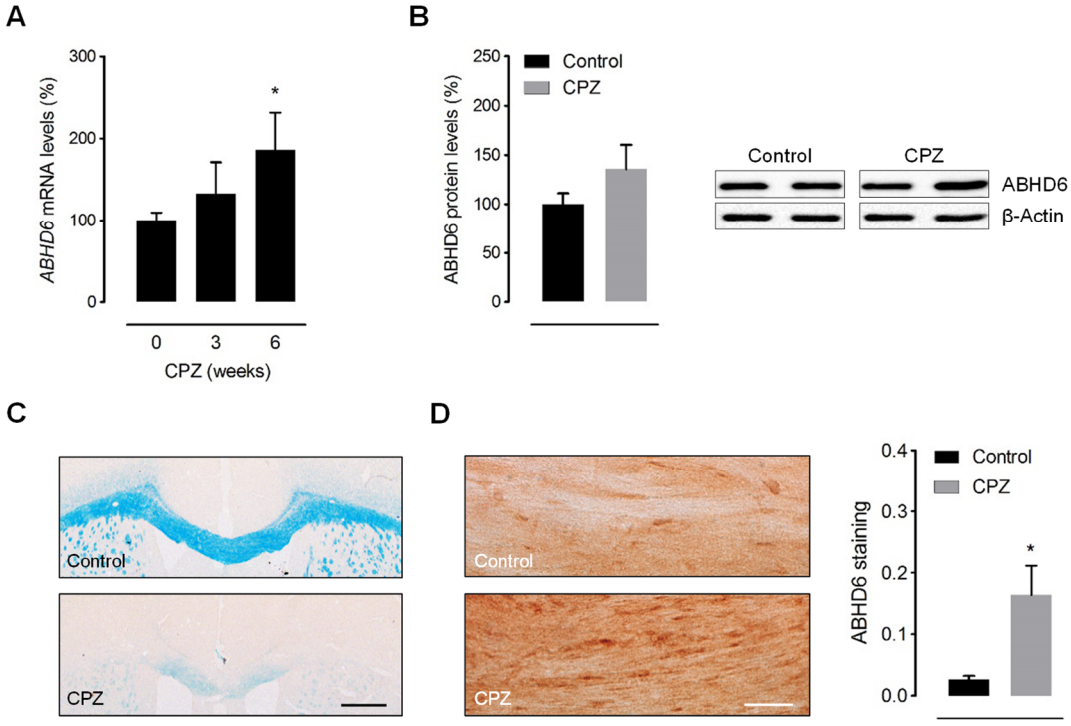

Figure 2. Demyelination by cuprizone feeding upregulates ABHD6 expression. (**A**) RT-qPCR quantification of *Abhd6* in brain tissue from mice fed a cuprizone containing diet for 3 or 6 weeks (n = 6-7 mice). Expression levels were normalized to *Gapdh* and *Hprt1* and presented relative to that measured in control mice. (**B**) Western blot analysis of 2-AG hydrolytic enzyme ABHD6 in brain samples from mice treated with cuprizone for 6 weeks (n = 4-5 mice). (**C**) Representative images depicting luxol fast blue (LFB) myelin staining and (**D**) immunoperoxidase labeling of ABHD6 in coronal brain sections from mice fed a cuprizone containing diet for 6 weeks and untreated controls. Analysis of immunostained area showed a substantial increase in ABHD6 expression in demyelinated corpus callosum (n = 3 mice). Scale bars: 500 µm (LFB) and 50 µm (ABHD6). CPZ, cuprizone. *$p < 0.05$ versus mice fed a control diet; Student's t-tests.

To study the effects of ABHD6 blockade during primary demyelination we chose a short-term cuprizone administration protocol consisting in toxin feeding for 3 weeks. Mice were daily treated with the brain permeant ABHD6 inhibitor KT182 (2 mg/Kg) (Hsu et al. 2013) or its vehicle (**Figure 3A**). Partial demyelination of the corpus callosum occurred in vehicle-treated mice after 3 weeks of cuprizone administration, as evidenced by histological evaluation of LFB and MBP staining (**p < 0.01 vs control mice) (**Figures 3B** and **C**). Notably, analysis of tissue sections from mice that received KT182 showed an attenuated myelin damage following 3 weeks of cuprizone feeding ($^{\#}p$ < 0.05 vs vehicle-treated mice) (**Figures 3B** and **C**).

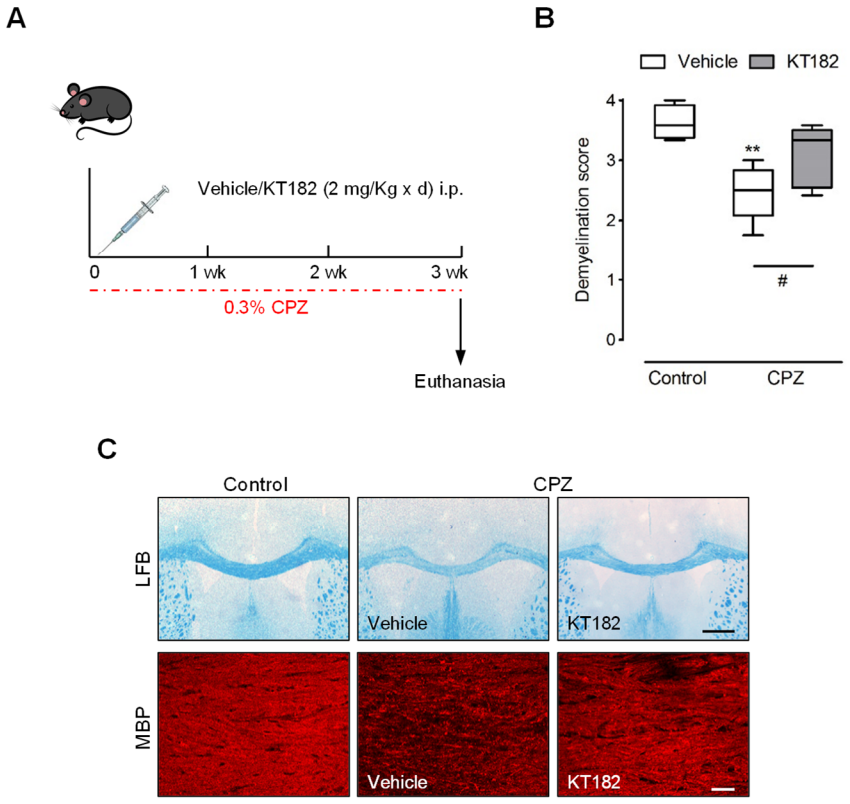

Figure 3. ABHD6 inactivation attenuates demyelination by cuprizone feeding. (**A**) Mice were fed cuprizone containing diet for 3 weeks and treated in parallel with KT182 (2 mg/Kg) or vehicle. (**B**) Analysis of luxol fast blue (LFB) staining and myelin basic protein (MBP) immunolabeling in corpus callosum slices from mice fed a cuprizone containing diet in comparison to control tissue sections. Administration of the ABHD6 inhibitor was associated to a significant attenuation of demyelination by cuprizone (n = 4-5 mice). Myelin damage was scored from 4 (normal myelin) to 0 (complete demyelination). Representative images showing LFB and MBP staining in the corpus callosum of control and cuprizone-treated mice that received KT182 or vehicle are shown in **C**. Scale bars: 500 µm (LFB) and 50 µm (MBP). CPZ, cuprizone. **p < 0.01 versus mice fed a control diet, $^{\#}p$ < 0.05 versus vehicle-treated mice; Student´s t-tests.

Amelioration of myelin pathology by KT182 was associated to a substantial suppression of inflammation evidenced by a reduced amount of both CD11b$^+$-microglia/macrophages and GFAP$^+$-astrocytes in the corpus callosum of mice treated with the ABHD6 inhibitor (**Figures 4A** and **B**). By contrast, administration of KT182 did not modulate the recruitment of NG2$^+$ OPCs to the demyelinated corpus callosum (**Figures 4A** and **B**). Altogether, these data support the hypothesis that ABHD6 blockade engages myelin protective and anti-inflammatory effects during primary demyelination.

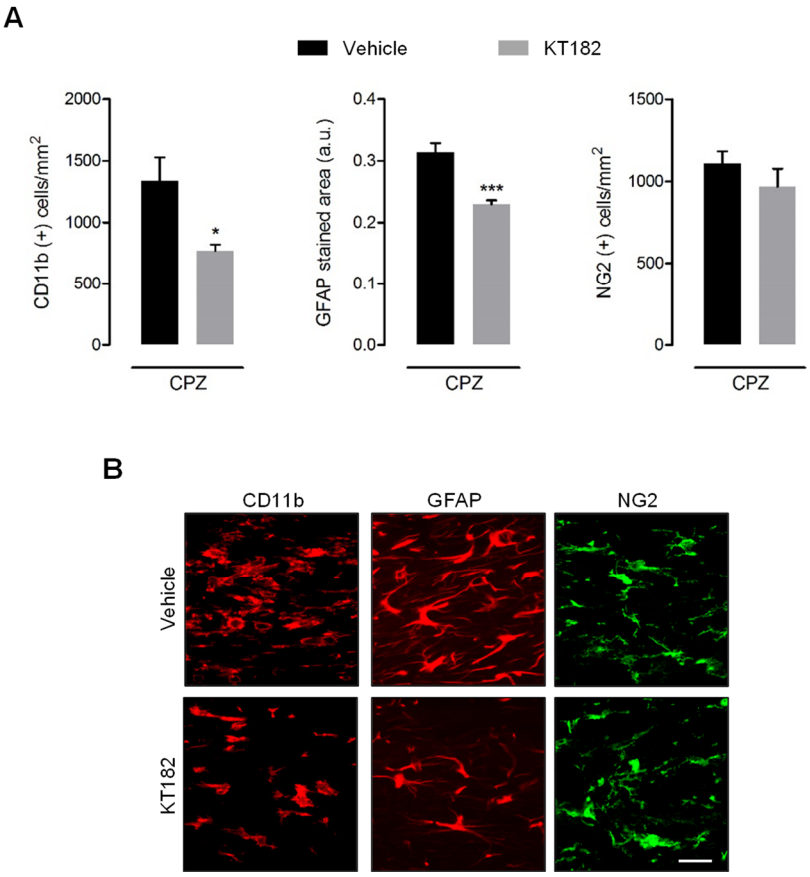

Figure 4. ABHD6 blockade modulates inflammatory reaction associated to cuprizone feeding. Glial reactivity was quantified in brain sections from mice treated with KT182 (2 mg/Kg) or vehicle during a 3 week cuprizone administration protocol. (**A**) Administration of the ABHD6 inhibitor was associated to a reduced presence of CD11b$^+$ microglia/macrophages and GFAP$^+$ astrocytes in demyelinated corpus callosum, without changes in the number of NG2$^+$ OPCs (*n* = 4-5 mice). (**B**) Representative images depict immunolabeling of CD11b, GFAP and NG2 in the corpus callosum of cuprizone-treated mice that received KT182 or vehicle. Scale bar: 25 µm. CPZ, cuprizone. *p < 0.0 and ***p < 0.001; Student´s *t*-tests.

2.2. ABHD6 blockade does not accelerate myelin repair

Previous studies have established a proof of principle that inhibition of 2-AG hydrolysis can promote remyelination and functional recovery of demyelinated axons through a variety of mechanisms (Arévalo-Martín et al. 2003; Feliú et al. 2017; Gomez et al. 2010). Based on our previous observations, we next sought to evaluate the efficacy of ABHD6 to promote the repair of damaged myelin in the cuprizone model. With this aim, mice were treated with cuprizone for 6 weeks and subsequently administered KT182 or vehicle daily over a 2 week interval starting at day 1 after cuprizone withdrawal (**Figure 5A**). Double-blind analysis of tissue sections stained for LFB and MBP showed significant improvement of myelination scores 2 weeks after cuprizone removal in vehicle-treated mice (*$p < 0.05$ vs mice treated with cuprizone for 6 weeks) (**Figures 5B** and **C**). However, myelination scores in mice treated with KT182 were similar to that determined in vehicle-treated mice, indicating that ABHD6 inactivation does not accelerate remyelination of damaged corpus callosum (**Figures 5B** and **C**).

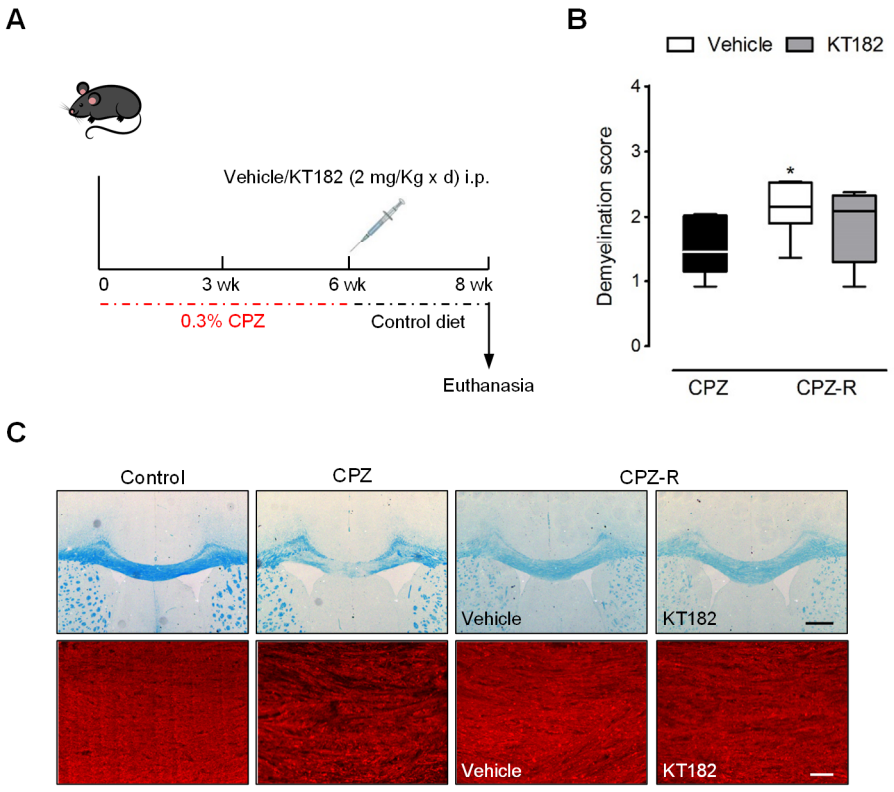

Figure 5. ABHD6 inactivation does not improve spontaneous remyelination in the cuprizone model. (**A**) Mice treated with cuprizone for 6 weeks were randomly selected for daily treatment with KT182 (2 mg/Kg) or vehicle during a 2-week remyelination phase. (**B**, **C**) LFB and MBP immunostaining revealed extensive demyelination at 6 weeks of cuprizone administration and partial recovery 2 weeks after toxin withdrawal. Double blind scoring of LFB/MBP staining showed no differences between mice treated with KT182 or vehicle during the recovery phase (n = 6 mice). Scale bars: 500 µm (LFB) and 50 µm (MBP).

Because preventive administration of KT182 attenuates microglia and astrocyte reactivity during cuprizone intoxication (**Figure 4**), we next evaluated the effect of the ABHD6 inhibitor over the 2 week remyelination phase on these cells types. In contrast to our results during the 3-week demyelination period, mice treated with KT182 upon cuprizone withdrawal did not exhibit changes in the number of $CD11b^+$ cells or the extent of GFAP immunostaining in the remyelinating corpus callosum, as compared to vehicle-treated animals (**Figures 6A** and **B**). Altogether, these results suggest that inhibition of ABHD6 is a powerless strategy to promote myelin repair and reduce gliosis during the recovery phase of cuprizone intoxication.

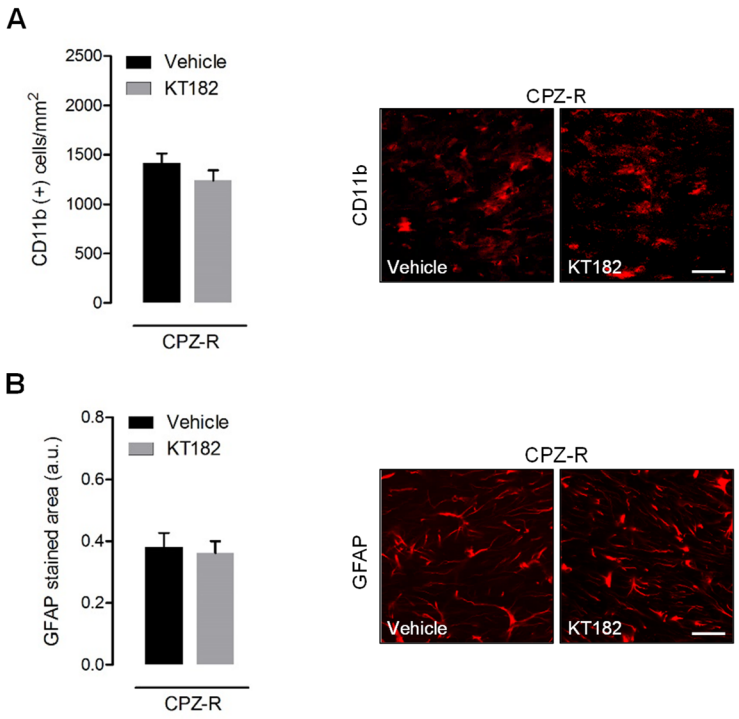

Figure 6. Blockade of ABHD6 does not modulate the extent of astrocyte and microglia reactivity during remyelination. Mice treated with KT182 (2 mg/Kg) or vehicle for 2 weeks upon withdrawal from cuprizone feeding (6 weeks) (*n* = 5-6 mice) were assayed for the presence of $GFAP^+$ astrocytes and $CD11b^+$ microglia in the corpus callosum. Quantification of immunostained sections showed no effect of the ABHD6 inhibitor on either cell type. Scale bars: 25 µm.

3. Prophylactic ABHD6 inactivation in experimental autoimmune encephalomyelitis

The utility of targeting ABHD6 in MS is hypothesized on the basis that the inhibitor WWL70 (Li et al. 2007; Marrs et al. 2010) attenuates clinical disability in the EAE mouse model of the disease (Wen et al. 2015). However, the relative contribution of central versus peripheral ABHD6 to the control of EAE disease progression has not been investigated. In this study, we addressed this issue by comparing the efficacy of two novel ABHD6 inhibitors with different blood-brain barrier permeability, namely KT182 and KT203. The brain permeant compound KT182 readily crosses the blood brain barrier and inactivates brain ABHD6 upon systemic administration whereas the activity of KT203 is restricted to peripherally expressed ABHD6 (Hsu et al. 2013).

3.1. Efficacy of KT182 and KT203 compounds to target brain ABHD6

In order to corroborate the differential efficacy of KT182 and KT203 to inactivate brain ABHD6 *in vivo*, we treated naive mice with a single injection of either compound and we evaluated the serine-hydrolase activity profile in brain samples. With this aim, we carried out gel-based activity based protein profiling (ABPP) experiments in brain proteomes incubated with the broad spectrum SH-directed probe FP-Rh. The ABPP assay showed positive reactivity of ABHD6 (~35 kDa) with FP-Rh detected by in-gel fluorescence scanning and we observed that the brain permeant compound KT182 effectively bound to the active site of the hydrolase ABHD6 (thus blocking probe labelling of the enzyme) 4 and 24 h after acute injection (**Figure 7**). Consistent with previous results of Hsu and collaborators (Hsu et al. 2013), the inhibitor KT182 showed good selectivity against other brain serine hydrolases when administered *in vivo* although we observed some cross-reactivity with FAAH, at the dose tested. As expected, the peripherally restricted compound KT203 exhibited no inhibitory activity at brain ABHD6 following acute administration to naive mice (**Figure 7**).

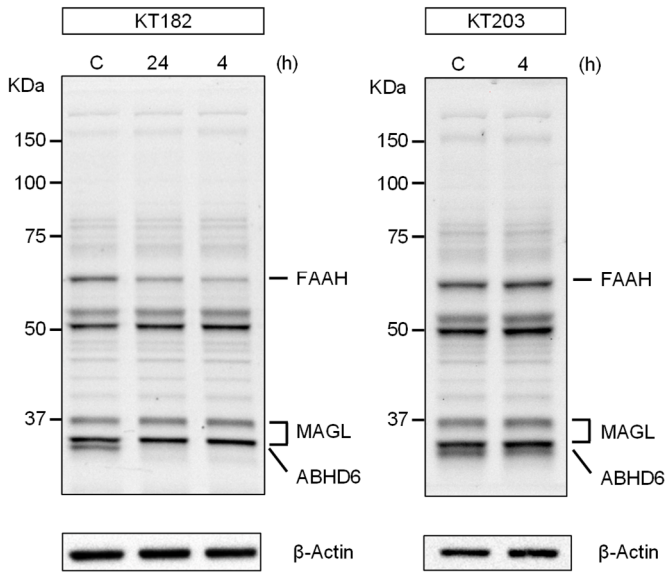

Figure 7. Brain serine hydrolase activity profiles of the ABHD6 inhibitors KT182 and KT203 *in vivo* determined by competitive ABPP. Brain membranes from mice treated with a single dose of KT182, KT203 (2 mg/Kg) or vehicle and sacrificed at the indicated time-points were subjected to gel-based competitive ABPP with the FP-Rh (*n* = 4 mice per condition). Compound KT182 produced complete and sustained inactivation of ABHD6 while KT203 showed negligible inhibition of serine hydrolase activity in the brain of naive mice.

3.2. Clinical efficacy of central and peripheral ABHD6 inhibitors in the EAE model

To determine the efficacy of both compounds during EAE disease progression we chose a prophylactic regimen starting on the day after MOG injection consisting in the administration of a daily i.p. injection of ABHD6 inhibitors (2 mg/Kg) or vehicle. Evaluation of EAE disease progression showed significant amelioration of motor disability in mice that were treated with KT182 (**Figure 8A**). By contrast, treatment with the peripherally restricted ABHD6 inhibitor KT203 under a similar treatment schedule failed to modulate the course of EAE disease progression (**Figure 8B**). However,

comparison of motor scores at 30 dpi did not reveal significant differences concerning neurological disability between treatment groups (**Figure 8C**). To further examine whether long-term ABHD6 blockade ameliorates motor dysfunction in immunized mice, we assessed the functional status of the corticospinal tract in the recovery phase of the disease. EAE induction was associated to a significant increase in corticospinal tract conduction latency as measured *in vivo* at 30 dpi (**Figure 8D**). Nevertheless, this functional deficit was not significantly attenuated in mice treated with KT182 or KT203 (**Figure 8D**). In all, these results suggest that ABHD6 blockade engages only modest protective effects during EAE progression, which require enzyme inactivation in the CNS at early disease stages.

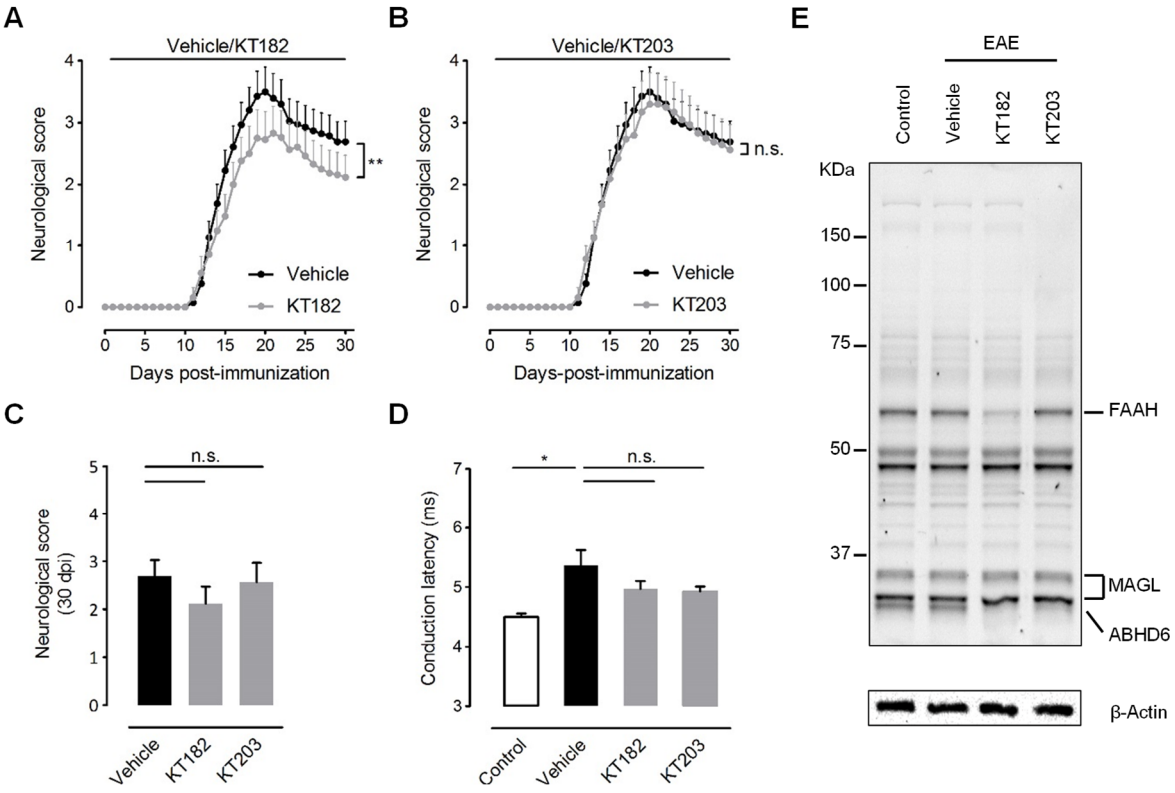

Figure 8. *In vivo* efficacy of ABHD6 inhibitors in the EAE model of multiple sclerosis. (**A**) Daily administration of the brain permeant compound KT182 (2 mg/Kg) starting at 0 dpi transiently ameliorated motor disability during the time-course of EAE as revealed by comparison of neurological score curves (n = 19-21 mice, $^{**}p$ = 0.0018; Mann-Whitney U-test). (**B**) Treatment with the peripherally restricted ABHD6 inhibitor KT203 (2 mg/Kg) did not affect neurological disability during EAE progression (n = 16-21 mice). (**C**) Comparison of motor scores at 30 dpi did not reveal significant differences between treatment groups. Data in **A**-**C** are representative of 3 independent EAE experiments pooled together. (**D**) Measurement of corticospinal tract conduction latency at 30 dpi indicated similar disability in EAE mice treated with ABHD6 inhibitors or vehicle (n = 5-10 mice). (**E**) ABPP of brain proteomes from EAE mice at 30 dpi. Animals were daily treated with KT182, KT203 or vehicle and sacrificed for analysis 24 h after the last injection. Both KT182 and KT203 showed complete inhibition of brain ABHD6 in EAE mice. Images are representative of at least 3 independent ABPP assays. n.s., not statistically significant. $^{*}p < 0.05$, Student's t-test.

In order to verify the target inhibition following treatment with both compounds in our experimental model, we next tested the serine-hydrolase inhibitory profile of brain samples from EAE mice daily treated with KT182 and KT203. We found that either ABHD6 inhibitor completely inactivated ABHD6 in the chronic phase of EAE (30 dpi) (**Figure 8E**). Comparison between serine hydrolase activity profiles from naive and EAE mice (**Figures 7** and **8E**) indicates that our *in vivo* treatment schedule with KT182 effectively inhibited brain ABHD6 during the whole time-course of the EAE, whereas KT203 inhibitory activity was restricted to the periphery during the immunization and early acute phases. Both inhibitors are equally effective at targeting ABHD6 at chronic stages, when disease progression engages blood-brain barrier breakdown and drug access to the CNS.

3.3. ABHD6 inhibitors do not attenuate inflammatory responses in chronic EAE

According to previous observations, the therapeutic benefits resulting from ABHD6 blockade in the EAE model are associated to a marked suppression of inflammatory responses. In this regard, the ABHD6 inhibitor WWL70 attenuated the presence of microglia/macrophages and the expression of inflammatory mediators such as TNFα and IL1β in chronic EAE disease (Wen et al. 2015). Nonetheless, recent work from this laboratory indicates that WWL70 suppresses the production of prostaglandin E2 in microglia by ABHD6 independent mechanisms, which are likely to contribute to the therapeutic efficacy of this inhibitor in the EAE model (Tanaka et al. 2017). Importantly, KT182 failed to suppress microglial PGE2 production in this study (Tanaka et al. 2017), suggesting that it does not elicit the described off-target anti-inflammatory effects *in vitro* or *in vivo*.

Aiming at elucidating the anti-inflammatory potential of pharmacological ABHD6 inhibition in the EAE model, we next evaluated the extent of inflammatory reaction in immunized mice treated with KT182 and KT203. Histological analysis of spinal cord sections from animals sacrificed at 30 dpi showed a slight, non-significant reduction in the number of inflammatory lesions (**Figures 9A** and **B**) and in the presence of $CD11b^{+}$ microglia/macrophages (**Figures 9C** and **D**) associated to mice treated with KT182, that was not evident in the KT203-treated group. These observations are consistent with motor score results, which show a modest efficacy of the systemic compound to attenuate neurological disability during the time-course of EAE disease without significant differences between treatment groups at 30 dpi (**Figures 8A** and **C**).

We next measured the expression of several inflammation markers in spinal cord and brain tissue of mice chronically treated with KT182 and KT203. RT-qPCR analysis of tissue samples obtained at the end of the experiment showed up-regulation in mRNA levels for the pro-inflammatory markers *Iba-1*, *COX-2*, *TNFα* and *IL1β* in the spinal cord and to a lower extent, in the striatum and hippocampus of EAE mice (**Figure 9E**). However, the expression of the different inflammatory molecules in each brain area was similar between vehicle, KT182 and KT203 treatment groups (**Figure 9E**). Altogether, these results indicate that preventive ABHD6 blockade does not attenuate inflammatory responses associated to tissue damage in the chronic phase of EAE.

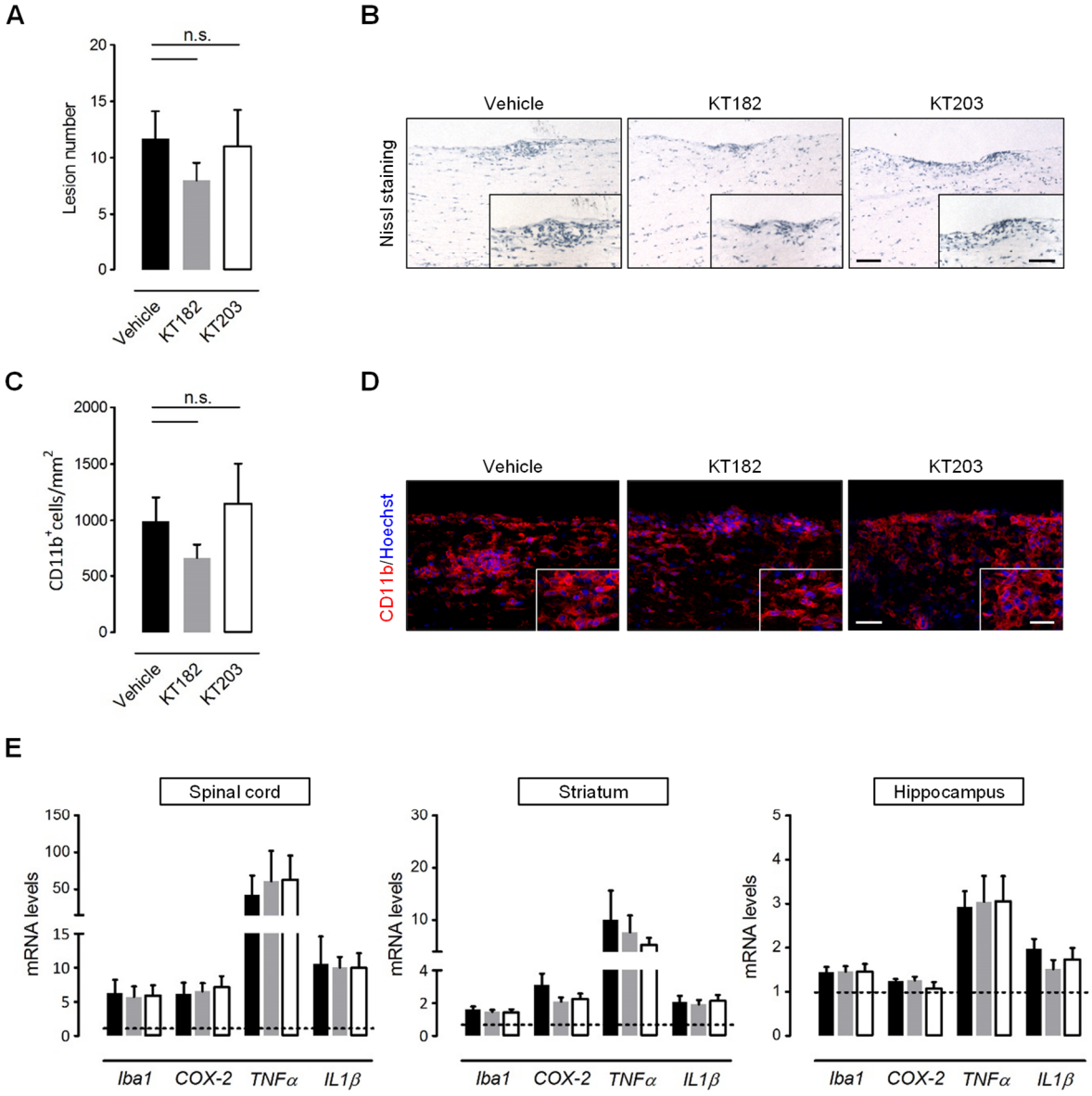

Figure 9. ABHD6 inhibition does not modulate inflammatory responses in chronic EAE disease. Quantification of infiltrating lesions (**A**) and microglia/macrophages (**C**) in lumbar spinal cord white matter from EAE mice showed no significant anti-inflammatory effects associated to the administration of the ABHD6 inhibitors KT182 and KT203 (*n* = 6-8 mice). Representative images show Nissl staining (**B**) and CD11b immunolabeling (**D**) in spinal cord longitudinal sections from immunized mice treated with KT182, KT203 or vehicle. Scale bars in **B**: 100 µm and 50 µm (insert); in **D**: 50 µm and 25 µm (insert). (**E**) Expression analysis of inflammatory markers *Iba1*, *COX-2*, *TNFα*, *iNOS* and *IL1β* determined by RT-qPCR in the spinal cord, striatum and hippocampus of EAE mice. Results were adjusted to *Gapdh* and *Hprt1* levels as endogenous references and normalized to values in non-immunized mice. The number of mice included in the analysis was as follows: spinal cord *n* = 7-10, striatum *n* = 12-17 and hippocampus *n* = 11-16.

3.4. ABHD6 expression is not upregulated in chronic EAE

ABHD6 plays a minor role in 2-AG metabolism under physiological conditions and it is postulated that the potential benefits of ABHD6 inhibitors in neuroinflammatory diseases may depend on the extent of enzyme upregulation in injured tissue (Blankman et al. 2007; Wen et al. 2015). Thus, to further evaluate the role of ABHD6 during autoimmune demyelination, we looked at changes in the expression levels of the enzyme by RT-qPCR and western blot in EAE mice. ABHD6 gene expression levels in spinal cord and brain samples from immunized mice at 30 dpi were similar to that measured in control, non-immunized mice (**Figure 10A**). Consistently, assessment of ABHD6 protein levels using an affinity-purified antibody previously validated in knockdown studies (Thomas et al. 2013) showed no changes in the levels of the enzyme (**Figure 10B**). Collectively, these results suggest that, in our experimental conditions, the contribution of ABHD6 to 2-AG hydrolysis is not significantly upregulated in the recovery phase of EAE disease progression.

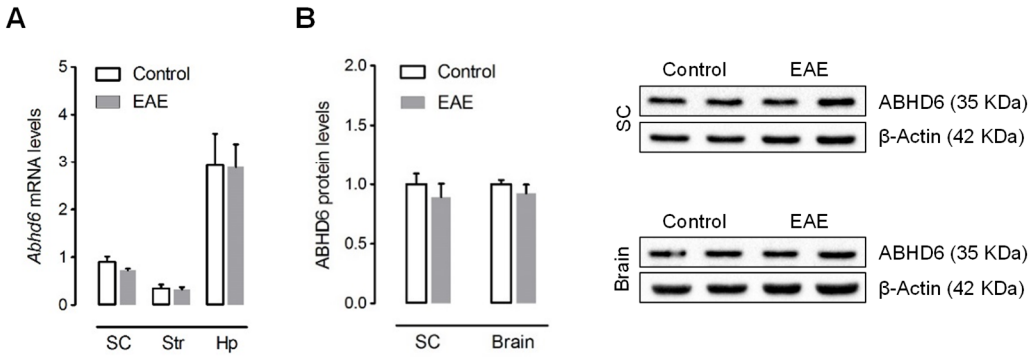

Figure 10. Analysis of ABHD6 expression in chronic EAE. (**A**) ABHD6 gene expression in spinal cord (SC; *n* = 5-10 mice), striatum (Str; *n* = 9-17 mice) and hippocampus (Hp; *n* = 8-16 mice) of EAE mice at 30 dpi determined by RT-qPCR. Results were adjusted to *Gapdh* and *Hprt1* levels as endogenous references. (**B**) Quantification and representative images of ABHD6 expression in tissue extracts from EAE mice analyzed by Western blot. ABHD6 levels were normalized to β-actin and referred to values in control animals (*n* = 3 mice). Data are presented as mean ± S.E.M.

3.5. Chronic ABHD6 blockade desensitizes brain CB_1 receptors

The limited efficacy of the CNS acting compound KT182 at late stages of EAE progression may be associated, at least in part, to the development of functional tolerance to the protective effects resulting from ABHD6 inhibition. Indeed, the sustained presence of elevated 2-AG levels causes pharmacological adaptations at the CB_1 receptor signaling level that may limit the therapeutic utility of endocannabinoid hydrolysis inhibitors in neurodegenerative conditions (Bernal-Chico et al. 2015; Schlosburg et al. 2010). Here, we specifically addressed the possibility that long-term ABHD6 blockade engages changes in CB_1 receptor function by means of [^{35}S]GTPγS and [^{3}H]CP55,950 autoradiography. Mice that received daily injections of KT182 for 30 days exhibited significant reductions in cannabinoid-agonist stimulated [^{35}S]GTPγS binding affecting mainly the striatum and the cerebellum (**Figures 11A** and **C**). Conversely, chronic administration of the peripherally restricted inhibitor ABHD6 was not associated to changes in [^{35}S]GTPγS binding.

Concerning CB_1 receptor expression studies, analysis of [^{3}H]CP55,950 binding in tissue sections showed that long-term treatment with KT182 and KT203 did not elicit significant alterations in receptor density in any of the brain areas analyzed (**Figures 11B** and **C**). In all, these results indicate that partial CB_1 receptor uncoupling from $G_{i/o}$ proteins takes place following chronic KT182 administration to EAE mice and is not associated to protein downregulation.

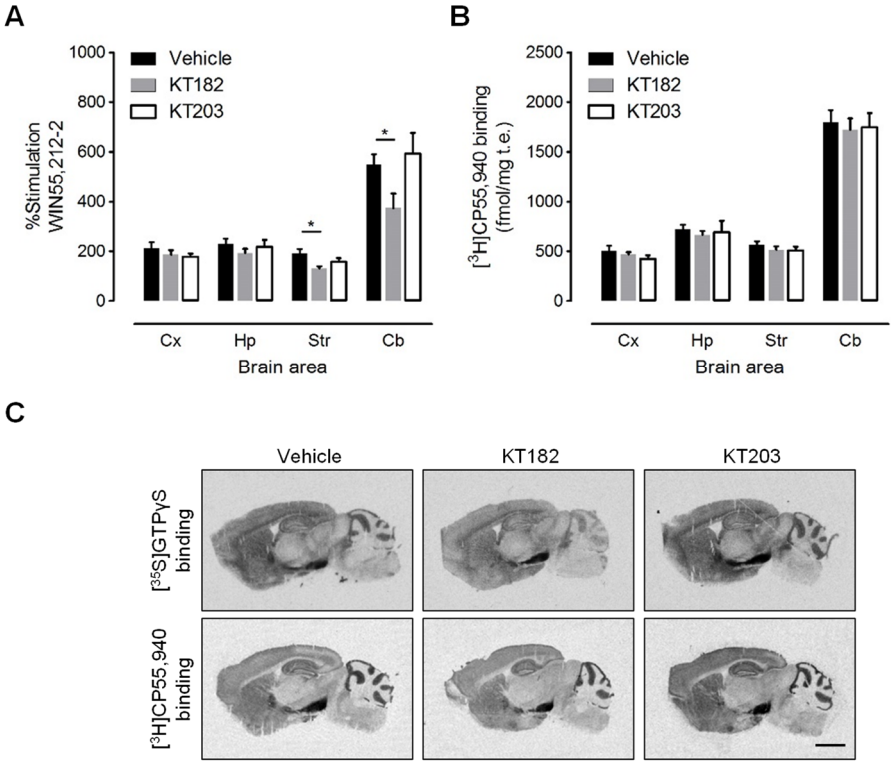

Figure 11. Chronic ABHD6 inactivation modulates CB_1 receptor functionality during EAE. (**A**) Quantification of cannabinoid-stimulated [^{35}S]GTPγS binding in brain sections from EAE mice chronically treated with brain permeant or peripherally restricted ABHD6 inhibitors. Statistical analysis indicated a significant difference between vehicle and KT182 treatment groups concerning the ability of the cannabinoid agonist WIN55,212-2 to stimulate [^{35}S]GTPγS binding in the striatum and cerebellum. (**B**) Expression levels of CB_1 receptors as determined by [^{3}H]CP55,940 autoradiography in the brain of EAE mice. (**C**) Representative autoradiograms showing WIN55,212- 2-stimulated [^{35}S]GTPγS binding and [^{3}H]CP55,940 binding in sagittal brain sections of EAE mice following treatment with KT182, KT203 or vehicle (*n* = 7-10 mice). Cx is cortex; Hp is hippocampus; Str is striatum; and Cb is cerebellum. Scale bar: 2 mm. **p* < 0.05, Student's t-test. Data correspond to mean ± S.E.M.

4. Effects of ABHD6 inhibitors on NMDA excitotoxicity to neuronal cultures

4.1. KT182 attenuates NMDA mediated cell death

The observation that chronic administration of KT182 induces CB_1 receptor loss-of-function supports the possibility that ABDH6 inactivation engages protective effects at a central level during EAE involving the activation of this cannabinoid receptor subtype. Neuronal CB_1 receptors exert symptom control in the EAE model through mechanisms that involve attenuation of excitotoxicity

as pathogenic mechanism (Maresz et al. 2007; Pryce et al. 2003). Thus, we next sought to investigate whether ABHD6 blockade attenuates cell death in an *in vitro* model of neuronal excitotoxicity induced by activation of NMDA receptors (Ruiz et al. 2014). We initially confirmed ABHD6 and CB_1 receptor gene expression in cultured cells by qPCR (**Figure 12A**). Application of KT182 for 30 min prior to stimulation with NMDA prevented the release of LDH by ~25% at the highest concentration tested (1 µM) (**Figure 12B**). However, KT182 blocked NMDA-stimulated cell death with an EC50 ~0.2 µM while the EC_{50} value for the inhibition of endogenous ABHD6 by KT182 is ~1 nM (Hsu et al. 2013). We next carried out ABPP assays to determine possible discrepancies between the concentrations of KT182 that inhibit ABHD6 and those that attenuate cell death in our culture system. Neurons were treated with KT182 followed by preparation of membrane proteomes that were probed with FP-Rh to detect ABHD6. In good agreement with the observations of Hsu et al. (2013), the ABPP assay in proteomes from cultured neurons showed that binding of the FP-Rh to ABHD6 was completely blocked by pretreating cells with 10 nM-1 µM KT182 *in situ* (**Figure 12D**). We corroborated these results using the serine hydrolase probe HT-01 that binds specifically to ABHD6 (Hsu et al. 2013). The fact that 10 nM and even higher concentrations of KT182 do not attenuate LDH release by NMDA while effectively targeting ABHD6 suggest that this enzyme does not play a role in mediating neuroprotection against excitotoxicity by KT182 in our culture system. To provide support for this hypothesis we tested the effect of a variety of ABHD6 inhibitors in neuronal cultures. Incubation with KT203, WWL70 and KT195 at effective concentrations that inactivate ABHD6 *in vitro* (1-2 µM) (Hsu et al. 2013; Marrs et al. 2010) (**Figure 12D**) failed to prevent neuronal excitotoxicity induced by NMDA (**Figure 12C**). These results demonstrate that KT182 is not targeting ABHD6 to attenuate cell death in cultured neurons.

We next evaluated the involvement of FAAH as mediator of neuronal protection by KT182. Ruling out a role of this enzyme as pharmacological target underlying the effects of the ABHD6 inhibitor KT182 in neuron cultures, incubation with two structurally unrelated FAAH inhibitors, namely URB597 and PF750 (1 µM), was ineffective in attenuating neurotoxicity by NMDA (**Figure 12C**).

4.2. KT182 attenuates mitochondrial calcium elevations during NMDA exposition

Under our experimental conditions, intense insults with NMDA are likely to result in calpain-mediated neurotoxicity through necrosis (Ruiz et al. 2014). Noteworthy, the 1,2,3-triazole urea (TU) ABHD6 blocker KT195 attenuates necrotic cell death of cultured fibroblast by preventing calcium overload of the mitochondria and permeability transition pore formation (Yun et al. 2014). As KT182 is a TU inhibitor optimized from KT195 (Hsu et al. 2013), we wondered about its ability to modulate mitochondrial calcium increase during NMDA excitotoxicity. To address this question we investigated whether KT182 modulates mitochondrial calcium homeostasis during NMDA excitotoxicity. In neurons transfected with the mitochondria-targeted indicator 2mtD4cpv, addition of NMDA induced a sustained increase in mitochondrial calcium levels that was reduced by 10% in the presence of KT182 (**Figures 12E-F**). Reminiscent of our results in excitotoxicity experiments, the ability of KT182 to attenuate mitochondrial calcium elevations by NMDA was not mimicked by the ABHD6 inhibitors KT203, KT195 or WWL70, nor by the FAAH blockers URB597 and PF750 (**Figure 12F**). Altogether, these results suggest that protection by KT182 during NMDA excitotoxicity may occur, at least in part, as a consequence of its ability to prevent calcium overload to the mitochondria.

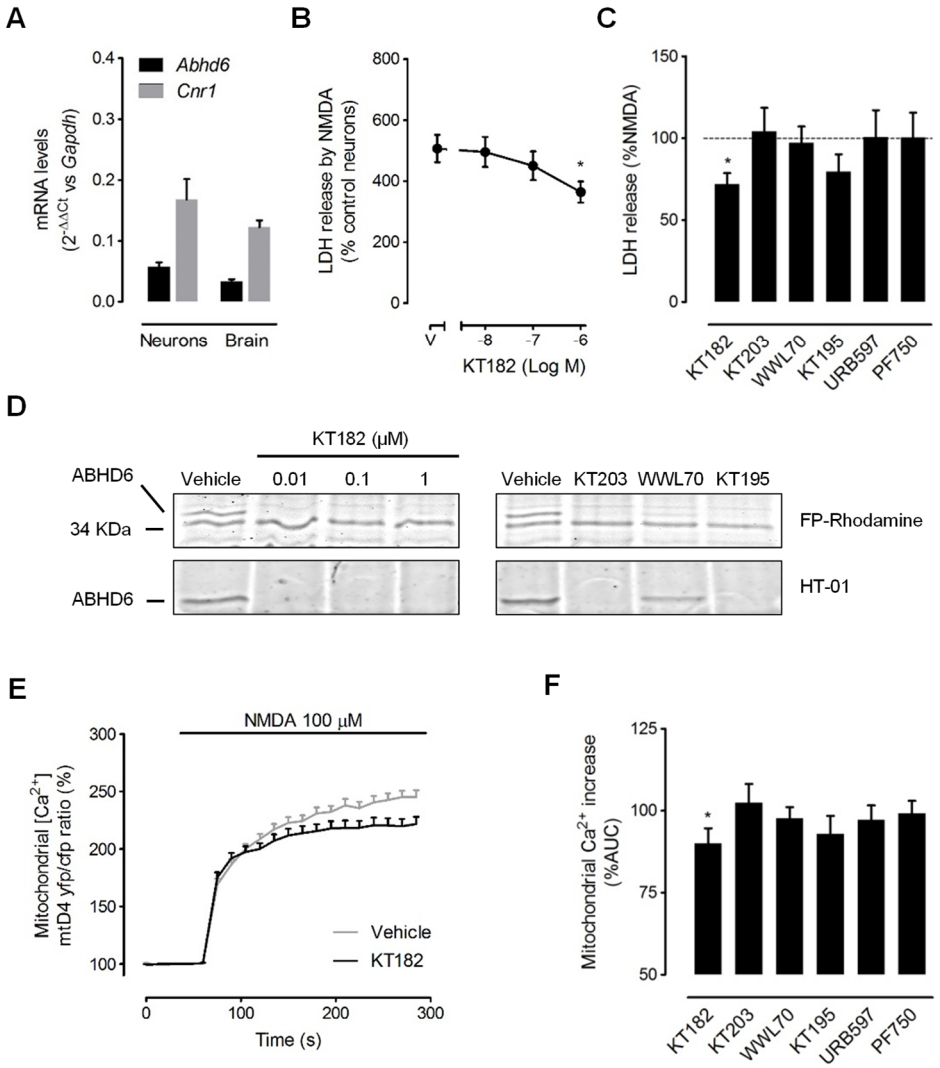

Figure 12. KT182 attenuates NMDA excitotoxicity and mitochondrial calcium uptake in cultured neurons. (**A**) *Abhd6* and *Cnr1* expression in primary cortical neurons determined by RT-qPCR (*n* = 3 cultures). Expression levels of both genes in mouse forebrain tissue are shown for a comparison (*n* = 7 mice). Results are presented as relative expression levels versus *Gapdh.* (**B**) The ability of KT182 to prevent neuronal excitotoxicity was determined in cells treated with KT182 or vehicle for 30 min prior to stimulation with NMDA (100 μM, 15 min). (**C**) ABHD6 does not regulate NMDA excitotoxicity. The protective efficacy of KT182 in excitotoxicity assays was not mimicked by the ABHD6 inhibitors KT203 (1 μM), KT195 (2 μM) and WWL70 (1 μM) or the FAAH inhibitors URB597 (1 μM) and PF750 (1 μM) (*n* = 10-16 cultures). (**D**) The ability of ABHD6 inhibitors to bind the enzyme was determined by competitive ABPP assay of proteomes from cultured neurons. Drugs were added to cells at the indicated concentrations prior to preparing membrane proteomes, followed by incubation with FP-Rh or HT-01 probes. A representative experiment of 2-3 independent assays is shown. (**E**, **F**) KT182 attenuates mitochondrial calcium uptake upon NMDA receptor activation. (**E**) Time-courses depict the increase in normalized yfp/cfp ratios evoked in neuron cultures transfected with 2mtD4cpv by continuous exposure to NMDA (100 μM) in the presence of K182 (1 μM) or vehicle (*n* = 62-80 cells). (**F**) Comparison of the area under the curve (AUC) calculated for each experimental condition revealed significant inhibition of mitochondrial calcium responses by KT182 but not by the alternative ABHD6 inhibitors KT203, KT195, WWL70 nor by the FAAH inhibitors URB597 and PF750 (*n* = 61-78 cells). Data are presented as mean ± S.E.M. of results from at least 3 different cultures. **p* < 0.05, Student's *t*-test or Mann-Whitney *U*-test.

Discussion

In the **first part of this work** we addressed a key unanswered question in the endocannabinoid field, concerning the anatomical localization of CB_1 receptors in oligodendrocytes. Taking advantage of electron microscopy techniques and newly generated transgenic mice, we report that hippocampal OPCs and myelinating OL in subcortical white matter of the adult mouse brain express low levels of CB_1 receptors *in situ*. On the other hand, we have evaluated for the first time, possible changes in myelin ultrastructure in mice lacking CB_1 receptors at the peak of myelination. Although EM analysis shows no major changes affecting myelin thickness, CB_1 receptor knockout mice exhibited a subtle increase in the number of myelinated axons within the caudal portion of the corpus callosum, supporting a role for CB_1 in regulating myelination.

The precise cellular and subcellular distribution of CB_1 receptors has been extensively analyzed for more than 2 decades using conventional immunohistochemistry, electron microscopy and electrophysiological techniques (Katona and Freund 2012). These studies have demonstrated that the CB_1 receptor is heterogeneously expressed in synaptic terminals throughout the brain, being the proportion and density of the receptor protein much higher in hippocampal inhibitory than in excitatory cells (Katona et al. 2006; Kawamura et al. 2006). More recently, the generation of transgenic mice lacking CB_1 receptors in phenotype-specific cell populations has allowed the unequivocal localization of these proteins in cells and subcellular compartments that express them at low densities, including glutamatergic neurons (Gutiérrez-Rodríguez et al. 2017) and astrocytes (Gutiérrez-Rodríguez et al. 2018; Han et al. 2012). In the same line, the combination of genetic exclusion and high resolution electron microscopy techniques has provided *bona fide* demonstration of CB_1 receptor presence in rodent brain mitochondria (Hebert-Chatelain et al. 2016). In all, cell-specific transgenic mice have proven an invaluable tool for the analysis of CB_1 receptor populations expressed at low levels in specific cellular, subcellular and intracellular locations. Concerning cells of the oligodendroglial lineage, the functional expression of CB_1 receptors in cultured OPCs and OL is well documented (Bernal-Chico et al. 2015; Gomez et al. 2015; Mato et al. 2009; Molina-Holgado et al. 2002). However, immunohistochemical analysis of rodent brain tissue has failed to provide conclusive evidence of CB_1 receptor expression in rodent oligodendroglia. Unfortunately, oligodendrocyte specific CB_1 receptor-knockout mice have not been generated hitherto and studies using viral strategies for *in vivo* knockdown purposes are equally lacking. In this scenario, we aimed at evaluating CB_1 receptor localization in OPCs and myelinating OLs of the adult mouse brain by applying high-resolution electron microscopy techniques to the analysis of wild-type and global CB_1 receptor knockout mice.

For the evaluation of CB_1 receptor expression in OPCs, we generated double mutant mice carrying global deletion of CB_1 receptors and expressing EYFP under *NG2* promoter. In this animals, OPC processes and CB_1 receptors can be identified at the electron microscopy level by DAB immunodeposits and deposition of gold particles, respectively, following application of combined immunolabeling techniques. In this study, we chose the hippocampus for immunohistochemical analysis because this structure exhibits high CB_1 receptor immunoreactivity and the precise localization of the CB_1 receptor protein has been extensively analyzed in this brain area using electron microscopy techniques (Gutiérrez-Rodríguez et al. 2018; Gutiérrez-Rodríguez et al. 2017; Han et al. 2012; Katona et al. 2006; Kawamura et al. 2006). A combined pre-embedding immunogold and immunoperoxidase method applied to brain tissue from NG2-$EYFP^{+/-}$-$CB_1^{+/+}$ and NG2-$EYFP^{+/-}$-$CB_1^{-/-}$ mice showed that at least 6% of OPCs within hippocampal *stratum radiatum* express CB_1 receptors in their plasma membrane at a density of 0.2 particles/µm. Noticeably, CB_1 receptor immunoparticle densities in receptor-positive inhibitory and excitatory terminals of the

NG2-EYFP$^{+/-}$-CB$_1^{+/+}$ mutants are in line with previous hippocampal data in wild-type mice (Gutiérrez-Rodríguez et al. 2017; Kawamura et al. 2006). According to these previous studies using high sensitive preembedding immunoelectron microscopy, the proportion of CB_1 receptor immunopositive inhibitory terminals in CA1 *stratum radiatum* is around 80% whereas only 20% of excitatory synaptic profiles express CB_1 receptors in this brain area (Gutiérrez-Rodríguez et al. 2017). Moreover, the CB_1 receptor was expressed at a density of 4-5 particles/µm in GABAergic terminals of the CA1 *stratum radiatum* and only of 0.3-0.4 particles/µm in excitatory terminals within the same area. In this study, we were able to detect CB_1 receptor expressed in GABAergic and glutamatergic terminals at densities of 5.9 and 0.7 particles/µm, respectively. This observation shows that our immunostaining procedure detects CB_1 receptors at the electron microscopy level with high specificity and sensitivity. Furthermore, our comparative analysis of CB_1 receptor gold particles in synaptic compartments and NG2$^+$ profiles of the same animals allows us to conclude that CB_1 receptors are present at lower density in OPCs than in glutamatergic cells of the rodent hippocampus. It is worth mentioning, however, that CB_1 receptor density values in OPCs are in line with previous reports addressing the expression of the receptor protein in other glial cell types, namely astrocytes. In this regard, a recent study determined that around 40% of astrocytes in hippocampal CA1 *stratum radiatum* express CB_1 receptors at a density of 0.1-0.15 particles/µm in wild-type mice (Gutiérrez-Rodríguez et al. 2018).

We studied the distribution of CB_1 receptors in myelinating OLs of the subcortical white matter by applying a pre-embeding immunogold to the analysis of brain tissue from wild-type and global CB_1 receptor knockout mice. In this case, we chose the corpus callosum for analysis due to the large number of mature OLs and their characteristic an easily identifiable morphology in this area. Quantification of immunogold particles in the corpus callosum of wild-type and CB_1 knockout mice, allowed us to conclude that around 27% myelinating OLs in this white matter tract express CB_1 receptors in their somatic plasma membrane. In the context of the above-mentioned results, these observations suggest that, in the adult rodent brain, the CB_1 receptor protein is expressed at a higher proportion in the somata of myelinating OLs than in the processes of OPCs. Caution is needed when interpreting these results, however, as we did not carry out a comparative analysis of CB_1 receptor distribution in OPCs and OLs of the same animals. Another limitation of this study is that we did not analyze the localization of CB_1 receptor immunoparticles in OPCs of the corpus callosum, due to the scarce detection of DAB immunopositive profiles in this myelinated tract.

In the context of previous work, the expression of CB_1 receptors in OPCs profiles and myelinating OLs of the adult mouse brain seems low, both in terms of proportion and density. However, research in the endocannabinoid field has consistently demonstrated that the physiological relevance of CB_1 receptor functions does not correlate with the expression levels of the protein. In this regard, several pharmacological actions of endogenous and exogenous cannabinoids rely on the activation of CB_1 receptors present at low levels in forebrain glutamatergic terminals. Indeed, analysis of mutant mice lacking CB_1 expression in cortical glutamatergic neurons and viral deletion strategies have demonstrated a crucial role of this receptor population in mediating neuroprotection (Monory et al. 2006), motor impairment and hypothermia (Monory et al. 2007) as well as in the control of fear memories (Metna-Laurent et al. 2012), stress-induced social alterations (Dubreucq et al. 2012) and anxiety (Rey et al. 2012). In the same regard, CB_1 receptors in hippocampal astrocytic processes have been crucially involved in synaptic plasticity and memory formation (Han et al. 2012; Navarrete and Araque 2010; Robin et al. 2018) while being the protein density in this cellular compartment even lower than in glutamatergic synapses within the same area. Finally, low CB_1 densities located at mitochondrial membranes control neuronal activity

through their implication in mitochondrial respiration, a process that is related to the memory formation (Hebert-Chatelain et al. 2016). Based on the above-mentioned evidences, it seems plausible to speculate that CB_1 receptors expressed in oligodendrocyte populations play relevant role in myelin formation, maintenance and/or repair despite being expressed at low levels in these cells.

Overall, the present study demonstrates CB_1 receptor expression in OPCs and myelinating OLs of the adult mouse brain, thus providing an anatomical substrate for the myelin protective and regenerative effects of cannabinoid-based medicines in MS. However, we still have a limited understanding on the oligodendrocyte-specific expression pattern of CB_1 receptors. A detailed and comparative analysis of CB_1 receptor distribution in white matter oligodendroglia has yet to be carried out in order to identify possible specific features associated to different receptor populations. Future studies designed to identify expression changes at particular developmental stages may help elucidate the biological roles of CB_1 receptors expressed by oligodendrocyte populations during myelin generation, plasticity and repair.

Several *in vitro* studies have reported that oligodendroglial CB_1 receptors modulate different aspects of the myelination process including OPC migration (Sanchez-Rodriguez et al. 2018), proliferation (Gomez et al. 2015) and differentiation (Gomez et al. 2010; Gomez et al. 2011). These observations, together with our present data showing *in situ* expression of CB_1 receptor by both OPCs and myelinating oligodendrocytes, suggest the involvement of these receptor populations in regulating myelination. Constitutive CB_1 receptor knockout mice have been extensively phenotyped during development and adulthood, but severe alterations in white matter tracts have not been reported. Nevertheless, it should be also born in mind that the dynamics of myelin formation have not been thoroughly analyzed in CB_1 receptor mutant mice. Thus, as a first approximation to analyze the role of CB_1 receptors in regulating myelination, in this study we evaluated myelin ultrastructure in subcortical white matter of mice bearing a global deletion of the *Cnr1* gene. In this regard, we considered two parameters, 1) the myelin thickness, as determined from *g*-ratio analysis, and 2) the number of myelinated axons, that were measured both in the rostral and caudal corpus callosum of wild-type and CB_1 receptor knockout mice at the peak of myelination (P30). Quantitative analysis of myelin *g*-ratio from electron microscopy images revealed no differences affecting myelin thickness in CB_1 receptor knockout mice. The fact that CB_1 receptor deficient mice do not exhibit severe alterations in callosal myelin may suggests that this protein is dispensable during myelin formation, or that there are other regulators for myelination that ultimately compensate for the loss of CB_1 receptors in juvenile mice. Further studies addressing myelin ultrastructure at early developmental stages may help elucidate this question.

Surprisingly, mice lacking CB_1 receptors exhibit a slight increase in the number of myelinated axons restricted to the caudal portion of the corpus callosum. This observation contrast the pro-myelinating effects associated to the activation of oligodendrocyte CB_1 receptors *in vitro*, which would lead us to expect an incomplete and/or delayed myelination in mice lacking this protein. However, the biological actions of CB_1 receptors in oligodendrocytes have been addressed using high concentrations of receptor agonists and it is unclear whether the effects of these compounds result from acute receptor activation or from protein downregulation. It is also worth emphasizing that the global ´loss of function´ approach used for the present study does not allow for investigating cell-type specific roles of CB_1 receptors in the myelin biogenesis. Myelination is a complex process regulated by a plethora of extrinsic factors that include a variety of molecules associated not only axons but also to astrocytes and microglia. Given the widespread distribution

of the CB_1 receptor in brain tissue, it seems plausible to speculate that receptor populations expressed by specific cell types will coordinately regulate oligodendrocyte lineage progression and myelination in a complex, and maybe opposite, manner. New insights on the relevance of oligodendrocyte CB_1 receptor expressed by OPCs and mature OLs in myelin biology will most likely come from the generation of constitutive and/or conditional mutant mice lacking the receptor protein in specific oligodendendrocyte populations. Moreover, these transgenic mice would be central to understand whether MS can benefit from targeting oligodendrocyte CB_1 receptors.

The **second part of this work** aimed at re-evaluating the utility of targeting ABHD6 as novel therapeutic strategy to treat MS, using both *in vivo* and *in vitro* models that mimic different aspects of the disease. Administration of the systemically acting inhibitor KT182 partially prevented demyelination and inflammatory responses associated to cuprizone feeding. However, blockade of ABHD6 did not engage remyelination-promoting effects following cuprizone administration. *In vitro*, KT182 was unable to protect OLs from excitotoxicity nor to promote the differentiation of OPCs into mature cells. On the other hand, prophylactic administration of KT182 elicited a mild attenuation of neurological disability in the EAE model of MS. This effect was not mimicked by the peripherally restricted compound KT203, suggesting that the benefits resulting from ABHD6 blockade during immune-mediated demyelination require enzyme inactivation in nervous tissue at early disease stages. Noticeably, the chronic administration of KT182 resulted in partial desensitization of CB_1 receptors in certain brain areas. Finally, excitotoxicity assays in cultured neurons showed unveiled an off-target activity of KT182, since this compound attenuated NMDA mediated cell death in ABHD6 independent manner. Overall, these results indicate that pharmacological ABHD6 blockade exerts only modest protective effects during immune-dependent and -independent white matter injury.

Glutamate excitotoxicity to OLs is a key pathogenic mechanism of white matter damage in MS and other pathological conditions of the CNS (Matute et al. 2001). In this context, we have evaluated the efficacy of ABHD6 blockade to attenuate excitotoxicity to OLs as possible mechanism of white matter protection during demyelinating insults. Results showed that inhibition of ABHD6 was not able to protect oligodendrocytes in culture from AMPA mediated cell death. This observation contrasts with previous data of our laboratory reporting that pharmacological inhibition of MAGL using JZL184 prevents OL excitotoxicity by mechanisms that include the activation of CB_1 receptors expressed by these cells by endogenously produced 2-AG and the subsequent attenuation of calcium overload, mitochondrial dysfunction and ROS generation (Bernal-Chico et al. 2015). It is worth mentioning that OL *in vitro* showed high expression levels of *Abhd6* as compared to *Magl*. A plausible explanation for these apparent discrepancy is that the expression levels of the enzyme are not expected to correlate with its role in 2-AG metabolism in oligodendroglia. Indeed, ABHD6 plays a minor role in the hydrolysis of this endocannabinoid in brain tissue, as compared to MAGL (Blankman et al. 2007).

Fostering OPC differentiation is considered a promising therapeutic strategy for the treatment of demyelinating diseases including MS (Kremer et al. 2015). Thus, in this work we also analyzed the potential of the ABHD6 inhibitor KT182 to accelerate the differentiation of cultured OPCs. By assessing the expression of the myelin protein MBP as readout of maturation we were able to determine that blockade of ABHD6 does not engage differentiation-promoting effects in cultured OPCs. This observation contrasts with the reported capability of the MAGL inhibitor JZL184 to accelerate OPC maturation through the activation of cannabinoid receptors (Gomez et al. 2010) that we confirmed in the present study. The positive results with JZL184 in excitotoxicity and

differentiation assays corroborate the efficacy of 2-AG production and signaling machinery in our experimental conditions and allows us conclude that ABHD6 inactivation in OPCs and OLs is not sufficient to promote 2-AG mediated beneficial effects through the activation of cannabinoid receptors present in these cells.

When examining the consequences of ABHD6 inactivation in the cuprizone model of demyelination we found a modest but significant attenuation of myelin damage in mice dosed with KT182 during 3 weeks of toxin administration. This finding mimics previous data from our laboratory and others showing beneficial effects associated to MAGL blockade in the cuprizone, EAE and TMEV models of MS (Bernal-Chico et al. 2015; Feliú et al. 2017; Hernández-Torres et al. 2014). Altogether, these observations support the utility of targeting 2-AG hydrolysis during primary and immune-dependent demyelination. It is worth mentioning that cuprizone administration in our experimental conditions was related to an increased ABHD6 expression, which suggest that the protective effects of its blockade in this animal model might be linked to an increased role of this enzyme in 2-AG metabolism during inflammatory conditions, as previously pointed out (Poursharifi et al. 2017). Regardless possible changes in the relative contribution of ABHD6 to 2-AG metabolism during cuprizone intoxication, targeting ABHD6 is less efficient than inactivating MAGL in terms of myelin protection in this mouse model (Bernal-Chico et al. 2015).

Arguing against the possibility that ABHD6 modulates the OPCs recruitment or proliferation capacity during primary demyelination, treatment with KT182 did not evoke changes in the number of OPCs in demyelinated corpus callosum. Together with our *in vitro* observations, this result suggest that the myelin-preserving efficacy of the ABHD6 inhibitor does not result from direct protective and/or remyelination promoting effects in oligodendrocyte lineage cells. By contrast, administration of KT182 elicited a significant decrease in the inflammatory response associated to cuprizone administration, as evidenced by the reduced recruitment of both microglia and astrocytes to the demyelinated corpus callosum. This finding suggest that the modulation of these cells by an elevated 2-AG tone may contribute, at least in part, to the myelin protection by ABHD6 blockade. This possibility is supported by a number of studies describing beneficial effects of cannabinoids in experimental models of neuroinflammation that involve the modulation of astrocyte and microglia responses. Indeed, these molecules, through the activation of cannabinoid and cannabinoid related receptors in glial cells, are able to reduce the production of proinflammatory cytokines, such as TNFα, IL-1β, IL-6 and IL-12 and other inflammatory mediators including nitric oxide (Eljaschewitsch et al. 2006; Ortega-Gutiérrez et al. 2005; Stella 2010). Whether attenuated reactivity of microglia and astrocytes results from cell-autonomous modulation or, in contrast, occurs as a consequence of ABHD6 blockade and elevated 2-AG levels in other cell types, remains to be addressed. Noticeably, although the key role of astrocytic MAGL in the termination of 2-AG signaling has been highlighted (Viader et al. 2015), ABHD6 inactivation modulates cuprizone induced astrogliosis more efficiently than MAGL blockade (Bernal-Chico et al. 2015). These results support the idea that each 2-AG metabolizing enzyme exert differential control of endocannabinoid signaling depending on the cell type (Poursharifi et al. 2017) also during myelin damage and repair, and point to a relevant role of ABHD6 in the regulation of astrocytic functions during myelin pathology *in vivo.*

The reported ability of MAGL inhibitors to promote myelin repair *in vivo* (Feliú et al. 2017), encouraged us to test the efficacy of ABHD6 blockade to accelerate remyelination in the cuprizone model. As expected from previous studies (Skripuletz et al. 2011), toxin withdrawal from the diet was associated to partial remyelination of damaged corpus callosum at the time point tested.

However, treatment with the ABHD6 inhibitor KT182 failed to enhance the repair of damaged myelin in the time-window analyzed in this study, as determined by the absence of changes in LFB and MBP immunostaining in damaged corpus callosum. This observation corroborates the lack of efficacy of ABHD6 inhibitors to modulate oligodendroglia *in vivo*. In addition, it is worth noting that the ABHD6 inhibitor was unable to elicit anti-inflammatory effects when administered under therapeutic schedule during the recovery phase. This result contrast the efficacy of this compound to reduce the presence of microglia and astrocytic cells under a prophylactic protocol and highlights the requirement of early ABHD6 inactivation for myelin protective purposes. Mechanistic considerations notwithstanding, our data indicate that ABHD6 blockade is not able to engage myelin repair mechanism in a pre-existing inflammatory environment.

An additional objective of this study was to examine the role of central and peripheral ABHD6 in the EAE model of chronic MS. Prophylactic administration of systemically active KT182 modestly attenuated during the time-course of EAE progression while treatment with the peripherally restricted inhibitor KT203 showed no effect. This finding likely indicates that protection from autoimmune demyelination by ABHD6 blockade requires early enzyme inactivation in nervous tissue. On the other hand, the lack of efficacy of the compound KT203 suggest that suppression of immune responses by peripherally expressed ABHD6 is a negligible mechanism in the beneficial activity of enzyme inhibitors during autoimmune inflammation. Noticeable, treatment with ABHD6 inhibitors did not attenuate inflammatory responses in the chronic phase of EAE. Importantly, the possibility that inhibitors did not effectively target the enzyme at this point was excluded by functional proteomic analysis. At this point, it is worth mentioning that the expression of ABHD6 was not significantly upregulated in spinal cord or brain tissue from EAE mice, in clear contrast to our results in the cuprizone model. This piece of data suggest that the contribution of ABHD6 to 2-AG hydrolysis during autoimmune demyelination may not differ from that in non-pathological conditions, and provides a plausible explanation for the limited protective effects of enzyme inhibitors in the EAE model. As discussed above in the context of cuprizone intoxication, our results in the EAE model suggest that ABHD6 is a less promising target than MAGL for the control of autoimmune demyelination.

Our results regarding the benefits of ABHD6 blockade during immune-dependent demyelination are in marked contrast to recent reports on the anti-inflammatory and protective efficacy of the ABHD6 inhibitor WWL70 administered under a therapeutic schedule to EAE mice (Wen et al. 2015). The discrepancies between our results and those reported by Wen et al. (2015) may reflect experimental differences concerning EAE induction protocols and drug administration procedures, which in turn might affect disease severity and modulate the efficacy of ABHD6 blockade in this mouse model of MS. In this regard, it is worth mentioning that chronic treatment with KT182 triggered a partial loss of CB_1 receptor functionality in certain brain areas including striatum and cerebellum, which might reduce therapeutic efficacy of the ABHD6 inhibitor during the chronic phase of EAE (Maresz et al. 2007; Pryce et al. 2003). However, this possibility does not account for the absence of beneficial effects of KT203 in the recovery phase of EAE. A more plausible explanation is that the marked suppression of inflammation and disease severity by the ABHD6 inhibitor WWL70 results, at least in part, from off-target activity driving attenuation of PG production by microglia, as recently pointed out from cell culture experiments (Tanaka et al. 2017).

Concerning the specificity of the ABHD6 inhibitors employed in this study, gel-based ABPP assays in naive and EAE mice showed some limited cross-reactivity at FAAH associated to the administration of KT182. However, the possibility that FAAH inhibition might mediate the transient

amelioration of EAE by KT182 seems unlikely. FAAH inactivation, as determined by proteomic analysis, was only partial following both acute and chronic administration of KT182, and the question remains whether this effect renders significant increases in the levels of the endocannabinoid AEA as to engage therapeutic benefits in EAE mice. In this regard, it is noteworthy that FAAH knockout mice do not exhibit improved EAE severity during the acute inflammatory phase of the disease despite possessing 15-fold augmented endogenous brain levels of AEA (Cravatt et al. 2001; Webb et al. 2008). This neurological profile of FAAH null mice in the EAE model contrast with the early efficacy of KT182 to attenuate motor disability that observed in this study. Indeed, Importantly, FAAH knockout mice exhibit normal CB_1 receptor expression and function (Cravatt et al. 2001; Falenski et al. 2010), which contrasts the loss of CB_1 receptor coupling ability that we observed following chronic treatment with KT182. Altogether, these results suggest that both the therapeutic benefits and molecular adaptations following administration of KT182 result mainly from ABHD6 inhibition.

Long-term administration of cannabinoid agonists is associated to dramatic down regulation of brain CB_1 receptors and functional tolerance to cannabinoid behavioral effects (Blair et al. 2009; Sim et al. 1996). MAGL blockade with high doses of irreversible inhibitors mimic these pharmacological adaptations at the CB_1 receptor level that limit the therapeutic potential of these compounds (Bernal-Chico et al. 2015; Schlosburg et al. 2010). Concerning ABHD6, our results unveil that long-term inhibition of this enzyme during inflammatory demyelination induces a partial desensitization of CB_1 receptors in the absence of significant protein down regulation. The loss of CB_1 receptor functional ability was restricted to brain structures with high white matter to grey matter ratios and that exhibit significant inflammatory pathology in the EAE model of MS, namely the striatum and the cerebellum (Mandolesi et al. 2015). In this scenario, the emerging hypothesis is that ABHD6 inactivation promotes local and significant elevations in 2-AG levels that engage CB_1 receptor (and possibly CB_2 receptor) signaling through $G_{i/o}$ proteins in inflammatory conditions and that ultimately result in a partial attenuation of receptor function.

Attenuation of neuronal excitotoxicity by CB_1 receptors is a principal mechanism for symptom control by cannabinoids and endocannabinoids in MS and other neurological conditions (Maresz et al. 2007; Marsicano et al. 2003; Pryce et al. 2003). Based on these evidences, we sought to investigate the potential efficacy of ABHD6 inactivation to modulate neuronal excitotoxicity. In neuron cultures, the ABHD6 inhibitor KT182 partially prevented NMDA-mediated cell death and mitochondrial calcium overload. However, the protective effect of KT182 was not mimicked by alternative ABHD6 inhibitors that effectively targeted the enzyme in our culture system, as demonstrated by functional proteomic analysis. In all, these results suggest that the compound KT182 prevents NMDA-stimulated excitotoxicity to cultured neurons by ABHD6 independent mechanisms that involve the attenuation of mitochondrial calcium uptake. These findings are reminiscent of recent results showing that the serine hydrolase inhibitor KT195 blocks mitochondrial calcium overload and necrotic cell death in lung fibroblasts (Yun et al. 2014). Based on observations from cultured cells and isolated mitochondria, these authors propose that KT195 is not directly targeting the serine residues in the mitochondrial calcium uniporter (MCU) but instead modulating a novel pathway implicated in the regulation of calcium uptake by the MCU in fibroblasts. Notably, compound KT182 is a 1,2,3-TU derivative of KT195 with improved potency and selectivity for ABHD6 (Hsu et al. 2013). In our culture system, KT195 was less efficient than KT182 in attenuating NMDA-stimulated mitochondrial calcium uptake and cell death, but the similarities in the chemical structure of both compounds point to the possibility that they act at a common off-target. Indeed, the MCU has been centrally involved in the control of mitochondrial calcium uptake

and excitotoxic neuronal death (Qiu et al. 2013). Although in this study we do not provide definitive evidence showing MCU regulation by KT182, it is possible that this compound will be targeting a non-identified serine hydrolase implicated in regulating mitochondrial calcium uptake during neuronal excitotoxicity.

Mitochondrial injury and subsequent energy insufficiency are considered major cause of neurological impairments in the EAE model and key mediators of MS pathogenesis. Nevertheless, the mechanisms leading to mitochondrial dysfunction in human disease and rodent models, however, remain unclear (Nikić et al. 2011; Sadeghian et al. 2016; Witte et al. 2014). At the light of our *in vitro* observations, the possibility emerges that off-target activity of KT182 preserving mitochondrial function leads to neuroprotection by the ABHD6 inhibitor during EAE. However, the hypothesis that attenuation of mitochondrial injury is the sole mechanism underlying the beneficial effects of KT182 in the EAE model seems unlikely if considering the ability of the compound to engage CB_1 desensitization (present report) and the accumulating evidence on the benefits of ABHD6 inactivation in neurodegenerative, inflammatory contexts (Alhouayek et al. 2013; Naydenov et al. 2014). In conclusion, the present study demonstrates that targeting ABHD6 does not elicit marked anti-inflammatory and neuroprotective effects in the EAE mouse model of MS.

Conclusions

Decades of research have demonstrated that the endocannabinoid system offers the potential to relieve symptomatology in MS. Nowadays, a rational exploitation of the system in the clinical practice is hampered by a limited understanding of how cannabinoid-based medicines regulate the biology of OPC and OLs. In this context, a key unanswered question in the endocannabinoid field is whether and to what extent cells of the oligodendrocyte lineage in a tissue environment express CB_1 receptors. On the other hand, targeting the endocannabinoid hydrolytic enzyme ABHD6 might offer a novel therapeutic opportunity in MS that has not yet been evaluated in detail.

The main **Conclusions** of this Thesis are the following:

I. The first part of this work provides solid evidence that OPCs and myelinating OLs in the adult mouse brain express low levels of CB_1 receptors in their plasma membrane and that lack of the receptor protein is associated to subtle changes affecting myelin ultrastructure at the peak of myelination. As a whole, these findings support the possibility that CB_1 receptor in oligodendrocyte populations contribute to fine-tune the myelination process and provide an anatomical basis for the myelin protective and regenerative effects of cannabinoid-based medicines in MS.

II. Blockade of ABHD6 elicits only modest beneficial effects in mouse models of primary and immune-dependent demyelination and does not engage protective or differentiation promoting effects in cultured oligodendroglia and/or neurons. In the context of previous studies, these observations suggest that ABHD6 is a less promising target than MAGL for the engagement of endocannabinoid-mediated protective effects in MS.

Altogether, these findings broaden current understanding on the role and therapeutic potential of the endocannabinoid system in MS and will pave the way for future studies aiming at improving the benefit to risk ratio of currently available cannabis-based medicines for the treatment of this medical condition.

References

Aguirre A, Dupree JL, Mangin JM, Gallo V. 2007. A functional role for EGFR signaling in myelination and remyelination. Nat Neurosci 10:990-1002.

Ahrendsen JT, Macklin W. 2013. Signaling mechanisms regulating myelination in the central nervous system. Neurosci Bull 29:199-215.

Alhouayek M, Masquelier J, Cani PD, Lambert DM, Muccioli GG. 2013. Implication of the anti-inflammatory bioactive lipid prostaglandin D2-glycerol ester in the control of macrophage activation and inflammation by ABHD6. Proc Natl Acad Sci U S A 110:17558-63.

Alhouayek M, Masquelier J, Muccioli GG. 2014. Controlling 2-arachidonoylglycerol metabolism as an anti-inflammatory strategy. Drug Discov Today 19:295-304.

Almeida RG, Czopka T, Ffrench-Constant C, Lyons DA. 2011. Individual axons regulate the myelinating potential of single oligodendrocytes in vivo. Development 138:4443-50.

André A, Gonthier MP. 2010, The endocannabinoid system: its roles in energy balance and potential as a target for obesity treatment. Int J Biochem Cell Biol 42:1788-801.

Arévalo-Martín A, Vela JM, Molina-Holgado E, Borrell J, Guaza C. 2003. Therapeutic action of cannabinoids in a murine model of multiple sclerosis. J Neurosci 23:2511-6.

Atwood BK, Mackie K. 2010. CB2: a cannabinoid receptor with an identity crisis. Br J Pharmacol 160:467-79.

Baggelaar MP, van Esbroeck AC, van Rooden EJ, Florea BI, Overkleeft HS, Marsicano G, Chaouloff F, van der Stelt M. 2017. Chemical Proteomics Maps Brain Region Specific Activity of Endocannabinoid Hydrolases. ACS Chem Biol 12:852-861.

Baker D, Pryce G, Croxford JL, Brown P, Pertwee RG, Makriyannis A, Khanolkar A, Layward L, Fezza F, Bisogno T and others. 2001. Endocannabinoids control spasticity in a multiple sclerosis model. FASEB J 15:300-2.

Baker D, Pryce G, Jackson SJ, Bolton C, Giovannoni G. 2012. The biology that underpins the therapeutic potential of cannabis-based medicines for the control of spasticity in multiple sclerosis. Multiple Sclerosis and Related Disorders 1:11.

Barca-Mayo O, Lu QR. 2012. Fine-Tuning Oligodendrocyte Development by microRNAs. Front Neurosci 6:13.

Barnett MH, Prineas JW. 2004. Relapsing and remitting multiple sclerosis: pathology of the newly forming lesion. Ann Neurol 55:458-68.

Baumann N, Pham-Dinh D. 2001. Biology of oligodendrocyte and myelin in the mammalian central nervous system. Physiol Rev 81:871-927.

Bengtsson SL, Nagy Z, Skare S, Forsman L, Forssberg H, Ullén F. 2005. Extensive piano practicing has regionally specific effects on white matter development. Nat Neurosci 8:1148-50.

Benito C, Romero JP, Tolón RM, Clemente D, Docagne F, Hillard CJ, Guaza C, Romero J. 2007. Cannabinoid CB1 and CB2 receptors and fatty acid amide hydrolase are specific markers of plaque cell subtypes in human multiple sclerosis. J Neurosci 27:2396-402.

Berdyshev EV. 2000. Cannabinoid receptors and the regulation of immune response. Chem Phys Lipids 108:169-90.

Bernal-Chico A, Canedo M, Manterola A, Victoria Sánchez-Gómez M, Pérez-Samartín A, Rodríguez-Puertas R, Matute C, Mato S. 2015. Blockade of monoacylglycerol lipase inhibits oligodendrocyte excitotoxicity and prevents demyelination in vivo. Glia 63:163-76.

Berrendero F, Sánchez A, Cabranes A, Puerta C, Ramos JA, García-Merino A, Fernández-Ruiz J. 2001. Changes in cannabinoid CB(1) receptors in striatal and cortical regions of rats with experimental allergic encephalomyelitis, an animal model of multiple sclerosis. Synapse 41:195-202.

Bisogno T. 2008. Endogenous cannabinoids: structure and metabolism. J Neuroendocrinol 20 Suppl 1:1-9.

Bisogno T, Howell F, Williams G, Minassi A, Cascio MG, Ligresti A, Matias I, Schiano-Moriello A, Paul P, Williams EJ and others. 2003. Cloning of the first sn1-DAG lipases points to the spatial and temporal regulation of endocannabinoid signaling in the brain. J Cell Biol 163:463-8.

Bitsch A, Schuchardt J, Bunkowski S, Kuhlmann T, Brück W. 2000. Acute axonal injury in multiple sclerosis. Correlation with demyelination and inflammation. Brain 123 (Pt 6):1174-83.

Blair RE, Deshpande LS, Sombati S, Elphick MR, Martin BR, DeLorenzo RJ. 2009. Prolonged exposure to WIN55,212-2 causes downregulation of the CB1 receptor and the development of tolerance to its anticonvulsant effects in the hippocampal neuronal culture model of acquired epilepsy. Neuropharmacology 57:208-18.

Blankman JL, Long JZ, Trauger SA, Siuzdak G, Cravatt BF. 2013. ABHD12 controls brain lysophosphatidylserine pathways that are deregulated in a murine model of the neurodegenerative disease PHARC. Proc Natl Acad Sci U S A 110:1500-5.

Blankman JL, Simon GM, Cravatt BF. 2007. A comprehensive profile of brain enzymes that hydrolyze the endocannabinoid 2-arachidonoylglycerol. Chem Biol 14:1347-56.

Bolton C, Paul C. 1997. MK-801 limits neurovascular dysfunction during experimental allergic encephalomyelitis. J Pharmacol Exp Ther 282:397-402.

Bouaboula M, Poinot-Chazel C, Bourrié B, Canat X, Calandra B, Rinaldi-Carmona M, Le Fur G, Casellas P. 1995. Activation of mitogen-activated protein kinases by stimulation of the central cannabinoid receptor CB1. Biochem J 312 (Pt 2):637-41.

Browne P, Chandraratna D, Angood C, Tremlett H, Baker C, Taylor BV, Thompson AJ. 2014. Atlas of Multiple Sclerosis 2013: A growing global problem with widespread inequity. Neurology 83:1022-4.

Busquets-Garcia A, Puighermanal E, Pastor A, de la Torre R, Maldonado R, Ozaita A. 2011. Differential role of anandamide and 2-arachidonoylglycerol in memory and anxiety-like responses. Biol Psychiatry 70:479-86.

Bénard G, Massa F, Puente N, Lourenço J, Bellocchio L, Soria-Gómez E, Matias I, Delamarre A, Metna-Laurent M, Cannich A and others. 2012. Mitochondrial CB_1 receptors regulate neuronal energy metabolism. Nat Neurosci 15:558-64.

Cabranes A, Pryce G, Baker D, Fernández-Ruiz J. 2006. Changes in CB1 receptors in motor-related brain structures of chronic relapsing experimental allergic encephalomyelitis mice. Brain Res 1107:199-205.

Cabranes A, Venderova K, de Lago E, Fezza F, Sánchez A, Mestre L, Valenti M, García-Merino A, Ramos JA, Di Marzo V and others. 2005. Decreased endocannabinoid levels in the brain and beneficial effects of agents activating cannabinoid and/or vanilloid receptors in a rat model of multiple sclerosis. Neurobiol Dis 20:207-17.

Cadas H, Gaillet S, Beltramo M, Venance L, Piomelli D. 1996. Biosynthesis of an endogenous cannabinoid precursor in neurons and its control by calcium and cAMP. J Neurosci 16:3934-42.

Castillo PE, Younts TJ, Chávez AE, Hashimotodani Y. 2012. Endocannabinoid signaling and synaptic function. Neuron 76:70-81.

Centonze D, Bari M, Rossi S, Prosperetti C, Furlan R, Fezza F, De Chiara V, Battistini L, Bernardi G, Bernardini S and others. 2007. The endocannabinoid system is dysregulated in multiple sclerosis and in experimental autoimmune encephalomyelitis. Brain 130:2543-53.

Centonze D, Muzio L, Rossi S, Cavasinni F, De Chiara V, Bergami A, Musella A, D'Amelio M, Cavallucci V, Martorana A and others. 2009. Inflammation triggers synaptic alteration and degeneration in experimental autoimmune encephalomyelitis. J Neurosci 29:3442-52.

Chakrabarti A, Onaivi ES, Chaudhuri G. 1995. Cloning and sequencing of a cDNA encoding the mouse brain-type cannabinoid receptor protein. DNA Seq 5:385-8.

Chang A, Staugaitis SM, Dutta R, Batt CE, Easley KE, Chomyk AM, Yong VW, Fox RJ, Kidd GJ, Trapp BD. 2012. Cortical remyelination: a new target for repair therapies in multiple sclerosis. Ann Neurol 72:918-26.

Charles P, Hernandez MP, Stankoff B, Aigrot MS, Colin C, Rougon G, Zalc B, Lubetzki C. 2000. Negative regulation of central nervous system myelination by polysialylated-neural cell adhesion molecule. Proc Natl Acad Sci U S A 97:7585-90.

Chen DH, Naydenov A, Blankman JL, Mefford HC, Davis M, Sul Y, Barloon AS, Bonkowski E, Wolff J, Matsushita M and others. 2013. Two novel mutations in ABHD12: expansion of the mutation spectrum in PHARC and assessment of their functional effects. Hum Mutat 34:1672-8.

Chen Y, Liu X, Vickstrom CR, Liu MJ, Zhao L, Viader A, Cravatt BF, Liu QS. 2016. Neuronal and Astrocytic Monoacylglycerol Lipase Limit the Spread of Endocannabinoid Signaling in the Cerebellum. eNeuro 3.

Chew LJ, Coley W, Cheng Y, Gallo V. 2010. Mechanisms of regulation of oligodendrocyte development by p38 mitogen-activated protein kinase. J Neurosci 30:11011-27.

Chiarlone A, Bellocchio L, Blázquez C, Resel E, Soria-Gómez E, Cannich A, Ferrero JJ, Sagredo O, Benito C, Romero J and others. 2014. A restricted population of CB1 cannabinoid receptors with neuroprotective activity. Proc Natl Acad Sci U S A 111:8257-62.

Choi DW. 1988. Glutamate neurotoxicity and diseases of the nervous system. Neuron 1:623-34.

Colognato H, Tzvetanova ID. 2011. Glia unglued: how signals from the extracellular matrix regulate the development of myelinating glia. Dev Neurobiol 71:924-55.

Compston A, Coles A. 2008. Multiple sclerosis. Lancet 372:1502-17.

Consroe P, Musty R, Rein J, Tillery W, Pertwee R. 1997. The perceived effects of smoked cannabis on patients with multiple sclerosis. Eur Neurol 38:44-8.

Cravatt BF, Demarest K, Patricelli MP, Bracey MH, Giang DK, Martin BR, Lichtman AH. 2001. Supersensitivity to anandamide and enhanced endogenous cannabinoid signaling in mice lacking fatty acid amide hydrolase. Proc Natl Acad Sci U S A 98:9371-6.

Cravatt BF, Giang DK, Mayfield SP, Boger DL, Lerner RA, Gilula NB. 1996. Molecular characterization of an enzyme that degrades neuromodulatory fatty-acid amides. Nature 384:83-7.

Croxford JL, Pryce G, Jackson SJ, Ledent C, Giovannoni G, Pertwee RG, Yamamura T, Baker D. 2008. Cannabinoid-mediated neuroprotection, not immunosuppression, may be more relevant to multiple sclerosis. J Neuroimmunol 193:120-9.

Dendrou CA, Fugger L, Friese MA. 2015. Immunopathology of multiple sclerosis. Nat Rev Immunol 15:545-58.

DePaula-Silva AB, Hanak TJ, Libbey JE, Fujinami RS. 2017. Theiler's murine encephalomyelitis virus infection of SJL/J and C57BL/6J mice: Models for multiple sclerosis and epilepsy. J Neuroimmunol 308:30-42.

Devane WA, Hanus L, Breuer A, Pertwee RG, Stevenson LA, Griffin G, Gibson D, Mandelbaum A, Etinger A, Mechoulam R. 1992. Isolation and structure of a brain constituent that binds to the cannabinoid receptor. Science 258:1946-9.

Di Filippo M, Pini LA, Pelliccioli GP, Calabresi P, Sarchielli P. 2008. Abnormalities in the cerebrospinal fluid levels of endocannabinoids in multiple sclerosis. J Neurol Neurosurg Psychiatry 79:1224-9.

Di Marzo V, De Petrocellis L. 2010. Endocannabinoids as regulators of transient receptor potential (TRP) channels: A further opportunity to develop new endocannabinoid-based therapeutic drugs. Curr Med Chem 17:1430-49.

Dinh TP, Freund TF, Piomelli D. 2002. A role for monoglyceride lipase in 2-arachidonoylglycerol inactivation. Chem Phys Lipids 121:149-58.

Dubreucq S, Matias I, Cardinal P, Häring M, Lutz B, Marsicano G, Chaouloff F. 2012. Genetic dissection of the role of cannabinoid type-1 receptors in the emotional consequences of repeated social stress in mice. Neuropsychopharmacology 37:1885-900.

Eljaschewitsch E, Witting A, Mawrin C, Lee T, Schmidt PM, Wolf S, Hoertnagl H, Raine CS, Schneider-Stock R, Nitsch R and others. 2006. The endocannabinoid anandamide protects neurons during CNS inflammation by induction of MKP-1 in microglial cells. Neuron 49:67-79.

Falenski KW, Thorpe AJ, Schlosburg JE, Cravatt BF, Abdullah RA, Smith TH, Selley DE, Lichtman AH, Sim-Selley LJ. 2010. FAAH-/- mice display differential tolerance, dependence, and cannabinoid receptor adaptation after delta 9-tetrahydrocannabinol and anandamide administration. Neuropsychopharmacology 35:1775-87.

Fancy SP, Baranzini SE, Zhao C, Yuk DI, Irvine KA, Kaing S, Sanai N, Franklin RJ, Rowitch DH. 2009. Dysregulation of the Wnt pathway inhibits timely myelination and remyelination in the mammalian CNS. Genes Dev 23:1571-85.

Feliú A, Bonilla Del Río I, Carrillo-Salinas FJ, Hernández-Torres G, Mestre L, Puente N, Ortega-Gutiérrez S, López-Rodríguez ML, Grandes P, Mecha M and others. 2017. 2-Arachidonoylglycerol Reduces Proteoglycans and Enhances Remyelination in a Progressive Model of Demyelination. J Neurosci 37:8385-98.

Fernández-Ruiz J. 2009. The endocannabinoid system as a target for the treatment of motor dysfunction. Br J Pharmacol 156:1029-40.

Fernández-Ruiz J, García C, Sagredo O, Gómez-Ruiz M, de Lago E. 2010. The endocannabinoid system as a target for the treatment of neuronal damage. Expert Opin Ther Targets 14:387-404.

Fernández-Ruiz J, Pazos MR, García-Arencibia M, Sagredo O, Ramos JA. 2008. Role of CB2 receptors in neuroprotective effects of cannabinoids. Mol Cell Endocrinol 286:S91-6.

Fiskerstrand T, H'mida-Ben Brahim D, Johansson S, M'zahem A, Haukanes BI, Drouot N, Zimmermann J, Cole AJ, Vedeler C, Bredrup C and others. 2010. Mutations in ABHD12 cause the neurodegenerative disease PHARC: An inborn error of endocannabinoid metabolism. Am J Hum Genet 87:410-7.

Flores AI, Narayanan SP, Morse EN, Shick HE, Yin X, Kidd G, Avila RL, Kirschner DA, Macklin WB. 2008. Constitutively active Akt induces enhanced myelination in the CNS. J Neurosci 28:7174-83.

Follett PL, Rosenberg PA, Volpe JJ, Jensen FE. 2000. NBQX attenuates excitotoxic injury in developing white matter. J Neurosci 20:9235-41.

Forrest AD, Beggs HE, Reichardt LF, Dupree JL, Colello RJ, Fuss B. 2009. Focal adhesion kinase (FAK): A regulator of CNS myelination. J Neurosci Res 87:3456-64.

Franklin RJ. 2002. Why does remyelination fail in multiple sclerosis? Nat Rev Neurosci 3:705-14.

Franklin RJM, Ffrench-Constant C. 2017. Regenerating CNS myelin - from mechanisms to experimental medicines. Nat Rev Neurosci 18:753-69.

Freeman SA, Desmazières A, Simonnet J, Gatta M, Pfeiffer F, Aigrot MS, Rappeneau Q, Guerreiro S, Michel PP, Yanagawa Y and others. 2015. Acceleration of conduction velocity linked to clustering of nodal components precedes myelination. Proc Natl Acad Sci U S A 112:E321-8.

Furusho M, Dupree JL, Nave KA, Bansal R. 2012. Fibroblast growth factor receptor signaling in oligodendrocytes regulates myelin sheath thickness. J Neurosci 32:6631-41.

Fünfschilling U, Supplie LM, Mahad D, Boretius S, Saab AS, Edgar J, Brinkmann BG, Kassmann CM, Tzvetanova ID, Möbius W and others. 2012. Glycolytic oligodendrocytes maintain myelin and long-term axonal integrity. Nature 485:517-21.

Galabova-Kovacs G, Catalanotti F, Matzen D, Reyes GX, Zezula J, Herbst R, Silva A, Walter I, Baccarini M. 2008. Essential role of B-Raf in oligodendrocyte maturation and myelination during postnatal central nervous system development. J Cell Biol 180:947-55.

Galve-Roperh I, Rueda D, Gómez del Pulgar T, Velasco G, Guzmán M. 2002. Mechanism of extracellular signal-regulated kinase activation by the CB(1) cannabinoid receptor. Mol Pharmacol 62:1385-92.

Galve-Roperh I, Sánchez C, Cortés ML, Gómez del Pulgar T, Izquierdo M, Guzmán M. 2000. Anti-tumoral action of cannabinoids: involvement of sustained ceramide accumulation and extracellular signal-regulated kinase activation. Nat Med 6:313-9.

Gao Y, Vasilyev DV, Goncalves MB, Howell FV, Hobbs C, Reisenberg M, Shen R, Zhang MY, Strassle BW, Lu P and others. 2010. Loss of retrograde endocannabinoid signaling and reduced adult neurogenesis in diacylglycerol lipase knock-out mice. J Neurosci 30:2017-24.

Gérard CM, Mollereau C, Vassart G, Parmentier M. 1991. Molecular cloning of a human cannabinoid receptor which is also expressed in testis. Biochem J 279 (Pt 1):129-34.

Giera S, Deng Y, Luo R, Ackerman SD, Mogha A, Monk KR, Ying Y, Jeong SJ, Makinodan M, Bialas AR and others. 2015. The adhesion G protein-coupled receptor GPR56 is a cell-autonomous regulator of oligodendrocyte development. Nat Commun 6:6121.

Gómez del Pulgar T, Velasco G, Guzmán M. 2000. The CB1 cannabinoid receptor is coupled to the activation of protein kinase B/Akt. Biochem J 347:369-73.

Gomez O, Arevalo-Martin A, Garcia-Ovejero D, Ortega-Gutierrez S, Cisneros JA, Almazan G, Sánchez-Rodriguez MA, Molina-Holgado F, Molina-Holgado E. 2010. The constitutive production of the endocannabinoid 2-arachidonoylglycerol participates in oligodendrocyte differentiation. Glia 58:1913-27.

Gomez O, Sanchez-Rodriguez A, Le M, Sanchez-Caro C, Molina-Holgado F, Molina-Holgado E. 2011. Cannabinoid receptor agonists modulate oligodendrocyte differentiation by activating PI3K/Akt and the mammalian target of rapamycin (mTOR) pathways. Br J Pharmacol 163:1520-32.

Gomez O, Sanchez-Rodriguez MA, Ortega-Gutierrez S, Vazquez-Villa H, Guaza C, Molina-Holgado F, Molina-Holgado E. 2015. A Basal Tone of 2-Arachidonoylglycerol Contributes to Early Oligodendrocyte Progenitor Proliferation by Activating Phosphatidylinositol 3-Kinase (PI3K)/AKT and the Mammalian Target of Rapamycin (MTOR) Pathways. J Neuroimmune Pharmacol 10:309-17.

Gorzkiewicz A, Szemraj J. 2018. Brain endocannabinoid signaling exhibits remarkable complexity. Brain Res Bull 142:33-46.

Grigoriadis N, van Pesch V, Group P. 2015. A basic overview of multiple sclerosis immunopathology. Eur J Neurol 22 Suppl 2:3-13.

Gulyas AI, Cravatt BF, Bracey MH, Dinh TP, Piomelli D, Boscia F, Freund TF. 2004. Segregation of two endocannabinoid-hydrolyzing enzymes into pre- and postsynaptic compartments in the rat hippocampus, cerebellum and amygdala. Eur J Neurosci 20:441-58.

Gutiérrez-Rodríguez A, Bonilla-Del Río I, Puente N, Gómez-Urquijo SM, Fontaine CJ, Egaña-Huguet J, Elezgarai I, Ruehle S, Lutz B, Robin LM and others. 2018. Localization of the cannabinoid type-1 receptor in subcellular astrocyte compartments of mutant mouse hippocampus. Glia 525:1417-31.

Gutiérrez-Rodríguez A, Puente N, Elezgarai I, Ruehle S, Lutz B, Reguero L, Gerrikagoitia I, Marsicano G, Grandes P. 2017. Anatomical characterization of the cannabinoid CB1 receptor in cell-type-specific mutant mouse rescue models. J Comp Neurol 525:302-318.

Hájos N, Katona I, Naiem SS, MacKie K, Ledent C, Mody I, Freund TF. 2000. Cannabinoids inhibit hippocampal GABAergic transmission and network oscillations. Eur J Neurosci 12:3239-49.

Han J, Kesner P, Metna-Laurent M, Duan T, Xu L, Georges F, Koehl M, Abrous DN, Mendizabal-Zubiaga J, Grandes P and others. 2012. Acute cannabinoids impair working memory through astroglial CB1 receptor modulation of hippocampal LTD. Cell 148:1039-50.

Harrington EP, Zhao C, Fancy SP, Kaing S, Franklin RJ, Rowitch DH. 2010. Oligodendrocyte PTEN is required for myelin and axonal integrity, not remyelination. Ann Neurol 68:703-16.

Hashimotodani Y, Ohno-Shosaku T, Tsubokawa H, Ogata H, Emoto K, Maejima T, Araishi K, Shin HS, Kano M. 2005. Phospholipase Cbeta serves as a coincidence detector through its Ca2+ dependency for triggering retrograde endocannabinoid signal. Neuron 45:257-68.

Hebert-Chatelain E, Desprez T, Serrat R, Bellocchio L, Soria-Gomez E, Busquets-Garcia A, Pagano Zottola AC, Delamarre A, Cannich A, Vincent P and others. 2016. A cannabinoid link between mitochondria and memory. Nature 539:555-59.

Herkenham M, Lynn AB, Johnson MR, Melvin LS, de Costa BR, Rice KC. 1991. Characterization and localization of cannabinoid receptors in rat brain: a quantitative in vitro autoradiographic study. J Neurosci 11:563-83.

Herkenham M, Lynn AB, Little MD, Johnson MR, Melvin LS, de Costa BR, Rice KC. 1990. Cannabinoid receptor localization in brain. Proc Natl Acad Sci U S A 87:1932-6.

Hernandez M, Casaccia P. 2015. Interplay between transcriptional control and chromatin regulation in the oligodendrocyte lineage. Glia 63:1357-75.

Hernández-Torres G, Cipriano M, Hedén E, Björklund E, Canales Á, Zian D, Feliú A, Mecha M, Guaza C, Fowler CJ and others. 2014. A reversible and selective inhibitor of monoacylglycerol lipase ameliorates multiple sclerosis. Angew Chem Int Ed Engl 53:13765-70.

Howlett AC. 2002. The cannabinoid receptors. Prostaglandins Other Lipid Mediat 68-69:619-31.

Hsu KL, Tsuboi K, Chang JW, Whitby LR, Speers AE, Pugh H, Cravatt BF. 2013. Discovery and optimization of piperidyl-1,2,3-triazole ureas as potent, selective, and in vivo-active inhibitors of α/β-hydrolase domain containing 6 (ABHD6). J Med Chem 56:8270-9.

Hua T, Vemuri K, Pu M, Qu L, Han GW, Wu Y, Zhao S, Shui W, Li S, Korde A and others. 2016. Crystal Structure of the Human Cannabinoid Receptor CB. Cell 167:750-762.e14.

Human protein Atlas.2013. www.proteinatlas.org

Ishibashi T, Dakin KA, Stevens B, Lee PR, Kozlov SV, Stewart CL, Fields RD. 2006. Astrocytes promote myelination in response to electrical impulses. Neuron 49:823-32.

Ishii A, Furusho M, Dupree JL, Bansal R. 2014. Role of ERK1/2 MAPK signaling in the maintenance of myelin and axonal integrity in the adult CNS. J Neurosci 34:16031-45.

Ishii A, Fyffe-Maricich SL, Furusho M, Miller RH, Bansal R. 2012. ERK1/ERK2 MAPK signaling is required to increase myelin thickness independent of oligodendrocyte differentiation and initiation of myelination. J Neurosci 32:8855-64.

Jean-Gilles L, Feng S, Tench CR, Chapman V, Kendall DA, Barrett DA, Constantinescu CS. 2009. Plasma endocannabinoid levels in multiple sclerosis. J Neurol Sci 287:212-5.

Kahn MA, Kumar S, Liebl D, Chang R, Parada LF, De Vellis J. 1999. Mice lacking NT-3, and its receptor TrkC, exhibit profound deficiencies in CNS glial cells. Glia 26:153-65.

Kano M, Ohno-Shosaku T, Hashimotodani Y, Uchigashima M, Watanabe M. 2009. Endocannabinoid-mediated control of synaptic transmission. Physiol Rev 89:309-80.

Karram K, Goebbels S, Schwab M, Jennissen K, Seifert G, Steinhäuser C, Nave KA, Trotter J. 2008. NG2-expressing cells in the nervous system revealed by the NG2-EYFP-knockin mouse. Genesis 46:743-57.

Katona I, Freund TF. 2008. Endocannabinoid signaling as a synaptic circuit breaker in neurological disease. Nat Med 14:923-30.

Katona I, Freund TF. 2012. Multiple functions of endocannabinoid signaling in the brain. Annu Rev Neurosci 35:529-58.

Katona I, Urbán GM, Wallace M, Ledent C, Jung KM, Piomelli D, Mackie K, Freund TF. 2006. Molecular composition of the endocannabinoid system at glutamatergic synapses. J Neurosci 26:5628-37.

Katz Sand I. 2015. Classification, diagnosis, and differential diagnosis of multiple sclerosis. Curr Opin Neurol 28:193-205.

Kawamura Y, Fukaya M, Maejima T, Yoshida T, Miura E, Watanabe M, Ohno-Shosaku T, Kano M. 2006. The CB1 cannabinoid receptor is the major cannabinoid receptor at excitatory presynaptic sites in the hippocampus and cerebellum. J Neurosci 26:2991-3001.

Keough MB, Jensen SK, Yong VW. 2015. Experimental demyelination and remyelination of murine spinal cord by focal injection of lysolecithin. J Vis Exp 26.

Kim S, Kim SH, Kim H, Chung AY, Cha YI, Kim CH, Huh TL, Park HC. 2008. Frizzled 8a function is required for oligodendrocyte development in the zebrafish spinal cord. Dev Dyn 237:3324-31.

Kinney HC, Volpe JJ. 2018. Volpe´s Neurology of the Newborn (Sixth Edition). Elsevier 176-88.

Kipp M, Nyamoya S, Hochstrasser T, Amor S. 2017. Multiple sclerosis animal models: a clinical and histopathological perspective. Brain Pathol 27:123-37.

Kirby BB, Takada N, Latimer AJ, Shin J, Carney TJ, Kelsh RN, Appel B. 2006. In vivo time-lapse imaging shows dynamic oligodendrocyte progenitor behavior during zebrafish development. Nat Neurosci 9:1506-11.

Kmietowicz Z. 2010. Cannabis based drug is licensed for spasticity in patients with MS. BMJ 340:c3363.

Koch M, Kingwell E, Rieckmann P, Tremlett H. 2009. The natural history of primary progressive multiple sclerosis. Neurology 73:1996-2002.

Kozak KR, Prusakiewicz JJ, Marnett LJ. 2004. Oxidative metabolism of endocannabinoids by COX-2. Curr Pharm Des 10:659-67.

Kremer D, Akkermann R, Küry P, Dutta R. 2018. Current advancements in promoting remyelination in multiple sclerosis. Mult Scler:1352458518800827.

Kremer D, Küry P, Dutta R. 2015. Promoting remyelination in multiple sclerosis: current drugs and future prospects. Mult Scler 21:541-9.

Lau BK, Cota D, Cristino L, Borgland SL. 2017. Endocannabinoid modulation of homeostatic and non-homeostatic feeding circuits. Neuropharmacology 124:38-51.

Lee S, Leach MK, Redmond SA, Chong SY, Mellon SH, Tuck SJ, Feng ZQ, Corey JM, Chan JR. 2012. A culture system to study oligodendrocyte myelination processes using engineered nanofibers. Nat Methods 9:917-22.

Leterrier C, Bonnard D, Carrel D, Rossier J, Lenkei Z. 2004. Constitutive endocytic cycle of the CB1 cannabinoid receptor. J Biol Chem 279:36013-21.

Li W, Blankman JL, Cravatt BF. 2007. A functional proteomic strategy to discover inhibitors for uncharacterized hydrolases. J Am Chem Soc 129:9594-5.

Ligresti A, Cascio MG, Pryce G, Kulasegram S, Beletskaya I, De Petrocellis L, Saha B, Mahadevan A, Visintin C, Wiley JL and others. 2006. New potent and selective inhibitors of anandamide reuptake with antispastic activity in a mouse model of multiple sclerosis. Br J Pharmacol 147:83-91.

Liu J, Wang L, Harvey-White J, Osei-Hyiaman D, Razdan R, Gong Q, Chan AC, Zhou Z, Huang BX, Kim HY and others. 2006. A biosynthetic pathway for anandamide. Proc Natl Acad Sci U S A 103:13345-50.

Long JZ, Li W, Booker L, Burston JJ, Kinsey SG, Schlosburg JE, Pavón FJ, Serrano AM, Selley DE, Parsons LH and others. 2009. Selective blockade of 2-arachidonoylglycerol hydrolysis produces cannabinoid behavioral effects. Nat Chem Biol 5:37-44.

Loría F, Petrosino S, Mestre L, Spagnolo A, Correa F, Hernangómez M, Guaza C, Di Marzo V, Docagne F. 2008. Study of the regulation of the endocannabinoid system in a virus model of multiple sclerosis reveals a therapeutic effect of palmitoylethanolamide. Eur J Neurosci 28:633-41.

Lublin FD. 2014. New multiple sclerosis phenotypic classification. Eur Neurol 72 Suppl 1:1-5.

Lucchinetti C, Brück W, Parisi J, Scheithauer B, Rodriguez M, Lassmann H. 2000. Heterogeneity of multiple sclerosis lesions: implications for the pathogenesis of demyelination. Ann Neurol 47:707-17.

Lundgaard I, Luzhynskaya A, Stockley JH, Wang Z, Evans KA, Swire M, Volbracht K, Gautier HO, Franklin RJ, Attwell D and others. 2013. Neuregulin and BDNF induce a switch to NMDA receptor-dependent myelination by oligodendrocytes. PLoS Biol 11:e1001743.

Lutz B, Marsicano G, Maldonado R, Hillard CJ. 2015. The endocannabinoid system in guarding against fear, anxiety and stress. Nat Rev Neurosci 16:705-18.

Mandolesi G, Gentile A, Musella A, Fresegna D, De Vito F, Bullitta S, Sepman H, Marfia GA, Centonze D. 2015. Synaptopathy connects inflammation and neurodegeneration in multiple sclerosis. Nat Rev Neurol 11:711-24.

Mangin JM, Li P, Scafidi J, Gallo V. 2012. Experience-dependent regulation of NG2 progenitors in the developing barrel cortex. Nat Neurosci 15:1192-4.

Manterola A, Bernal-Chico A, Cipriani R, Canedo-Antelo M, Moreno-García Á, Martín-Fontecha M, Pérez-Cerdá F, Sánchez-Gómez MV, Ortega-Gutiérrez S, Brown JM and others. 2018. Deregulation of the endocannabinoid system and therapeutic potential of ABHD6 blockade in the cuprizone model of demyelination. Biochem Pharmacol 157:189-201.

Maresz K, Pryce G, Ponomarev ED, Marsicano G, Croxford JL, Shriver LP, Ledent C, Cheng X, Carrier EJ, Mann MK and others. 2007. Direct suppression of CNS autoimmune inflammation via the cannabinoid receptor CB1 on neurons and CB2 on autoreactive T cells. Nat Med 13:492-7.

Marinelli S, Pacioni S, Bisogno T, Di Marzo V, Prince DA, Huguenard JR, Bacci A. 2008. The endocannabinoid 2-arachidonoylglycerol is responsible for the slow self-inhibition in neocortical interneurons. J Neurosci 28:13532-41.

Maroso M, Szabo GG, Kim HK, Alexander A, Bui AD, Lee SH, Lutz B, Soltesz I. 2016. Cannabinoid Control of Learning and Memory through HCN Channels. Neuron 89:1059-73.

Marques S, Zeisel A, Codeluppi S, van Bruggen D, Mendanha Falcão A, Xiao L, Li H, Häring M, Hochgerner H, Romanov RA and others. 2016. Oligodendrocyte heterogeneity in the mouse juvenile and adult central nervous system. Science 352:1326-9.

Marrs WR, Blankman JL, Horne EA, Thomazeau A, Lin YH, Coy J, Bodor AL, Muccioli GG, Hu SS, Woodruff G and others. 2010. The serine hydrolase ABHD6 controls the accumulation and efficacy of 2-AG at cannabinoid receptors. Nat Neurosci 13:951-7.

Marsicano G, Goodenough S, Monory K, Hermann H, Eder M, Cannich A, Azad SC, Cascio MG, Gutiérrez SO, van der Stelt M and others. 2003. CB1 cannabinoid receptors and on-demand defense against excitotoxicity. Science 302:84-8.

Marsicano G, Lafenêtre P. 2009. Roles of the endocannabinoid system in learning and memory. Curr Top Behav Neurosci 1:201-30.

Marsicano G, Lutz B. 1999. Expression of the cannabinoid receptor CB1 in distinct neuronal subpopulations in the adult mouse forebrain. Eur J Neurosci 11:4213-25.

Marsicano G, Wotjak CT, Azad SC, Bisogno T, Rammes G, Cascio MG, Hermann H, Tang J, Hofmann C, Zieglgänsberger W and others. 2002. The endogenous cannabinoid system controls extinction of aversive memories. Nature 418:530-4.

Martin-Fernandez M, Jamison S, Robin LM, Zhao Z, Martin ED, Aguilar J, Benneyworth MA, Marsicano G, Araque A. 2017. Synapse-specific astrocyte gating of amygdala-related behavior. Nat Neurosci 20:1540-48.

Mato S, Alberdi E, Ledent C, Watanabe M, Matute C. 2009. CB1 cannabinoid receptor-dependent and -independent inhibition of depolarization-induced calcium influx in oligodendrocytes. Glia 57:295-306.

Matsuda LA, Lolait SJ, Brownstein MJ, Young AC, Bonner TI. 1990. Structure of a cannabinoid receptor and functional expression of the cloned cDNA. Nature 346:561-4.

Matute C, Alberdi E, Domercq M, Pérez-Cerdá F, Pérez-Samartín A, Sánchez-Gómez MV. 2001. The link between excitotoxic oligodendroglial death and demyelinating diseases. Trends Neurosci 24:224-30.

Matute C, Sánchez-Gómez MV, Martínez-Millán L, Miledi R. 1997. Glutamate receptor-mediated toxicity in optic nerve oligodendrocytes. Proc Natl Acad Sci U S A 94:8830-5.

McCarthy KD, de Vellis J. 1980. Preparation of separate astroglial and oligodendroglial cell cultures from rat cerebral tissue. J Cell Biol 85:890-902.

McDonald JW, Althomsons SP, Hyrc KL, Choi DW, Goldberg MP. 1998. Oligodendrocytes from forebrain are highly vulnerable to AMPA/kainate receptor-mediated excitotoxicity. Nat Med 4:291-7.

McKenzie IA, Ohayon D, Li H, de Faria JP, Emery B, Tohyama K, Richardson WD. 2014. Motor skill learning requires active central myelination. Science 346:318-22.

Mecha M, Carrillo-Salinas FJ, Feliú A, Mestre L, Guaza C. 2016. Microglia activation states and cannabinoid system: Therapeutic implications. Pharmacol Ther 166:40-55.

Mecha M, Feliú A, Machín I, Cordero C, Carrillo-Salinas F, Mestre L, Hernández-Torres G, Ortega-Gutiérrez S, López-Rodríguez ML, de Castro F and others. 2018. 2-AG limits Theiler's virus induced acute neuroinflammation by modulating microglia and promoting MDSCs. Glia 66:1447-63.

Mechoulam R. 1970. Marihuana chemistry. Science 168:1159-66.

Metna-Laurent M, Marsicano G. 2015. Rising stars: modulation of brain functions by astroglial type-1 cannabinoid receptors. Glia 63:353-64.

Metna-Laurent M, Soria-Gómez E, Verrier D, Conforzi M, Jégo P, Lafenêtre P, Marsicano G. 2012. Bimodal control of fear-coping strategies by CB_1 cannabinoid receptors. J Neurosci 32:7109-18.

Mi S, Miller RH, Lee X, Scott ML, Shulag-Morskaya S, Shao Z, Chang J, Thill G, Levesque M, Zhang M and others. 2005. LINGO-1 negatively regulates myelination by oligodendrocytes. Nat Neurosci 8:745-51.

Möbius W. 2010. Electron Microscopy of the Mouse Central Nervous System. Methods in Cell Biology (Volume 96). Elsevier Inc. Academic Press, p. 475.

Mogha A, D'Rozario M, Monk KR. 2016. G Protein-Coupled Receptors in Myelinating Glia. Trends Pharmacol Sci 37:977-87.

Molina-Holgado E, Vela JM, Arévalo-Martín A, Almazán G, Molina-Holgado F, Borrell J, Guaza C. 2002. Cannabinoids promote oligodendrocyte progenitor survival: involvement of cannabinoid receptors and phosphatidylinositol-3 kinase/Akt signaling. J Neurosci 22:9742-53.

Monory K, Blaudzun H, Massa F, Kaiser N, Lemberger T, Schütz G, Wotjak CT, Lutz B, Marsicano G. 2007. Genetic dissection of behavioural and autonomic effects of Delta(9)-tetrahydrocannabinol in mice. PLoS Biol 5:e269.

Monory K, Massa F, Egertová M, Eder M, Blaudzun H, Westenbroek R, Kelsch W, Jacob W, Marsch R, Ekker M and others. 2006. The endocannabinoid system controls key epileptogenic circuits in the hippocampus. Neuron 51:455-66.

Morales P, Reggio PH. 2017. An Update on Non-CB. Cannabis Cannabinoid Res 2:265-273.

Munro S, Thomas KL, Abu-Shaar M. 1993. Molecular characterization of a peripheral receptor for cannabinoids. Nature 365:61-5.

Murray TJ. 2009. The history of multiple sclerosis: the changing frame of the disease over the centuries. J Neurol Sci 277 Suppl 1:S3-8.

Narayanan SP, Flores AI, Wang F, Macklin WB. 2009. Akt signals through the mammalian target of rapamycin pathway to regulate CNS myelination. J Neurosci 29:6860-70.

Naruse M, Ishizaki Y, Ikenaka K, Tanaka A, Hitoshi S. 2017. Origin of oligodendrocytes in mammalian forebrains: a revised perspective. J Physiol Sci 67:63-70.

Navarrete M, Araque A. 2008. Endocannabinoids mediate neuron-astrocyte communication. Neuron 57:883-93.

Navarrete M, Araque A. 2010. Endocannabinoids potentiate synaptic transmission through stimulation of astrocytes. Neuron 68:113-26.

Navarro G, Morales P, Rodríguez-Cueto C, Fernández-Ruiz J, Jagerovic N, Franco R. 2016. Targeting Cannabinoid CB2 Receptors in the Central Nervous System. Medicinal Chemistry Approaches with Focus on Neurodegenerative Disorders. Front Neurosci 10:406.

Nave KA, Ehrenreich H. 2014. Myelination and Oligodendrocyte Functions in Psychiatric Diseases. JAMA Psychiatry 71:582-4.

Nave KA, Werner HB. 2014. Myelination of the nervous system: mechanisms and functions. Annu Rev Cell Dev Biol 30:503-33.

Navia-Paldanius D, Savinainen JR, Laitinen JT. 2012. Biochemical and pharmacological characterization of human α/β-hydrolase domain containing 6 (ABHD6) and 12 (ABHD12). J Lipid Res 53:2413-24.

Naydenov AV, Horne EA, Cheah CS, Swinney K, Hsu KL, Cao JK, Marrs WR, Blankman JL, Tu S, Cherry AE and others. 2014. ABHD6 blockade exerts antiepileptic activity in PTZ-induced seizures and in spontaneous seizures in R6/2 mice. Neuron 83:361-71.

Nikić I, Merkler D, Sorbara C, Brinkoetter M, Kreutzfeldt M, Bareyre FM, Brück W, Bishop D, Misgeld T, Kerschensteiner M. 2011. A reversible form of axon damage in experimental autoimmune encephalomyelitis and multiple sclerosis. Nat Med 17:495-9.

Nomura DK, Morrison BE, Blankman JL, Long JZ, Kinsey SG, Marcondes MC, Ward AM, Hahn YK, Lichtman AH, Conti B and others. 2011. Endocannabinoid hydrolysis generates brain prostaglandins that promote neuroinflammation. Science 334:809-13.

Okamoto Y, Morishita J, Tsuboi K, Tonai T, Ueda N. 2004. Molecular characterization of a phospholipase D generating anandamide and its congeners. J Biol Chem 279:5298-305.

Oliveira da Cruz JF, Robin LM, Drago F, Marsicano G, Metna-Laurent M. 2016. Astroglial type-1 cannabinoid receptor (CB1): A new player in the tripartite synapse. Neuroscience 323:35-42.

Ortega-Gutiérrez S, Molina-Holgado E, Arévalo-Martín A, Correa F, Viso A, López-Rodríguez ML, Di Marzo V, Guaza C. 2005. Activation of the endocannabinoid system as therapeutic approach in a murine model of multiple sclerosis. FASEB J 19:1338-40.

Palazuelos J, Davoust N, Julien B, Hatterer E, Aguado T, Mechoulam R, Benito C, Romero J, Silva A, Guzmán M and others. 2008. The CB(2) cannabinoid receptor controls myeloid progenitor trafficking: involvement in the pathogenesis of an animal model of multiple sclerosis. J Biol Chem 283:13320-9.

Palmer AE, Giacomello M, Kortemme T, Hires SA, Lev-Ram V, Baker D, Tsien RY. 2006. Ca2+ indicators based on computationally redesigned calmodulin-peptide pairs. Chem Biol 13:521-30.

Pasquali L, Lucchesi C, Pecori C, Metelli MR, Pellegrini S, Iudice A, Bonuccelli U. 2015. A clinical and laboratory study evaluating the profile of cytokine levels in relapsing remitting and secondary progressive multiple sclerosis. J Neuroimmunol 278:53-9.

Patricelli MP, Giang DK, Stamp LM, Burbaum JJ. 2001. Direct visualization of serine hydrolase activities in complex proteomes using fluorescent active site-directed probes. Proteomics 1:1067-71.

Paxinos G, Franklin K. 2012. Paxinos and Franklin´s the Mouse Brain in Stereotaxic Coordinates (4th Edition). Elsevier Inc. Academic Press.p.360.

Pertwee RG, Howlett AC, Abood ME, Alexander SP, Di Marzo V, Elphick MR, Greasley PJ, Hansen HS, Kunos G, Mackie K and others. 2010. International Union of Basic and Clinical Pharmacology. LXXIX. Cannabinoid receptors and their ligands: beyond CB_1 and CB_2. Pharmacol Rev 62:588-631.

Peters A, Folger C. 2013. A website entitled "The fine structure of the aging brain". J Comp Neurol 521:1203-6.

Pfeiffer SE, Warrington AE, Bansal R. 1993. The oligodendrocyte and its many cellular processes. Trends Cell Biol 3:191-7.

Piomelli D. 2003. The molecular logic of endocannabinoid signalling. Nat Rev Neurosci 4:873-84.

Piro JR, Benjamin DI, Duerr JM, Pi Y, Gonzales C, Wood KM, Schwartz JW, Nomura DK, Samad TA. 2012. A dysregulated endocannabinoid-eicosanoid network supports pathogenesis in a mouse model of Alzheimer's disease. Cell Rep 1:617-23.

Pitt D, Werner P, Raine CS. 2000. Glutamate excitotoxicity in a model of multiple sclerosis. Nat Med 6:67-70.

Polman CH, Reingold SC, Banwell B, Clanet M, Cohen JA, Filippi M, Fujihara K, Havrdova E, Hutchinson M, Kappos L and others. 2011. Diagnostic criteria for multiple sclerosis: 2010 revisions to the McDonald criteria. Ann Neurol 69:292-302.

Poursharifi P, Madiraju SRM, Prentki M. 2017. Monoacylglycerol signalling and ABHD6 in health and disease. Diabetes Obes Metab 19 Suppl 1:76-89.

Procaccini C, De Rosa V, Pucino V, Formisano L, Matarese G. 2015. Animal models of Multiple Sclerosis. Eur J Pharmacol 759:182-91.

Pryce G, Ahmed Z, Hankey DJ, Jackson SJ, Croxford JL, Pocock JM, Ledent C, Petzold A, Thompson AJ, Giovannoni G and others. 2003. Cannabinoids inhibit neurodegeneration in models of multiple sclerosis. Brain 126:2191-202.

Pryce G, Cabranes A, Fernández-Ruiz J, Bisogno T, Di Marzo V, Long JZ, Cravatt BF, Giovannoni G, Baker D. 2013. Control of experimental spasticity by targeting the degradation of endocannabinoids using selective fatty acid amide hydrolase inhibitors. Mult Scler 19:1896-904.

Puighermanal E, Marsicano G, Busquets-Garcia A, Lutz B, Maldonado R, Ozaita A. 2009. Cannabinoid modulation of hippocampal long-term memory is mediated by mTOR signaling. Nat Neurosci 12:1152-8.

Qiu J, Tan YW, Hagenston AM, Martel MA, Kneisel N, Skehel PA, Wyllie DJ, Bading H, Hardingham GE. 2013. Mitochondrial calcium uniporter Mcu controls excitotoxicity and is transcriptionally repressed by neuroprotective nuclear calcium signals. Nat Commun 4:2034.

Reich DS, Lucchinetti CF, Calabresi PA. 2018. Multiple Sclerosis. N Engl J Med 378:169-80.

Rey AA, Purrio M, Viveros MP, Lutz B. 2012. Biphasic effects of cannabinoids in anxiety responses: CB1 and GABA(B) receptors in the balance of GABAergic and glutamatergic neurotransmission. Neuropsychopharmacology 37:2624-34.

Richardson WD, Young KM, Tripathi RB, McKenzie I. 2011. NG2-glia as multipotent neural stem cells: fact or fantasy? Neuron 70:661-73.

Rivers LE, Young KM, Rizzi M, Jamen F, Psachoulia K, Wade A, Kessaris N, Richardson WD. 2008. PDGFRA/NG2 glia generate myelinating oligodendrocytes and piriform projection neurons in adult mice. Nat Neurosci 11:1392-401.

Robin LM, Oliveira da Cruz JF, Langlais VC, Martin-Fernandez M, Metna-Laurent M, Busquets-Garcia A, Bellocchio L, Soria-Gomez E, Papouin T, Varilh M and others. 2018. Astroglial CB1 Receptors Determine Synaptic D-Serine Availability to Enable Recognition Memory. Neuron 98:935-944.

Rodriguez JJ, Mackie K, Pickel VM. 2001. Ultrastructural localization of the CB1 cannabinoid receptor in mu-opioid receptor patches of the rat Caudate putamen nucleus. J Neurosci 21:823-33.

Rosenberg SS, Kelland EE, Tokar E, De la Torre AR, Chan JR. 2008. The geometric and spatial constraints of the microenvironment induce oligodendrocyte differentiation. Proc Natl Acad Sci U S A 105:14662-7.

Rueda D, Galve-Roperh I, Haro A, Guzmán M. 2000. The CB(1) cannabinoid receptor is coupled to the activation of c-Jun N-terminal kinase. Mol Pharmacol 58:814-20.

Ruiz A, Alberdi E, Matute C. 2014. CGP37157, an inhibitor of the mitochondrial Na+/Ca2+ exchanger, protects neurons from excitotoxicity by blocking voltage-gated Ca2+ channels. Cell Death Dis 5:e1156.

Sadeghian M, Mastrolia V, Rezaei Haddad A, Mosley A, Mullali G, Schiza D, Sajic M, Hargreaves I, Heales S, Duchen MR and others. 2016. Mitochondrial dysfunction is an important cause of neurological deficits in an inflammatory model of multiple sclerosis. Sci Rep 6:33249.

Sampaio-Baptista C, Khrapitchev AA, Foxley S, Schlagheck T, Scholz J, Jbabdi S, DeLuca GC, Miller KL, Taylor A, Thomas N and others. 2013. Motor skill learning induces changes in white matter microstructure and myelination. J Neurosci 33:19499-503.

Sanchez-Rodriguez MA, Gomez O, Esteban PF, Garcia-Ovejero D, Molina-Holgado E. 2018. The endocannabinoid 2-arachidonoylglycerol regulates oligodendrocyte progenitor cell migration. Biochem Pharmacol 157:180-88.

Savinainen JR, Saario SM, Laitinen JT. 2012. The serine hydrolases MAGL, ABHD6 and ABHD12 as guardians of 2-arachidonoylglycerol signalling through cannabinoid receptors. Acta Physiol (Oxf) 204:267-76.

Schlosburg JE, Blankman JL, Long JZ, Nomura DK, Pan B, Kinsey SG, Nguyen PT, Ramesh D, Booker L, Burston JJ and others. 2010. Chronic monoacylglycerol lipase blockade causes functional antagonism of the endocannabinoid system. Nat Neurosci 13:1113-9.

Scholz J, Klein MC, Behrens TE, Johansen-Berg H. 2009. Training induces changes in white-matter architecture. Nat Neurosci 12:1370-1.

Seehusen F, Baumgärtner W. 2010. Axonal pathology and loss precede demyelination and accompany chronic lesions in a spontaneously occurring animal model of multiple sclerosis. Brain Pathol 20:551-9.

Serafini B, Rosicarelli B, Magliozzi R, Stigliano E, Capello E, Mancardi GL, Aloisi F. 2006. Dendritic cells in multiple sclerosis lesions: maturation stage, myelin uptake, and interaction with proliferating T cells. J Neuropathol Exp Neurol 65:124-41.

Shao Z, Yin J, Chapman K, Grzemska M, Clark L, Wang J, Rosenbaum DM. 2016. High-resolution crystal structure of the human CB1 cannabinoid receptor. Nature.

Shin D, Lin ST, Fu YH, Ptácek LJ. 2013. Very large G protein-coupled receptor 1 regulates myelin-associated glycoprotein via Gαs/Gαq-mediated protein kinases A/C. Proc Natl Acad Sci U S A 110:19101-6.

Shire D, Calandra B, Rinaldi-Carmona M, Oustric D, Pessègue B, Bonnin-Cabanne O, Le Fur G, Caput D, Ferrara P. 1996. Molecular cloning, expression and function of the murine CB2 peripheral cannabinoid receptor. Biochim Biophys Acta 1307:132-6.

Sieber SA, Cravatt BF. 2006. Analytical platforms for activity-based protein profiling--exploiting the versatility of chemistry for functional proteomics. Chem Commun (Camb):2311-9.

Sim FJ, Lang JK, Waldau B, Roy NS, Schwartz TE, Pilcher WH, Chandross KJ, Natesan S, Merrill JE, Goldman SA and others. 2006. Complementary patterns of gene expression by human oligodendrocyte progenitors and their environment predict determinants of progenitor maintenance and differentiation. Ann Neurol 59:763-79.

Sim LJ, Hampson RE, Deadwyler SA, Childers SR. 1996. Effects of chronic treatment with delta9-tetrahydrocannabinol on cannabinoid-stimulated [35S]GTPgammaS autoradiography in rat brain. J Neurosci 16:8057-66.

Simons M, Nave KA. 2015. Oligodendrocytes: Myelination and Axonal Support. Cold Spring Harb Perspect Biol 8:a020479.

Skripuletz T, Gudi V, Hackstette D, Stangel M. 2011. De- and remyelination in the CNS white and grey matter induced by cuprizone: the old, the new, and the unexpected. Histol Histopathol 26:1585-97.

Snaidero N, Simons M. 2014. Myelination at a glance. J Cell Sci 127:2999-3004.

Soliven B. 2001. Calcium signalling in cells of oligodendroglial lineage. Microsc Res Tech 52:672-9.

Sperber BR, McMorris FA. 2001. Fyn tyrosine kinase regulates oligodendroglial cell development but is not required for morphological differentiation of oligodendrocytes. J Neurosci Res 63:303-12.

Spitzer S, Volbracht K, Lundgaard I, Káradóttir RT. 2016. Glutamate signalling: A multifaceted modulator of oligodendrocyte lineage cells in health and disease. Neuropharmacology 110:574-85.

Stankoff B, Aigrot MS, Noël F, Wattilliaux A, Zalc B, Lubetzki C. 2002. Ciliary neurotrophic factor (CNTF) enhances myelin formation: a novel role for CNTF and CNTF-related molecules. J Neurosci 22:9221-7.

Stella N. 2010. Cannabinoid and cannabinoid-like receptors in microglia, astrocytes, and astrocytomas. Glia 58:1017-30.

Stevens B, Porta S, Haak LL, Gallo V, Fields RD. 2002. Adenosine: a neuron-glial transmitter promoting myelination in the CNS in response to action potentials. Neuron 36:855-68.

Stover JF, Lowitzsch K, Kempski OS. 1997. Cerebrospinal fluid hypoxanthine, xanthine and uric acid levels may reflect glutamate-mediated excitotoxicity in different neurological diseases. Neurosci Lett 238:25-8.

Strachan-Whaley M, Rivest S, Yong VW. 2014. Interactions between microglia and T cells in multiple sclerosis pathobiology. J Interferon Cytokine Res 34:615-22.

Sugiura T, Kobayashi Y, Oka S, Waku K. 2002. Biosynthesis and degradation of anandamide and 2-arachidonoylglycerol and their possible physiological significance. Prostaglandins Leukot Essent Fatty Acids 66:173-92.

Sugiura T, Kondo S, Sukagawa A, Nakane S, Shinoda A, Itoh K, Yamashita A, Waku K. 1995. 2-Arachidonoylglycerol: a possible endogenous cannabinoid receptor ligand in brain. Biochem Biophys Res Commun 215:89-97.

Tanaka M, Moran S, Wen J, Affram K, Chen T, Symes AJ, Zhang Y. 2017. WWL70 attenuates PGE2 production derived from 2-arachidonoylglycerol in microglia by ABHD6-independent mechanism. J Neuroinflammation 14:7.

Tanimura A, Yamazaki M, Hashimotodani Y, Uchigashima M, Kawata S, Abe M, Kita Y, Hashimoto K, Shimizu T, Watanabe M and others. 2010. The endocannabinoid 2-arachidonoylglycerol

produced by diacylglycerol lipase alpha mediates retrograde suppression of synaptic transmission. Neuron 65:320-7.

Thomas G, Betters JL, Lord CC, Brown AL, Marshall S, Ferguson D, Sawyer J, Davis MA, Melchior JT, Blume LC and others. 2013. The serine hydrolase ABHD6 Is a critical regulator of the metabolic syndrome. Cell Rep 5:508-20.

Thompson AJ, Baranzini SE, Geurts J, Hemmer B, Ciccarelli O. 2018. Multiple sclerosis. Lancet 391:1622-36.

Tsai HH, Niu J, Munji R, Davalos D, Chang J, Zhang H, Tien AC, Kuo CJ, Chan JR, Daneman R and others. 2016. Oligodendrocyte precursors migrate along vasculature in the developing nervous system. Science 351:379-84.

Vercellino M, Masera S, Lorenzatti M, Condello C, Merola A, Mattioda A, Tribolo A, Capello E, Mancardi GL, Mutani R and others. 2009. Demyelination, inflammation, and neurodegeneration in multiple sclerosis deep gray matter. J Neuropathol Exp Neurol 68:489-502.

Viader A, Blankman JL, Zhong P, Liu X, Schlosburg JE, Joslyn CM, Liu QS, Tomarchio AJ, Lichtman AH, Selley DE and others. 2015. Metabolic Interplay between Astrocytes and Neurons Regulates Endocannabinoid Action. Cell Rep 12:798-808.

Walter L, Dinh T, Stella N. 2004. ATP induces a rapid and pronounced increase in 2-arachidonoylglycerol production by astrocytes, a response limited by monoacylglycerol lipase. J Neurosci 24:8068-74.

Wang S, Sdrulla AD, diSibio G, Bush G, Nofziger D, Hicks C, Weinmaster G, Barres BA. 1998. Notch receptor activation inhibits oligodendrocyte differentiation. Neuron 21:63-75.

Webb M, Luo L, Ma JY, Tham CS. 2008. Genetic deletion of Fatty Acid Amide Hydrolase results in improved long-term outcome in chronic autoimmune encephalitis. Neurosci Lett 439:106-10.

Weiner HL. 2004. Multiple sclerosis is an inflammatory T-cell-mediated autoimmune disease. Arch Neurol 61:1613-5.

Weissert R. 2013. The immune pathogenesis of multiple sclerosis. J Neuroimmune Pharmacol 8:857-66.

Wen J, Ribeiro R, Tanaka M, Zhang Y. 2015. Activation of CB2 receptor is required for the therapeutic effect of ABHD6 inhibition in experimental autoimmune encephalomyelitis. Neuropharmacology 99:196-209.

White R, Gonsior C, Bauer NM, Krämer-Albers EM, Luhmann HJ, Trotter J. 2012. Heterogeneous nuclear ribonucleoprotein (hnRNP) F is a novel component of oligodendroglial RNA transport granules contributing to regulation of myelin basic protein (MBP) synthesis. J Biol Chem 287:1742-54.

Wingerchuk DM, Carter JL. 2014. Multiple sclerosis: current and emerging disease-modifying therapies and treatment strategies. Mayo Clin Proc 89:225-40.

Witte ME, Mahad DJ, Lassmann H, van Horssen J. 2014. Mitochondrial dysfunction contributes to neurodegeneration in multiple sclerosis. Trends Mol Med 20:179-87.

Witting A, Chen L, Cudaback E, Straiker A, Walter L, Rickman B, Möller T, Brosnan C, Stella N. 2006. Experimental autoimmune encephalomyelitis disrupts endocannabinoid-mediated neuroprotection. Proc Natl Acad Sci U S A 103:6362-7.

Witting A, Walter L, Wacker J, Möller T, Stella N. 2004. P2X7 receptors control 2-arachidonoylglycerol production by microglial cells. Proc Natl Acad Sci U S A 101:3214-9.

Woodhams SG, Chapman V, Finn DP, Hohmann AG, Neugebauer V. 2017. The cannabinoid system and pain. Neuropharmacology 124:105-120.

Xiao J, Wong AW, Willingham MM, van den Buuse M, Kilpatrick TJ, Murray SS. 2010. Brain-derived neurotrophic factor promotes central nervous system myelination via a direct effect upon oligodendrocytes. Neurosignals 18:186-202.

Xiao L, Ohayon D, McKenzie IA, Sinclair-Wilson A, Wright JL, Fudge AD, Emery B, Li H, Richardson WD. 2016. Rapid production of new oligodendrocytes is required in the earliest stages of motor-skill learning. Nat Neurosci 19:1210-7.

Ye P, Carson J, D'Ercole AJ. 1995. In vivo actions of insulin-like growth factor-I (IGF-I) on brain myelination: studies of IGF-I and IGF binding protein-1 (IGFBP-1) transgenic mice. J Neurosci 15:7344-56.

Yun B, Lee H, Ghosh M, Cravatt BF, Hsu KL, Bonventre JV, Ewing H, Gelb MH, Leslie CC. 2014. Serine hydrolase inhibitors block necrotic cell death by preventing calcium overload of the mitochondria and permeability transition pore formation. J Biol Chem 289:1491-504.

Zonouzi M, Scafidi J, Li P, McEllin B, Edwards J, Dupree JL, Harvey L, Sun D, Hübner CA, Cull-Candy SG and others. 2015. GABAergic regulation of cerebellar NG2 cell development is altered in perinatal white matter injury. Nat Neurosci 18:674-82.

Zou S, Kumar U. 2018. Cannabinoid Receptors and the Endocannabinoid System: Signaling and Function in the Central Nervous System. Int J Mol Sci 19.

eman ta zabal zazu

Universidad del País Vasco
Euskal Herriko Unibertsitatea

Endokannabinoide sistemaren potentzial terapeutikoa esklerosi anizkoitzean: Oligodendrozitoetako CB_1 hartzaileen eta ABHD6 entzimaren inguruko froga berriak

DOCTOREGO TESIA

Andrea Manterola Juaristi
Biologian lizentziatua
Tesi-Zuzendariak: Susana Mato Santos eta Carlos Matute Almau
Neurozientziak Saila
Euskal Herriko Unibertsitatea UPV/EHU – Neurozientziak Saila
Achucarro Basque Center for Neuroscience
2019an, Leioan

Doktorego tesi honetan aurkeztutako datuen zati bat argitalpen hauen parte izan da:

1. Manterola A, Bernal-Chico A, Cipriani R, Ruiz A, Pérez-Samartín A, Moreno-Rodríguez M, Hsu K-L, Cravatt B, Brown JM, Rodríguez-Puertas R, Matute C*, Mato S* (2018). Re-examining the potential of targeting ABHD6 in multiple sclerosis: efficacy of systemic and peripherally restricted inhibitors in experimental autoimmune encephalomyelitis. *Neuropharmacology* 18: 181-191.
2. Manterola A, Bernal-Chico A, Cipriani R, Canedo-Antelo M, Moreno-García Á, Martín-Fontecha M, Pérez-Cerdá F, Sánchez-Gómez MV, Ortega-Gutiérrez S, Brown JM, Hsu KL, Cravatt B, Matute C, Mato S (2018) Deregulation of the endocannabinoid system and therapeutic potential of ABHD6 blockade in the cuprizone model of demyelination. *Biochem Pharmacol* 141: 189-201.

Doktorego tesi hau ahalbidetu duen finantzazioa: Eusko Jaurlaritzaren 2014-2015 ikasturtean doktoreak ez diren ikertzaileak prestatzeko Doktoratu Aurreko Programako laguntza (PRE_2014_1_32). Ekonomia eta Lehiakortasun Ministerioa (SAF2013-45084-R eta SAF2016-75292-R laguntzak), Eusko Jaurlaritza (IT702-13 laguntza), CIBERNED (PRY-15-404 laguntza), ARSEP Fundazioa eta WOP Fundazioa.

Laburpena

Esklerosi anizkoitza (EA) nerbio sistema zentraleko (NSZ) hanturazko gaixotasunik ohikoena da, gazteen artean desgaitasun neurologikoak sortzen dituena. Gaixotasun honen etiologia zehatza ezagutzen ez den arren, jakina da oligodendrozitoen heriotzarekin eta neuronen endekapenarekin erlazionatutako hanturazko lesioak eragiten dituzten kausa genetiko eta ingurugiroko faktore desberdinen parte hartzea existitzen dela. Paziente desberdinen arteko hanturazko lesioen konposizioa berdina ez den arren, lesio gehienek izaten dituzte T-linfozitoak eta makrofagoak. Hauez gain, zitokinak eta beste hainbat hanturazko eragile askatuz, aktibatutako mikrogliek eta astrozitoek ere hartzen dute parte lesioen garapenean. EA errepikari-atzerakari akutuaren sintomak askotan itzulgarriak izan ohi dira. Hala ere, gaixo gehienek EA sekundarioki progresiboa garatzen dute, non axoien endekapen itzulezinak desgaitasun iraunkorra eragiten duen. Aipatutako EA-ren sintomen arintze hori NSZ-ko **oligodendrozitoen zelula aintzindariek** (OPC) **oligodendrozito heldu mielinizatzaileetan** (OL) bihurtzeko duten ahalmenarekin erlazionatuta egon ohi da nolabait. Horrela, kronikoki desmielinizatutako lesioek OPC-en diferentziazioa inhibituta izatea dute ezaugarri. Ildo honetan, OPC-en diferentziazioa eta mielinaren birsortzea eragin dezaketen molekulen sintesia estrategia terapeutiko garrantzitsua kontsideratzen da EA-ren arloan.

Endokannabinoide sistemak EA-ren sintomatologia murrizteko potentziala duela frogatu dute urteetan zehar eginiko ikerketek. Jakina da marihuana landarean (*Cannabis sativa* L.) aurkitzen diren agonista kanabinoideek EA-ren animali ereduetan sintomak krontrolatzeko ahalmena dutela, babes neuronala, hanturaren aurkako eraginak eta birsortze mekanismoak eskaitzen dituztelarik. Eragin onuragarri hauek neuronetako **CB_1 hartzaileen** eta batik bat zelula hematopoietikoetan adierazten diren CB_2 hartzaileen aktibaziori esker ematen dira. *In vitro* eginiko ikerketen arabera, oligodendrozito leinuko zelulek CB_1 hartzaileak dentsitate baxuan adierazten dituzte eta hauek kannabinoideek EA-an dituzten efektu onuragarrien eraginean parte hartu dezaketela uste da. Hala ere, zelula hauek CB_1 hartzailea *in situ* adierazten dutela frogatzen duten datu fidagarrien falta oztopo bat izan da hartzaile populazio hauek EA-an izan dezaketen garrantzia ulertzeko. Bestalde, kannabisean oinarritutako sendagaien erabilgarritasuna mugatua dela dirudi, askotan, NSZ-ko CB_1 hartzaile populazio zabalaren aktibazioaren ondorioz, efektu ez desiragarriak eragiten baitituzte. Beraz, gaur egungo ikerketen helburu nagusia kannabinoideen efektuak zelula espezifikoetara murriztu eta onura/arrisku ratioa hobetu dezaketen sendagaiak sortzea da.

Endogenoki sintetizatzen diren kannabinoideen artean, , **2-arakidonoilglizerola** (2-AG) babes neuronalaren eragile kontsideratzen da hanturazko prozesuetan. NSZ-ean, 2-AG-a monoazilglizerol lipasa (MAGL) entzimak degradatzen du nagusiki. Bestalde, maila baxuagoan, **ABHD familiako hidrolasa 6** (α/β-hydrolase domain-containing, ABHD6) entzima ere gai da 2-AG-a hidrolizatzeko. MAGL entzimaren inhibitzaileak kannabinoide agonista exogenoek dituzten onura berdinak eragiteko gai dira EA-ren testuinguruan. Hala ere, MAGL entzima kronikoki inhibitzeak eragin ez desiragarriak sortzen dituela ikusi da, horien artean **garuneko CB_1 hartzaileen desentsibilizazioa eta tolerantzia funtzionala**. Eragin hauek entzima honen inhibitzaileen erabilgarritasun terapeutikoa zalantzan jartzen dute. Bestalde, ebidentzia berriek ABHD6 entzima inhibitzeak efektu ez desiragarririk gabeko eragin terapeutikoak izan ditzakeela proposatzen dute, hain zuzen ere EA-rekin erlazionatutako sintomak modulatuz. Hala ere, ABHD6 entzimak oligodendrozitoetan eta gai zurian dituen eragin biologikoak oso gutxi aztertu dira.

Testuinguru honetan, doktorego tesi honen helburu nagusia endokannabinoide sistemak mielinaren biologian duen betebeharra aztertzea izan da, EA gaixotasunari enfasi handia emanez.

Gure **helburu espezifikoak** honakoak izan dira:

1. Helburua. CB_1 hartzaileen lokalizazio ultraegiturala aztertzea sagu helduen garuneko OPC eta OL helduetan eta, bestalde, CB_1 hartzailea adierazten ez duten saguek mielinaren ultraegituran izan ditzaketen aldaketa posibleak aztertzea.

2. Helburua. Gaixotasunaren alde desberdinak antzeratzen diztuzten *in vivo* eta *in vitro* ereduak erabiliz, EA-ren testuinguruan ABHD6 entzima inhibitzea estrategia terapeutiko oparoa izan daitekeen aztertzea.

Doktorego tesi honen **emaitzak** 2 ataletan banatzen dira:

Lehenengo atalean, mikroskopia elektronikoko teknikak erabiliz, sagu helduen hipokanpoko OPC-en %6-ak eta gorputz kailukarako oligodendrozitoen %27-ak CB_1 hartzailea adieratzen dutela ikusi dugu. Gainera, hartzaileen dentsiteak konparatuz, OPC-ek bukaera sinaptikoek baino CB_1 hartzaile adierazpen maila txikiagoa dutela deskribatu dugu. Bestalde, CB_1 hartzailearen faltak mielinaren ultraegituran aldaketa handirik eragiten ez duela ikusi dugu garapeneko mielinizazioaren punturik gorenean.

Emaitzen **bigarren atalean**, gai zuriaren kaltearen testuinguruan eta erreminta farmokologikoak erabiliz, ABHD6 entzima inhibitzeak efektu onuragarri arinak soilik eragiten dituela ikusi dugu. KT182 inhibitzailea era profilaktikoan administratzeak desgaitasun neurologikoen hobetze txiki bat besterik ez du eragiten entzefalomielitis autoimmune esperimentalaren (EAE) animali ereduan. Periferiara murriztutako KT203 inhibitzailea, ordea, ez da gai efektu babesgarri hori eragiteko, onura terapeutikoak izateko NSZ-ko ABHD6-a gaixotasunaren lehen faseetan inhibitu beharra dagoela adieraziz. EAE-ren fase kronikoan aldiz, ez KT182-a ez KT203-a ez dira hanturazko erantzuna murrizteko gai. Kuprizonak eragindako desmielinizazio primarioaren kasuan berriz, ABHD6-a inhibitzeak mielinaren kaltea eta astrogliaren bitarteko hantura murrizten ditu. Hala ere, entzima hau desmielinizatutako testuinguru batean inhibituz gero, ez da mielinaren birsortzea bultzatzeko gai. Bestalde, ABHD6-a inhibitzeak ez du kultibatutako oligodendrozitoak exzitotoxizitatetik babesteko ez hauen diferentziazioa bultzatzeko ahalmenik, hauek KT182-ak eragindako mielinaren babesaren mekanismo bitartekariak izan daitezkeela baztertuz. Alderantziz, KT182 inhibitzailea kultibatutako neuronetan NMDA-k eragindako heriotza eta mitokondrien kaltzio mailen igoera murrizteko gai da ABHD6-arekin zer ikusirik ez daukan mekanismo baten bitartez. Entzimaren blokeo kronikoari dagokionez, gure datuek ABHD6-ren inhibitzaileak denbora luzez administratzeak garuneko zenbait areatako CB_1 hartzaileen funtzio galera eragiten duela erakusten dute.

Laburbilduz, emaitza hauek EA-ren testuinguruan ABHD6 entzima inhibitzearen potentzial terapeutikoa mugatua dela erakusten dute. Bestalde, zelula oligodendroglialek, bai OPC eta bai oligodendrozito mielinizatzaileek, CB_1 hartzailea adierazten dutela erakusten duten frogak aurkeztu ditugu. Aurkikuntza honek hainbat gauza iradoki ditzake, alde batetik, hartzaile populazio hauek, nolabait, mielinizazioaren erregulazioan parte hartu dezaketela, eta bestetik, kannabinoideek EA-an dituzten onurak, neurri batean bada ere, oligodendrozitoek adierazitako CB_1 hartzaileen aktibazioaren ondorioz gerta daitezkeela. Guztira, datu hauek EA-n endokannabinoide sistemak izan dezakeen inplikazioaren inguruko jakintzari informazioa gehitzen diote.

Sarrera

1. Oligodendrozitoak eta mielina

Oligodendrozitoak (OLak) lehendabiziz Pío del Río-Hortegak deskribatu zituen 1921-ean eta nerbio sistema zentralean (NSZ) **mielina** sortzeaz arduratzen diren zelula glialak dira. Mielina nerbio zelulen axoiak estaltzen dituen izaera koipetsuko mintz zelularra da eta ezinbestekoa da nerbio bulkaden garraioa era egokian gerta dadin. Horrez gain, mielinak sostengu metabolikoa ere eskeintzen die axoiei (Nave and Werner, 2014).

Zelula oligodendroglialak zelula aintzindari neural multipotenteetatik sortzen dira garapen enbrionarioaren azken faseetan, seinale espezifikoak jaso eta oligodendrozitoen traskripzio faktore 2-a (oligodendrocyte transcription factor 2, olig 2) adierazten hasten direnean. Lehen diferentziazio fase honetan, zelulek oligodendrozitoen aintzindari zelula (OPC) izena hartzen dute (Naruse et al., 2017). OPC hauek markatzaile bereizgarriak adierazten dituzte, horien artean plaketetatik eratorritako hazkunde faktore alfa (platelet derived growth factor receptor alpha, PDGFRα) eta neurona-glia antigeno 2- proteoglikanoa (neuron-glial antigen 2, NG2) (Richardson et al., 2011). Oligodendrozito heldu mielinizatzaile (OL) gehiengoak jaio eta ondorengo lehen etapetan (saguetan lehen 10 aste inguruetan, gizakietan berriz lehen 5-10 urteetan) sortzen dira OPC-etatik. Hala ere, garun helduetan hainbat zelulek OPC izaten jarraitzen dute (Simons and Nave, 2015), aktibitate neuronalean gertatzen diren aldaketen aurrean OL-etan bihurtu eta mielina sortzeko gaitasuna erakusten dutelarik. Prozesu honek, sortu berri diren zirkuituen kondukzioa hobetuz, NSZ-aren pastizitate eta ikasketa prozesuak ahalbidetzen dituela proposatzen da (McKenzie et al., 2014; Xiao et al., 2016).

1.1. Mielinaren formazio eta birmoldaketa

1.1.1. Oligodendrozitoen diferentziazioa

OPCak OL bihurtzeko jasaten duten diferentziazio prozesua hainbat heltze etapa desberdinez osatzen da. Hori horrela izanda, heltze etapa bakoitzean zelulek morfologia eta markatzaile bereizgarriak adierazten dituzte (Baumann and Pham-Dinh, 2001). Lehen etapan, PDGFRα eta NG2 adierazteagatik bereizten diren zelula horiek, O4 markatzailea adierazten hasi eta morfologia konplexuagoa garatuz, pre-OL-etan bihurtzen dira. Momentu honetan, zelulek beraien mugitzeko ahalmena galtzen duten arren, ugaritzeko gai izaten jarraitzen dute. Aurrerago, aitzindari helduago hauek mielinaren sorkuntzarekin erlazionatuta dagoen 2',3'-zikliko nukleotido-3'-fosfodiesterasa (2',3'-cyclic nucleotide-3'-phosphodiesterase, CNPasa) proteina adierazten hasi eta zelula OL pre-mielinizatzaileetan bihurtzen dira. Azken fasean, zelula hauek oligodendrozito heldu (Mature myelinating OL) izatera pasatzen dira, mielina sortzeko ezin bestekoak diren proteinak adieraziz, horien artean mielinaren proteina proteolipidoa (myelin proteolipid protein, PLP) eta mielinaren oinarrizko proteina (myelin basic protein, MBP) (**1. Irudia**).

Mielinaren sorkuntza era egokian gerta dadin, hainbat urrats gertatu behar dira: OPCen proliferazioa, migrazioa eta diferentziazioa. Urrats hauek guztiak oso ondo kontrolatutako pausoak dira, bai **faktore intrazelularren** bitartez eta bai **seinale exogenoen** bitartez ere (Almeida et al., 2011). Esan beharra dago oligodendrozitoak , *in vitro*, mielina sortu eta finkatutako axoiak eta karbonozko nanofibrak estaltzeko gai direla (Rosenberg et al., 2008; Lee et al., 2012). Honen arabera, seinalizazio bidirekzionalaren beharra nahiko mugatua dela uste da, hau da, oligodendrozitoek mielinizatzeko joera izango lukete baina, etengabeko mielinizazioa ekiditeko, seinale inhibitorioak jasoko lituzkete hainbat tokitan (Nave and Ehrenreich, 2014).

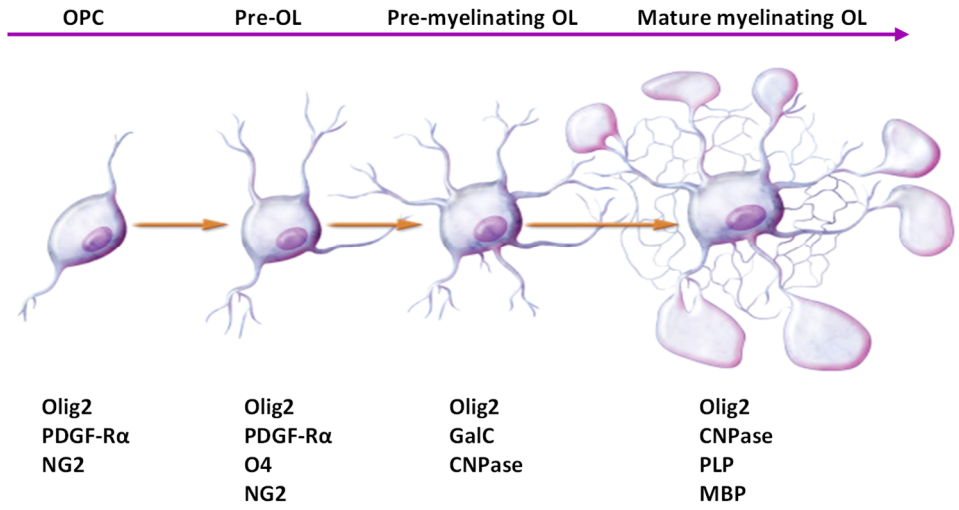

1.Irudia. Oligodendrozito leinu-ko zelulen diferentziazio etapa desberdinen markatzaileak. Irudiak oligodendrozito leinuaren pregresioa erakusten du, oligodendrozitoen zelula antzindarietatik (OPC) hasi eta oligodendrozito mielinizatzaile helduetaraino (Mature myelinating OL). Kinney and Volpe, 2018 –en oinarritua.

Erregulatzaile traskripzionalak dira, oligodendrozitoen kromatinaren birmoldaketa, histonen eraldaketa eta DNA aren metilazioa eraginez, zelula horien diferentziazio eta heltze prozesuak erregulatzen dituzten **seinale intrazelularrak** (Hernandez and Casaccia, 2015). OPC-ak ugaritzeko gaitasun haundia duten zelula bipolarrak dira, kromatina traskripzionalki-aktiboa izateagatik nabarmentzen direnak. Horrela, ziklo zelularreko gene asko eta diferentziazio prozesuak ahalbidetzen dituzten geneak inhibitzen dituzten faktoreak (Adibidez: *Hes5*, *Tcf7l2*, *Id2/Id4*, *Sox5*, *Sox6*, *Sox11*…) adierazten dituzte. Hauek zelulak ugaritzen jarraitzea eta mielinarekin erlazionatutako geneak ez adieraztea bermatuko dute. Heltze prozesua berriz bi eratara erregulatuko da, alde batetik mielinarekin erlazionatutako geneak erreprimitzen dituzten faktoreak inhibitzeko gai diren molekulen bitartez (*E2f4* eta *Yy1* barne), eta bestetik, mielinarekin erlazionatutako geneen adierazpena positiboki erregulatuko duten faktoreen (*Myrf* eta *Sox 10* barne) bitartez. Garrantzitsua da azpimarratzea, askotan, gene desberdinen adierazpen maila eta proteinen ugaritasuna ez datozela bat, mikroRNA desberdinek RNA mezularien egonkortasuna baldintzatzen baitute oligodendrozito leinuaren progresioaren beste erregulazio metodo bezala (Barca-Mayo and Lu, 2012).

Seinale extrazelularrak berriz axoietatatik datozten seinale juxtatakrinoek, matrize extrazelularreko (ECM) elementuek eta mikroglia/makrofago eta astrozitoek askatutako faktore disolbagarriek osatzen dituzte (Nave and Werner, 2014). Seinale kilikarien artean honako hauek bereiz daitezke: axoietako neurregulina /ErbB hartzailearen arteko seinalizazioa (Lundgaard et al., 2013), ECM-ko lamininak eragindako oligodendrozitoetako integrina eta distroglikano hartzaileen aktibazioa (Colognato and Tzvetanova, 2011), astrogliako leukemia faktore inhibitzailearen (LIF) bitarteko seinalizazioa (Ishibashi et al., 2006), hazkuntza faktore epidermala (EGF) (Aguirre et al., 2007), intsulina hazkuntza I faktorea (IGF-I) (Ye et al., 1995), fibroblastoen hazkuntza faktorea (FGF) (Furusho et al., 2012), faktore neurotrofiko ziliarra (CNTF) (Stankoff et al., 2002), garunetik deribatutako faktore neurotrofikoa (BDNF) (Xiao et al., 2010) eta neurotrofina 3-a (NT-3) (Kahn et al., 1999) besteak beste. Bestalde, mielinizazioaren kontrol negatiboa atxikidura-zelularreko hainbat molekulek eragiten dute, horien artean, Atxikidura molekula neural polisialilatua (PSA-

NCAM) (Charles et al., 2000), Jagged1/Notch-1 seinalizazioa (Wang et al., 1998), LINGO-1/RhoA seinalizazioa (Mi et al., 2005) eta wingless/int (Wnt) ligandoak (Fancy et al., 2009).

Aurkikuntza azpimarragarrien arabera, **G-proteinei** atxikitutako hartzaileek (GPCR) mielinizazio prozesuaren hainbat etapa erregulatzen dituzte. (Mogha et al., 2016). Adibidez, garapeneko lehen faseetan, Wnt ligandoek OPC-en heltzea negatiboki erregulatzen dute GPCR-ei lotu eta β-kateninaren translokazioa eta ondorengo Tcf/Lef traskripzioaren aktibazioa eraginez (Kim et al., 2008). Aldi berean, Wnt bidezko seinalizazioak, Cxcl12- ren seinalizazioarekin batera, Cxcr4 GPCR-aren aktibazioa burutuz, OPCen migrazioa ere erregulatzen du (Tsai et al., 2016). Bestalde, Gpr56/Adgrg1 atxikidura proteinak OPC-ek ugaritze ahalmena mantentzea bermatzen du, $G\alpha_{12/13}$ -areakin duen interakzioaren bitartez, diferentziazio prozesua inhibitzen duen RhoA proteina aktibatuz. Horregatik, GPCR-en adierazpen maila jeitsi egiten da oligodendrozito premielinizatzaileetan eta ia aurkiezina bihurtu oligodendrozito heldu mielinizatzaileetan (Giera et al., 2015). Azkenik, rodopsina familiako Gpr17 eta Gpr37 proteinak heltze prozesuaren erregulatzaile oso garrantzitsuak kontsideratzen dira. Gpr17-a zelula premielinizataileetan adierazi eta oligodendrozito heldu mielinizatzaileetan galtzen den bitartean, Gpr37-ren adierazpena mantendu egiten da oligodendrozito helduetan. Bi proteinek oligodendrozitoen diferentziazioa $G\alpha_{i/o}$-en bidezko seinalizazioari esker inhibitzen dute, AMP zikliko mailak jaitsiz eta Raf-MAPH-ERK bidea aktibatuz. Bide honen eraginez, ERK1/2 ez da nukleora traslokatzen eta, beraz, *Myrf* traskripzio fakore pro-mielinizatzailearen maila jaitsi eta Hes56 proteina inhibitorioaren adierazpen maila igotzen da (Shin et al., 2013).

Azkenik, kontutan hartu behar da mielinizazio prozesua, axoietatik askatutako **neurotrasmisoreen** bitartez, neuronen aktibitateak ere modulatzen duela. Neurotrasmisore horien artean adenosina (Stevens et al., 2002), glutamatoa (Mangin et al., 2012) eta GABA (Zonouzi et al., 2015) aurkitzen dira besteak beste. Glutamatoaren bitartekoa da orainarte gehien aztertu den ´neurotrasmisoreen bidezko mielinizazioaren erregulazioa´. Ezagutzen denaren arabera, AMPA/kainato hartzaile ionotropikoen aktibazioak OPC-en ugaritzea inhibitzen duen bitartean, NMDA hartzaile metabotropikoen aktibazioak zelulen heltze eta diferentziazioa bultzatzen du (Spitzer et al., 2016).

Seinale guzti hauek integratzeaz eta diferentziazio maila egokia lortzeaz gain, oligodendrozitoek mielinizazio aktiboa era egokian bukatu eta mielinaren mantenua bermatu behar dute. Prozesu hau erregulatzen duten molekulen artean Fyn eta FAK kinasak aurki ditzakegu, eta baita kaltzioa ere (Ca^{2+}), bigarren mezulari gisa jokatuz, PKC, ERKs, CREB eta Ca^{2+}/kalmodulina kinasa II eta IV-en aktibazioa eragin eta mielinizazioa erregulatzen duena (Soliven, 2001).

Fyn kinasaren adierazpena nagusi da oligodendrozitoen diferentziazio prozesuan eta beharrezkoa mielinizazioa eta MBP-ren itzulpena era egokian gerta daitezen (White et al., 2012). Horregatik, Fyn adierazten ez duten saguek hipomielinizazioa eta oligodendrozito galera erakusten dute gai zurian (Sperber and McMorris, 2001). Horren antzera, FAK kinasak ECM ko seinaleak barneratu eta oligodendrozitoen zitoeskeletoan aldaketak eragiten ditu diferentziazioa eta mielinizazioa bultzatuz. FAK adierazten ez duten saguek ere arazoak erakusten dituzte oligodendrozitoen prozesu zelularren hazkuntzan (Forrest et al., 2009).

Gako extrazelular askok (neurregulina 1, BDNF, IGF-1 eta FGF besteak beste) beraien eragina mitogenoz aktibatutako proteina kinasak (MAPK)/extrazelularki erlazionatutako kinasak (ERK) osatutako seinalizazio bidea aktibatuz burutzen dituzte (Ahrendsen and Macklin, 2013). Adibidez, FGR1/2 dierazten ez duten saguek ERK proteina gutxiago aktibatzen dute eta, nahiz eta hasieran oligodendrozito normalak adierazi, mielinizazio prozesua ez dute ondo burutzen. (Furusho et al.,

2012). Bestalde, ERK1/2-ren baldintzapeko ablazioak diferentziazio akastuna eta dismielinizazioa eragiten ditu (Galabova-Kovacs et al., 2008; Ishii et al., 2012). Horrez gain, p38 MAPK bideak positiboki erregulatzen du oligodendrozitoen diferentziazioa, ERK eta kinasa c-Jun N-terminal (JNK) proteinen bitartez, c-Jun-ek eragiten duen mielinarekin erlazionatutako geneen inhibizioa blokeatuz (Chew et al., 2010). NSZ helduan ERK1/2 aren ablazioa eraginez gero, mielinarekin erlazionatutako geneen adierazpena jaitsi egiten da axoien endekapen berantiarra, astrogliosia eta oligodendrozitoen galera eraginez. Aurkikuntza hauek guztiek argi erakusten dute ERK1/2 MAPK seinalizazioak mielinaren eta axoien osotasunaren mantenuan duen garrantzia (Ishii et al., 2014).

Fosfatidilinositol-3-kinasa (PI3K)/akt eta rapamizinaren ugaztun itua-k (mTOR) osatzen dituzten seinalizazio bideek ere badute garrantzia seinale extrazelularrak (neuregulinak, integrinak, IGF-1, NT-3 eta LIF besteak beste) barneratzeko orduan (Ahrendsen and Macklin, 2013). Akt-ren bitarteko seinalizazioa, ur gora, bigarren mezulari lipidikoek aktibatzen dute eta, ur behera, Fyn-ek eta FAK-ek (Colognato and Tzvetanova, 2011). Hainbat estrategia molekular erabiliz, laborategi desberdinek, Akt/mTOR bitarteko seinalizazioa NSZ-eko mielinzazioaren erregulatzaile nagusienetako bat dela erakutsi dute. Horrela, oligodendrozitoetan Akt konstitutiboki aktibo aurkitzeak NSZ-aren hipermielinizazioa eragiten duela ikusi da, nahiz eta OPC-en biziraupena ez kaltetu (Flores et al., 2008). Bestalde, fosfatasa eta tensina homologoa (PTEN) adierazten ez duten saguek ere hipermielinizazioa erakuten dute NSZ-ean, PTEN-ek Akt-ren aktibatzailea den PIP3 aren produkzioa murriztu egiten baitu (Harrington et al., 2010). Hala ere, deskribatu denaren arabera, PTEN-en delezioak eragindako Akt/mTOR-en gehiegizko aktibazioak ondoriotzat ematen duen hipermielinizazioak axoien endekapena sortzen du, beraz, ez dirudi estrategia terapeutiko bezela erabili daitekeenik desmielinizazioa eragiten duten gaixotasunetan.

1.1.2. Mielinaren biogenesia eta konpaktazioa

OPC-ak zelula multipolarrak dira eta beraien prozesuak filopodioen antzera hedatu egiten dira (Kirby et al., 2006). Neuronen axoiarekin lehen kontaktua egiten dutenean, OPC-en prozesuek atzera egin dezakete edo kontrakoa, egonkortu. Egonkortuz gero, mintz espezializatu bat eratzen da, komunikazio axogliala sortu eta lehen aipatutako seinale guztiak martxan jarriz (**2. Irudia**).

Jaio osteko garapenean, oligodendrozitoen mielina mintza 5,000 μm^2 hasi daiteke eguneko (Pfeiffer et al., 1993). Mielina heldua 160 mintz geruza izatera hel daiteke eta mielina segmetuak, internodo bezala ezagutuak, 1.7 mm izaterarte heda daitezke (Nave and Werner, 2014). Mikroskopio elektroniko bidezko analisiek erakutsi dutenaren arabera, estruktura hau triangelu forma duen oligodendrozito mintzaren hedadura bakarrak osatzen du. Horrela, kanpoen dagoen geruza oligodendrozitoarekin kontaktuan aurkitzen da eta barneko geruza, ´inner tongue´ bezala ezagutzen dena, berriz, neuronaren axoiarekin kontaktuan. Mielinizazio prozesua 2 mugimendu nagusietan oinarritzen da; Alde batetik, ´wrapping´ izena hartzen duena, non ´inner tongue´-a axoiaren inguaruan hedatzen joaten den lehenago sortutako geruzen azpitik mielina geruza berriak sortuz, eta bestalde, Ranvier nodoen alde banatara eta internodoaren luzera haundituz gertatzen den hedapen laterala. Mielinaren garapen egokiak kanal zitoplasmatikoak dituen sistema konplexu baten eraketaren beharra ere badu. Sistema hau mikrotubuluz eta garraio besikulaz osatua egon ohi da eta sintetizatu berri diren mielinaren osagarriak oligodendrozitoaren somatik hedatzen ari den barne geruzara heltzea bermatzen du (**2. Irudia**). Kanal zitoplasmatiko hauek betirako irauten duten arren, kopurua asko jaisten da garapeneko mielinizazioa amaitzen denean (Snaidero and Simons, 2014). Oligodendrozito eta axoien artean gertatzen den komunikazio honek mielina estruktura dinamiko-plastikoa izatea eragiten du.

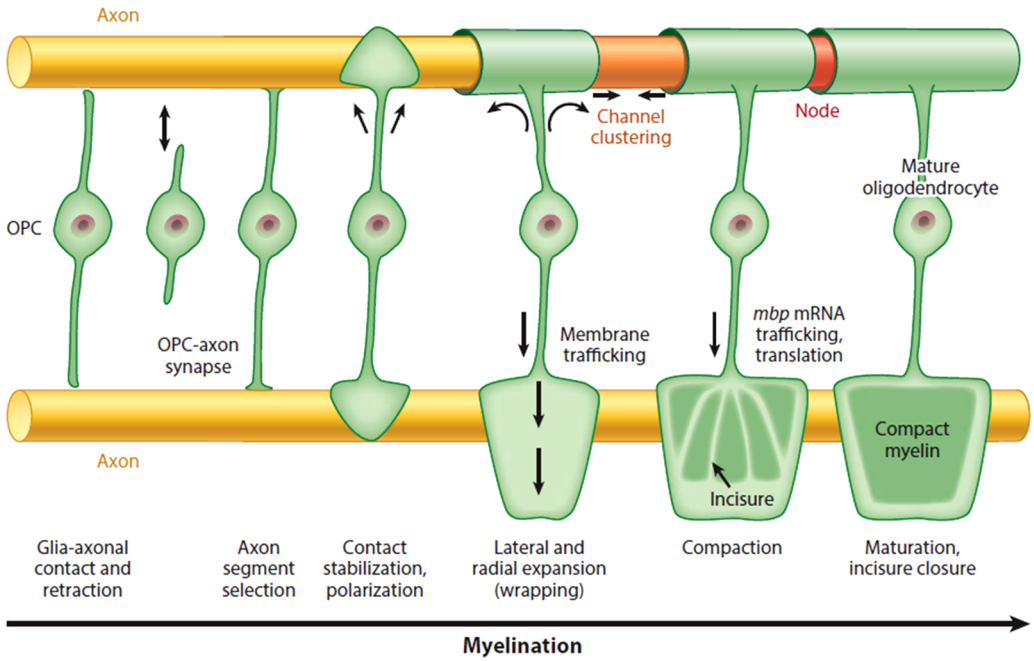

2. Irudia. Mielinizazio prozesuaren irudi eskematikoa. OPC-ak axoiekin kontaktua sortu ostean mielinizazio prozesua hasten da. Irudiaren beheko partean mielina mintza kiribildu gabe ikus dezakegu. Axon, Axoia; OPC-axon synapse, OPC eta axoiaren arteko kontaktua; Glia-axonal contact and retraction, Glia eta axoiaren arteko kontaktua eta OPCaren atzera-egitea; Axon segment selection, Axoi zatiaren hautaketa; Contact stabilization polarization, Kontaktuaren egonkortzea eta polarizazioa; Membrane trafficking, Mintzeko zirkulazioa; Incisure, Kanala; Node, Ranvier nodoa; *mbp* mRNA trafficking and traslation, *mbp* mRNA-ren garraio eta itzulpena; Compact myelin, mielina konpaktatua; Maturation, Heltzea. Nave and Werner, 2014-etik hartua.

Azkenik, mielinarean konpaktazioa gertatzen da. Konpaktazio prozesu hau, garapeneko lehen etapetan, mielinaren kanpokaldeko geruzetan hasi eta bai radialki eta bai longitudinalki zabalduz joaten da. Ondo jakina da MBP eta CNPasa proteinek ezinbesteko eginbeharra betetzen dutela prozesu honetan (Snaidero and Simons, 2014). MBP proteina kodifikatzen duen mRNA oligodendrozitoaren nukleotik mielinaren barne geruzetara garraiatzen da, bertan itzulpena gertatzen delarik. Ondoren, proteina kanpo geruzetara garraiatzen da eta bertan hasten da konpaktazioa. Bestalde, CNPasa barne geruzetan bi mielina geruzen arteko espazioa mantentzeaz arduratzen da, hedatzen jarraitu behar duen geruza atal horretan mielinaren konpaktazio goiztiarra ekidinez.

1.1.3. Mieliaren plastizitate eta birmoldaketa

Esan bezala, mielina estruktura dinamiko bat da eta, hainbat ikerketek erakutsi duten modura, aktibitate neuronalean gertatuko aldaketei erantzuteko gai da. Garun heldu osasuntsuetan, hainbat seinaleri erantzunez, mielina sortzen duten oligodendrozitoak etengabe garatzen dira OPC-etatik (Rivers et al., 2008). Prozesu honek, mielina berria sortuz, sodio kanalak nodoetan elkartuz (Freeman et al., 2015) eta energi-produkziorako sustratoak transferituz (Fünfschilling et al., 2012), sortu berriak diren zirkuituen bulkadak era egokian garatzea ahalbidetzen du. Testuinguru honetan, erresonantzia magnetikoen (MRI) bitartez, gizakiak zeregin konplexu bat burutzeko entrenatzen

diren bitartean gai zurian aldaketak gertatzen direla ikusi da (Bengtsson et al., 2005; Scholz et al., 2009), eta baita arratoietan ere, hauek entrenamendu motoreak burutzen dituzten bitartean (Sampaio-Baptista et al., 2013). Horrez gain, oligodendrozito berrien generazioa inhibituz gero, *de novo*- mielinizazioa blokeatu egiten dela ikusi da, ikasteko gaitasunean akatsak sortuz (McKenzie et al., 2014). Guztira, mielinaren birmoldaketak ikaste eta oroimenaren eraketan eginbehar esanguratsua betetzen duela erakutsi dute aurkikuntza hauek.

1.2. Esklerosi anizkoitza

Mielinaren haustura nerbio sistema zentral eta periferikoko gaixotasun desmielinizatzaileen zantzu patologiko nagusiena da. Gaixotasun desmielinizatzaile hauek bi talde nagusitan banatzen dira, alde batetik genetikoak diren leukodistrofiak, eta bestetik, adoleszentzia edo gaztaroan garatzen diren eskuratutako gaixotasun desmielinizatzaileak.

Esklerosi anizkoitza (EA) lehen aldiz Jean-Martin Charcotek deskribatu zuen 1868-an eta desmielinizazio fokuak sortzen dituen NSZ-ko hanturazko gaixotasun kroniko bezala ezagutzen da. EA pertsona heldu gaztei eragiten dien gaixotasun ezgaitzaile neurologikorik ohikoena da. EA-ren atlas data basearen arabera (Atlas of MS data base, 2013), 2.3 milioi pertsonek jasaten dute gaixotasun hau munduan, herrialde garatuetan eragin sozio-ekonomiko garrantzitsuak eraginez. Salbuespenak izanda ere, gaixotasun honen distribuzio globala hasi egiten da ekuatoretik aldentzean. Bestalde, gaxoen bi heren inguru emakumeak dira eta sexuen arteko desberdintasun hau handitu egin da azken urteetan. Uste denaren arabera, bai faktore genetikoak eta bai ingurugiro-faktoreak dira desberdintasun horien arduradun (Browne et al., 2014).

EA gaixotasun oso konplexua da, fenotipo kliniko eta patologiko desberdinak erakusten dituena. Hala ere, **desmielinizazioa**, **hantura** eta **endekapen neuronal/axonala** dira patologia honen ezaugarririk nagusienak (Compston and Coles, 2008). EA-ren etiologia argi ezagutzen ez den arren, gehien onartua dagoen teoriaren arabera, gaixotasuna linfozito autoerreaktiboak barrera hematoentzefalikoa zeharkatuz hasten da, NSZ-ko gliaren aktibazioa eta neuro-endekapena eragiten dutelarik (Weiner, 2004). Aipatu beharra dago, azken urteetan oligodendrozitoen heriotza primarioak eta desgaitasun axonal goiztiarrak garrantzia hartu dutela EA-ren sortze eta progresioa eragin dezaketen mekanismo etiopatologiko alternatibo gisa.

1.2.1. Esklerosi anizkoitz moten klasifikazioa

EA-ren diagnostiko irizpidea aldatu egin da denboraren poderioz, ikerkuntzaren eboluzio eta teknologi berrien garapenari esker. Berreritze ratioan, MRI-an eta gaixotasunaren progresioan oinarrituta, EA mota desberdinetan klasifikatzen da, Lublinek 2014an definitu (Lublin, 2014) eta 2017-ko McDonal irizpidean deskribatzen den bezela (Thompson et al., 2018).

EA errepikari-atzerakaria (RRMS). Gaixotasunaren formarik ohikoena. EA mota honen ezaugarririk nagusiena osatze garaiez jarraitutako aurreikusi eziniko erasoak dira. Eraso bakoitzaren artean, gaixoek nolabaiteko egonkortasuna erakusten dute, gaixotasunaren progresio esanguratsurik jasan gabe. (**3. Irudia**). EA-ren Diagnosi Taula Internazionalaren arabera, eraso baten definizioa honakoa da: ´Pazienteak sintomak edo hanturazko desmielinizazio akutu tipikoaren ezaugarrizko seinaleak erakusten ditu NSZ-an, gutxienez 24 iraupenarekin eta infekziorik gabe´ (Polman et al., 2011). Gutxi gora behera, gaixoen %85 inguruk mota honetako EA pairatzen dute, hasiera batean bada ere. Hala ere, paziente askok denboraren poderioz EA sekundarioki progresiboa garatzen dute. Berriki deskribatu denez, batzuetan pazienteek eraso bakar bat jasan dezaketela deskribatu da. Gertaera honi ´Klinikoki isolatutako sindromea´ (CIS) deitu zaio eta EA errepikari-atzerakarien espektroaren barruan kontsideratzen da (Lublin, 2014) (**3. Irudia**).

EA Sekundarioki Progresiboa (SPMS). EA mota hau pairatzen duten gaixoek lehendabizi EA errepikari-atzerakaria izan dute, gerora, itzulezinezko beherakada neurologikoa sortzen duen etapa progresiboa garatuz (Pasquali et al., 2015) (**3. Irudia**). Mota honetako gaixoen %40-ek lehen erasoa jasan eta 20 urte ingurura garatzen dute etapa progresiboa. Kasu gehienetan, SPMS-ak errepikari-atzerakari fasean kaltetutako NSZ-ko areekin zerikusia duten funtzio neurologikoen beherakada graduala sortzen du (Katz Sand, 2015).

EA Primarioki Progresiboa (PPMS). Mota honetako EA duten gaixoek funtzio neurologikoen beherakada progresiboa jasaten dute hasieratik, aurreikusi eziniko erasoak sekula izaten ez dituztelarik (**3. Irudia**). EA kasu guztien artean %10 inguruk izaten dute gaixotasunaren forma hau (Koch et al., 2009). Normalean RRMS-a baino beranduago azaltzen da denboran eta gaixoek pronostiko larriagoa izaten dute.

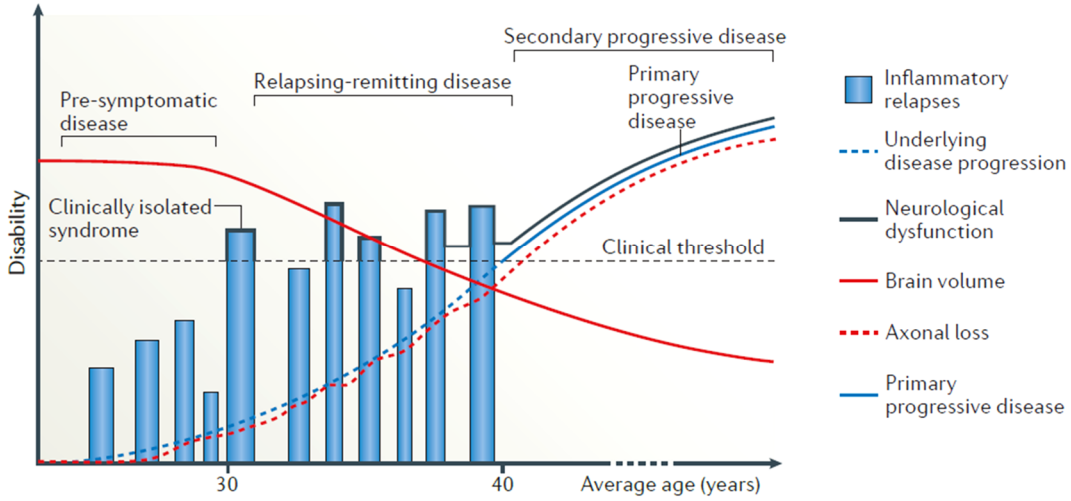

3. Irudia. EA mota derberdinak eta bakoitzak dituen ezaugarriak (disfuntzio neurologikoa, garun atrofia eta galera axonala) azaltzen dituen eskema. Clinically isolated syndrome, Klinikoki isolatutako sindromea; Relapsing-remitting disease, gaixotasun errepikari-atzerakaria; Secondary progressive disease, EA sekundarioki progresiboa; Primary progressive disease, EA primarioki progresiboa; Clinical threshold, Atari klinikoa; Average age (years), Adinaren batezbestekoa (urteak); Inflammatory relapses, Hanturazko erasoak; Underlying disease progresion, Kliniko bihurtu arteko gaixotasunaren progresioa; Neurological dysfunction, Disfuntzio neurologikoa; Brain volume: Garunaren bolumena; Axonal loss: Axoien galera. Dendrou et al., 2015-tik hartua hartua.

1.2.2. Esklerosi anizkoitzaren etiologia eta patofisiologia

EA-ren garapena hainbat faktore desberdinekin erlazionatua izan da, bai ingurumen faktoreekin (D bitaminaren falta, obesitatea, tabako kontsumoa…) eta baita fakotore genetiko eta epigenetikoekin ere (Giza leukozito antigenoaren (HLA) edo Histokonpatibilitate konplexuaren (MHC) familiako geneekin zerikusia dutenak batik bat) (Thompson et al., 2018). Gaixoetan egininko azterketa histopatologiko xehek EA-ko lesioen artean heterogeneotasun handia dagoela erakutsi dute, gaixotasunaren hasiera eta progresioa mekanismo etipopatogeniko konplexuek gidatzen dituztela iradokituz. (Lucchinetti et al., 2000). Urteak pasa ahala, EA gaixotasunaren ezaugarri desberdin hauek antzeratzen dituzten hainbat animali-eredu garatu dira (**1. Kaxa**).

Sistema immuneraren erregulazio akatsa EA-n gertatzen den NSZ-ren kaltearen bitartekari nagusia kontsideratzen da (Grigoriadis et al., 2015). Prozesu honen arduradun nagusiak zelula dendritikoak dira, barrera hematoentzefalikoa zeharkatu eta zitokina desberdinak askatuz, T zelulen diferentziazioa eragiten dutenak. Horrela, IL-12 zitokinak $CD4^+$ T zelulak IFNγ askatzen duten Th11 zelula laguntzaileetan (Th11 helper cells) bihurtzea eragiten du. Bestalde, IL-23-aren presentziak $CD4^+$ T zelulak IL-17-a askatzen duten Th17 zeluletan bihurtzen ditu (Serafini et al., 2006). Aktibatutako T zelula hauek hainbat eragin patogeniko izaten dituzte. Alde batetik, barrera hematoentzefalikoaren iragazkortasuna handitzen dute matrizeko metalopreinasak eta oxigeno espezie erradikalak sortuz. Gainera, monozitoak muinetik errekrutatu eta makrofagoen, mikroglien eta astrozitoen aktibazioa burutuko duten zitokinak askatzen dituzte. Erantzun gisa, zelula aktibo hauek hanturaren bitartekariak eta oxigeno/oxido-nitriko espezie erradikalak askatzen dituzte, azkenik, mielinaren haustura eta axoien endekapena bultzatuz (Strachan-Whaley et al., 2014). Beste alde batetik, $CD8^+$ T zelulek ere askatzen dituzte hantura eragiten duten bitartekariak (IL-17 eta limfotoxina besteak beste) eta beraien presentzia axoien endekapenarekin erlazionatu da (Bitsch et al., 2000). Hauez gain badira patogenesian parte hartzen duten beste zelula batzuk ere, horien artean ´Natural killer´ bezala ezagutzen diren zelulek zitokina desberdinak askatu eta B zelulek berriz antigorputzak eta auto-antigorputzak sortzen dituzte.

Ikuspuntu nagusiak EA-ren garapena sistema inmunearen erregulazio faltak sortzen duela dioen arren, hainbat gaixotan, sortu berri diren lesioetan, oligodendrozitoen apoptosi goiztiarra eta mikroglien aktibazioa deskribatu dira zelula immuneen absentzian (Lucchinetti et al., 2000; Barnett and Prineas, 2004). Aurkikuntza honen arabera, autoimmunitatea, EA duten paziente batzuen kasuan gutxienez, **oligodendrozitoen apoptosi primarioaren** osteko gertakizun bat izan liteke. Deskribapen histopatologiko horietan oinarrituta, EA-ko lesioak 3 talde nagusietan banatzen dira. Ohikoenak I eta II patroiak betetzen dituztenak dira, beraien ezaugarri nagusia fagozito mononuklear eta T zelulen presentzia delarik (II patroiko lesioen kasuan baita immunoglobulinen presentzia ere). Aldiz, III patroiko lesioen kasuan oligodendrozitoen apoptosia eta mielinaren barruko geruzetatik hasten den oligodendropatia dira ezaugarri nagusiak (Reich et al., 2018). PPMS eta SMPS pairatzen dituzten gaixoen kasuan, lesio desmielinizatzaile aktiboak aurkitzea ez dan hain ohikoa, lesio inaktiboak baizik. Lesio inaktibo hauek ongi definitutako desmielinizazio fokoak izaten dira, makrofagoen ausentzian, axoien dentsitate murriztua eta lesioaren inguruan mikroglia aktiboak izateagatik definitzen direnak (**4. Irudia**).

Azken urteetan, **neuro-endekapena** EA-an gertatzen den ezgaitasun neurologikoaren kausa primarioa izan daitekeela proposatzen duen teoriak indar handia hartu du, alterazio sinaptikoa eta galera axonal/neuronala deskribatu baitira EA-ren testuinguruan (Centonze et al., 2009; Vercellino et al., 2009; Seehusen and Baumgärtner, 2010). Gainera, neuro-endekapena gaixotasunaren lehen faseetan gertatu daitekeela uste da, eta ez beti mielina galeraren ondorioz (Seehusen and Baumgärtner, 2010). Horri dagokionez, hainbat ebidentziek **glutamatoak eragindako exzitotoxizitatea** EA-an neuro-endekapena eragiten duten mekanismo nagusienetako bat dela bermatzen dute. Bai neuronak eta bai oligodendrozitoak oso sentikorrak dira glutamato-hartzaileen gehiegizko aktibazio baten aurrean (Choi, 1988; Matute et al., 2001). Gehiegizko aktibazio honek kaltzioaren sarrera masiboa eragiten du, mitokondrien mintzaren despolarizazioa eta oxigeno espezie erreaktiboen askatzea eraginez, zelularen heriotza bideratuko duten seinalizazio bideak aktibatzen dituelarik. Ildo honetan, EA duten pazienteen likido zefalorrakideoan glutamato kontzentrazio haundiak topatu direla aipatu beharra dago (Stover et al., 1997), edota glutamato hartzaileen (AMPA/kainato eta NMDA) antagonistak eragindako efektu babesgarriak deskribatu direla ere (Bolton and Paul, 1997; Pitt et al., 2000), glutamatoaren teoriari pisua emanez.

1. Kaixa: EA-ren sagu-ereduak

Animali-ereduen garapena oso garrantzitsua izan da EA ikertzerako orduan, baita ikuspegi terapeutikoaren aldetik ere. Giza EA-ren ikuspuntu guztiak erreplikatzen dituen eredurik existitu ez arren, badira gaixotasunaren hainbat arlo aztertzeko garatu diren eredu asko.

Entzefalomielitis autoimmune esperimentala (EAE) (Procaccini et al., 2015)

- *Indukzioa*: Mielinaren proteinekin eginiko emultsio antigeniko baten inokulazioaren bitartez. Erantzun immunea indartzeko, sarritan adjubantearen eta toxina pertussisaren laguntza behar izaten da.
- *Mekanismoa*: T zelula autoerreaktiboak NSZ-ra sartzen dira, bertako astrozito eta mikroglien aktibazioa eraginez, eta ondorioz, odoletik makrofagoak eta monozitoak errekrutatuz.
- *Ezaugarriak*: Garun eta bizkar muinaren desmielinizazioa eta endekapen neurologikoa. Lehen sintomak indukzio osteko 9-12. egunean agertzen dira: buztan eta atzeko hanken ahultasuna, aurreko hanken paralisiarekin jarraituz.
- *Aplikazioak*: Sistema immunearan aktibazioa, hantura eta eragile immunomodulatorioen erabilera terapeutikoa aztertu.
- *EAE motak*:
  - *EAE errepikari-atzerakaria Biozzi ABH edo SJL/J saguetan:* MBP_{84-104} edo $PLP_{139-151}$-arekin buruturiko immunizazioak erasoen frekuentzia aztertzea ahalbidetzn du.
  - *EAE kronikoa C57BL/6J saguetan:* $MOG_{35–55}$- arekin buruturiko immunizazioak gaixotasun akutua eragiten du, indarberritze partzial batez jarraitua gaixotasunaren fase kronikoan.
  - *EAE sagu diabetiko ez obesoetan (NOD):* MOG_{35-55} –aren bidezko immunozazioak EA errepikari-atzerakaria sortzen du, erasorik gabeko fase kroniko batez jarraitua.
  - *EAE sagu transgenikoetan:* MOG_{35-55}-aren aurkako T zelulak dituzten (2D2) eta B zelula gehiego adierazten dituzten saguak (IgH MOG). Oso egokiak dira, *in vitro*, zelulen aktibazioa eta funtzioa ulertzeko.

Desmielinizazioa sortzen duten eredu toxikoak

1. <u>*Kuprizona bidezko desmielinizazioa*</u> (Kipp et al., 2017)

- *Indukzioa:* Kuprizona (bis-cyclohexanone-oxaldihydrazone) dietan.
- *Mekanismoa:* Kuprizona kupre kelatzaile bat da, era selektiboan oligodendrozito helduen heriotza eragiten duena, ondorioz, desmielinizazioa eraginez. Eredu honetan NSZ-ko gliaren aktibazioa ikus daiteke ia T zelulen presentziarik gabe. OL-en apoptosia kuprizonak mitokondriei eragindako kalteagatik gertatzen dela uste da.
- *Ezaugarriak*: Kuprizona irensteak oso desmielinizazio errepikakorra sortzen du hainbat garuneko areatan. Gelditu gabeko tratamenduak, 5-6 astetan, erabateko desmielinizazioa eragiten du. Honi, janari normalera itzuliz gero, bermielinizazio fase batek jarraitzen dio.
- *Aplikazioak*: Desmielinizazio primarioa sortzen duten mekanismoak aztertu eta bermielinizazioa bultzatu dezaketen estrategia terapeutikoak frogatzea.

2. <u>*Lisolezitina bidezko desmielinizazioa*</u> (Keough et al., 2015)

- *Indukzioa:* Lisolezitina (LPC) daraman txertoa garun eta bizkar-muinean.
- *Mekanismoa:* Fosfolipasa A2-aren aktibatzaile honek desmielinizazio fokalak sortzen ditu bere izaera detergenteak mielina suntsitzen duelako. Erantzun immunearekin erlazionatua dagoen desmielinizazioa ez izan arren, T eta B zelulak infiltratzen dira (NSZ-aren hobetzea bultzatzen dutenak). Txertoa eman eta 5-6 astetara erabateko bermielinizazioa gertatzen da.
- *Aplikazioak:* Desmielinizazio primarioa eta bermielinizazioa eragiten dituzten mekanismoak ezagutu eta hauek tratatzeko balio dezaketen estrategia terapeutikoak frogatzea.

Karraskarien Theilerren entzefalomielitis birusa (TMEV) (DePaula-Silva et al., 2017)

- *Indukzioa:* TMEV bezalako picornabirusen bitarteko infekzioa.
- *Mekanismoa:* TMEV-aren aurkako $CD4^+$ T zelulek askatutako zitokinek desmielinizazioa bultzatuko duten mikroglia/makrofagoen aktibazioa eragiten dute. Eredu honetan axoien kaltea desmielinizazioren aurretik gertatzen da, neuro-endekapenak T zelulen eta makrofagoen errekrutamendua eragin dezakeela proposatuz. Eredu egokia de EA primarioki progresiboa aztertzeko.
- *Ezaugarriak*: Sintoma nagusiak, 30-60 egunetara agertzen direnak, koordinazio motore kaltetua, inkontinentzia eta axoien endekapena dira.
- *Aplikazioak*: Axoien endekapena eragiten duten mekanismoak aztertu eta berau ekidin dezaketen molekulak aztertzea.

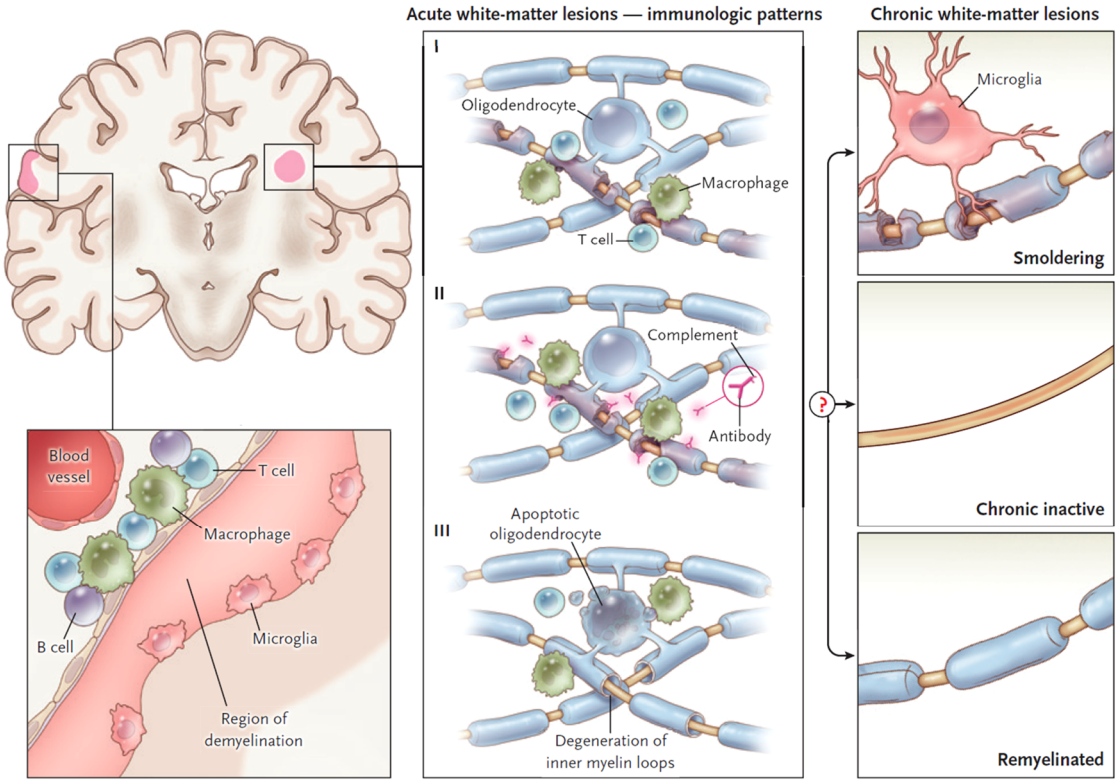

4. Irudia. EA-an aurki daitezkeen lesio motak. Hiru lesio akutu mota bereiz daitezke. I eta II patroiak betetzen dituztenak dira ohikoenak eta sistema immunearen erregulazio faltaren ondorioz agertzen direla uste da. Aldiz, III patroiko lesioek oligodendrozitoen apoptosi primarioa erakusten dute. Fase akutuaren ostean, axoi batzuk bermielinizatu (Remyelinated) egiten dira, beste batzuk aldiz egoera inaktibo kroniko (Chronic inactive) batean mantentzen dira eta, azkenik, lesio batzuk kronikoki aktibo (Smoldering) jarraitzen dute luzaroan. Reich et al., 2018 -etik hartua.

Lesio gehienek kronikoki desmielinzatuta jarraitzen duten arren, kasu batzuetan mielinaren ´konponketa´ espontaneo bat gertzen da . Lesio horiei ´shadow plaques´deitzen zaie (Chang et al., 2012). **Bermielinizazioa** erantzun fisiologiko gisa ulertu eta mielinaren berreskuratzea eragiten duen prozesu birsortzaile bezela deskribatzen da. Prozesu hau OPC-ak errekrutatu eta oligodendrozito heldu mielinizatzaileetan desberdintzeko gaitasunari esker gertatzen da (Franklin and Ffrench-Constant, 2017; Kremer et al., 2018) , originala baino meheagoa den mielina geruza bat sortuz (**5. Irudia**). OPC-en aktibazioa eta errekrutamendua burutzen duten mekanismoak ez dira oraindik guztiz ezagutzen. Uste denaren arabera, **mikrogliak** dira NSZ-eko ehunen kaltea antzematen duten lehen zelulak. Hauek, aktibatzean, seinalizazio molekula desberdinak askatzen dituzte bertako **astrozitoak** aktibatuz, erantzun gisa faktore desberdinak askatu eta OPC-en modulazioa burutuko dutelarik (Franklin and Ffrench-Constant, 2017).

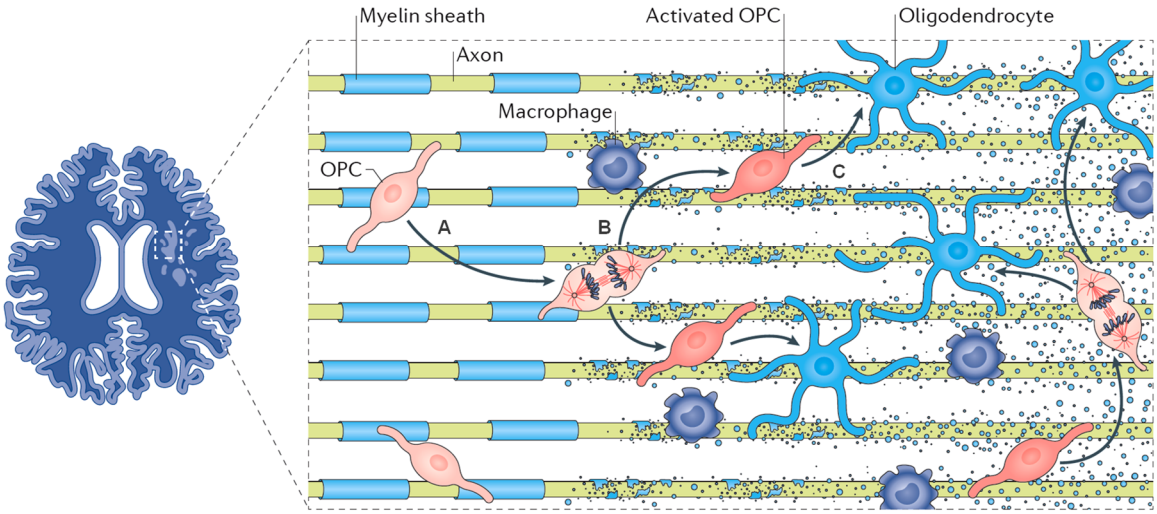

5. Irudia. Bermielinizazioa azaltzen duen irudi eskematikoa. Bermielinizazioa lortzeko honako pausoak era egokian gertatu behar dira: OPC-en errekrutamendua (**A**), ugaritzea (**B**) eta diferentziazioa (**C**), lesionatutako eremuan oligodendrozito mielinizatzaile berriak sortuz. Franklin and Ffrench-Constant, 2017-tik hartua.

EA-n bermielinizazioa gertatzen dela jakina den arren, prozesu hau denboren poderioz ez eraginkor bihurtzen dela ikusi da, endekapen neurologikoaren areagotzea bultzatuz (Franklin, 2002). Hainbat ikerkuntzen arabera, bermielinizazio ahalmen galera hau kaltetutako eremuetan OPC-ek diferentziatzeko gaitasuna galtzen dutelako gertatzen da (Kremer et al., 2018). Horrexegatik, zelula hauen diferentziazioa bultza dezaketen estrategia terapeutikoak garatzea oso gai garrantzitsua bihurtu da EA-ren inguruko ikerkuntzan.

1.2.3. Esklerosi anizkoitzaren tratamendurako gaur eguneko estrategiak

Gaur egun EA tratatzeko existitzen diren ia terapia guztiak tratamendu gaixotasun-eraldatzaileak dira (disease-modifying agents, DMTs). DMT hauek maila desberdinetan aritzen dira, besteak beste antigeno aurkezpenari eraginez edo erantzun immune periferikoa ekidinez (Weissert, 2013). Terapia mota hauek baliogarriak dira EA errepikari-atzerakaria duten gaixoetan eraso kopuruak murriztu eta bizi kalitatea hobetzeko (Wingerchuk and Carter, 2014). Hala ere, gaur egungo DMT-ak ez dira gai neuro-endekapen mekanismoek indarra hartzen duteneko EA-ren fase progresiboak hobetzeko. Beraz, NSZ-a hanturatik babestu eta mielinaren eta neuronen birsorkuntza bultza dezaketen tratamenduak garatzea ezinbestekoa helburua da.

2. **Endokannabinoidea sistema**

Garuneko endokannabinoide sistema hainbat funtzio, besteak beste mugimendua, kognizioa, memoria, aldartea, gorputzaren temperatura edo eta apetitua erregulatzen dituen sistema neuromodulatzailea da. Endokannabinoide sistema hau hartzaile kannabinoideek, estekatzaile endogenoek eta hauen biosintesia eta degradazioa burutzen dituzten entzimek osatzen dute. Hartzaile kannabinoideak **Δ^9-Tetrahidrokannabinolaren** (**Δ^9-THC**) itu nagusiak dira. Δ^9-THC-a marihuana belarretik (*Cannabis sativa* L) datorren konposatu bat da, 5000 urteetan zehar olgeta droga eta sendagarri gisa ibili izan dena.

2.1. Garuneko hartzaile kannabinoideak

1964an konfiskatutako hashish-etik lehen aldiz Δ^9-THC-a isolatu ondoren (Gaoni and Mechoulam, 1964), estruktura antzekoa zuten konpostatu asko sintetizatu ziren. Horrek lehenengo hartzaile kannabinoidea identifikatzea ahalbidetu zuen, zeini kannabinoide hartzaile 1 (**CB_1 hartzailea**) izena eman zitzaion. Hurrengo urteetan hartzaile hau arratoien garun kortexetik klonatzea lortu zen, (Matsuda et al., 1990), baita gizakien testikulu eta garunetik (Gérard et al., 1991) eta azkenik, sagu garunetik ere (Chakrabarti et al., 1995). Ez askoz beranduago, bigarren hartzaile bat identifikatu zen arratoietan (Munro et al., 1993) eta saguetan (Shire et al., 1996) eta honi kannabinoide hartzaile 2 deitu zitzaion (**CB_2 hartzailea**).

CB_1 eta CB_2 hartzaileak G proteinei loturiko hartzeileen superfamiaren parte dira. Hartzaile mota hauek domeinu desberdinez osatzen dira: Domeinu N-terminala, glikosilazio lekuak aurkezten dituena, Domeinu C-terminala, G proteinei lotzen zaiena eta mintzarteko 7 domeinu. Lehendabiziz egin ziren ikerketek erakutsi zutenez, CB_1 hartzaileak batez ere garunean adierazten dira, CB_2 hartzaileak, aldiz, sistema immune periferikoko zeluletan. Hartzaile bakoitzak seinalizazio bide espezifikoak aktibatzen dituzten arren, biek elkarbanatzen dute G_i proteinei lotzeko ahalmena (Howlett, 2002). Azken ikerketek CB_1 proteinaren kristal egitura (Hua et al., 2016; Shao et al., 2016) eta agonista lotzearekin batera hartzaileak jasaten dituen aldaketak deskribatu dituzte. Aurkikuntza hauek asko lagundu dute hartzaileen eta beroiei lotzen zaizkien molekulen ezaugarriak ulertzen.

Garunean, CB_1 hartzaileen adierazpena zabala eta heterogeneo da. Horrela, proteina hau gehien adierazten duten areak memoria eta ikasketarekin erlazionaturikoak (**hipokanpoa eta kortexa**), aktibitate motorearekin erlazionaturikoak (**zerebeloa eta ganglio basala**), jokabide emozionalekin erlazionaturikoak (**amigdala**) eta minarekin erlazionaturikoak (**hipotalamoa**) dira besteak beste (Zou and Kumar, 2018).

Distribuzio zelularrari dagokionez, NSZ-aren barruan, CB_1 hartzaileak **neurona helduetan** adierazten dira batik bat. Zehazki, hartzaile hauek neurona GABAergikoetan kontzentrazio handietan adierazten dira, eta maila askoz baxuagoan zelula glutamatergikoetan (**7. Irudia**) (Marsicano and Lutz, 1999; Kawamura et al., 2006; Gutiérrez-Rodríguez et al., 2017). Hartzaileen gehiengoa **axoien bukaera presinaptikoetan** adierazten dira, non, neurotrasmisoreen liberazioa negatiboki erregulatuz, sinapsien homeostasia bermatzen duten (**7.** eta **8. Irudiak**) (Katona and Freund, 2012). Ikerketa anatomiko eta funtzional askok erakutsi dutenaren arabera, **bukaera postsinaptikoetan** ere adierazten dira CB_1 hartzaileak, non dirudienez, erregulazio prozesu autonomoak burutzen dituzten (Rodriguez et al., 2001; Marinelli et al., 2008; Maroso et al., 2016). Bestalde, CB_1 hartzaileen presentzia **zelula glialetan** ere deskribatu da. Zehazki, mikroskopio elekotronikoz burututako analisien bitartez, **astrozitoek** CB_1 kopuru detektagarriak adierazten dituztela ikusi da (Han et al., 2012; Gutiérrez-Rodríguez et al., 2018). Dentsitate txikietan adierazten diren arren, astrozitoetako CB_1 hartzaileek astrozito eta neuronen arteko komunikazioan eginkizun

garrantzitsua betetzen dute, jokabide eta memoria prozesuetan partez hartuz (Metna-Laurent and Marsicano, 2015; Oliveira da Cruz et al., 2016; Robin et al., 2018). Hainbat *in vitro* buruturiko ikerketek beste glia-zelulek ere, bai mikrogliek (Stella, 2010) eta bai oligodendrozitoek (Gomez et al., 2010; Bernal-Chico et al., 2015), CB_1 hartzaileak adierazten dituztela iradokitzen dute. Hala ere, *in vivo* zelula hauetan CB_1 hartzaileek ze distribuzio eta zein eginkizun fisiologiko betetzen dituzten oraindik ez da argi ezagutzen.

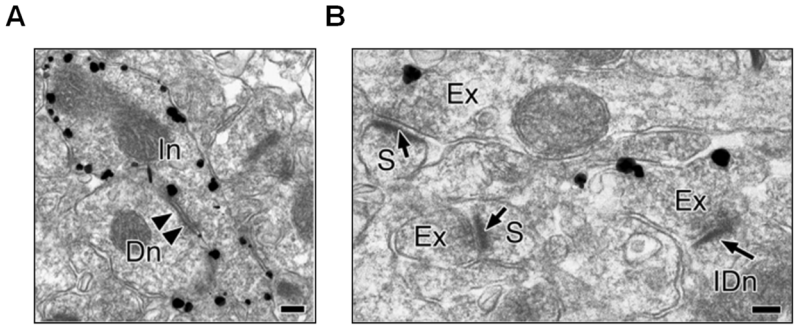

7. Irudia. Saguen hipokanpoan CB_1 hartzaileen kokapena zein den erakusten duten mikroskopio elektroniko bidez lorturiko irudiak. Argazkiek CB_1 hartzaileak markatzen dituzten partikulak erakusten dituzte amaiera sinaptiko inhibitorio (In) (**A**) eta kitzikatzaileetan (Ex) (**B**). Dendrita (Dn), Arantza dendritikoa (S). Kawamura et al., 2006-tik hartua.

Beste GPCR-ekin gertatzen den bezala, CB_1 hartzaileak **mintz plasmatikoan** aurkitzen dira batik bat. Hala ere, azken ikerketen arabera, hartzaile hauek konpartimendu intrazelularretan ere adierazten dira, besteak beste **endosometan** (Leterrier et al., 2004) eta **mitokondrietan** (Bénard et al., 2012; Hebert-Chatelain et al., 2016). Gainera, mitokondrietako CB_1 hartzaileek memoria prozesuetan eta neuronen energi-metabolismoan eginbehar garrantzitsuak betetzen dituztela deskribatu da.

Kannabinoideen **CB_2 hartzaileei** dagokionez, sistema immune periferikoko zelula eta ehunak dira proteina hau gehien adierazten dutenak, eta uste denaren arabera, hauek dira kannabinoideen efektu immunomodulatzaileen bitartekari nagusiak (Berdyshev, 2000; Howlett, 2002). Hauen artean, makrofagoak, $CD4^+$ eta $CD8^+$ T zelulak, B zelulak, ´natural killer´-ak , monozitoak eta neutrofilo polimorfonuklearrak dira CB_2 hartzaile maila altuenak erakusten dituzten zelulak. NSZ osasuntsuan berriz, CB_2 hartzaileak adierazten diren edo ezaren eztabaida existitzen da (Atwood and Mackie, 2010). Horren inguruan, kultibatutako zeluletan burututako Ikerketa farmakologiko batzuk astrozitoek eta mikrogliek CB_2 hartzaile gutxi batzuk adierazten dituztela diote (Stella, 2010; Gomez et al., 2011). Hala ere, NSZ-an hantura ematen denean, **mikrogliak** CB_2 hartzailea adierazten dutela eta adierapen maila zelularen aktibazio mailarekin erlazionatuta dagoela ongi deskribatu da (Mecha et al., 2016). Mikroglietako CB_2 hartzaile horiek zelulen migrazioa eta infiltrazioa erregulatzen dituzte neuro-endekapen prozesuetan (Fernández-Ruiz et al., 2008; Navarro et al., 2016). Hori horrela izanda, CB_2 hartzaileen aktibazioak milaka erantzun immuneei eragiten die. Beraz, kannabinoideek mikroglietako eta sistema immune periferikoko zeluletako CB_2 hartzaileen aktibazioaren bitartez erakusten dituzten hanturaren aurkako eraginak eta neuronetan CB_2

hartzaileen presentzia oso urria dela eta kontutan hartuta, CB_2 selektiboki aktibatzen duten drogen garapenak etorkizun handiko eta efektu psikoaktibo gabeko estrategia terapeutikoa dirudi.

Endokannabioideak, CB_1 eta CB_2 hartzaileak aktibatzeko gaitasuna izateaz gain, beste hartzaile batzuei ere lotu daitezke (Gorzkiewicz and Szemraj, 2018). Adibidez, TRPV1 kanal ionikoek, (normalean pH baxuen eta kapsaizinaren aurrean erantzuten dutenak) hainbat *N*-arakidonoildopamina eta baita ***N*-arakidonoiletanolamina** (**anandamida, AEA**) lotzeko ahalmena dute. (Di Marzo and De Petrocellis, 2010). Kannabinoideak lotzeko ahalmena duten beste hartzaileen artean, peroxisoma proliferatzailez aktibatutako hartzaileak (PPARs), katioi kanal ez selektibo TRPA1 edo TRPM8-ak, 5-HT3-aren antzera estekatzaile bidez aktibatzen diren kanal ionikoak, GPR55 bezalako hartzaile metabotropikoak, glizina eta nikotinaren hartzaileak eta boltai-menpeko kanal ionikoak aurki ditzakegu.

2.2. Endokannabinoideen produkzio eta seinalizazio makineria

Endokannabinoideak mintz zelularreko osagarriak erabiliz sintetizatzen diren mezulari lipidikoak dira. Nahiz eta hainbat molekula identifikatu diren, bi dira endokannabinoide nagusienak: ***N*-arakidonoiletanolamina** (anandamida, AEA) (Devane et al., 1992) eta **2-arakidonoilglizerola** (**2-AG**) (Sugiura et al., 1995). Biak **beharraren arabera** (on demand) sintetizatzen dira, normalean kaltzio intrazelular mailen igoerei erantzunez (Pertwee et al., 2010). Nahiz eta bi endokannabinoideek izan CB_1 eta CB_2 hartzaileetara lotzeko ahalmena, bakoitzak erantzun biologikoak era desberdinetara erregulatzen dituzte (Busquets-Garcia et al., 2011). Esan beharra dago, 2-AG-a kannabinoide hartzaileen agonista osoa den bitartean, AEA-k gehienetan agonista partzial bezala jokatzen duela (Howlett, 2002). Gainera, NSZ-an 2-AG mailak AEA-renak baino 200-800 aldiz altuagoak izan ohi dira (Sugiura et al., 2002) eta, uste denaren arabera, bera da CB_1 hartzaile presinaptikoei lotuz, funtzio sinaptikoa kontrolatzen duen endokannabinoidea (Katona and Freund, 2008).

Endokannabinoideen sintesi eta degradazioa ongi erregulatutako prozesuak dira. AEA sintesi nagusiena kaltzio menpeko ***N*-aziltransferasak** (**NAT**) burutzen du. Honek **azido arakidonikoa** (**AA**) fosfatidilkolinatik fosfatidiletanolaminara tranferitzen du ***N*-azilfosfatidiletanolamina** (**NAPE**) sortuz (Cadas et al., 1996). Bigarren pausoan, N-arakidonil-fosfatidiletanolaminaren Fosfolipasa D-ak (**NAPE-PLD**) katalizatutako erreakzioan, NAPE-tik AEA lortzen da (Okamoto et al., 2004). Alternatiboki, fosfolipasa C-ak (**PLC**) ere hidroliza dezake NAPE-a, produktu bezala fosfo-AEA emanez. Ondoren, fosfo-AEA fosfatasen akzio bitartez defosforilatua izango da AEA lortuz (Liu et al., 2006). Gehienetan aktibitate neuronalak eragindako AEA-ren askatzea kaltzioren menpekoa izan ohi den arren, neuronetan gertatzen den kaltzioaren sarrera ez da AEA sintezia eragiten duen mekanismo bakarra. Hainbat GPCR ren aktibazioak, hoien artean dopaminaren D2 hartzaileenak, edo glutamatoaren hartzaile metabotropikoenak ($mGlu_{1/5}$) edo azetilkolinaren hartzaile M3 muskarinikoenak, AEA ren sintesia eragin dezake (Piomelli, 2003).

2-AG-ren sintesi bide nagusia PLC-ak eragindako mintzeko fosfatidilinositolen hidroliasiaren bitartekoa da, produktu gisa **1,2-diazilglizerola** (**DAG**) sortuz. Ondoren, mintzean integraturik aurkitzen den **diazilglizerol lipasa** (**DGLα/β**) entzimak DAG-a 2-AG-an bihurtzen du (Bisogno et al., 2003; Bisogno, 2008). DGLα edo DGLβ adierazten ez duten saguak erabilita egin diren ikerketen arabera, NSZ-an α forma da 2-AG-aren sintesiaz arduratzen dena, β forma gibelean nagusi den bitartean (Gao et al., 2010; Tanimura et al., 2010). Neuronetan, 2-AG-aren sintesia mintzaren despolarizazioaren edo $mGlu_{1/5}$ edo M_1/M_3 bezalako GPCR hartzaileen aktbazio bitartez gerta daiteke (Hashimotodani et al., 2005; Kano et al., 2009).

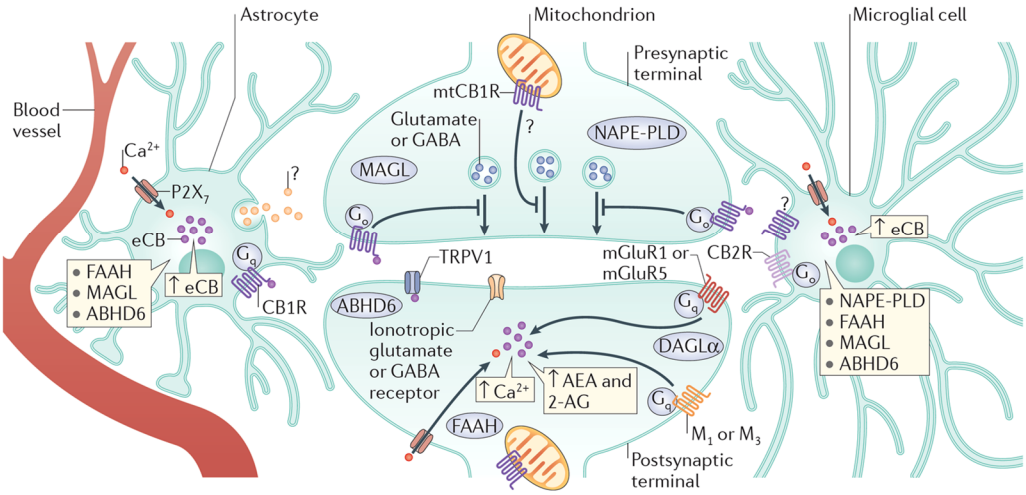

8. Irudia. Neurona eta glia-zeluletako endokannabinoide sistema. CB_1 hartzaileak (CB_1R) bukaera presinaptikoetan adierazi ohi dira, normalean $G_{i/o}$ proteinei lotuta. 2-AG edo AEA bidezko neuronetako CB_1 hartzaileen aktibazioak neurotrasmisioa murrizten du zelula presinaptikoan. CB_1 hartzaileak bai neurona presinaptiko zein postsinaptikoetako mitokondrietan ere adierazten dira ($mtCB_1R$). Hauen aktibazioak fosforilazio oxidatiboa eta ATP-aren sintesia inhibitzen ditu. AEA-ak TRPV1 hartzaileak ere aktibatu ditzake, korronte postsinaptikoak haundituz. 2-AG-ak berriz $GABA_A$ hartzaile postsinaptikoak aktiba ditzake. Despolarizazio postsinaptikoak (hainbat hartzaileren aktibazioak eragindakoa, glutamatoaren hartzaile matabotropikoak barne) 2-AG-aren sintesia martxan jartzea eragiten du diazilglizerol lipasa-α (DAGLα) entzimaren akzioaren bitartez. Orduan, sortu berri den 2-AG horrek akzio atzerakoia eraginez, presinapsian aurkitzen diren CB_1 hartzaileak aktibatzen ditu trasmisio sinaptikoa erreprimituz. 2-AG-a degradatzen duen entzima nagusia monoazilglizerol lipasa (MAGL) da, bukaera presinaptikoan eta astrozitoetan adierazten dena. Bestalde, ABHD familiako α-β-hidrolasa domeinu 6-ak (ABHD6) produkzio tokietako 2-AG mailak erregulatzen ditu. AEA sintetizatzen duen entzima nagusia N-azil fosfatidil etanolamina-fosfolipasa D-a (NAPE-PLD) da, bukaera postsinaptikoan ere agertzen den arren, batik bat bukaera presinaptikoan adierazten dena. Aldiz, AEA hidrolizatzen duen entzima (FAAH) bai bukaera pre zein postsinaptikoetan adierazten da. Mikroglia zelulek hantura prozesuekin erlazionatuta dauden CB_2 hartzaileak adierazten dituzte. Horrez gain, astrozitoek G_q-proteinei lotutako CB_1 hartzaileak adierazten dituzte, behin aktibatuta kaltzio intrazelularraren nibelen gorakada eraginez, ´gliotrasmisoreen´ liberazioa bultzatzen dutenak. Astrozitoetan eta mikroglia zeluletan endokannabinoideen sintesia ATP-ak eragindako P_2X_7 hartzaileen aktibazioaren bitartez gertatu ohi da. Lutz et al., 2015-etik hartua.

Glia-zeluletako endokannabinoideen produkzioari dagokionez, Kultibatutako astrozito eta mikroglietan P_2X_7 hartzaile ionotropikoen aktibazioak, kaltzio intrazelularraren nibelen igoera eraginez, 2-AG-ren sintesia bultzatzen du (Walter et al., 2004; Witting et al., 2004). *In vitro*, OPC-ek eta OL-ak ere 2-AG-a modu konstitutiboan sintetizatzen dute (Gomez et al., 2010; Bernal-Chico et al., 2015). Hala ere, zelula hauetan endokannabinoideen sintesia erregulatzen duten seinale extrazelularrak zeintzuk diren ez da argi ezagutzen. Bide metabolikoen kasuan, endokannabinoideak normalean, **serin hidrolasa** espezifikoen akzioaren bitartez, hidrolisi bidez degradatzen dira. Hala ere, bide oxidatiboak ere deskribatu dira (**9. Irudia**).

Bi endokannabinoide nagusien metabolismoa intrazelularki gertatzen den prozesua den arren, ez da molekula hauentzat espezifikoa den transportadorerik deskribatu, beraz, hauek zelula barrura nola iristen diren ez dago oso argi. Behin zelula barruan, AEA **gantz azidoen amido hidrolasak** (**FAAH**) degradatzen du nagusiki (Cravatt et al., 1996), produktu bezala AA eta etanolamina sortuz

(**8.** eta **9. Irudiak**). FAAH-ren akzioaz gain, **N-aziletanolaminaren azido amidasa hidrolasak** (**NAAA**) ere hidroliza dezake AEA. Bestalde, 2-AG-aren entzima hidrolizatzaile nagusia **monoazilglizerol lipasa** (**MAGL**) da (Dinh et al., 2002). MAGL nerbio sistema osoan adierazten den eta 2-AG totalaren %85 inguru hidrolizatzen duen entzima da, produktu gisa AA eta glizerola sortuz (Savinainen et al., 2012). Entzima hidrolitiko hauek lokalizazio desberdina izaten dute, horrela, FAAH batik bat bukaera postsinaptikoetan adierazten den bitartean, MAGL bukaera presinaptikoetako CB_1 hartzaileen inguruan adierazten da (**9. Irudia**) (Gulyas et al., 2004). Neuronetan adierazteaz gain, FAAH eta MAGL entzimen adierazpena zelula glialetan ere deskribatu da (Lutz et al., 2015). Astrozitoetako MAGL-ak berezeki neuronen artean seinalizatzen duen 2-AG-ren degradazioan parte hartu eta endokannabinoideetatik prostaglandina pro-inflamatorioak sortzeko ahalmena duela deskribatu da (Viader et al., 2015; Chen et al., 2016).

MAGL-az gain, beranduago deskribatu diren beste bi entzima ere badira 2-AG-a hidrolizatzeko gai, **ABHD familiako hidrolasa 6** eta **12** (α/β-hydrolase domain containing 6 and 12, ABHD6/ABHD12) hain zuzen ere (Blankman et al., 2007) (**10. irudia**). Beraien sekuentzien artean %20-ko homologia bakarrik existitzen den arren, biek antzeko 2-AG kopurua hidrolizatzen dute. ABHD6-a 30KDa-ko mintz proteina integrala da, gune aktiboa zelula barnera begira duena. Gune aktibo horren ezaugarri nagusia S148-D278 eta H306 amino azidoen adierazpena da (Blankman et al., 2007; Navia-Paldanius et al., 2012). Entzima hau sistema immuneko zeluletan, hesteetan eta garunean maila altuan adierazten da (Human Protein Atlas). Zelula barneko lokalizazioari dagokieonez, ABHD6-a gehien bat bukaera postsinaptiko glutamatergikoetan adierazten da, baina baita bukaera GABAergikoetan edo astrozito eta mikroglietan ere (Marrs et al., 2010). NSZ-an, ABHD6-aren aktibitate entzimatikorik altuena kortex frontalean, hipokanpoan, gorputz ildaskatuan eta zerebeloan deskribatu da. (Baggelaar et al., 2017). Egoera fisiologikoetan, entzima honek 2-AG kopuru totalaren %4 inguru hidrolizatzen du. Hala ere, esan beharra dago ABHD6-ak, endokannabinoide horrez gain, beste substratu batzuen degradazioan ere parte hartzen duela (Navia-Paldanius et al., 2012). Hainbat ikerketek erakutsi dutenaren arabera, NSZ kaltetuta duten karraskarietan ABHD6-aren adierazpen maila igotzeaz gain, hau farmakologikoki inhibitzeak efektu onuragarriak eragiten ditu (Poursharifi et al., 2017). Horren arabera, egoera fisiologikoekin konparatuz, zenbait hanturazko prozesutan ABHD6-ak 2-AG kopuru totalaren proportzio altuagoa hidrolizatzen duela uste da.

ABHD12-a ere mintzeko proteina integrala da eta honek ere gune aktiboa zelula barrura begira aukezten du. Entzima hau 2-AG totalaren %9-aren hidrolisiaz arduratzen da (Blankman et al., 2007). Proteina hau kodifikatzen duen genean (*Abhd12*) gertatuko mutazioak PHARC (polyneuropathy, hearing loss, ataxia, retinitis pigmentosa and cataract) izenarekin ezagutzen den neuro-endekapenezko gaixotasun batekin erlazionatzen dira (Fiskerstrand et al., 2010; Blankman et al., 2013; Chen et al., 2013). Hori dela eta, proteina honek NSZ-aren mantenuan ezinbesteko eginkizuna betetzen duela pentsatuz, kannabinoideen inguruko ikerkuntzak ABHD12-aren inhibizioa estrategia terapeutiko gisa erabiltzea baztertu egin du.

Azken hamarkadetan asko azpimarratu da hantura prozesuetan 2-AG-ren hidrolisitik sortutako AA-k duen garrantzia. AA-k **ziklooxigenasa-2**-aren (COX-2) substratu gisa jokatzen du prostaglandinen (PG) sintesian (**9. Irudia**). Zehazki, MAGL-aren menpeko 2-AG-aren hidrolisia hantura eragiten duten prostaglandinak sintetizatzeko erabiltzen den AA-ren iturri nagusia dela frogatu da (Nomura et al., 2011). Beraz, MAGL edo ABHD6-a inhibitzeak izan ditzakeen onurak prostaglandinen produkzioa murriztearekin erlazionatuta egon daitezkeela uste da, eta ez seinalizazio endokannabinoidea indartzearekin bakarrik (Nomura et al., 2011; Piro et al., 2012).

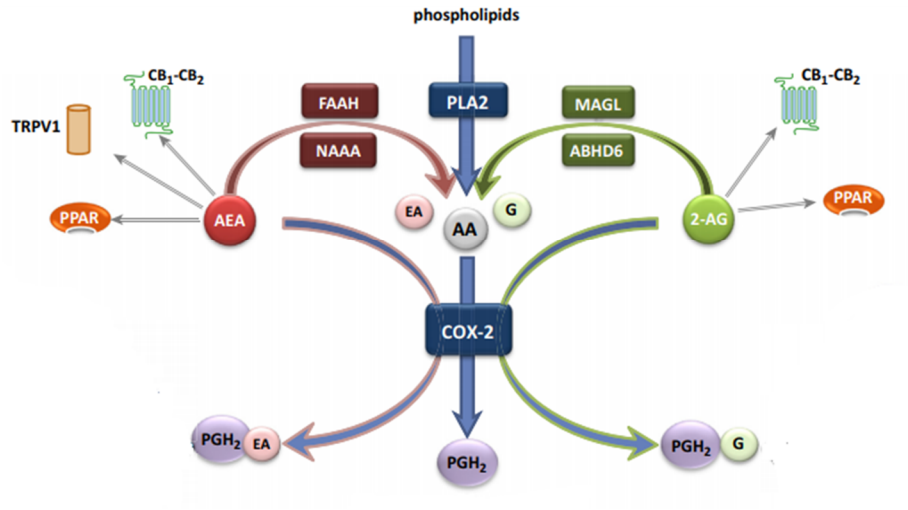

9. Irudia. Endokannabinoideen hidrolisi bideak. Monoazilglizerol lipasak (MAGL) eta α/β hidrolasa 6-ak (ABHD6) 2-arakidonoilglizerola (2-AG) hidrolizatzen dute azido arakidonikoa (AA) eta glizerola (G) emanez. Gantz azidoen amido hidrolasak (FAAH) eta N-aziletanolaminaren azido amidasa hidrolasak (NAAA) *N*-arakidonoiletanolamina (AEA) degradatzen dute, AA eta etanolamina (EA) sortuz. AA ziklooxigenasa-2-ak (COX-2) oxidatu egiten du PGH2-a emanez, prostaglandina sintetasek erabiliko dutena prostaglandina (PG) desberdinak sintetizatzeko. 2-AG eta AEA ere zuzenean oxida ditzake COX-2-ak, PG-glizerol esterrak (PG-G) eta PG-etanolaminak (PG-EA) eratuz**.** Alhouayek et al., 2014-tik moldatua.

Bestalde, 2-AG-ren eta AEA-ren bitarteko seinalizazioa metabolismo oxidatiboz ere erregulatu daiteke. COX-2 entzimak bi endokannabinoide hauek zuzenean oxidatzeko ahalmena du, produktu gisa PG glizerol esterrak (PG-G) eta PG glizerol etanolaminak (PG-EA) sortuz (Kozak et al., 2004) (**9. Irudia**). Deskribatu berri den metobolismo bide honen garrantzia oraindik aztertzen ari den arren, ABHD6-a inhibitzeak ahalbidetutako COX-2 bidezko 2-AG-ren oxidaziotik sortutako D2-glizerol prostaglandina lipidikoa makrofagoen aktibazioaren kontrolarekin erlazionatu da (Alhouayek et al., 2013). Ikerketa desberdinetan oinarrituta, COX-2-a inhibitzeak aurkezten dituen hanturaren aurkako efektuak endokannabinoide mailetan gertatutako igoerarekin erlazionatuta egon daitezkeela uste da, eta ez prostaglandinen sintesia murriztearekin bakarrik (Alhouayek et al., 2014).

2.3. CB_1 hartzaile bidezko seinalizazioa

CB_1 hartzaileen aktibazioa zelula motaren, estekatzaile motaren eta estekatzaile-hartzaile arteko erlazio motaren arabera aldatzen diren hainbat erantzun zelularrekin erlazionatuta dago. Agonista hartzaileari lotzen zaionean, G proteinen menpeko eta ez menpeko seinalizazio bideak martxan jartzen dira. CB_1 hartzailearen aktibazio kanonikoa **$G_{i/o}$ proteinen** aktibazioarekin erlazionatuta dago. Aktibazio honek GTP-a GDP-az ordezkatu eta α-subunitatea βγ dimerotik askatzea eragiten du. Puntu horretan, biek, bai α-subunitateak eta bai βγ dimeroak, efektore desberdinekin elkarrekintzak sortzeko ahamena dute. Aktibatutako α_i subunitateak **adenilil ziklasa**-ren (**AC**) inhibizioa eragiten du, adenosina monosfosfato ziklikoaren (cAMP) mailak jaitsi eta **proteina kinasa A**-ren (**PKA**) menpeko seinalizazioa murriztuz (seinalizazio bide hau CB_2 aren aktibazioak ere burutzen du) (Howlett, 2002). Aldi berean, βγ dimeroek beste seinalizazio bide batzuk aktibatzen

dituzte, horien artean, **mitogenoz-aktibatutako proteina kinasen** (**MAPK; ERK**, **c-Jun** eta **p38**) bidezko seinalizazioa (Bouaboula et al., 1995; Rueda et al., 2000; Galve-Roperh et al., 2002). Azaldu bezala, CB_1 hartzaileek bukaera sinpatikoetan neurotrasmisoreen askatzea murrizten dute. Hori **boltai menpeko kaltzio kanal** (**VGCC**) eta **barne potasio kanal errektifikatzaileen** (**GIRK**) aktibazioari esker gertatzen da (Howlett, 2002). Gainera, CB_1 hartzaileek zelulen biziraupen eta diferentziazioarekin erlazionatutako seinalizazio bideak ere aktibatzen dituzte, horien artean **fosfatidilinositol 3-kinasa** bidea (**PI3K/Akt**) (Gómez del Pulgar et al., 2000), **zeramiden biosintesia** (Galve-Roperh et al., 2000) eta **mTOR** bidea (Puighermanal et al., 2009). CB_1 hartzaileen aktibazio ez kanonikoa berriz zelula motaren araberako G proteina alternatiboen aktibazioaren bitartez gertatzen da. Adibidez, funtzio sinaptikoaren erregulazioan eginbehar garrantzitsua betez, astrozitoetako CB_1 hartzaileek kaltzioaren askatzea eragiten dute **$G_{q/11}$ proteinei** lotzeko duten ahalmenaren ondorioz (Navarrete and Araque, 2008). Azkenik, hainbat ikerketek erakutsi dutenez, CB_1 hartzaileek CB_1/CB_1 oligomeroak eta beste GPCR-ekin heterodimeroak sortzen dituzte (Morales and Reggio, 2017), CB_1 hartzailearen aktibazio hutsez ulertu ez daitezkeen efektu farmakologikoak eraginez.

2.4. CB_1 hartzaile bidezko nerbio Sistema zentralaren erregulazioa

CB_1 hartzaile neuronalak glutamato eta GABA-ren liberazioa erregulatzeko gai dira bukaera presinaptikoetan. Neuro-enkapenezko gaixotasunetan neuronen exzitotoxizitatea prozesu patogeniko gakoa kontsideratzen da. Honekin erlazionatuta, CB_1 hartzaileak transmisio kitzikatzailea mugatzeko duen ahalmena efektu neuro-babesgarriekin erlazionatu da (Katona and Freund, 2008; Chiarlone et al., 2014). CB_1 hatzaileen bidezko trasmizioaren inhibizioa **despolarizazio bidez induzitutako inhibizioaren supresioa** eta **kitzikapena** (**DSI**, **DSE**) bezala ezagutzen diren epe laburreko plastizitate forma bereziekin erlazionatuta dagoela ikusi da (Katona and Freund, 2012). Gainera, CB_1 hartzaileak GABA edo glutamato liberazioaren **epe luzeko depresioaren** (**LTD**) funtsezko bitartekariak dira (Castillo et al., 2012). Bestalde, **gliotrasmisoreen liberazioa** kontrolatzeko ahalmena dutelako, astrozitoetako CB_1 hartzaileak ere funtzio sinaptikoarekin erlazionatu dira (Navarrete and Araque, 2010; Martin-Fernandez et al., 2017). Honi dagokionez, garrantzitsua da aipatzea astrozitoetako CB_1 hartzaileak kannabinoideek hipokanpoan eragindako LTD-aren arduradunak direla deskribatu dela (Han et al., 2012).

NSZ-ean, CB_1 hartzaileek eragindako transmizio sinpatikoaren birmoldaketa hainbat eta hainbat akzio biologikoren arduraduna da. **Memoria eta ikasketa** prozesuak erregulatzeaz gain (Marsicano and Lafenêtre, 2009), CB_1 hartzaileek **nozizepzioan** (Woodhams et al., 2017), **jokabide motoreen** (Fernández-Ruiz, 2009), **antsietate** eta **stressarekiko erantzunen** (Lutz et al., 2015), **apetitu** eta **ahorakin jokabideen** (Lau et al., 2017) erregulazioan ere parte hartzen dute besteak beste. Hori horrela dela, CB_1 hartzaileen bitarteko seinalizazioaren erregulazio galera hainbat NSZ-eko gaixotasunekin erlazionatu da (Fernández-Ruiz et al., 2010). Kannabinoideek glutamato homeostasia mantenduz, exzitotoxizitatea, kalte oxidatiboa eta hantura murrizteko duten ahalmenak endokannabinoide sistema neuro-endekapeneko gaixotasunak tratatzeko etorkizun handiko itu terapeutikoa dela iradokitzen du.

3. **Endokannabinoide sistema eta esklerosi anizkoitza**

3.1. Endokannabinoide sistemaren erregulazio galera esklerosi anizkoitzean

Endokannabinoide sistema esklerosi anizkoitzarekin erlazionatuta dagoela adierazten duten hainbat ikerketa existitzen dira. Hauek EA-dun gaixoetan eta animali ereduetan sistemaren alterazioak deskribatzen dituzte.

Hartzaileei dagokieonez, EAE ereduko animalietan, hauek sagu osasuntsuekin konparatzean, CB_1 hartzaile kopuru baxuagoa deskribatu da (Berrendero et al., 2001; Cabranes et al., 2006; Palazuelos et al., 2008). Kuprizona ereduan aldiz, CB_1 hartzaile nibel altuagoak neurtu dira (Manterola et al., 2018). Desadostasun honen arrazoia bi ereduen artean neuro-endekapen mailarekiko dagoen desberdintasuna izan daitekeela uste da, EAE ereduan neuronen galera handia baitago eta kuprizona ereduan berriz, oso txikia (Skripuletz et al., 2011). Bestalde, CB_2 hartzaileari dagozkien mRNA eta proteina mailetan igoerak gertatzen direla nahiko argi ikusi da bai EA gaixoetan eta baita gaixotasunaren animali ereduetan ere (Maresz et al., 2007; Loría et al., 2008; Palazuelos et al., 2008). Aurkikuntza hauek kannabinoide hartzaile mota honek animali eredu desberdinetan hantura kontrolatzeko gaitasuna duela dioten lan desberdinekin bat datoz.

EA gaixotasuna pairatzen duten pertsonen garunean, likido zefalorrakideoan eta plasman, pertsona osasuntsuetan baina AEA maila altuagoak topatu dira (Eljaschewitsch et al., 2006; Centonze et al., 2007; Jean-Gilles et al., 2009). Hala ere, EA duten pazienteetan AEA maila baxuagoak ere deskribatu izan dira (Di Filippo et al., 2008). Bestalde, animali ereduetan eginiko aurkikuntzak nahiko eztabaidatsuak dira, AEA maila baxuagoak (Cabranes et al., 2005; Manterola et al., 2018), altuagoak (Baker et al., 2001; Centonze et al., 2007) eta aldatu gabeak (Witting et al., 2006) aurkitu baitira. EA gaixo eta EAE ereduko saguetan, AEA kontzentrazio altuak NAPE-PLD entzimaren adierazpen maila altuagoekin eta FAAH-ren adierazpen maila baxuagoekin erlazionatu dira (Baker et al., 2001; Centonze et al., 2007).

2-AG-ari dagokionez, ikerketa gehienek, bai animali ereduetan (Maresz et al., 2007; Manterola et al., 2018) baita EA duten gaixoen likido zefalorrakideoan (Centonze et al., 2007) eginikoek, endokannabinoide honen kontzentrazioa aldatzen ez dela adierazten dute. Hala ere, EAE saguetan 2-AG kontzentrazio altuagoak ere deskribatu izan dira (Baker et al., 2001). Endokannabinoide hau degradatzen duten entzimei begiratuz gero, animali eredu desberdinetan MAGL (Manterola et al., 2018) eta ABHD6-aren (Wen et al., 2015) adierazpen mailen igoera nabarmendu da.

3.2. Endokannabinoide sistemaren potentzial terapeutikoa esklerosi anizkoitzean

Kannabisarekin auto-medikatzen ziren gaixoek erasoen maiztasunean, espastizitatean eta dardaren kontrolean zituzten hobekuntzetan oinarrituta (Consroe et al., 1997), kannabinoideek EA-n izan dezaketen potentzial terapeutikoa luzaroan aztertu da. Horrela, exogenoki emandako agonista kannabinoideek **neuro-endekapena**, **desmielinizazioa** eta **hantura murriztu** eta **bermielinzazioa bultzatzen** dutela ikusi da (Arévalo-Martín et al., 2003; Cabranes et al., 2005; Maresz et al., 2007; Palazuelos et al., 2008).

Kannabinoideek dituzten hanturaren aurkako efektu gehienak CB_2 hartzaileen aktibazioaren bitartez eragindako T zelulen eta mikroglien funtzioen kontrolaren ondorioz gertatzen direla nahiko ongi deskribatu da (Eljaschewitsch et al., 2006; Maresz et al., 2007). Hala ere, EA-ren progresioa kontrolatzeko CB_1 hartzaileen aktibazioa beharrezkoa dela jakina da. Bereziki, neuronetako CB_1 hartzaileek exzitotoxizitateak eta hanturak eraginiko neuro-endekapenaren kontrola burutzen dutela ikusi da EAE animali ereduan (Pryce et al., 2003; Maresz et al., 2007; Croxford et al., 2008). Uste denaren arabera, CB_1 hartzaileek neuro-endekapenaren aurrean eskeintzen duten babesa proteina hauek transmizio kitzikatzailea kontrolatu eta biziraupenarekin erlazionatutako bideak aktibatzeko duten ahalmenari esker gertatzen da (Marsicano et al., 2003; Monory et al., 2006).

Kannabinoideek EA-an izan dezaketen potentzial terapeutikoen inguruko ikerketak EA gaixoetan espastizitatea tratatzeko erabiltzen den Sativex®-en komertzializazioa ahalbidetu du. Botika hau ahoko mukosetan ematen den ´spray´ bat da eta, 1:1 proportzioan, Δ^9-THC eta kannabidiolaz

osaturik dago (Kmietowicz, 2010). Hala ere, ikerketa desberdin askok erakutsi dutenaren arabera, kannabinoide exogenoen erabilerak efektu ez desiragarriak sortzen dituzte, horien artean psikoaktibitatea eta oroimen arazoak. Efektu hauek garuneko CB_1 hartzaile guztiak modu ez espezifikoan aktibatzeagatik agertzen dira. Beraz, EA-ren inguruko gaur egungo ikerketen helburua CB_1 eta CB_2 hartzaileen aktibazioak dakartzan efektu onuragarriak mantendu eta ez desiragarriak murriztuko dituzten terapien garapena da. Testuinguru honetan, AEA eta 2-AG-a degradatzen dituzten entzimen inhibizioaren bitartez endokannabinoide hauen kontzentrazioa handitzea estrategia itxaropentxu gisa proposatu da.

FAAH entzima farmakologikoki eta genetikoki **inhibitzeak** AEA mailen igoera eragiten du du NSZ-ko ehunetan (Cravatt et al., 2001). EA-ri dagokionez, hainbat ikerketek FAAH entzima inhibitzeak animali eredu desberdinetan espastizitatea murrizten duela diote (Baker et al., 2001; Ligresti et al., 2006; Pryce et al., 2013). Horrela izanda ere, FAAH entzima inhibitzeak gaixotasunaren progresioan eragiten dituen efektuak oso gutxi aztertu dira. Aztertu denaren arabera, FAAH entzima adierazten ez duten saguek EAE-ren fase akutuan ez dute desberdintasunik erakusten sagu basatiekin (WT) konparatuz gero, gaixotasunaren arintze fasean berriz, fenotipo babesle apala besterik ez dute aurkezten (Webb et al., 2008).

2-AG-ari dagokionez, animali ereduetan eginiko hainbat ikerketek **MAGL**-ren **inhibitzaileek** hantura eta kalte neurologikoak murrizteko eta bermielizazioa bultzatzeko gaitasuna dutela frogatu dute (Hernández-Torres et al., 2014; Bernal-Chico et al., 2015; Feliú et al., 2017; Mecha et al., 2018). Zoritxarrez, MAGL entzima luzaroan inhibitzeak efektu ez desiragarriak ere eragiten ditu, garuneko CB_1 hartzeileen desentsibilizazioa eta tolerantzia funtzionala besteak beste (Schlosburg et al., 2010), entzima hau inhibitzen duten farmakoen erabilera zalantzan jarriz.

Beste alde batetik, **ABHD6 entzima inhibitzeak**, bai sistema periferikoan zein NSZ-ean**,** 2-AG kontzentrazioak era finean erregulatzea ahalbidetzen duela proposatzen da, testuinguru patologikoetan efektu onuragarriak izanik. Partikularki, ABHD6-a farmakologikoki inhibitzeak, sinapsietan eta makrofago periferikoetan 2-AG kontzentrazio mailen igoera eraginez, efektu anti-epileptikoak eta hanturaren aurkakoak sortu ditzakeela ikusi da (Alhouayek et al., 2013; Naydenov et al., 2014). Gainera, efektu babesgarri hauek dosi kronikoen ostean mantendu egiten direla frogatu da, efektu ez desiragarririk eragin gabe (Long et al., 2009). Berriki, ABHD6 entzima inhibitzeak EA-ren testuinguruan efektu onuragarriak dituela erakusten duen lan bat argitaratu da. Bertan, inhibitzaile sistemiko bat erabiliz, WWL70, entzimaren blokeoak saguak EAE-ren aurka babesten dituela ikusi da, hanturaren aurkako efektu indartsuak erakutsiz (Wen et al., 2015). Hala ere, ikertzaile talde berdineko kideek WWL70-ak mikroglietan, ABHD6-arekin zer ikusirik ez duten mekanismoen bitartez, prostagladinen produkzioa murrizten duela deskribatu dute, inhibitzailearen erabilerak *in vivo* eragindako onurak mekanismo honekin erlazionatuta egon daitezkeela proposatuz (Tanaka et al., 2017). Gainera, hantura autoimmunearen kontrolean **sistema zentral eta periferikoko ABHD6** populazioen parte hartzea zein izan daitekeen sekula ez da aztertu.

3.3. Oligodendrozitoetako CB_1 hartzaileen zeregina esklerosi anizkoitzean

Kannabinoideek EA-dun gaixoetan eta animali ereduetan mielina babesteko eta bermielinizazioa bultzatzeko duten gaitasunak OPC-ak eta OL-ak konposatu hauen itu zuzenak izan daitezkeela irakokitzen du. Gai honen inguruko ikerketak hasi ziren garaian eginiko autorradiografia lanen arabera, helduen gai zuriko traktuek ez zuten CB_1 hartzailerik adierazten (Herkenham et al., 1991). Beranduago, EA-dun gaixoetan *postmortem* eginiko analisi immunohistokimikoek lesioetako

OPC-ek eta OL-ek CB_1 hartzailea adierazten dutela iradoki zuten (Benito et al., 2007). Hala ere, gizaki eta saguen NSZ mailan eginiko ikerketak ez dira zelula oligodendroglialek CB_1 hartzailea adierazten dutela era fidagarrian erakusteko gai izan.

Oligodendrozitoek CB_1 hartzailea adierazten dutela dioen ideiak indarra hartu duela gutxi argitaraturiko lan bati esker. Bertan, zelula bakarren sekuentziazioa burutuz, OPC-etatik hasi eta OL helduetaraino, oligodendrozito leinuko ia populazio guztiek *Cnr1* transkritoak adierazten dituztela frogatzen da (Marques et al., 2016) (**10. Irudia**). Aipatu beharra dago, horrez gain, gizakien garuneko gai zuri subkortikaleko OPC $A2B5^+$-etan ere aurkitu direla *Cnr1* transkritoak (Sim et al., 2006). Hartzaileaz gain, olidodendrozito zelulek 2-AG endokannabinoidea sintetizatu eta degradatzeko behar diren entzimak (*Daglb* and *Mgll*) ere adierazten dituzte. Aurkikuntza honek oligodendrozito zelulek, 2-AG-a sortu eta beraien mintzeko CB_1 hartzaileak aktibatuz, kontrol autokrinoa burutu dezaketela iradokitzen du (Gomez et al., 2010; Bernal-Chico et al., 2015; Gomez et al., 2015).

Orain arte, CB_1 hartzaileek OPC eta OL-etan izan ditzaketen betebehar biologikoak asko ikertu dira *in vitro* sistemetan. Horren inguruan, duela gutxiko ikerketek erakutsi dutenaren arabera, OPC-ek sortutako 2-AG-ak, mintzean dituzten CB_1 hartzaileen aktibazioaren bitartez, zelula hauen migrazioa bultzatzen du (Sanchez-Rodriguez et al., 2018). Bestalde, kultibatutako zelutan, ERK/MAPK eta PI3K/Akt/mTOR seinalizazio bideen bitartez, CB_1 hartzaileen aktibazioak OPC-en diferentziazioa eragiten dutela deskribatu da (Gomez et al., 2010; Gomez et al., 2011; Gomez et al., 2015). Zelulen biziraupenari dagokionez, gure laborategiko datuek CB_1 hartzailearen aktibazioak OL-ak heriotza exzitotoxikotik babesten dituela frogatu dute (Bernal-Chico et al., 2015). Beraz, *in vitro* eginiko aurkikuntza guzti hauek hainbat gauza iradokitzen dituzte, alde batetik, zelula oligodendrogialetan adierazitako CB_1 hartzaileek mielinizazio prozesuan zereginen bat izan dezaketela, eta bestetik, hartzaile populazio hauek EA-ren testuinguruan kannabinoideek dituzten onuren bitartekari izan daitezkeela. Hala ere, oligodendrozitoetan CB_1 hartzaileen adierazpena era fidagarrian frogatzen duten datuen faltak asko mugatu du hauen funtzio biologikoa ulertzea.

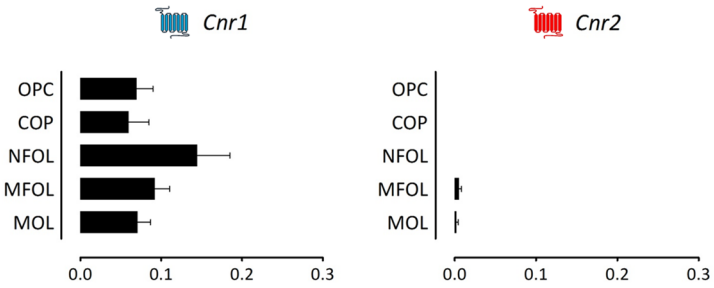

10. Irudia. *Cnr1* eta *Cnr2* transkritoen adierazpena oligodendrozito leinuko zeluletan. Zelula bakarreko sekuentziazio datuak http://linnarssonlab.org/oligodendrocytes/-tik lortu dira. NFOL-ak dira *Cnr1* adierazpen maila altuena erakusten duten zelulak**.** *Cnr2*-aren adierazpena berriz ia detektaezina da leinuko zelula guztieztan. OPC, Oligodendrozitoen zelula aintzindaria; COP differentiation-committed oligodendrocyte precursors, diferentziazioarekin konprometitutako zelula aintzindariak; NFOL newly formed oligodendrocytes, Oligodendrozito sortu berriak; MFOL myelin forming oligodendrocytes, Oligodendrozito mielinizatzaileak; MOL mature oligodendrocytes, Oligodendrozito helduak.

Helburuak

EA-ren testuinguruan kannabisetik eratorritako konposatuek potentzial terapeutikoa dutela oso ezaguna da. Analisi transkriptomiko eta *in vitro* eginiko entsegu farmakologikoen arabera, OPC-ek eta oligodendrozito helduek, maila baxuan bada ere, CB_1 hartzaileak adierazten dituzte. Aurkikuntza hauetan oinarrituta, konposatu kannabinoideen efektu onuragarriak, neurri batean bada ere, oligodendrozitoetako CB_1 hartzaileen aktibazioarekin erlazionatuta egon daitezkeela uste da. Hala ere, proteina hauek zelula hauetan duten adierazpen maila baxuaren ondorioz, oso zaila izan da CB_1 hartzaileek oligodendrozito leinuko zeluletan duten distribuzioa aztertzea. Gaur egun, oligodendrozitoek *in situ* CB_1 hartzailea adierazten dutela frogatzen duten datu fidagarriak falta dira eta hartzaile populazio hauek mielinaren biologian izan dezaketen betebeharra eztabaidazko gaia da. Bestalde, kannabinoide exogenoek, garuneko CB_1 hartzaileen populazio zabala aktibatzearen ondorioz, efektu ez desiragarriak eragiten dituztela jakina da. Gaur egungo ikerketek 2-AG-ren degradazioa inhibitzea eragin ez desiragarri gabeko estrategia terapeutiko aproposa izan daitekeela proposatzen dute. Garun ehunetan, 2-AG nagusiki monoazilglizerol lipasaren (MAGL) akzio bitartez degradatzen da eta, maila baxuagoan, baita ABHD familiako hidrolasa 6-aren (ABHD6) bitartez ere. Deskribatu denez, MAGL entzimaren inhibitzaileek eragin onuragarriak dituzte EA-ren animali ereduetan. Hala ere, hauen administrazio kronikoa garuneko CB_1 hartzaileen desentsibilizazioarekin eta tolerantzia funtzionalarekin erlazionatu da, entzima honen inhibizioaren potentzial terapeutikoa zalantzan jarriz. Bestalde, hainbat ebidentziek ABHD6 entzimaren inhibizioak 2-AG mailen erregulazio fina ahalbidetzen duela adierazten dute, EA-ren testuinguruan potentzial terapeutikoa duen itua dela proposatuz.

Beraz, hau guztia kontutan hartuta, Doktorego Tesi honen **helburu nagusia** endokannabinoide sistemak mielinaren biologian eta patologian dituen betebeharrak hobeto ezagutzea izan da, bereziki EA-ren testuinguruan oinarrituz.

Gure **helburu espezifikoak** honakoak izan ziren:

1. Helburua. Sagu helduen garuneko OPC eta OL helduetan CB_1 hartzaileen lokalizazio ultraegiturala aztertzea eta CB_1 hartzailea adierazten ez duten saguetan mielinaren ultraegituran aldaketa posibleak aztertzea.

2. Helburua. Gaixotasunaren alde desberdinak antzeratzen diztuzten *in vivo* eta *in vitro* ereduak erabiliz, EA-ren testuinguruan ABHD6 entzima inhibitzea estrategia terapeutiko oparoa izan daitekeen aztertzea.

Material eta Metodoak

1. Animaliak

Mikroskopio elektroniko bidezko analisietarako CB_1 hartzailea adiearazten ez zuten saguak (Marsicano et al. 2002) eta kumaldi bereko sagu basatiak erabili genituen, hemendik aurrera $CB_1^{-/-}$ eta $CB_1^{+/+}$ bezala adierazita agertuko direnak (kolonia aitzindariak adeitsuki Beat Lutz doktoreak emanak, Institute of Molecular Biology, Mainz, Alemania). Bestalde, *NG2* genearen menpe proteina fluoreszente horia (EYFP) adierazten zuten saguak erabili genituen (kolonia aitzindariak adeitsuki Jacqueline Trotter doktoreak emanak, Institute of Molecular Biology, Mainz, Alemania) (Karram et al. 2008). Sagu hauek CB_1 hartzailea adierazten ez zuten saguekin gurutzatu ziren, sagu mutante bikoitzak lortuz, EYFP proteinarentzat heterozigotoak eta bestalde $CB_1^{-/-}$ edo $CB_1^{+/+}$ zirenak (hemendik aurrera a NG2-$EYFP^{+/-}$-$CB_1^{+/+}$ eta NG2-$EYFP^{+/-}$-$CB1^{-/-}$ bezala adierazita agertuko direnak). Kuprizona bidezko desmielinizazio eta EAE animali ereduetarako C57BL/6 sagu basatiak erabili ziren, Charles River-en (Bartzelona, Espainia) erosiak. Oligodendrozito eta neuronen hazkuntza (Kultibo) primarioak burutzeko Euskal Herriko Unibertsitateko animaliategian hazitako Sprague Dawley arratoiak erabili ziren. Animali guztiak baldintza estandarretan (12 orduko argi/ilunpe zikloak) eta ura eta janaria *ad libitum* zutelarik mantendu ziren. Prozedura guztiak helburu zientifikoekin erabilitako animaliak babesteko Europako Zuzentarauarekin bat gauzatu ziren (2010/63/UE) eta Euskal Herriko Unibertsitateko Animaliekin egiten den Esperimentaziorako Etika Batzordeak (AEEB) eta Gipuzkoako Diputazioak onetsi eta kontrolatuak izan ziren. Animalien sufrimendua eta erabili beharreko animalien zenbakia murrizteko esfortzu guztiak egin ziren.

2. CB_1 hartzaileen lokalizazio ultraegiturala oligodendrozito populazioetan

2.1. Saguen sakrifizioa eta ehunen prozesamendua

Saguak Ketamina/xilazina (80/10 mg/Kg; Imalgene®, Mérial, France/Rompun®, Bayer, Alemania) zeraman txerto intraperitoneal baten bitartez anestesiatu ziren eta bihotzean zeharreko perfusioa burutu zitzaien ponpa peristaltiko baten laguntzaz, lehendabizi disoluzio fisiologikoarekin (0,9% NaCl; pH 7,4) eta ondoren %4 paraformaldehido, %0,1 glutaraldehido eta %0,2 azido pikriko zeramatzan disoluzio finkatzailearekin, 0,1 M fosfato tanpoian (PB; pH 7.4) prestatua. Perfusioaren ondoren, garunak %4 paraformaldehidotan post-finkatu ziren gau batez 4˚C-tan. Gorputz kailukara eta hipokanpoa zuten sekzio koronalak (40 µm-eko lodiera) bibratomo (VT1000S, Leica, Wetzlar, Alemania) bitartez lortu ziren eta %0,02 sodio azida zeraman 0,1 M PB-tan gorde ziren erabili arte.

2.2. Zilarrez anplifikatutako urrezko partikulen bidezko immuno-markaketa

Oligodendrozito heldu mielinizatzaileetan CB_1 hartzaileen lokalizazioa aztertu ahal izateko, zilarrez anplifikatutako urrezko partikulen bidezko immuno-markaketa aplikatu genien $CB_1^{-/-}$ eta $CB_1^{+/+}$ saguen garun ehunei. Ehun sekzioak %10 behi seruma (BSA; Sigma-Aldrich, St. Louis, MO, AEB), % 0,1% sodio azida eta %0,02 saponina zeramatzan Tris-HCl (TBS; pH 7,4) tanpoiak osatutako blokeo disoluzioan inkubatu ziren 30 minutuz giro tenperaturan. Jarraian, sekzioak, 2 egunez eta 4˚C-tan, CB_1 hartzailea ezagutzen duen untxian eginiko antigorputzarekin (1:500; ImmunoGenes, Budapest, Hungaria) inkubatu ziren. Antigorputz hau %0,004 saponina zeraman blokeo disoluzioan prestatua izan zen. %1 BSA/TBS-arekin hainbat garbiketa egin ondoren, sekzioak, 4 orduz eta giro tenperaturan, %0,1 sodio azida eta %0,004 saponina zeramatzan blokeo disoluzioan prestatutako 1.4 nm-ko urre partikula bati lotutako antigorputz sekundarioarekin inkubatu ziren, sagu IgG-ak ezagutzen dituen ahuntzean eginiko batekin hain zuzen ere. Ehunak %1 BSA/TBS-tan garbitu ziren gau oso batez. Ondoren, TBS-tan prestatutako %1 glutaraldehidotan post-finkatu eta ur destilatuarekin garbitu ziren. Urrezko partikulen tamaina zilar bidez anplifikatu zen, 12 minutuz eta ilunpetan, HQ Silver Kit-a (Nanoprobes) erabiliz. Hurrengo egunean, sekzioak osmifikatu egin ziren

(%1 OsO_4, 0,1 M PB-tan; pH 7,4) 30 minutuz. 0,1 M PB-tan 3x10 minutuko garbiketak egin ondoren, ehunak etanol kontzentrazio desberdinetatik (%50-tik %100ra) oxido propilenora pasatuz deshidratatu egin ziren. Segidan, sekzio guztiak erretxina epoxy-an (Sigma-Aldrich) sartu ziren, oxido propilenoaren kontzentrazioa pixkanaka murriztuz (Erretxina: OP; 1:3 30 minutuz, 1:1 ordu betez eta 3:1 2 orduz). Azkenik, ehunak erretxina berrian sartu ziren gau oso batez eta jarraian, polimerizatu zezaten, bi egun 60˚C-tan pasa zituzten. Argi mikroskopioz aztertu ondoren, intereseko ehun zatiak aukeratu eta erretxinaz eginiko kapsuletan itsatsi ziren. Sekzio semifinak (500 nm-ko lodiera) ultramikrotomo (RMC Boeckeler, Tucson, AZ, AEB) baten bitartez lortu ziren eta, ehuna identifikatu ahal izateko, %1 toluidina urdinarekin markatu. Behin intereseko ehun zatia azaleratzen hasten zela ikustean, sekzio ultrafinak (55-60 nm-ko lodiera) diamantezko laban (Diatome, Hatfield PA, AEB) baten bitartez lortu ziren eta nikelezko saretxoetan jaso. Mikroskopiora joan aurretik, sekzio ultrafin hauek %4 uranilo azetatoa (30 min) eta %2,5 berun zitratoa (30 min) erabiliz kontrastatu ziren.

2.3. Urre partikulen eta immunoperoxidasa metodoaren bidezko markaketa bikoitza

OPC-etan CB_1 hartzaileen lokalizazio ultraegiturala aztertu ahal izateko, immunoperoxidasa metodoan eta urrezko partikulekin markatutako antigorputzetan oinarritutako markaketa bikoitza aplikatu genien NG2-EYFP $^{+/-}$-CB1$^{+/+}$ eta NG2-EYFP $^{+/-}$-CB1$^{-/-}$ saguen garun ehunei. Hipokanpoa zuten sekzioak %1 hidrogeno peroxidoarekin (H_2O_2) tratatu ziren 15 minutuz giro tenperaturan. Hainbat aldiz TBS-arekin garbitu ondoren, sekzioak %10 behi seruma, %0,1 sodio azida eta %0,02 saponina zeramatzan Tris-HCl (TBS; pH 7,4) tanpoiak osatutako blokeo disoluzioan inkubatu ziren 30 minutuz giro tenperaturan. Jarraian, ehunak, 2 egunez eta 4˚C-tan, untxian egindako CB_1 hartzailearen aurkako (1:500; ImmunoGenes) eta arratoian egindako proteina berde fluoreszentearen (GFP) aurkako (1:2000; Nacalai Tesque, Kyoto, Japon) antigorputzekin inkubatu ziren. Antigorputz hauek %0,004 saponina zeraman blokeo disoluzioan prestatu ziren. %1 BSA/TBS-arekin hainbat garbiketa egin ondoren, sekzioak, 4 orduz eta giro tenperaturan, 1.4 nm-ko urre partikula bati lotutako sagu IgG-ak ezagutzen dituen ahuntzean eginiko antigorputz (1:200; Nanoprobes Inc.) eta arratoi IgG-ak ezagutzen dituen zaldian eginiko biotinilatutako antigorputz sekundarioekin (1:200; Vector Laboratories, Burlingame, CA, AEB) inkubatu ziren. Antigorputz hauek %0,1 sodio azida eta %0,004 saponina zeramatzan disoluzioan prestatu ziren. %1 BSA/TBS-arekin garbitu ondoren, ehunak abidina-biotina konplexuarekin tratatu ziren (ABC; Elite, Vector laboratories). Gau osoz %1 BSA/TBS-arekin garbitu ondoren, %1 glutaraldehidotan post-finkatu ziren. Segidan, urre partikulak zilarrarekin anplifikatu eta immunoperoxidasa erreakzioa garatu zen, kromogeno gisa 3´diaminobenzidina (DAB) erabiliz (Roche Diagnostics, Mannheim, Alemania). Azkenik, ehunak osmifikatu, deshidratatu eta epoxy erretxinan sartu ziren, aurretik aipatutako metodologia jarraituz.

2.4. Urre eta immunoperoxidasa bidezko markaketen semi-kuantifikazioa

Urre eta immununoperoxidasa bidezko metodoak $CB_1^{+/+}$, $CB_1^{-/-}$, NG2-EYFP$^{+/-}$-$CB_1^{+/+}$ eta NG2-EYFP$^{+/-}$-$CB_1^{-/-}$ saguei (*n* = 3-5 kondizio bakoitzeko) aplikatu zitzaizkien. Ehunak argi mikroskopioz ebaluatuz, markaketa egokia erakusten zuten gorputz kailukara edo hipokanpoko *stratum radiatum*-eko zatiak aukeratu eta bertatik lortu ziren sekzio ultrafinak. Baldintzak estandarizatu eta negatibo faltsuak saihesteko asmotan, ehun bakoitzeko 20 sekzio ultrafin bakarrik jaso ziren.

Sekzio ultrafinen argazkiak Euskal Herriko Unibertsitateko SGIKER zerbitzuan lortu ziren sCMOS (Hamamatsu Photonics France, Cerdañola, Espainia) kamara bati lotutako Jeol JEM 1400 Plus mikroskopio elektronikoa erabiliz (Jeol, Tokio, Japon). Oligodendrozito helduen ebaluaziorako,

argazkiak 4,000-8,000 X-ko handipenekin atera ziren, OPC-en kasuan berriz, 8,000-15,000 X-ko handipenekin. Gorputz kailukarako oligodendrozito mielinizatzaileak beraien ezaugarri bereizgarrietan oinarrituta identifikatu ziren, besteak beste, heterokromatina agregakin ugariko nukleoa edo nukleoa inguratzen duen zitoplasma fina (Peters and Folger 2013). Hipokanpoko *stratum radiatum*-eko OPC-en prozesuak berriz DAB agregakinen presentziagatik identifikatu ahal izan ziren. Bukaera sinaptiko inhibitzaile eta kitzikatzaileetako CB_1 hartzaileen dentsitatea kalkulatzeko animali bakoitzeko (n = 3), era sistematikoan eta 8,000 X-ko handipenarekin, 20 argazki atera ziren. Oligodendrozitoen, OPC-en eta bukaera sinaptikoen perimetroa kalkulatzeko Image-J softwarea (NIH, Bethesda, MD, AEB) erabili zen. Markaketa positiboa intereseko egiturak mintzean gutxienez partikula bat izatea kontsideratu zen. CB_1 hartzailearentzat positibo ziren oligodendrozito eta OPC prozesuen ehunekoa nahiz markaketen dentsitatea (partikula/ mintz µm), batezbesteko ± SEM eran aztertu ziren software estatistiko bat erabiliz. 22-38 oligodendrozito, 28-94 OPC-DAB positibo, 15-24 bukaera sinaptiko inhibitzaile eta 97-107 bukaera kitzikatzaile zenbatu ziren animaliko.

3. **Mielinaren ultraegituraren analisia**

3.1. Saguen sakrifizioa eta ehunen prozesamendua

Saguak tribromoetanola (Avertin, 0.2 mL animali 10 g-ko; Sigma- Aldrich) zeraman txerto introperitoneal baten bitartez anestesiatu ziren eta bihotzean zeharreko perfusioa burutu zitzaien ponpa peristaltiko baten laguntzaz, lehendabizi disoluzio fisiologikoarekin (0,9% NaCl; pH 7,4) eta ondoren, %4 paraformaldehido, %2,5 glutaraldehido eta %0,5 NaCl zeramatzan 0,1 M fosfato tanpoiak (PB; pH 7.4) osatutako disoluzio finkatzailearekin (Möbius et al., 2010). Perfusioaren ondoren, garunak disoluzio finkatzailean mantendu ziren gau batez 4˚C-tan eta %1 paraformaldehidotan gorde erabili arte. Gorputz kailukara zuten sekzio sagitalak (40 µm-eko lodiera) bibratomo bitartez lortu ziren. Ehun hauek 30 minutuz osmifikatu, deshidratatu, eta erretxinatan sartu ziren. Azkenik, mikroskopio elektronikoan ikusi ahal izateko, lehenago azaldutako protokoloa jasan zuten (ebaketa eta kontrastea). Baldintzak estandarrak izan zitezen, kumaldi bereko $CB_1^{+/+}$ eta $CB_1^{-/-}$ saguen (n = 3 kondizioko) ehunak paraleloki prozesatu ziren.

3.2. g-ratioen neurketa eta axoi mielinizatuen zenbaketa

Analisi hauek burutzeko, Euskal Herriko Unibertsitateko SGIKER zerbitzuko Jeol JEM 1400 Plus mikroskopio elektronikoa erabiliz, zoriz aukeratutako gorputz kailukara errostral eta kaudaleko eremuetan, 4,000 X haundipenarekin, 20 argazki atera ziren. *g*-ratioen kasuan, analisia zorizkoa zela bermatzeko, argazkiei 1.2 mm-ko sare bat gainjarri zitzaien. Horrela, sareko koadrante desberdinen elkartze puntuek zeharkatutako axoiak bakarrik aztertu ziren. *g*-ratio balioa kalkulatzeko, Image-J softwarearen bitartez, balio hauek neurtu ziren: 1) axoi gehi ´inner tongue´-aren azalera 2) zuntz osoaren azalera (**1. Irudia A**). Azalera balio hauetatik axoi gehi ´inner tongue´-aren diametroa (d_I) eta mielinizatutako zuntz osoaren diametroa (d_M) kalkulatu ziren. Azkenik, *g*-ratio balioak d_I/d_M eginez lortu ziren.

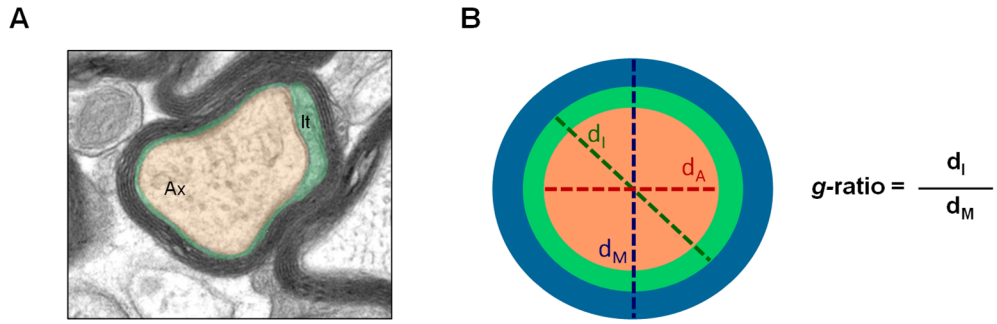

1. Irudia. *g*-ratio balioen neurketa mikroskopio elektronikoko irudietan. (**A**) axoia (Ax, laranja), ´inner tongue´-ga (It, berdea) eta mielina erakusten dituen mikroskopio elektronikoko irudi esanguratsua. (**B**) *g*-ratioa nola lortzen den adierazten duen diagrama eskematikoa.

4. **ABHD6 entzimaren inhibitzaileak**

ABHD6 entzimaren KT182 [4-[3'-(Hidroximetil)[1,1'-bifenil]-4-il]-1H-1,2,3-triazol-1-yl](2-frenil-1-piperidinil)-metanona] eta KT203 4'-[1-[[2-(Fenilmetil)-1-piperidinil]karbonil]-1H-1,2,3-triazol-4-yl]-[1,1'-bifenil]-3-azido karboxilikoa] inhibitzaile selektiboak Benjamin F. Cravatt doktorearen laborategian sintetizatu ziren The Scripps Research Institutoan (La Jolla, CA, AEB), lehenago deskribatu izan den bezala (Hsu et al. 2013). ABHD6-en WWL70 inhibitzailea [N-Metil-N-[[3-(4-piridinil) fenil]metil]-4'-(aminokarbonil)[1,1'-bifenil]-4-il azido karbamiko esterra], eta FAAH entzimaren PF750 [**N**-fenil-4-(kinolin-3-ilmetil)piperidina-1-karboxamida] eta URB597 [[3-(3-karbamoilfenil)fenil] *N*-ziklohexilkarbamatoa] inhibitzaileak Tocris Bioscience-i (Bristol, EB) erosi zitzaizkion. Azkenik, ABHD6 entzimaren KT195 [4-(4'-Metoxi[1,1'-bifenil]-4-il)-1H-1,2,3-triazol-1-il](2-fenil-1-piperidinil) metanona] inhibitzailea Cayman Chemical-i (Ann Arbor, MI, AEB) erosi zitzaion.

5. **Esklerosi anizkoitzaren animali ereduak**

5.1. Kuprizona bidezko desmielinizazio primarioa

Desmielinizazio primarioa 10 asteko saguei %0,3 kuprizona (bis-ziklohexanona oxaldihidrazona; Sigma-Aldrich) zeraman ehotutako sagu janaria (Altromin, Lemgo, Alemania), 3 edo 6 astez, jaten emanez eragin zen. Bermielinizazioa ikertzeko, kuprizona 6 astez administratu ondoren, saguak dieta arruntera itzuli ziren bi astez.

5.2. Entzefalomielitis auto-immune esperimentala (EAE)

EAE-a 10 asteko sagu emeetan induzitu zen 300 µl oligodendrozito glikoproteina 35-55 (MOG; 200 µg; CIPF, Valentzia, Espainia) eta 8mg/mL *Mycobacterium tuberculosis* H37Ra-arekin (8 mg/mL; DIFCO Laboratories, AEB) suplementaturiko Freunden adjubante osatugabea zeramaten txertoen bitartez. Immunizazio egunean eta immunizazio osteko (day post-immunization, dpi) bigarren egunean pertussis toxina (500 ng; Calbiochem, Merck Millipore, Burlington, MA, AEB) txertatu zitzaien intraperitonealki. Saguen pisua eta desgaitasun motorea egunero ebaluatu ziren, sintomak 0-tik 8-ra puntuatuz: 0, sintomarik ez; 1, buztan ahula; 2, buztan paralizatua; 3, buztan paralizatua eta ahultasuna atzeko hanketan; 4, buztan paralizatua eta hemiparalisia atzeko hanketan; 5, atzeko hanken paralisi totala; 6, atzeko hanken paralisi totala eta arazoak aurrekoetan; 7, tetraplegia; eta 8, hilzorian. Esperimentuaren amaieran, saguak Avertin-ekin (240 mg/Kg i.p.; Sigma-Aldrich)

anestesiatu eta, elektrodo bat garunean eta bestea L2 ornoan ipiniz, traktu kortikoespinaleko kondukzioa neurtu zitzaien (Bernal-Chico et al. 2015).

5.3. ABHD6 entzimaren inhibitzaileen administrazioa in vivo

ABHD6 entzimaren KT182 eta KT203 inhibitzaileak %15 DMSO, %4,25 polietilen glikol 400 (Sigma-Aldrich), %4,25 Tween-80 (Sigma-Aldrich) eta %76,5 disoluzio fisiologikoz osatutako eramailean disolbatu eta intraperitonealki txertatu ziren 2mg/kg dosian. Kuprizona ereduan, ABHD6 entzima inhibitzearen eraginak aztertzeko, saguak 21 egunez egunero txertatu ziren KT182 inhibitzailearekin edo eramailerekin soilik. Bermielinizazioa aztertzeko, 6 astez kuprizona irentsi zuten animalietatik, zoriz, talde bat aukeratu eta 2 astez KT182 edo eramailea txertatu zitzaien. Azkenik, EAE animali ereduan, saguek KT182-a, KT203-a edo eramailea zeraman txertoa jaso zuten egunero 30 egunez, 1 dpi-an hasita.

6. **Gelean garatutako aktibitatean oinarritutako proteinen profila (ABPP)**

ABHD6 entzimaren inhibitzaileen ABPP profila sagu naifen (*n* = 4) eta zoriz aukeratutako EAE-dun saguen garunean aztertu zen. Saguak isoflurano (IsoVet®; B Braun, Melsungen, Alemania) bitartez anestesiatu eta dekapitazioz sakrifikatu ziren. Ondoren, garunak -80°C-tan gorde ziren erabili arte. Ehun proteomak prestatzeko, garunak 20 mM HEPES, 250 mM sakarosa eta 2 mM DL-ditiotreitol (DTT) (pH 7.4) zeramatzan lisi tanpoian jarri eta kristal eta tefloizko homogeneizagailu baten laguntzaz homogeneizatu ziren. Ondoren, soberakinak kentzeko, homogeneizatutako garunei abiadura baxuko zentrifugazio bat eman zitzaien (3300 rpm, 5 min, 4°C). Jarraian, gainjalkina 45 minutuz 100,000 x g-tara zentrifugatu zen mintzez osatutako jalkinak lortzeko. Jalkinak garbitu eta 20 mM HEPES-etan (pH 7.4) berreseki ziren. ABHD6 entzimaren inhibitzaileen ahalmen blokeatzailea kortexetik isolatutako neuronetan ere aztertu zen. Horretarako, zelulak 30 minutuz KT182, KT203, WWL70 edo KT195-arekin inkubatu ziren 37 °C-tara. Ondoren, izotzetan hoztutako PBS-arekin garbitu eta lisi tanpoiaren 500 µl-tan lisatu ziren. Mintzak berriro ere ultrazentrifugazio (100,000 x g, 45 min, 4°C) bidez isolatu eta 20 mM HEPES-etan (pH 7.4) berreseki ziren pipetaren laguntzaz. Proteina totalen kontzentrazioak Bradford entsegu (Bio-Rad, Hercules, CA, AEB) bidez kalkulatu ziren eta lagin horiek -80 °C-tara gorde ziren ABPP esperimentuak egin arte. Geletan garatutako ABPP entseguak lehenago deskribatu bezala burutu ziren (Hsu et al., 2013). Ehunetatik lortutako proteinak 1-2 mg/mL-tara doitu ziren eta, 30 minutuz 37°C-tara, fluorofosfonato-rodamina (FP-Rh) (Patricelli et al. 2001) edo HT-01 (Hsu et al. 2013) sondekin inkubatu ziren (1 µM; adeitsuki Ku-Lung Hsu doktorek emanak, University of Virginia, Charlottesville, VA, AEB). Sondekin markatutako proteinak desnaturalizatu eta %10 akrilamidadun geletan kargatu ziren. Azkenik, gel horiek fluoreszentzia detektatzeko gai den ChemiDoc™ MP (Bio-Rad) imagen sistema batekin eskaneatu ziren (**2. Irudia**).

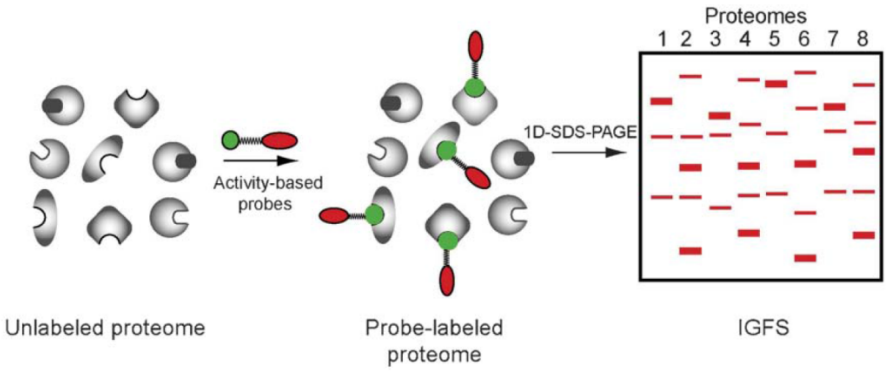

2. Irudia. Gelean garatutako aktibitatean oinarritutako proteinen profila (ABPP). ABPP sondek entzima aktiboetara lotzeko gaitasuna dute baina ez entzima inkatiboetara (inhibitzailea lotuta dutenak). Markatutako entzimak gelen fluoreszentziaren detekzio bidez ikusi daitezke, non beraien pisu molekularraren arabera identifikatuak izango diren. Sieber and Cravatt, 2006-tik hartua.

7. **Histologia eta analisi immunohistokimikoak**

7.1. Saguen sakrifizioa eta ehunen prozesamendua

Saguak Ketamina/xilazina (80/10 mg/Kg; Imalgene®) zeraman txerto intraperitoneal baten bitartez anestesiatu ziren eta bihotzean zeharreko perfusioa burutu zitzaien ponpa peristaltiko baten laguntzaz, lehendabizi disoluzio fisiologikoarekin eta ondoren 0,1 M PB-tan prestatutako %4 paraformaldehido zeraman disoluzio finkatzailearekin. Ondoren, garunak eta bizkar hezur muinak 3 orduz %4 paraformaldehidotan post-finkatu eta gau batez %20 sakarosatan kriobabestu ziren. Azkenik, ehun horiek Tissue-Tek OCT-arekin (Electron Microscopy Sciences, Hatfield, PA, AEB) babestu eta -80°C-tan gorde ziren. Garuneko sekzio koronalak eta bizkar hezur muinen luzetarako sekzioak (10 µm-ko lodiera) CM3050S kriostatoa (Leica) erabiliz lortu ziren eta -20°C-tan gorde erabili arte. Ehunen batzuk beste prozesamendu bat jasan zuten, hau da, post-finkatuak izan ondoren, %0,02 sodio azida zeraman 0,1 M PB-tan gorde ziren ondoren sekzioak (40 µm-ko lodiera) bibratomo bidez lortu ahal izateko.

7.2. Histologia

Kuprizonarekin tratatutako saguen garunetako sekzio koronalak (bregma 1 eta -1; Paxinos and Franklin, 2012), mielinaren ebaluaziorako, Luxol Fast Blue-arekin (LFB) markatu ziren. Horretarako, ehunak, gau batez eta 37-42°C-tara, % 95-ko etanola, %0,5 azido azetiko glazial eta %0,1 LFB solbente 38 (Sigma-Aldrich) zeramatzan disoluzio batekin tratatu ziren. Ondoren, sekzioak %0,01 litio karbonatoarekin (Sigma-Aldrich) tindugabetu ziren. Azkenik, alkohol kontzentrazio desberdinetatik pasatuz (%50-%100) ehunak deshidratatu eta jarraian DPX-arekin (Sigma-Aldrich) estali ziren. Bestalde, EAE ereduko saguen bizkar hezur muinen sekzioak, hanturazko infiltrazioen ebaluaziorako, Nissl-arekin markatu ziren. Horretarako, bizkar hezur muin ehunak xilenotik pasa eta jarraian, etanol kontzentrazioak jaitsiz, berhidratatu egin ziren. Ondoren, %1 toluidina urdina ur destilatuan disolbatu eta ehunak bertan sartu ziren. Azkenik, sekzioak garbitu, deshidratatu eta DPX-arekin estali ziren.

7.3. Immunofluoreszentzia eta immunoperoxidasa markaketak

Ehunak %5 serum (NGS) eta %0,2 Triton X-100 zeramatzan TBS-tan blokeatu ziren ordubetez. Jarraian, saguan eginiko MBP-aren aurkako (1:1000; Covance, Princeton, NJ, AEB), saguan eginiko GFAP-ren aurkako (1:40; Merck Millipore), untxian eginiko NG2-aren aurkako (1:200; Merck Millipore) edo arratoian eginiko CD11b-aren aurkako (1:100; Merck Millipore) antigorputz primarioekin inkubatu ziren gau osoz 4°C-tara. Hainbat garbiketen ondoren, ahuntzean egindako 388 edo 594 fluoroforoei konjugatutako antigorputz sekundarioak (1:400; Invitrogen, Carlsbad, CA, AEB) gehitu zitzaizkien antigorputz primarioak detektatu ahal izateko eta, bestalde, Hoechst 33258-a (5 µg/mL; Sigma-Aldrich) kromatina markatzeko. Azkenik ehunak Glycergel-a (Dako, Carpinteria, CA, AEB) erabiliz estali ziren.

Immunoperoxidasa metodoaren kasuan, garun ehunak lehendabizi 10 minutuz %1 H_2O_2 –arekin tratatu ziren giro tenperaturan. TBS-arekin hainbat aldiz garbitu ondoren, ehunak 30 minutuz %10 BSA, %0,1 sodio azida eta %0,002 saponina zeramatzan TBS-arekin blokeatu ziren. Jarraian, 3 egunez eta 4°C-tara, sekzioak untxian egindako ABHD6 entzimaren aurkako antigorputz primarioarekin (1:250; adeitsuki Mark Brown doktoreak emana, Cleveland Clinic Lerner Research Institute, Cleveland, OH, AEB) inkubatu ziren. Antigorputz primarioa ezagutzeko, ehunak zaldian eginiko untxi IgG-ak ezagutzen dituen biotinilatutako antigorputz sekundarioarekin (1:200; Vector Laboratories, Burlingame, CA, AEB) eta abidina-biotina konplexuarekin (ABC; Elite, Vector Laboratories) tratatu ziren. Immunoperoxidasaren erreakzioa DAB-a erabiliz burutu zen. Amaitzeko, sekzioak ur destilatuarekin garbitu eta DPX-a erabiliz estali ziren. Esperimentu bakoitzean kontrolak erabili genituen, antigorputz primariorik gehitu ez izanez gero markaketarik existitzen ez zela egiaztatzeko.

7.4. Irudien analisia

Ehun sekzioen argazkiak saio berean atera ziren Axiocam MRc5 kamara digital bati lotutako Zeiss Axioplan 2 mikroskopio bat erabiliz (Zeiss, Oberkochen, Alemania). Desmielinizazioa, hanturazko erantzuna (zelula glialen erreaktibitatea) eta ABHD6 entzimaren adierazpena ebaluatzeko gorputz kailukara erdialdean 2 argazki atera ziren 40X objektiboa erabiliz. Mielinaren kaltea ebaluatzeko LFB eta MBP markaketak 0-tik 4-ra puntuatu ziren, 0 mielinizazio totala eta 4 mielina normala izanik. Bizkar hezur muinetan hanturazko lesioen ebaluazioa egiteko berriz, 20X-ko objektiboarekin ateratako 45-50 argazki kontsekutibo aztertu ziren. Bestale, ehun hauetan $CD11b^+$ mikroglia/makrofagoen zenbaketa 40X-ko objektiboarekin gai zurian semi-kontsekutiboki ateratako 15-20 argazkitan burutu zen.

Immunohistokimia bidez burututako markaketak ebaluatzeko, fluoreszentziazko mikroskopioaren intentsitatea antigorputz primariorik gabeko kontroletan seinalerik ikusten ez zen puntuan ezarri zen. Zelula glialen immuno-markaketa Image J softwarea erabiliz neurtu zen. ABHD6 eta GFAP-aren aurkako antigorputzen kasuan, markatutako area 16 bit-era pasatako irudietan neurtu eta gorputz kailukararen area osoagatik zatituz kalkulatu zen (markatutako area/area totala). Mikroglia/makrofagoen kasuan, $CD11b^+$ zelulak banan banan zenbatu eta milimetro karratuko adierazi ziren (zelula totalak/ mm^2). Analisi guztiak gutxienez 4 saguko taldeetan burutu ziren.

8. **Gene adierazpenen analisia**

Saguak Ketamina/xilazina (80/10 mg/Kg; Imalgene®) zeraman txerto intraperitoneal baten bitartez anestesiatu eta 30 segunduz disoluzio fisiologikoarekin perfunditu ziren ponpa peristaltiko baten laguntzaz. Kuprizona ereduko animalien garuneko +1 eta -1 bregma (Paxinos and Franklin,

2012) nibelen arteko eta EAE ereduko saguen garuneko +1.1 eta +0.2 bregma nibelen arteko sekzioak isolatu ziren David Kopf garun zatitzaile bat erabiliz (Tujunga, CA, AEB). Garun zati horiek eta bizkar hezur muinak RNAlater-aren (Qiagen, Hilden, Alemania) bidez babestu ondoren -80°C-tan gorde ziren erabili arte.

Ehunen RNA totala RNeasy Protect Mini Kit-a (Qiagen) erabiliz erauzi zen eta kultibatutako zelulena berriz RNA Miniprep Kit-a (Agilent, Santa Clara, CA, AEB) erabiliz. cDNA-ren sintesia Superscript™ III erretrotranskriptasa-ren (Invitrogen) bitartez burutu zen ausazko hasleak erabiliz (*random primers*). Hasle zehatzak, DNA genomikoaren anplifikazioa ekiditeko, exoien lotuneetan diseinatu ziren Primer Express software-a (Applied Biosystems, Foster City, CA, AEB) erabiliz. Hasleen sekuentziak honakoak izan ziren: sagu eta arratoi *Abhd6* zuzena 5'-ACC GGA AAT TGT TTT TGG AAA TC-3' eta atzeranzkoa 5'-GCT AAT ATG TCT GCC CCC GA-3´; sagu *Iba1* zuzena 5'-GCA GGA AGA GAG GCT GGA GGG GAT C-3' eta atzeranzkoa 5'-CTC TTA GCT CTA GGT GGG TCT TGG G-3; sagu *IL1β* zuzena 5'- GAG AGT GTG GAT CCC AAG CAA TAC- 3' eta atzeranzkoa 5'-GAC AAA CCG TTT TTC CAT CTT CTT-3´; sagu *TNFα* zuzena 5'-GCC TCT TCT CAT TCC TGC TTG TGG CAG-3' eta atzeranzkoa 5'- GAC GTG GGC TAC AGG CTT GTC ACT CG-3´; sagu *COX2* zuzena 5'-GGG AGT CTG GAA CAT TGT GAA-3' eta atzeranzkoa 5'- GCA CAT TGT AAG TAG GTG GAC TGT-3´; arratoi *Gapdh* zuzena 5'-GAA GGT CGG TGT CAA CGG ATT T-3' eta atzeranzkoa 5'- CAA TGT CCA CTT TGT CAC AAG AGA A-3´; arratoi *Hprt1* zuzena 5'-ATG GAC TGA TTA TGG ACA GGA CTG A-3' eta atzeranzkoa 5'-ACA CAG AGG GCC ACA ATG TG-3´; sagu *Gapdh* zuzena 5'-TGC AGT GCC AGC CTC GTC -3' eta atzeranzkoa 5'-GCC ACT GCA AAT GGC AGC-3´; sagu *Hprt1* zuzena 5'- TAC TGT AAT GAT CAG TCA ACG GGG-3' eta atzeranzkoa 5'-GTT GAG AGA TCA TCT CCA CCA ATA AC- 3´. Denbora errealeko PCR kuantitatiboa dNTP-ak, Sso7d fusio polimerasa, $MgCl_2$-a, EvaGreen sonda eta egonkortzaileak daramatzan SsoFastTM EvaGreen Supermix-a (Bio-Rad) erabiliz burutu zen CFX96 Denbora-Errealeko PCR Detekzio Sistema (Bio-Rad) baten bitartez. Lagin bakoitzeko intereseko mRNA-en adierazpen mailak kurba estandar batean oinarrituta kalkulatu ziren eta emaitzak gene adierazpen erlatibo bezala aurkeztu ziren RNA estandar horren diluzio fakotoreetan oinarrituta edo $2^{-\Delta\Delta Ct}$ algoritmora erabiliz. Balioak *Gapdh* eta *Hprt1* geneen adierazpen mailetan oinarrituta normalizatu ziren.

9. **Autorradiografia**

Anestesiatutako saguak (IsoVet®) dekapitazio bitartez sakrifikatu ziren. Jarraian garunak atera eta -80°C-tan mantendu ziren erabili arte. Autorradiografia entseguak CM3050S kriostato (Leica) bidez lortutako 20 µm-ko lodieradun sekzioetan burutu ziren. CB_1 hartzailearen autorradiografietarako, sekzioak, 30 minutuz eta giro tenperaturan, 50 mM Tris-HCl eta %1 BSA zeramatzan tanpoian (pH 7.4) inkubatu ziren. Segidan, tanpoi berdinari 3 nM [^{3}H](−)-cis-3-[2-Hidroxi-4-(1,1-dimetilheptl) fenil]-trans-4-(3-hidroxipropil) ziklohexanola ([^{3}H]CP55,940; 150.2 Ci/mmol; ARC, San Louis, MA, AEB) gehitu zitzaizkion eta ehunak bertan inkubatu ziren 2 orduz 37°C-tara. Lotura ez espezifikoak zehazteko asmoz, ehun batzuen inkubazioari 10 µM CP55,940 ere gehitu zitzaien. Lotu gabeko erradioestekatzailea %1 BSA zeraman 50 mM Tris-HCl-arekin garbituz kendu zen. Lehortu ondoren, ehunak 21 egunez eta 4°C-tara film ^{3}H-sentikorretara (Kodak BioMax MR, Sigma-Aldrich) aplikatu ziren, horrela autorradiogramak lortuz. Agonista kannabinoide bidez estimulatutako [^{35}S]GTPγS autorradiografien kasuan, ehunak, 30 minutuz eta 30°C-tara, 50 mM HEPES, 0,2 mM EGTA, 3 mM $MgCl_2$, 100 mM NaCl eta %0,5 BSA zeramatzan tanpoian (pH 7.4) inkubatu ziren estekatzaile endogenoak kendu ahal izateko. Ondoren, tanpoi berdinari 1 mM DTT, 2 mM GDP, 3 mU/mL adenosina deaminasa eta 0,04 nM [^{35}S]GTPγS (1250 Ci/mmol; Perkin Elmer, Waltham, MA, AEB) gehitu zitzaizkion eta ehunak bertan 120 minutuz inkubatu ziren. Jarraian, garun sekzioak agonista kannabinoidea den WIN55,212-2-aren 1 µM-ekin inkubatu ziren. Lotura ez

espezifikoak 10 µM guanosina- 5-O-(3-tio) trifosfato-aren (GTPγS) presentzian determinatu ziren. Azkenik, sekzioak 50 mM Tris-HCl-tan (pH 7.4) garbitu, lehortu eta film ^{14}C-sentikorretara (Amersham Systems, GE Healthcare Europe GmbH) aplikatu ziren ^{14}C-polimero estandarren presentzian 2 egunez 4°C-tara. Bukatzeko, autorradiogramak eskaneatu eta Image J Sofware-a erabiliz analizatu ziren.

10. **Western blot analisiak**

Saguak Ketamina/xilazina (80/10 mg/Kg; Imalgene®) zeraman txerto introperitoneal baten bitartez anestesiatu eta 30 segunduz disoluzio fisiologikoarekin perfunditu ziren ponpa peristaltiko baten laguntzaz. +1 eta -1, edo +1.1 eta +0.2 bregma nibelen (Paxinos and Franklin, 2012) arteko sekzioak David Kopf garun zatitzaile bat erabiliz isolatu eta -80˚C-tara gorde ziren erabili arte. Ehunak kristal eta tefloizko homogeneizagailu baten laguntzaz homogeneizatu ziren proteasen inhibitzaile nahasketa bat (Mini EDTA-free tablets, Roche, Mannheim, Alemania) zeraman 200 µl RIPA-ren presentzian. Jarraian homogeneizatutako garunak 12,000 rpm-tara zentrifugatu ziren 10 minutuz eta 4°C-tara. Gainjalkinetako proteina kopurua Bradford entsegu (Bio-Rad) bidez kalkulatu zen. Lagin bakoitzeko 10 µg proteina %10 SDS-PAGE gelen bitartez banatu eta ondoren nitrozelulosazko mintzetara (Hybond ECL, GE Healthcare Europe GmbH, Bartzelona, Espainia) transferitu ziren. Lotura ez espezifikoak ekiditeko, mintzak, ordubetez eta giro tenperaturan, %5 BSA eta %1 NGS zeramatzan %0,05 Tween/TBS (TBST)-tan blokeatu ziren. Jarraian, proteinen detekziorako, mintz horiek blokeo disoluzioan prestatutako untxian eginiko ABHD6-aren aurkako antigorputz (1:500; adeitsuki J Mark Brown doktoreak emana), untxian eginiko MBP-aren aurkako antigorputz (1:5000; Merck Millipore) eta untxian eginiko β-aktinaren aurkako antigorputz (1:5000; Sigma-Aldrich) primarioekin inkubatu ziren, gau osoz eta 4˚C-tara. Hainbat garbiketen ondoren, mintzak peroxidasarekin konjugatutako antigorputz sekundarioekin (1:5000; Sigma-Aldrich) inkubatu eta kimioluminiszentzia erabiliz errebelatu ziren fabrikatzailearen argibideei jarraituz (Super Signal West Dura, Pierce, Rockford, IL, AEB). Azkenik, proteinen bandak ChemiDoc™ XRS imagen sistema (Bio-Rad) erabiliz identifikatu ziren. Banden seinalea Image-J Software-a erabiliz neurtu zen eta balioak β-aktinaren seinalean oinarrituz normalizatu ziren.

11. **Oligodendrozitoen kultiboak**

Glia zelulen kultibo mixtoak Sprague-Dawley arratoi jaioberriak (P0-P2) erabiliz burutu ziren lehenago deskribatutako prozedurak jarraituz (McCarthy and de Vellis 1980). Garunak garezurretatik atera eta kortex-ak isolatu ziren. Jarraian, kortex horien digestioa burutu zen hauek %0,25% tripsina eta %4 DNAsa zeramatzan HBSS medioarekin inkubatuz (15 min, 37°C). Ondoren, tamaina desberdinetako orratzetatik pasatuz (21 G eta 23 G), zelulen disoziazio mekanikoa burutu zen. Zelula hauek, zentrifugatu ostean, %10 FBS (HyClone™, Thermo Fisher Scientific, Waltham, MA, AEB) eta antibiotiko/antimikotiko disoluzioak zeramatzan Iscovek aldatutako Dulbecco-ren Medioan (Iscove´s Modified Dubelcco´s Medium, IMDM, Thermo Fisher Scientific) berreseki ziren. Ondoren, zelulak poli-D-lisina-rekin estalitako 75 cm^2 flaskoetan erein ziren eta bertan mantendu ziren 10-15 egunez 37°C-tara eta %5 CO_2-ren presentzian. Orduan, flaskoak, 2 orduz eta 37°C-tan, 400 rpm-tara astindu ziren mikrogliak kentzeko asmoz. Astrozito geruzaren gaineko OPC-ak flaskoak gau osoz 400 rpm-ra astinduz askatu ziren. Zelula esekiak 10 µm-ko nylon-ezko sare batetik pasatuz filtratu ziren eta Petri plaketan erein ordubetez. Ondoren, itsatsi gabeko zelulak beste Petri plaka batzuetan erein ziren 2 orduz. Prozesu horien ondoren geratutako zelula esekiak zentrifugatu eta 100 µg/mL transferrina, 60 ng/mL progesterona, 40 ng/ mL sodio selenitea, 5 µg/mL intsulina, 16 µg/mL putreszina eta 100 µg/ mL BSA zeramatzan Dulbecco-k aldatutako Eagle-en Medioan (Dulbecco's Modified Eagle's Medium, DMEM) berreseki ziren. Exzitotoxizitate esperimentuetarako

zelulak poli-D-lisina-z estalitako 48 putzutxoko plaketan erein ziren, dentsitatea 8×10^3 zelula/putzutxoko izanik. Bestalde, western-blot analisietarako 4×10^4 zelula/putzutxoko eta PCR entseguetarako 10^5 zelula/putzutxoko erein ziren, poli-D-lisina-z estalitako kristalezko kubreak zeramatzaten 24 putzutxoko plaketan. Zelulak 2 egunez PDGF-AA (5 ng/mL) eta bFGF (5 ng/mL) faktore mitotikoen presentzian mantendu ziren, zelula kopurua handitu eta diferentziazioa ekiditeko asmoz. Kultiboen purutasuna immunozitokimia bidez frogatu zen, horretarako zelula desberdinak markatzen dituzten antigorputzak erabiliz : Olig-2 (1:1000; Merck Millipore); PDGFRα (1:200; Santa Cruz Bio technology); GFAP (1:80; Merck Millipore) edo Iba-1 (1:2000; Wako, Richmond, VA, AEB). 2 eguneko hazkuntzaren ondoren Olig-2^+ zelulak totalen %95 ± 0.2 osatzen zutela frogatu zen. Gainontzeo zelulak astrozito GFAP$^+$ edo mikroglia Iba-1^+ bezala identifikatu ziren (*n* = 7 kultibo, 4 kristalezko kubre; 15 argazki kubreko). Kultibo berdinetan OPC PDGFRα^{+-}ak totalen %92.5 ± 0.5 osatzen zutela frogatu zen. Exzitotoxizitate esperimentuetarako OPC-en diferentziazioa bultzatu zen, hauek 1 edo 2 egunez faktore mitogenikorik gabeko eta triiodotironina (T3; 30 ng/mL), faktore neurotrofiko ziliarra (CNTF; 10 ng/mL) eta neurotrofina 3 (NT-3; 1 ng/mL) diferentziazio faktoreak zeramatzan medioan mantenduz.

12. **Oligodendrozitoen toxizitate entseguak**

Oligodendrozitoak 30 minutuz drogekin edo eramailearekin [DMSO %0,1-%0,2 (v/v) amaierako kontzentrazioa izanik] tratatu ziren eta jarraian AMPA eta ziklotiazida gehitu zitzaien (10 µM: 100 µM; Abcam, Cambridge, EB) 15 minutuz. Ondoren, medioa aldatu zitzaien eta gau osoz ABHD6 entzimaren KT182 eta MAGL entzimaren JZL184 (Cayman Chemical) inhibitzaileen presentzian inkubatu ziren. Zelulen bideragarritasuna estimulu exzitotoxikoa baino 24 ordu beranduago neurtu zen 3-(4,5-dimetiltiazol-2-yl)-2,5-difeniltetrazolium bromida (MTT; CellTiter 96® on-Radioactive Cell Proliferation Assay, Promega, Madison, WI, AEB) erabiliz. Produktu gisa lortutako koloredun formazana Synergy-HT fluorimetroaren (Bio-Tek Instruments, Winooski, VT, AEB) bitartez neurtu zen 570 nm-tako uhin luzeran. Gutxienez triplikadun 3 esperimentu independente burutu ziren kondizio bakoitzarentzat.

13. **Oligodendrozitoen diferentziazio entseguak**

OPC-en diferentziazioa bultzatzeko, zelula hauei faktore mitogenikorik gabeko eta T3 (30 ng/mL), CNTF (10 ng/mL) eta NT-3 (1 ng/mL) faktore diferentziatzaileak zeramatzan medio berria ipini zitzaien, KT182 eta JZL 184 inhibitzaileen presentzian edo ausentzian. Inhibitzaile hauek egunero gehitu zitzaizkien zelulei. Diferentziazio maila MBP proteinaren adierazpen mailak western-blot analisi bitartez neurtuz aztertu zen. Horretarako, zelulak 40 µL elektroforesi tanpoiarekin (sample buffer) lisatu eta %10 SDS-PAGE geletara ezarri ziren, aurretik azaldutako prozedura jarraituz. Gutxienez 3 esperimentu independente burutu ziren kondizio bakoitzarentzat.

14. **Neuronen Kultiboak**

Neuronen kultibo primarioak Sprague-Dawley arratoien E18 enbrioietatik lortu ziren lehenago desbribatua izan den prozedura jarraituz (Ruiz et al. 2014). Isoflurano (IsoVet®) bitartez anestesiatutako arratoi izorrak dekapitazioz sakrifikatu ziren eta enbrioiak atera zitzaizkien. Enbrioi hauek HBSS (Ca^{2+} eta Mg^{2+} gabe eta 10 mM glucosa eta 10 mM glizina gehituta) zuten Petri plaketan jaso ziren. Garunak atera eta kortexak isolatu ziren, odola eta meningeak ongi kenduta zeudela ziurtatuz. Kortex guztiak elkartu eta, 5 minutuz 37^{o}C-tara eta %5 CO_2-ren presentzian, %4 tripsina eta %0,25 DNAsa-rekin inkubatu ziren. Entzimen aktibitatea %0,02 B-27 (Gibco-Thermo Fisher Scientific), %0,01 Penizilina-estreptomizina-fungizona (Sigma-Aldrich), %0,002 glutamina eta %10 FBS (Gibco-Thermo Fisher Scientific) zeramatzan Neurobasal medioaren (NB; Gibco-Thermo Fisher

Scientific) 4 mL gehituz gelditu zen. Zentrifugatu ondoren (200 G, 5 min), jalkin bakoitza 1 mL NB+FBS-tan berreseki eta tamaina desberdinetako orratzetatik (21 G eta 23 G) pasatuz disoziatu zen. Zelula esekiak 40 µm-ko nylon-ezko sare (Millipore) batetik pasatuz filtratu eta poli-L-ornitina-az estalitako 48 putzutxoko plaketan erein ziren, dentsitatea 1×10^5 zelula/putzutxoko izanik. Mikroskopio konfokal bidezko zelula bakarren irudikapen esperimentuetarako, oinarria kristalezkoa duten plakatxoetan (Ibidi GmbH, Planegg/Martinsried, Alemania) erein ziren zelulak. 24 ordura medioa aldatu zitzaien, B27 zeraman serumik gabeko Neurobasal medioa gehituz. Medio horrekin 8-9 egun mantendu ziren 37°C-tara eta %5 CO_2-aren presentzian. Kaltzio mitokondrialaren analisirako, zelulak mitokondrien 2mtD4cpv adierazlea zeramaten plasmidoekin transfektatu ziren (adeitsuki Roger Tsien doktoreak emanak, University of California, La Jolla, CA, AEB). Transfekziorako, erein aurretik, Rat Neuron Nucleofector Kit-a (Lonza, Basel, Suitza) erabiliz, 4×10^6 neurona 3 µg cDNA-rekin elektroporatu ziren. Ondoren, azaldu bezala erein eta mantendu ziren.

15. **Neuronen toxizitate entseguak**

Neuronak 30 minutuz egon ziren drogen edo eramailearen presentzian. Ondoren, Ca^{2+} eta Mg^{2+} gabeko eta 10 mM glukosa, 2,6 mM $CaCl_2$ eta 10 mM glizina zituen HBSS medioan disolbatutako N-metil-D-aspartatoa (NMDA, 100 µM; Sigma-Aldrich) gehitu zitzaien 15 minutuz 37°C-tara. Jarraian, medioa aldatu zitzaien B27 zeraman Neurobasal medioa gehituz. Zelulen bideragarritasuna 24 ordu beranduago neurtu zen Citotox 96 entsegu kolorimetrikoa (Promega, Madison, WI, AEB) erabiliz. Metodo hau laktato deshidrogenasa (LDH) entzimak tetrazolio gatza formazanean bihurtzeko duen ahalmena neurtzean datza. Erreakzio kolorimetriko hau ,490 nm-ko uhin luzeran, Synergy-HT fluorimetroa (Bio-Tek Instruments) erabiliz neurtu zen. Gutxienez triplikadun 4 esperimentu independente burutu ziren kondizio bakoitzarentzat.

16. **Kaltzio mitokondrialaren neurketa**

Mitokondrien kaltzio erantzunak analisatu ahal izateko, 2mtD4cpv adierazlearekin transfektatutako neuronak, 20 mM HEPES, 10 mM glukosa, 2,6 mM $CaCl_2$ eta 10 mM glizina zeramatzan HBSS-tara (pH 7,4) pasatu ziren. Neurona horiek TCS SP8X mikroskopio konfokal (Leica) baten bitartez aztertu ziren. Zelulak 458 nm-ko uhin luzerara estimulatu ziren eta cfp eta yfp emisioak jaso ziren FRET ratioaren kuantifikaziorako. NMDA-ren aurrean neuronek izandako erantzuna aztertzeko, emisioak 5 minutuz 15 segunduro jaso ziren. Datuen analisirako, Petri plaka barruan 5-12 zelula inguruko populazio homogeneoak aukeratu ziren eta neuronen somak intereseko area gisa hautatu ziren (ROI). Balio ez espezifikoak kendu ondoren, datuak $R/R_0 \pm$ S.E.M. (%) gisa adierazi ziren, R denbora zehatz bateko yfp/cpf fluoreszentzia ratioa izanik eta R_0 berriz estimulurik gabe zelulek adierazten duten FRET-aren ratioa. Datuak estatistikoki konparatzeko, zelula bakoitzak NMDA aplikatu ondoren erakutsitako erantzun kurbaren azpiko area (area under the curve, AUC) neurtuz kalkulatu zen.

17. **Analisi estatistikoa**

Datuak batazbestekoa ± errore estandarra (SEM) bezala irudikatu dira eta *n*-ak laginarean tamaina adierazten du (animali edo kultibo kopurua). Analisi estatistikoak GraphPad Prism 6-aren 5.0 bertsioa erabiliz burutu ziren (GraphPad Software Inc. San Diego, CA, AEB). EAE ereduko kurtso tenporalak eta egoera motorearen puntuazioak ez parekatutako Mann-Whitney *U*-test-a erabiliz analizatu ziren. Barra moduan adierazitako egoera motorearen puntuazio datuak eta datu histologiko eta biokimikoak, normaltasun testa aplikatu ondoren, ez parekatutako Student-en *t*-testarekin edo Mann Whitney *U*-testarekin analizatu ziren. Kasu guztietan $< 0,05$ *p* balioak estatistikoki adierazgarriak kontsideratu ziren.

Emaitzak – 1. Helburua

EMAITZAK- 1. HELBURUA

1. CB_1 hartzaileen lokalizazio ultraegiturala oligodendrozitoen zelula aintzinadarietan

OPC-etan CB_1 hartzaileen lokalizazioa aztertu ahal izateko mikroskopio elektroniko (ME) bidez ikusi daitekeen markaketa bikoitza erabili genuen, alde batetik, inmunoperoxidasan, eta bestetik, zilarrez amplifikatatuko urrezko partikuletan oinarritutakoa hain zuzen ere. OPC-ak era egokian identifikatu ahal izateko, NG2 proteina kodifikatzen duen genearen promotorearen menpe proteina hori fluoreszentea (NG2-EYFP) adierazten duten sagu transgenikoak erabili genituen (Karram et al., 2008). Sagu hauen karakterizazioaren arabera, EYFP-a adierazten duten zelula gehienek, oligodendrozito heldugabeetan espero izatekoa den moduan, *Olig2* eta *Sox10* transkripzio faktoreak ere adierazten dituzte. Gainera, ez dituzte inondik inora oligodendrozito helduen markatzaileak adierazten. NG2-EYFP-arentzat heterozigotoak ziren saguak $CB_1^{+/-}$ saguekin gurutzatu genituen, NG2-$EYFP^{+/-}$-$CB_1^{+/+}$ eta NG2-$EYFP^{+/-}$-$CB_1^{-/-}$ mutante bikoitzak lortuz. Animali hauetan, OPC-ak EYFP proteinaren aurkako immunomarketak eragindako DAB metaketari esker identifikatu ziren, CB_1 hartzaileak, berriz, zilarrez amplifikatatuko urrezko partikulen presentzia bitartez (**1. Irudia**).

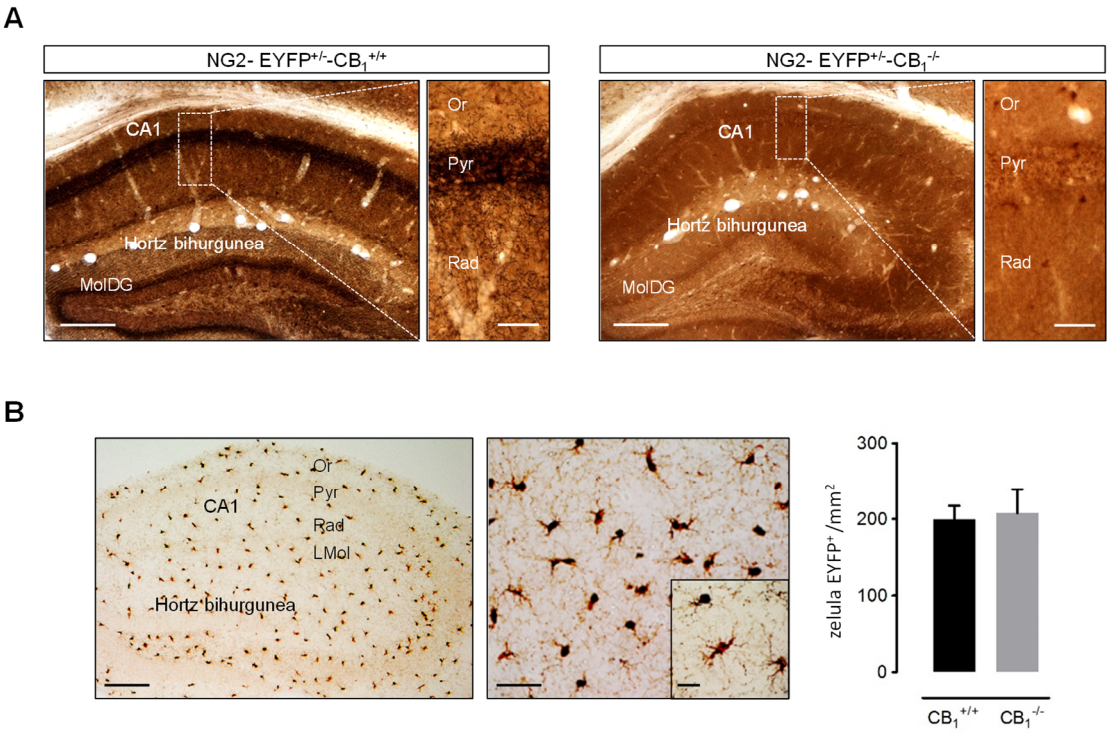

1. Irudia. CB_1 hartzailearen lokalizazioa NG2-$EYFP^{+/-}$-$CB_1^{+/+}$ saguen hipokanpoan. (**A**) Markaketa bikoitza erakusten duten irudi adierazgarriak. OPC-ak inmunoperoxidasa metodoaren bitartez markatuak ikusi daitezke, CB_1 hartzaileak berriz, zilarrez amplifikitatuko urrezko partikulen bidez. NG2-$EYFP^{+/-}$-$CB_1^{+/+}$ saguen hipokanpoko Pyr eta MoDG geruzetan CB_1 hartzaileen markaketa esanguratsua ikus daiteke. CB_1 markaketa xehetasun handiagoan erakusten duten irudiak aurkezten dira alboan. NG2-$EYFP^{+/-}$-$CB_1^{-/-}$ saguen hipokanpoan markaketa bereizgarri hau ikustezina da, erabilitako CB_1 aren aurkako antigorputza espezifikoa dela frogatuz. (**B**) EYFP-aren aurkako inmunoperoxidasa bidezko markaketa NG2-$EYFP^{+/-}$-$CB_1^{+/+}$ saguen hipokanpoan. Bertan, NG2 zelulen morfologia eta distribuzio adierazgarria ikus daiteke. NG2 zelulen kopuruari dagokionez, analisi kuantitatiboak ez du desberdintasunik adierazten NG2-$EYFP^{+/-}$-$CB_1^{+/+}$ eta NG2-$EYFP^{+/-}$-$CB_1^{-/-}$ animalien artean. (*n* = 3 sagu taldeko). CA1, *cornu ammonis*; Or, *stratum oriens*; Pyr, *stratum pyramidale*; Rad, *stratum radiatum*; MoDG, hortz bihurgune molekularra. eskala barrak: 200 µm eta 25 µm (**A**); 200 µm, 50 µm eta 25 µm (**B**).

NG2-EYFP$^{+/-}$-CB$_1^{+/+}$ saguen hipokanpoan CB$_1$ hartzaileen markaketa lehendabizi argi-mikroskopio bitartez egiaztatu zen. Aldez aurretiko deskribapen lanekin bat eginez (Hájos et al., 2000; Gutiérrez-Rodríguez et al., 2017), haritsu itxurako markaketa esanguratsua hauteman genuen hipokanpoko CA1 eta CA3-an, batik bat hortz bihurgunean, geruza piramidalean eta *stratum radiatum*-ean. NG2-EYFP$^{+/-}$-CB$_1^{-/-}$ saguen hipokanpoan markaketa ikustezina zela egiaztatzean, seinalea espezifikoa zela frogatu ahal izan genuen (**1. Irudia A**). Bestalde, NG2-EYFP$^{+/-}$-CB$_1^{+/+}$ animali transgenikoetan, DAB seinaleak NG2 zelulen distribuzio uniforme eta ezaguna jarraitzen zuela frogatu genuen (Karram et al., 2008). Azkenik, DAB-arentzat positibo ziren zelulen kopuruari dagokionez, NG2-EYFP$^{+/-}$-CB$_1^{-/-}$ eta NG2-EYFP$^{+/-}$-CB$_1^{+/+}$ saguen artean desberdintasunik ez zegoela egiaztatu genuen (**1. Irudia A** eta **B**).

Ultraegitura mailako azterketa egitean, NG2-EYFP$^{+/-}$-CB$_1^{+/+}$ saguen *stratum radiatum*-ean, dendritekin sinaptatzen duten bukaera inhibitorioek CB$_1$ hartzailea markatzen zuten partikula ugari erakusten zituztela ikusi genuen (Hájos et al., 2000; Gutiérrez-Rodríguez et al., 2017) (**2. Irudia C**). Espero bezala, beraien morfologia bereizgarriagatik identifikatutako sinapsi kitzikatzaileetan askoz partikula gutxiago antzeman genituen (**2. Irudia C**). Berriro ere, NG2-EYFP$^{+/-}$-CB$_1^{-/-}$ saguen garun ehunean markaketa desagertu egiten zela egiaztatu genuen, ibilitako antigorputza espezifikoa zela frogatuz.

ME-ko irudietan, OPC-ak eta beraien prozesuak DAB markaketari esker identifikatuak izan ziren (**2. Irudia A**). NG2-EYFP$^{+/-}$-CB$_1^{+/+}$ saguetan, zelula horien %10,5 ± %0,72 -ak mintz zitoplasmatikoan zilar partikularen bat adierazten zutela ikusi genuen (**2. Irudia B**), NG2-EYFP$^{+/-}$-CB$_1^{-/-}$ saguen kasuan berriz %4,4 ± %0,40-ak (***p < 0.0001; **2. Irudia B**). Bi genotipoen arteko konparaketak, hipokanpoko *stratum radiatum*-eko NG2 zelulen %6 inguruk CB$_1$ hartzailea adierazten dutela erakusten du. DAB arentzat positiboak ziren profiletan, zilar partikulen dentsitatea 0,2 partikula/ µm-koa dela kalkulatu genuen (**2. Irudia D**). Era berean, garun area berdinean, sinapsietako CB$_1$ hartzaileen dentsitateak ere kalkulatu genituen. Emaitzen arabera, OPC-ek sinapsi kitzikatzaileek baino dentsitate baxuagoa erakusten dute (**p < 0.01) (**2. Irudia D**). Guztira, emaitza hauek sagu helduen hipokanpoko OPC-ek CB$_1$ hartzailea maila oso baxuan adierazten dutela iradokitzen dute.

2. CB$_1$ hartzaileen lokalizazio ultraegiturala oligodendrozito mielinizatzaileetan

Oligodendrozito heldu mielinizatzaileetan CB$_1$ hartzaileen lokalizazio ultraegiturala aztertu ahal izateko, zilarrez amplifikatatuko urrezko partikuletan oinarritutako markaketa metodoa aplikatu genien sagu basati (CB$_1^{+/+}$) eta CB$_1$ hartzailea adierazten ez zuten saguen (CB$_1^{-/-}$) garun ehunei. NG2-EYFP$^{+/-}$-CB$_1^{+/+}$ saguekin gertatzen zenaren antzera, CB$_1$ hartzailearen markaketa tipikoa bereizi genuen CB$_1^{+/+}$ animalien hipokanpoan (**3. Irudia A**). Berriro ere, CB$_1^{-/-}$ saguen ehunean markaketa desagertu egiten zela frogatu genuen, erabilitako antigorputzaren espezifizitatea beste behin frogatuz (**3. Irudia A**).

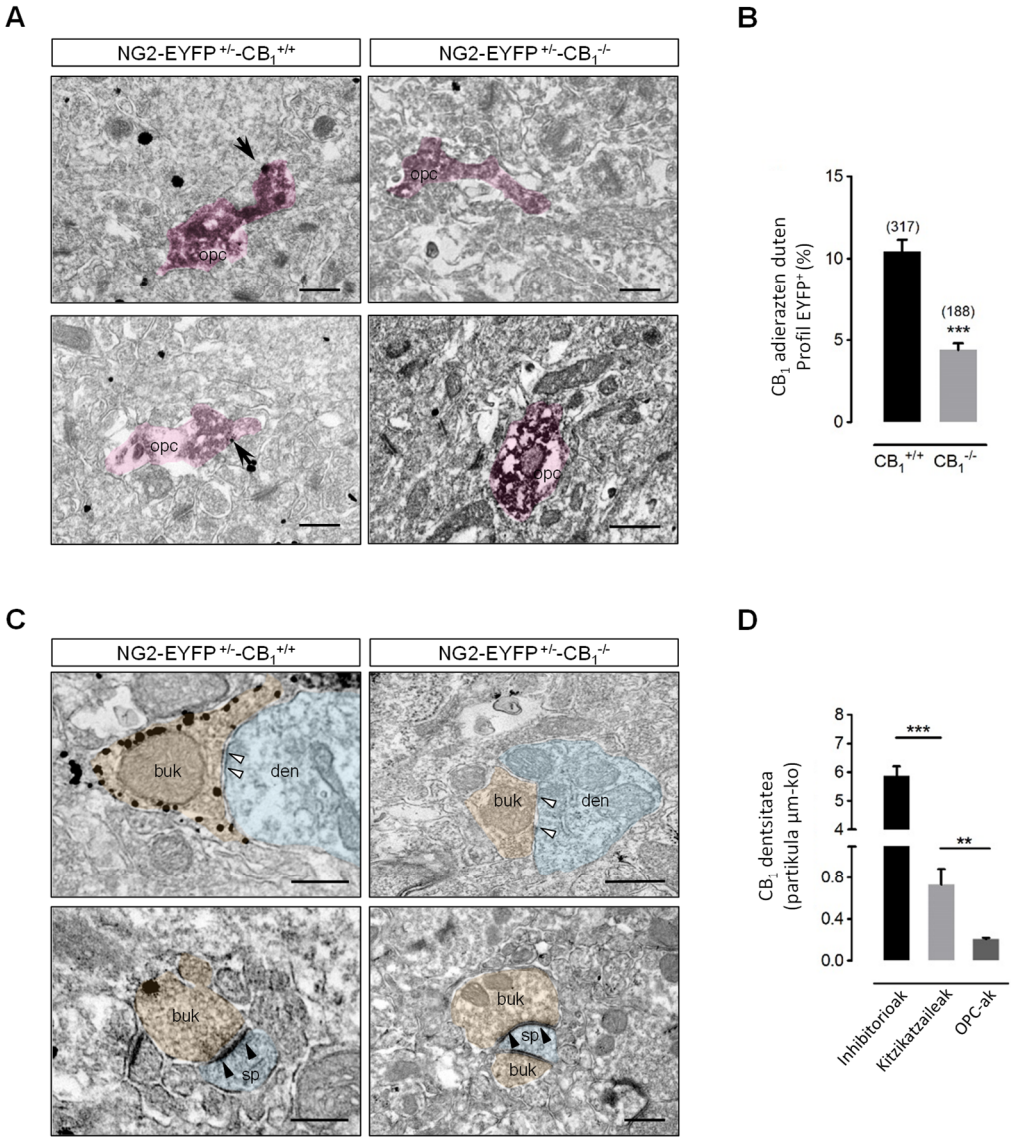

2. Irudia. CB_1 hartzaileen lokalizazioa saguen hipokanpoko oligodendrozitoen zelula aintzindarietan. (**A**) Mikroskopio elektronikoko argazki esanguratsuak. Bertan, NG2-$EYFP^{+/-}$ saguen garuneko sekzio koronaletan egindako zilarrez intensifikatutako urrezko partikulen bidezko CB_1 hartzaileen markaketa eta immunoperoxidasa bidezko EYFP zelulen markaketa ikus daitezke. OPC-en prozesuetan CB_1 hartzaileak markatzen dituzten urre partikulak (gezi beltzak) mintz plasmatikoan agertzen dira. Eskala barra: 500 nm. (**B**) CB_1 hartzailea adierazten duten OPC prozesuen zenbaketa NG2-$EYFP^{+/-}$ saguetan. CB_1 hartzailea adierazten duten prozesu DAB positibo gutxiago zenba daitezke NG2-$EYFP^{+/-}$-$CB_1^{-/-}$ saguetan (*n* = 5 sagu grupoko), erabilitako antigorputza espezifikoa dela frogatuz. Parentesi arteko zenbakiek zenbatutako OPC kopurua adierazten dute. (**C**) CB_1 hartzailearen distribuzioa NG2-$EYFP^{+/-}$ animalien bukaera sinaptikoetan. Eskala barra: 500 nm. Gezi-buru txuriak, sinapsi inhibitorioak; gezi-buru beltzak, sinapsi kitzikatzaileak; den, dendrita (urdinez); opc, oligodendrozitoen zelula aintzindaria (arroxez), sp, arantza dendritikoa (urdinez); buk, bukaera sinaptikoa (laranjaz). (**D**) CB_1 hartzaileen dentsitatea (partikula/mintz plasmatiko µm) NG2-$EYFP^{+/-}$-$CB_1^{+/+}$ saguen *stratum radiatum*-eko OPC-tan, bukaera inhibitorioetan eta bukaera kitzikatzaileetan kalkulatu zen (*n* = 3-5 sagu taldeko). $^{**}p < 0.01$ eta $^{***}p < 0.001$, Studenten *t*-testa.

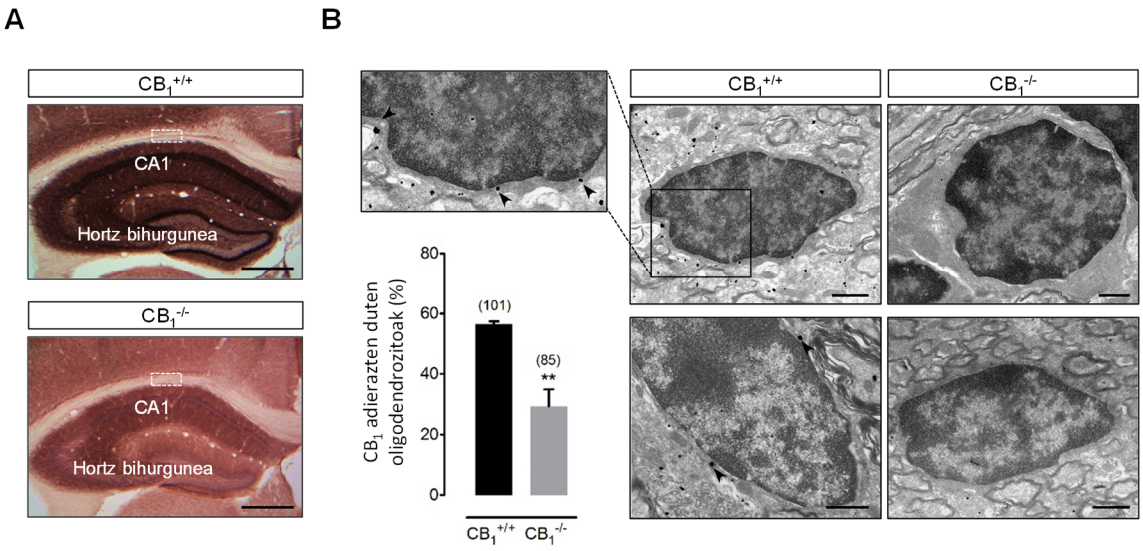

3. Irudia. CB_1 hartzaileen adierazpena sagu helduen garuneko oligodendrozito mielinizatzaileetan. (**A**) CB_1 hartzailearen markaketaren espezifikotasuna. Zilarrez intensifikatutako urre partikulen bidezko markeketa metodoa aplikatu zitzaien 60 eguneko sagu basati ($CB_1^{+/+}$) eta CB_1 hartzailea adierazten ez zuten saguen ($CB_1^{-/-}$) garun ehunei. Irudietan CB_1 hartzailearen markaketa tipikoa ikus daiteke, $CB_1^{-/-}$ saguetan desagertu egiten dena. Karratutxo zuriek mikroskopio elektronikoan aztertutako gai zuri areak seinalatzen dituzte. Eskala barra: 200 µm. (**B**) CB_1 hartzailearen lokalizazio ultraegiturala gorputz kailukarako oligodendrozito heldu mielinizatzaileetan. CB_1 hartzailea markatzen duten urre partikulak oligodendrozito somen (gezi beltzak) mintz plasmatikoan lokalizatzen dira. $CB_1^{-/-}$ saguetan, CB_1 hartzailea adierazten duten oligodendrozito kopurua adierazgarriki baxuagoa da (n = 3 sagu taldeka). Parentesi arteko zenbakiek zenbatutako oligodendrozito kopurua adierazten dute. $^{**}p < 0.01$; Studenten t-testa. Eskala barra: 1 µm.

CB_1 hartzailearen immuno-markaketa argi mikroskopio bitartez egiaztatu ondoren, ME bidez aztertu nahieko gai zuri area aukeratu eta sekzio ultrafinak egin ziren (**3. Irudia A**). Oligodendrozito heldu mielinizatzaileak beraien morfologia eta ezaugarri bereizgarrietan oinarrituta identifikatu ziren. Ezaugarri hauen artean nukleo elektrodentsoa edo nukleoa inguratzen duen zitoplasma fina aurki daitezke. Zelula horietan CB_1 hartzaileak zilarrez intentsifikatutako urre partikulen bidez identifatu ziren. $CB_1^{+/+}$ saguetan, zelula horien %56.4 ± %0.9 -ak somaren mintz zitoplasmatikoan zilar partikularen bat adierazten zutela ikusi genuen (**3. Irudia B**), $CB_1^{-/-}$ saguen kasuan %29.3 ± %5.7%-ak ($^{**}p < 0.01$). Bi genotipoen arteko konparaketak sagu helduen gorputz kailukarako oligodendrozito mielinizatzaileen %27 inguruk CB_1 hartzailea adierazten dutela erakusten du (**3. Irudia B**).

3. Mielinaren ultraegituraren ebaluazioa CB_1 adierazten ez duten saguetan

CB_1 hartzailea adierazten ez duten saguak asko erabili izan dira NSZ-an ikerketa desberinak burutzeko. Hori horrela izanda, inoiz ez dira mielinari dagokion anormaltasunik deskribatu. Kannabinoide hartzaile hau adierazten ez duten animaliek mielinan alterazio handirik ez aurkezteak esanahia desberdinak izan ditzake. Alde batetik, baliteke mielizazio prezesuan proteina honek betebehar garrantzitsurik ez izatea, eta bestetik, posible litzateke CB_1 hartzaileen gabezia konpentsatu dezakaten faktore desberdinak existitzea. Hala ere, esan beharra dago CB_1 hartzailea adierazten ez duten saguetan mielinaren ultraegitura ez dela sakonki aztertu.

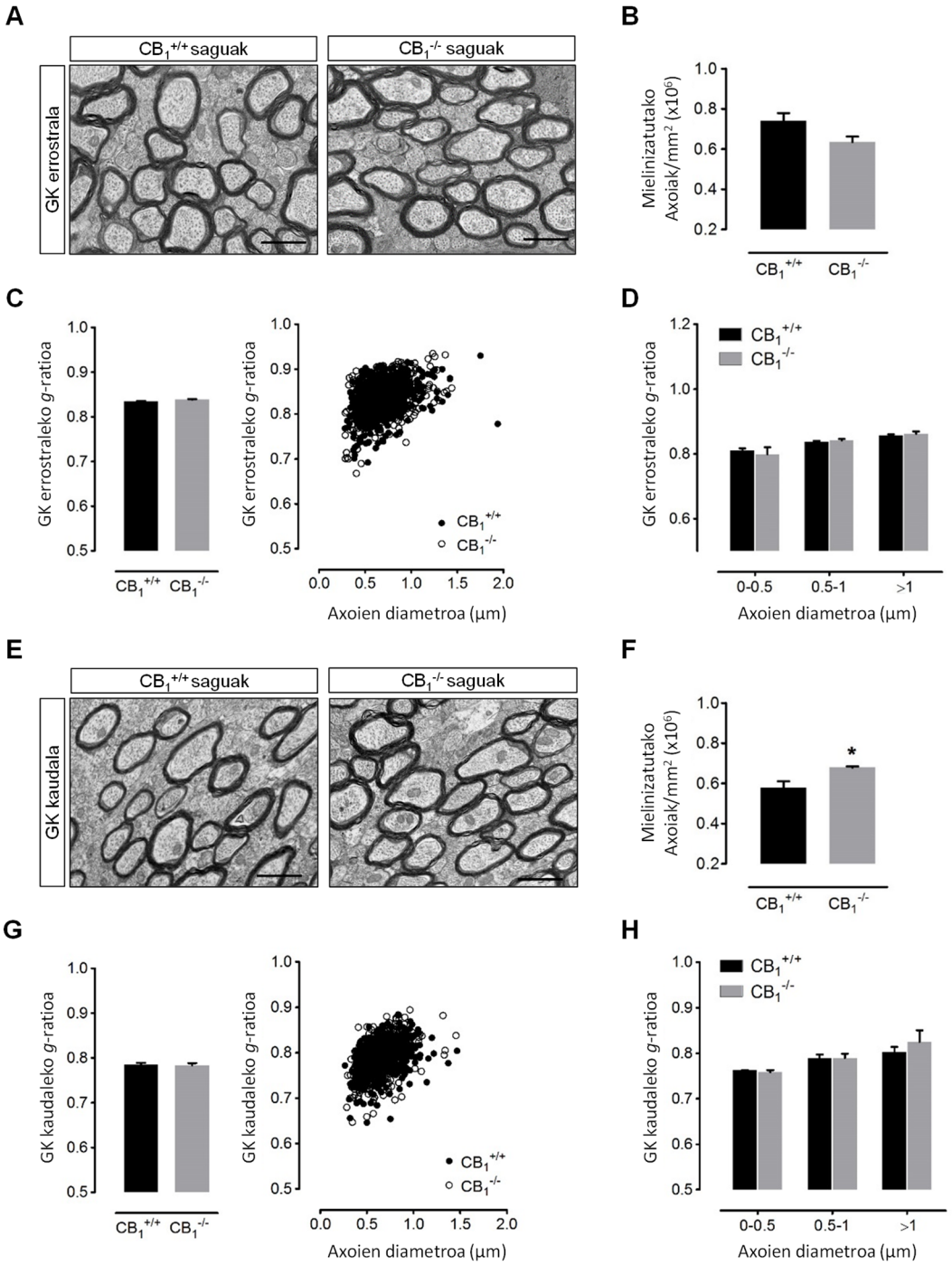

4. Irudia. CB_1 hartzailea adierazten ez duten saguen gorputz kailukara (GK) errostral eta kaudalaren analisia. (**A**, **E**) Mikroskopio elektronikoko irudi esanguratsuek 30 eguneko (P30) sagu basati ($CB_1^{+/+}$) eta CB_1 hartzailea adierazten ez duten sagueen ($CB_1^{-/-}$) gorputz kailukarako zeharka moztutako axoiak erakusten dituzte. Eskala barra: 1 µm. (**B**, **F**) Mielinizatutako axoien dentsiatea sagu $CB_1^{-/-}$ eta WT-etan. CB_1 hartzailea adierazten ez duten saguek mielinizatutako axoi gehiago dituzte gorputz kailukara kaudalean. (**C**, **G**) Gorputz kailukara rostral eta kaudaleko *g*-ratioen batazbestekoak puntu gisa adierazten dituen grafikoa, y-ardatzak axoien kalibrea irudikatzen du. (**D**, **H**) *g*-ratioak axoi kalibreen arabera banatuta erakusten dituen histograma itxurako grafikoa. $CB_1^{-/-}$ saguek ez dute desberdintasunik adierazten mielinaren lodierari dagokionez. Axoi mielinizatu kopurua aztertzeko gutxienez 827 axoi zenbatu ziren eta *g*-ratioen analisirako gutxienez 103 axoi neurtu ziren, animaliko 1600 μm^2 area totala aztertuz (n = 3 sagu taldeko). *$p < 0.05$; Studenten t-testa.

Horregatik, gure hurrengo helburua garapeneko mielinizazioaren momentu gorenean (jaio osteko 30. eguna, P30), $CB_1^{-/-}$ saguek mielinaren ultraegituran izan ditzaketen ´aldaketa´posibleak aztertzea izan zen. Horretarako, mielinaren lodiera (*g*-ratioa) eta mielinizatutako axoien dentsitatea aztertu genituen gorputz kailukara errostral eta kaudalean (**4. Irudia A** eta **E**). Mielinaren lodierari dagokionez, CB_1 hartzailea adierazten ez duten saguek kumaldi bereko sagu basatiekiko desberdintasunik adierazten ez dutela frogatu genuen, ez gorputz kailukara errostralean (**4. Irudia A** eta **C**) ez kaudalean (**4. Irudia E** eta **G**). Alterazioak axoi kalibre zehatz batzuetan aurki daitezkeen ikusi ahal izateko, *g*-ratioak axoien kalibreen arabera banatu genituen. Kasu honetan ere ez genuen desberdintasunik aurkitu bi genitipoen artean, ez axoi txiki ez handietan (**4. Irudia D** eta **H**). Emaitza hauen arabera, $CB_1^{-/-}$ saguek ez dute inongo alteraziorik mielinaren lodierari dagokionez. Hala ere, ME bidezko analisi honen bitartez, $CB_1^{-/-}$ saguek gorputz kailukara kaudalean mielinizatutako axoi kopuru pixka bat handiagoa azaltzen dutela ikusi genuen (**4. Irudia F**). Aurkikuntza honek CB_1 hartzaileek mielinaren formazio eta manteinuan nolabaiteko inplikazioa izan dezaketela proposatzen du.

Emaitzak – 2. Helburua

EMAITZAK – 2. HELBURUA

1. *In vitro* oligodendrozitoetan ABHD6 entzima inhibitzearen efektuak

1.1. ABHD6-ren blokeoak ez ditu oligodendrozitoak heriotz-exzitotoxikotik babesten

Oligodendrozitoak glutamato hartzaileen gehiegizko aktibazioarekiko oso sentikorrak dira, (Matute et al., 1997; McDonald et al., 1998; Follett et al., 2000) eta, hainbat ikerketen arabera, glutamatoak oligodendrozitoei eragindako exzitotoxizitatea EA gaixotasunean desmielinizazioa eragiten duen mekanismo etiopatogeniko garrantzitsua izan daiteke (Matute et al., 2001). Ildo horretan, 2-AG-a hidrolizatzen duen MAGL entzima inhibitzeak EA animali ereduetan dituen onurak oligodendrozitoak exzitotoxizitatetik babestearekin erlazionatuta daude (Hernández-Torres et al., 2014; Bernal-Chico et al., 2015). Testuinguru honetan, gure laborategiko aurretiko datuek erakutsitakoaren arabera, 2-AG-ak, CB_1 hartzaileak aktibatzearen bitartez, kultibatutako oligodendrozitoak glutamato hartzaileen aktibazio bidezko heriotzetik babesten ditu. Gainera, babes hau indartu egiten da MAGL farmakologikoki inhibitzen denean (Bernal-Chico et al., 2015). Emaitza hauetan oinarrituta, 2-AG-a hidrolizatzen duen ABHD6 entzima inhibitzeak oligodendrozitoak exzitoxizitatetik babesteko gaitasuna duen aztertu nahi izan genuen. Lehenengo, kultibatutako oligodendrozitoek, beste hainbat entzimen artean, ABHD6-a adierazten dutela frogatu genuen qPCR analisi bitartez (**1. Irudia A**). Entseguan erabilitako ABHD6 entzimaren KT182 inhibitzailearen kontzentrazio bat bera ere (10 nM-1 µM) ez zen gai izan oligodendrozitoak AMPA-k eragindako heriotzetik babesteko (**1. Irudia B**). Aurretiko aurkikuntza konfirmatuz, MAGL entzimaren JZL184 inhibitzaileak hazkuntza bereko oligodendrozitoak babesteko gaitasuna erakutsi zuen (**p* < 0.05 eramailearekin tratatutako kultiboekin konparatuz) (**1. Irudia C**). Honek, gure kondizio esperimentaletan, oligodendrozitoek 2-AG-a sortu eta honen bitartez seinalizatzeko gaitasuna dutela konfirmatzen du. Emaitza hauek ABHD6-a inhibitzeak oligodendrozitoen aurkako exzitotoxizitatea modulatzeko gaitasunik ez duela iradokitzen dute.

1.2. ABHD6-a inhibitzeak ez du oligodendrozitoen heltzea bultzatzen

Bermielinizazioa berezko prozesu bat da eta era egokian gerta dadin OPC-ak oligodendrozito mielinizatzaileetan diferentziatu behar dira. EA dutenen garunetan OPC asko dauden arren, zelula hauek diferentziatzeko ahalmen murriztua izaten dute. Horregatik, EA-ren inguruko ikerteta arloan, OPC hauen diferentziatzeko ahalmena handitzea helburu garrantzitsu bihurtu da (Kremer et al., 2015). Honi dagokionez, MAGL-aren inhibizioa 2-AG mailak igo eta, *in vitro,* OPC-en diferentziazioa bultzatu (Gomez et al., 2010) eta *in vivo* bermielinizazio eragiteko gai dela (Feliú et al., 2017) deskribatu da. Ikerketa hauetan oinarrituta, KT182-ak arratoi jaio berrietatik hazitako OPC-en diferentziazioa bultzatzeko izan zezakeen ahalmena aztertu genuen. Diferentziazio prozesu basala eragiteko hazkuntza medioko mitogenoak kendu eta hormona tiroideoa, CNTF-a eta NT-3-a gehitu genituen 48-96 orduz. Zelulen diferentziazio mailak MBP adierazpen nibelak western-blot bidez neurtuz aztertu genituen (**1. Irudia D**). ABHD6 entzimaren KT182 inhibitzaileren kontzentrazio desberdinen (10 nM-1 µM) presentzia ez zen MBP adierazpen mailak igotzeko gai izan 96 ordura (**1. Irudia E**). Aurretiko aurkikuntzekin (Gomez et al., 2010) bat eginez, MAGL entzimaren JZL184 inhibitzaileak, denbora tarte berdinean, OPC-en diferentziazioa bizkortzeko gaitasuna azaldu zuen (**p* < 0.05 eramailearekin tratatutako zelulekin konparatuz) (**1. Irudia E**). Emaitza hauek ABHD6-aren blokeoa OPC-en heltze prozesua bizkortzeko gai ez dela adierazten dute.

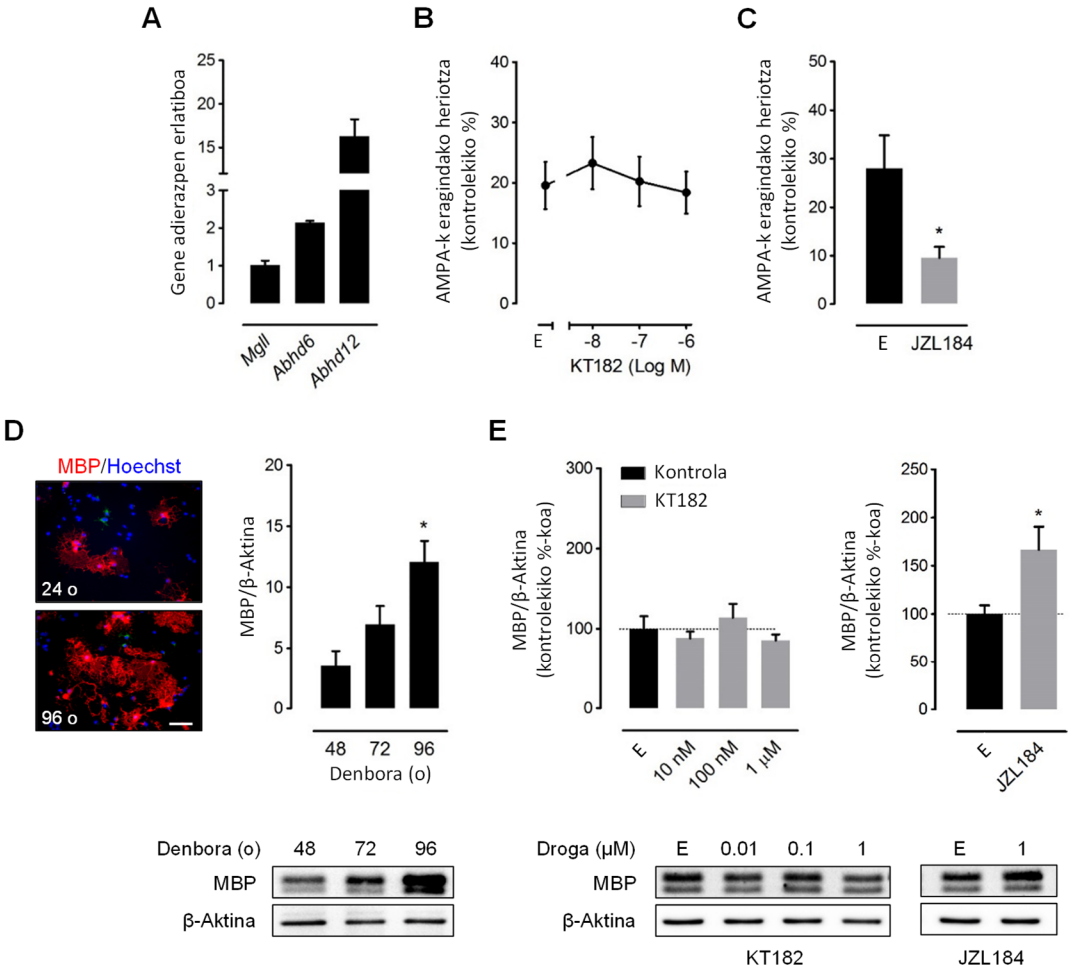

1. Irudia. ABHD6 entzimaren blokeoa kultibatutako oligodendrozitoetan. (**A**) Kultibatutako oligodendrozitoetan *Abhd6*, *Abhd12* eta *Mgll* adierazpen mailak RT-qPCR bidez neurtu, *Gapdh*-aren adierazpen mailekiko normalizatu eta *Mgll* adierazpen mailekiko irudikatu ziren. (**B**, **C**) ABHD6-ren inhibizioak ez du oligodendrozitoen exzitotoxizitatea murrizten. Grafikoek AMPA+ zikolotiazidak (10 µM:100 µM, 15 min) eragindako exzitotoxizitatea jasan zuten zelulen bideragarritasuna erakusten dute, bai ABHD6-aren KT182 inhibitzailearen (**B**) bai MAGL-en JZL184 inhibitzailearen (**C**) presentzian (*n* = 4 zelula hazkuntza). (**D, E**) ABHD6-a inhibitzeak ez du OPC-en diferentziazioa bultzatzen. (**D**) 48-96 orduz T3 hormonaren presentzian hazitako zelulen western-blot bitartez neurtutako MBP adierazpen mailak (*n* = 3 zelula hazkuntza). Irudi esanguratsuek immunozitokimia bidezko MBP-earen markaketa erakusten dute oligodendrozitoen diferentziazio fase desberdinetan. Eskala barra: 50 µm. (**E**) 96 orduz frogatutako KT182 inhibitzailearen kontzentrazio bakar baten presentzia ez da MBP-aren adierazpen maila igotzeko gai (*n* = 3 zelula hazkuntza). 96 orduz aplikatutako MAGL entzimaren JZL184 inhibitzaileak MBP adierazpen mailaren igoera eragiten du zelula hazkuntza berdinetan. **p* < 0.05 48 orduz diferentziatutako OPC-ekin (**C**) edo eramailearekin (**E**) tratatuako zelulekin konparatuz (**E**); Studenten *t*-testa.

2. ABHD6 entzima inhibitzearen ondorioak kuprizona bidezko desmielinizazio primarioan

2.1. ABHD6-aren blokeoa kuprizonak eragindako hantura eta desmielinizazioa murrizteko gai da

Gure laborategiko aurretiko emaitzek MAGL entzima farmakologikoki inhibitzeak kuprizonak eragindako hantura eta desmielinizazioa murrizteko gaitasuna duela erakusten dute (Bernal-Chico et al., 2015). Ikerketa lan honetan, ABHD6 entzimak kuprizonan oinarritutako animali ereduan duen eragina aztertu nahi izan dugu. Helburu honekin, lehendabizi, kuprizona bidezko tratamenduak ABHD6 entzimaren adierazpenean eragindako aldaketa posibleak analizatu genituen. qRT-PCR analisi bitartez, kuprizonak entzimaren transkripzio mailan denbora menpeko igoera eragiten zuela ikusi genuen. (**p* < 0.05 sagu kontrolekin konparatuz) (**2. Irudia A**). Western-blot bidezko ABHD6 proteinaren kuantifikazioak igoera ez adierazgarria (%36 ± 25) erakutsi zuen kuprizona 6 astez administratu ondoren (**2. Irudia B**). Kuprizonak ABHD6 adierazpen mailetan eragin ditzakeen efektuak sakonkiago aztertzeko asmotan, immunohistokimia bitartez entzima markatu genuen desmielinizatutako gorputz kailukaran. Emaitzen arabera, kuprizona 6 astez administratzeak ABHD6-aren adierazpenean igoera handia eragin zuen saguen gai zurian (**2. Irudia C** eta **D**). Elkarrekin, datu hauek kuprizona bidezko desmielinizazio primarioa ABHD6 entzimaren adierazpen mailen igoerarekin erlazionatuta dagoela iradokitzen dute.

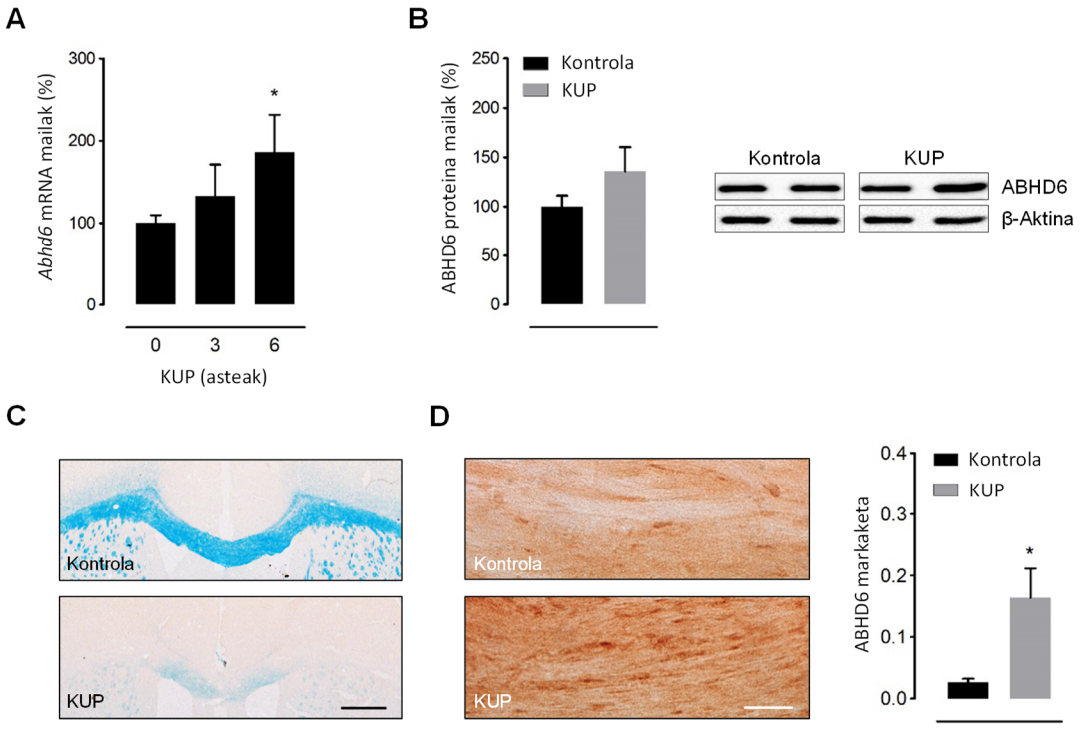

2. Irudia. Kuprizona bidezko desmielinizazioak ABHD6 adierazpen mailaren igoera eragiten du. (**A**) RT-qPCR bidezko *Abhd6* genearen adierazpen mailaren neurketa 3 edo 6 astez kuprizonarekin tratatutako animalien garun ehunean. (*n* = 6-7 sagu). Adierazpen mailak *Gapdh* eta *Hprt1*-enekin normalizatu eta kontrolen adierazpen mailekiko irudikatuta agertzen dira. (**B**) 6 astez kuprizonarekin tratatutako saguen garun ehunean eginiko western-blot analisia (*n* = 4-5 sagu). (**C**) Luxol fast blue (LFB) bidezko mielinaren markateta erakusten duten irudi esanguratsuak. Saguak 6 astez kuprizonarekin tratatzeak gorputz kailukararen desmielinizazioa eragiten du. (**D**) Immunoperoxidasa bidezko ABHD6-aren markaketa 6 astez kuprizonarekin tratatuko saguen gorputz kailukaran. Markatutako arearen arabera, kuprizonak ABHD6-aren adierazpen mailan igoera eragiten du gai zurian (*n* = 3 sagu). Eskala barrak: 500 µm (LFB) eta 50 µm (ABHD6). Ku, kuprizona. **p* < 0.05 dieta kontrola zuten saguekin konparatuz; Studenten *t*-testa.

Kuprizona bidezko desmielinizazio primarioan ABHD6 entzima inhibitzeak izan ditzakeen eraginak aztertzeko asmotan, 3 asteko kuprizona administrazio protokoloa aukeratu genuen. Saguek toxina janariarekin nahastuta irentsi zuten. Sagu horiei ABHD6 entzimaren KT182 inhibitzailea (2 mg/Kg) (Hsu et al., 2013) edo eramailea bakarrik zeraman txerto intraperitoneala eman zitzaien egunero. Kuprizona administratzen hasi eta 3 astetara eginiko LFB eta MBP markaketa bidezko analisiek eramailearekin tratatutako saguen gorputz kailukararen desmielinizazio partziala erakutsi zuten (**$p < 0.01$ kontrol saguekin konparatuz) (**3. Irudia B** eta **C**). Analisi berdinek KT182 bidezko tratamendua kuprizonak eragindako desmielinizazioa murrizteko gai zela erakutsi zuten ($^{\#}p < 0.05$ eramailearekin tratatutako saguekin konparatuz) (**3. Irudia B** eta **C**).

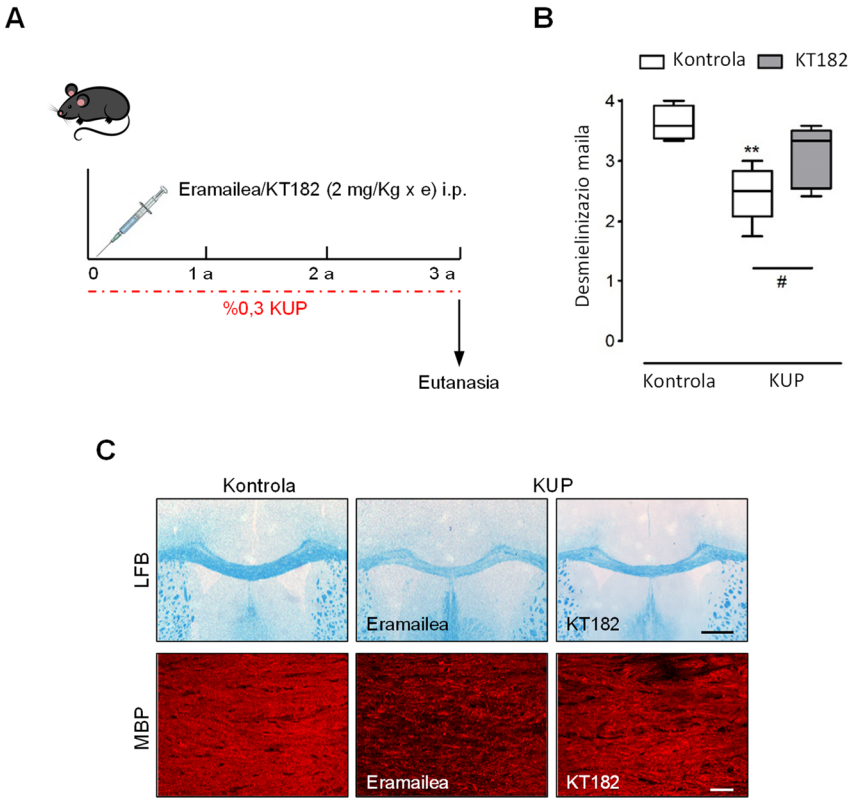

3. **Irudia**. ABHD6-aren inhibizioa kuprizonak eragindako desmielinizazioa murrizteko gai da. **(A)** Saguei 3 astez kuprizona administratu zitzaien dietan eta KT182 (2 mg/Kg) edo eramailea zeraman txerto bat eman zitzaien egunero. **(B)** Luxol fast blue (LFB) markaketa eta mielinaren proteina basikoaren (MBP) immunomarkaketa kuprizonarekin tratatutako saguen eta sagu kontrolen gorputz kailukaran. Mielinaren kaltea 4-tik (itxura normaleko mielina) 0-ra (desmielinizazio totala) puntuatu zen. KT182 edo eramailearekin tratatu ziren saguen gorputz kailukaran eginiko LFB eta MBP markaketen irudi esanguratsuak ikus daitezke **C**-n. Eskala barrak: 500 µm (LFB) eta 50 µm (MBP). KU, Kuprizona. **$p < 0.01$ dieta kontrola zuten saguekin konparatuz, $^{\#}p < 0.05$ eramailearekin tratatutako saguekin konparatuz; Studenten *t*-testa.

KT182-arekin tratatuak izan ziren animalien gorputz kailukaran CD11b$^+$-microglia/makrofago eta GFAP$^+$- astrozito kopuru baxuagoa aurkitu genuen eramailearekin tratu ziren saguen gorputz kailukararekin konparatuz, ABHD6-aren inhibitzaileak eragindako desmielinizazioaren murrizketa hanturazko erantzunen murrizketarekin erlazionatuta dagoela iradokituz (**4. Irudia A** eta **B**). Bestalde, KT182-aren bidezko tratamenduak ez zuen NG2$^+$ OPC-en kopuruan aldaketarik eragin (**4. Irudia A** eta **B**). Emaitza hauek, guztira, desmielinizazio primarioan zehar ABHD6-aren blokeoak efektu babesgarri eta hanturaren aurkakoak dituela adierazten dute.

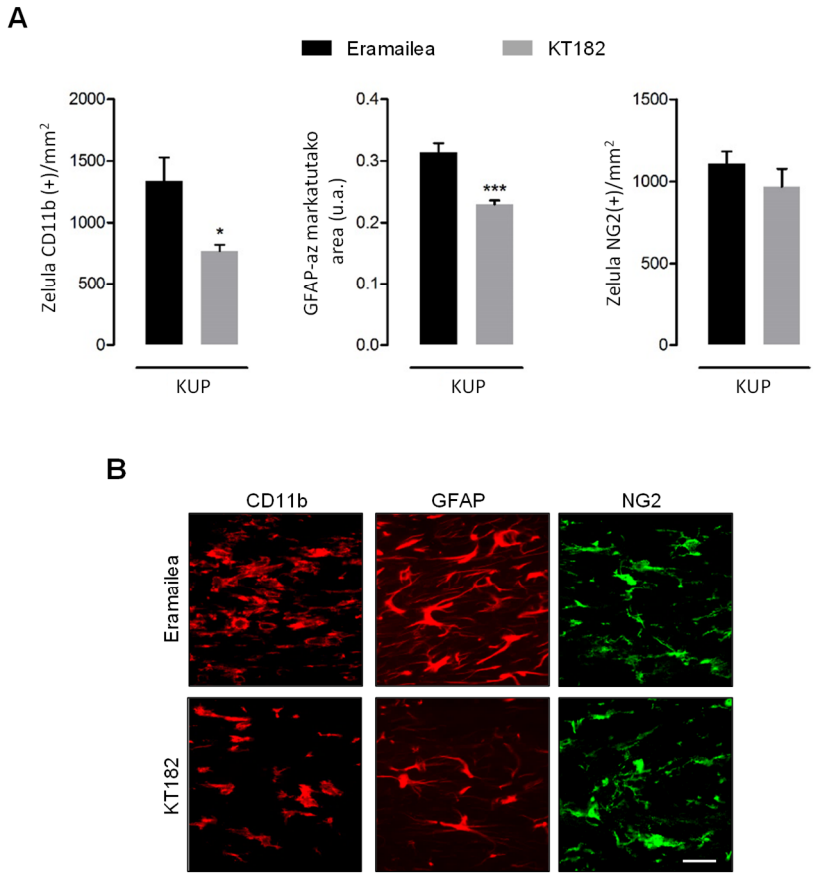

4. Irudia. ABHD6-aren inhibizio farmakologikoak kuprizonak eragindako hanturaren aurkako efektuak ditu. 3 astez kuprizona irentsi eta KT182 (2 mg/Kg) edo eramailearekin tratatu ziren saguen gorputz kailukaran erreaktibitate gliala neurtu zen. (**A**) KT182-arekin tratatutako desmielinizatutako saguen gorputz kailukaran CD11b$^+$-microglia/makrofago eta GFAP$^+$- astrozito gutxiago zenbatu ziren eramailarekin tratutako saguetan baino. Bestalde, konposatu honek ez zuen eraginik izan NG2$^+$ OPC-en kopuruan (*n* = 4-5 sagu). (**B**) Desmielinizatutako saguen gorputz kailukaran eginiko CD11b, GFAP eta NG2-en markaketak adierazten dituzten irudi esanguratsuak ikus daitezke. Eskala barrak: 25 µm. Ku, kuprizona. *p < 0.0 eta ***p < 0.001; Studenten *t*-testa.

2.2. ABHD6 entzima inhibitzeak ez du bermielinizazio prozesua bizkortzen

Hainbat ikerketen arabera, 2-AG endokannbinoidearen hidrolisia inhibitzeak, mekanismo desberdinen bitartez, bermielinizazioa eta desmielinizatutako axoien berreskuratzea eragiteko gaitasuna du (Arévalo-Martín et al., 2003; Gomez et al., 2010; Feliú et al., 2017). Gure aurretiko aurkikuntzetan oinarrituta, ABHD6-a inhibitzeak kuprizonak eragindako mielinaren birsortzea bultzatzeko ahalmena duen aztertu nahi izan genuen. Helburu honekin, saguei 6 astez kuprizona administratu eta jarraian, bi astez, janari arrunta eman genien. Kuprizona kendu eta hurrengo egunetik hasita, egunero KT182-arekin edo eramaile soilarekin tratatu genituen (**5. Irudia A**). LFB eta MBP-az markatutako gorputz kailukaran itsu-itsuka eginiko analisiek mielinaren birsortze partziala erakutsi zuten kuprizona kendu eta bi astez eramailearekin tratatu ziren saguetan (*p < 0,05 kuprizonarekin 6 astez tratatu ziren saguekin konparatuz) (**5. Irudia B** eta **C**). Hala ere, KT182 inhibitzailearekin tratatutako saguek ez zuten eramailearekin tratatutakoek baina birsortze eraginkorragoa azaldu, ABHD6-aren blokeoa gorputz kailukarako bermielinizazioa bizkortzeko gai ez dela iradokituz (**5. Irudia B** eta **C**).

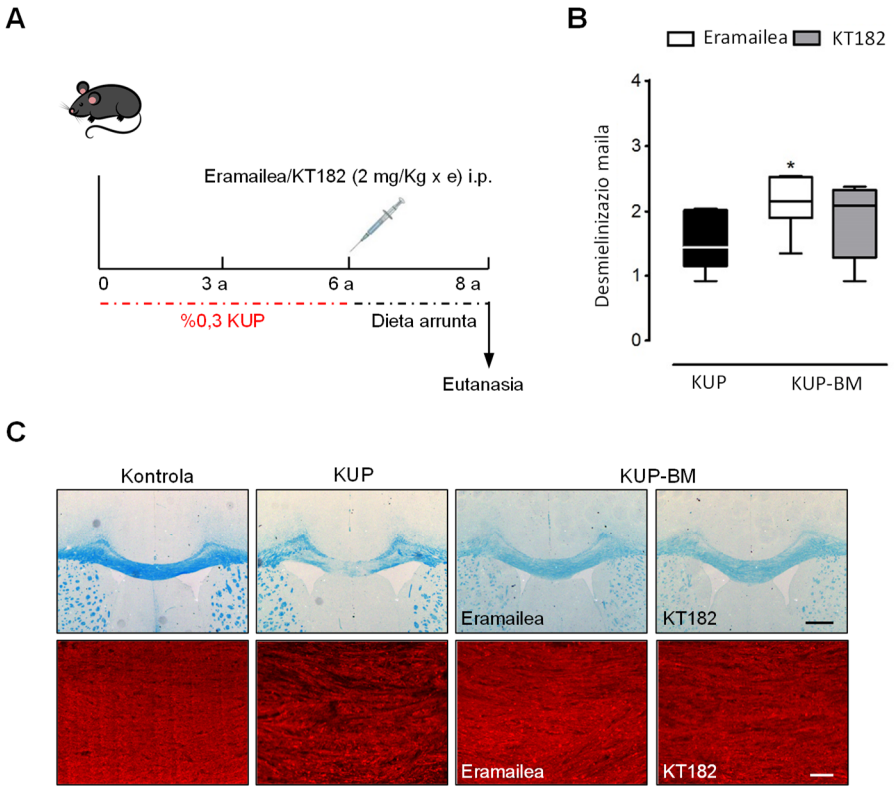

5. Irudia. ABHD6-ren blokeoa ez da gai bermielinizazio prozesua bizkortzeko kuprizonaren animali ereduan. (**A**) 6 astez kuprizonarekin tratatutako sagu guztien artean, ausaz talde bat bermielinizazio fasean KT182 (mg/Kg) edo eramailearekin tratatzeko aukeratu zen. (**B**, **C**) LFB eta MBP markaketek kuprizonarekin 6 astez tratatutako saguek gorputz kailukara desmielinizatuta zutela eta 2 astez janari arruntera itzultzean mielinaren birsortze partziala gertatu zela erakusten dute. Itsu-itsuka eginiko LFB eta MBP markaketen puntuazioak ez du desberdintasunik erakusten KT182-arekin edo eramailearekin tratatutako animalien artean (*n* = 6 sagu). Eskala barrak: 500 µm (LFB) eta 50 µm (MBP).

Kuprizonak eragindako desmielinizazio primarioan KT182-aren bidezko tratamenduak mikroglien eta astrozitoen erreaktibitatea murrizteko gaitasunean (**4. Irudia**) oinarrituz, hurrengo pausoan inhibitzaile honek, bermielinizazio fasean, zelula mota hauengan izandako efektu posibleak aztertu genituen. Kasu honetan, $CD11b^+$ eta $GFAP^+$ zelulei dagokionez, KT182-arekin eta eramailearekin tratatutako saguen gorputz kailukaren artean ez genuen aldaketarik antzeman (**6. Irudia A** eta **B**). Aurkikuntza hauen arabera, ABHD6-aren inhibizioa ez da hobetze fasean mielinaren berreskuratzea bultzatu eta gliosia murrizteko etorkizun haundiko estrategia.

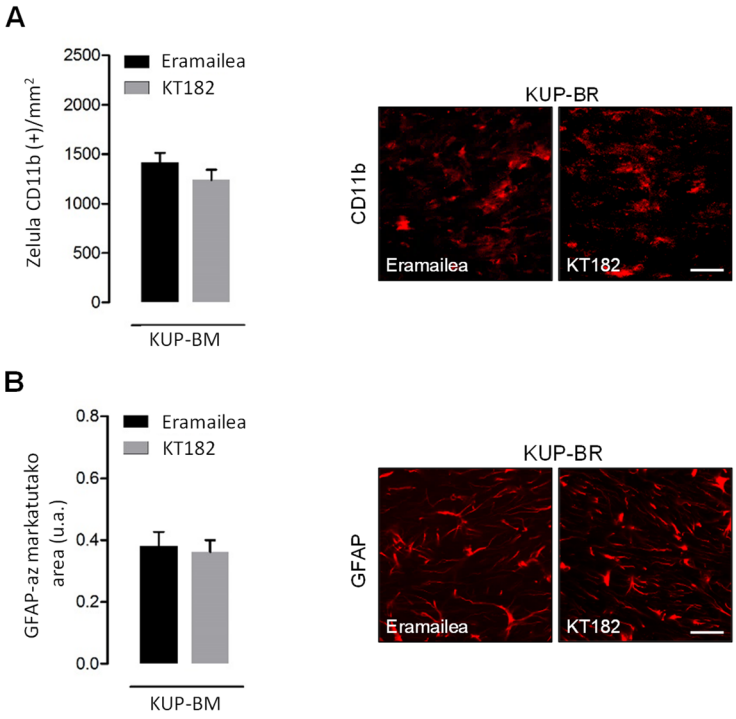

6. Irudia. ABHD6-a inhibitzeak ez du astrozito eta mikroglien erreaktibitatea modulatzen bermielinizazio fasean. $GFAP^+$ astrozitoen eta $CD11b^+$ mikroglien ebaluazioa KT182 (2 mg/Kg) edo eramailearekin tratatutako saguen gorputz kailukaran (*n* = 5-6 sagu). Kuantifikazioen arabera, hobetze fasean, KT182 inhibitzaileak ez du eraginik zelula hauengan. Eskala barrak: 25 µm.

3. **ABHD6-aren inhibizio profikatikoa entzefalomielitis autoimmune esperimentalean**

WWL70 inhibitzaileak (Li et al., 2007; Marrs et al., 2010) EAE animali ereduan gaixotasunaren desgaitasun klinikoak murrizteko duen gaitasunak (Wen *et al.*, 2015), ABHD6-aren inhibizioa EA-ren tratamendurako estrategia terapeutiko egokia izan daitekeela iradokitzen du . Hala eta guztiz ere, EAE-ren kontrolean sistema periferikoko ABHD6-ak eta sistema zentraleko ABHD6-ak izan dezaketen ekarpena ez da sekula aztertu. Ikerketa lan honetan, barrera hematoentzefalikoa zeharkatzeko ahalmen desberdina duten ABHD6 entzimaren bi inhibitzaile berriren bitartez, zalantza honi erantzuna ematen saiatu gara. Erabilitako inhibitzaile hauek barrera hematoentzefalikoa zeharka dezakeen KT182 konposatua eta periferiako ABHD6-a bakarrik inhibitu dezakeen KT203 konposatua izan dira hain zuzen ere (Hsu et al., 2013).

3.1. KT182 eta KT203 konposatuek garuneko ABHD6-ra lotzeko duten gaitasuna

In vivo KT182 eta KT203 konposatuek garuneko ABHD6-a lotzeko duten gaitasun desberdina egiaztatzeko, sagu naifak bi inhibitzaileen (2 mg/kg) txerto bakarrarekin tratatu genituen. Ondoren, beraien garuneko ehunetan aktibitatean oinarritutako (ABPP) serin hidrolasen inhibizio profila aztertu genuen. Horretarako, garunetatik lortutako proteomak espektro zabaleko FP-Rh sondarekin inkubatu eta ondoren gel batetik pasa genituen. ABBP entsegu hauetan, pisu molekularrari esker, ABHD6-ari dagokion banda (~35 kDa) identifikatu ahal izan genuen. Horrela, KT182-arekin tratatuko saguek , 4 eta 24 ordutara, garuneko ABHD6-a inhibituta zutela frogatu genuen (**7. Irudia**). Hsu eta lankideen (Hsu et al., 2013) datuekin bat eginez, KT182 inhibitzaileak ABHD6-arekiko selektibitatea erakutsi zuen. Hala ere, erabilitako dosian, inhibitzaile honek FAAH-ren inhibizio partziala burutzen zuela detektatu genuen. Espero bezala, KT203 inhibitzaileak ez zuen erakutsi garuneko ABHD6-a inhibitzeko gaitasunik (**7. Irudia**).

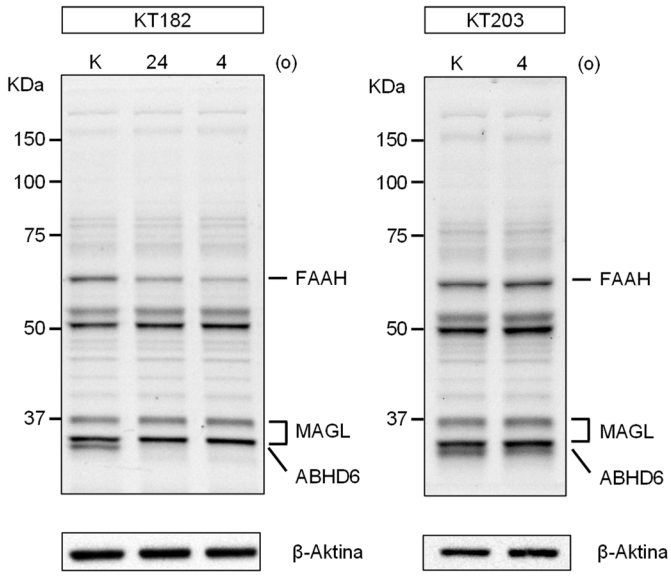

7. Irudia. KT182 eta KT203 inhibitzaileekin tratatutako saguen garuneko serin-hidrolasen profila ABPP entsegu bitartez. Inhibitzaileen (2 mg/Kg) edo eramailearen txerto bakarrarekin tratatutako saguak irudian agertzen diren denboren barruan sakrifikatu eta hauen garunen proteomak FP-Rh sondarekin inkubatu ziren (*n* = 4 sagu kondizio bakoitzeko). KT182 konposatua garuneko ABHD6-aren inhibizio total eta iraunkorra eragiteko gai da, KT203 inhibitzaileak, berriz, ez du sagu naifen garunera heltzeko gaitasunik.

3.2. ABHD6 zentral eta periferikoaren eraginkortasun klinikoa EAE animali ereduan

EAE animali ereduan bi inhibitzaileen efikazia terapeutikoa aztertu ahal izateko administrazio protokolo profilaktikoa aukeratu genuen. Beraz, saguak MOG txertoaren hurrengo egunetik hasi eta egunero ABHD6-aren inhibitzaile (2 mg/Kg) edo eramailearekin tratatu genituen txerto intraperitoneal bitartez. Gaixotasunaren progresioaren ebaluazioak erakutsitakoaren arabera, KT182 inhibitzailearekin tratatutako saguek desgaitasun motore baxuagoa erakutsi zuten eramailearekin tratatutakoekin konparatuz (**8. Irudia A**). Protokolo berdina jarraituz, KT203-arekin burututako tratamendua berriz ez zein gai izan gaixotasunaren progresioa modulatzeko (**8. Irudia**

B). Hala ere, azkeneko egunean (gaixotasunaren indukzioren osteko 30. eguna (30 dpi)) burututako desgaitasun motoreen konparaketak ez zuen tratamenduen arteko desberdintasunik erakutsi (**8. Irudia C**). Esperimentuaren amaieran (30 dpi) ABHD6-a kronikoki inhibitzeak EAE-rekin erlazionatutako desgaitasun motorea modulatzeko izan dezakeen gaitasuna sakonago aztertzeko asmoarekin, traktu kortikoespinalaren egoerari erreparatu genion. EAE-ren garapenak traktu kortikoespinaleko kondukzioaren latentzian igoera bat eragin zuela ikusi genuen (**8. Figura D**). KT182 edo KT203 inhibitzaileekin burututako tratamenduak ordea ez zuten latentzia hori era adierazgarrian murrizteko ahalmenik aurkeztu (**8. Irudia D**). Emaitza hauek guztira, ABHD6-aren inhibizioak EAE-an efektu babesle txikiak bakarrik eragiten dituela iradokitzen dute. Gainera, eragin babesle horiek gerta daitezen gaixotasunaren hasierako faseetan NSZ-ko ABHD6-aren inhibizioa beharrezkoa dela adierazten dute.

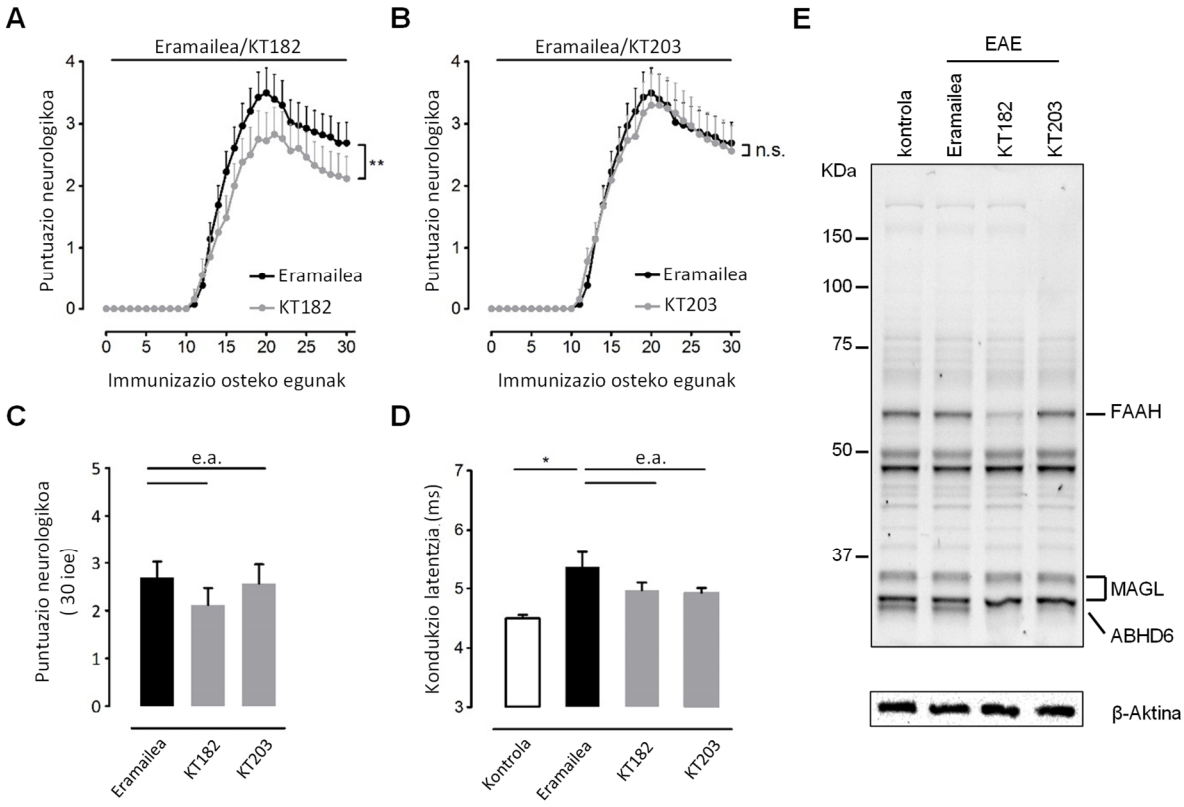

8. Irudia. ABHD6 entzimaren inhibitzaileen eraginkortasuna EAE animali ereduan (**A**) Egoera motorearen puntuazioak erakusten dituen grafikoan ikus daitekeen bezala, lehen egunetik hasitako KT182 (2 mg/Kg) bidezko tratamendua EAE-ak eragindako desgaitasunak murrizteko gai da (n = 19-21 sagu, $^{**}p$ = 0.0018; Mann-Whitney U-testa). (**B**) Barrera hematoentzefalikoa zeharkatzeko gai ez den KT203 (2 mg/Kg) bidezko tratamendua berriz ez da EAE-aren progresioa modulatzeko gai (n = 16-21 sagu). (**C**) Egoera motorearen puntuazioen konparaketak ez du tratamendu taldeen artean desberdintasunik erakusten. **A**-**C** puntuetan agertzen diren datuek hiru esperimentu independente irudikatzen dituzte. (**D**) Traktu kortikoespinaleko kondukzio latentziek antzeko desgaitasunak erakusten dituzte bai eramailearekin eta bai ABHD6-aren inhibitzaileekin tratatutako saguetan. (**E**) Esperimentuaren bukaeran (30 dpi) KT182, KT203 edo eramailearekin tratatutako saguen garunekin eginiko ABPP entsegua. Animaliak egunero tratatu ziren inhibitzaile edo eramailearekin. Azken txertoa eman eta 24 ordu beranduago sakrifikatu ziren animaliak. Biek, KT182 eta KT203 inhibitzaileek erakutsi zuten EAE kronikoa zuten animalien garuneko ABHD6-a inhibitzeko gaitasuna. Irudiak gutxienez hiru ABPP entsegu desberdinen adierazgarri dira. e.a., ez adierazgarria. $^{*}p < 0.05$, Studenten t-testa.

Gure gaixotasunaren animali ereduan, inhibitzaileekin burututako tratamenduaren ondoren ABHD6-aren inhibizio patroia zein zen ezagutzeko, ABBP entseguaz baliotu ginen. Bertan, bai KT182 eta bai KT203-rekin tratatutako saguek EAE-ren fase kronikoan garuneko ABHD6-a inhibituta zutela frogatu genuen (**8. Irudia E**). Sagu naifetan eta EAE saguetan burututako serin hidrolasen profila (**7.** eta **8. Irudia E**) konparatuz gero, KT182 bidezko tratamenduak garuneko ABHD6-a EAE-ren progresio osoan zehar inhibitu zuela antzeman dezakegu. Aldiz, KT203 bidezko tratamenduak gaixotasunaren lehen faseetan periferiako ABHD6-a bakarrik inhibitu zezakeela ikus dezakegu. EAE-ren fase kronikoan berriz, bi inhibitzaileek aurkeztu zuten garuneko ABHD6-a blokeatzeko gaitasuna, gaixotasunak barrera hematoentzefalikoaren haustea eragiten baitu, KT203 NSZ-ra heltzea ahalbidetuz.

3.3. ABHD6-ren inhibitzaileak ez dira EAE-ak eragindako hantura murrizteko gai

Aurretiko aurkikuntzen arabera, ABHD6-aren inhibizioak EAE-an aurkezten dituen onurak hanturaren aurkako efektuekin erlazionaturik daude. Horrela, ABHD6-aren WWL70 inhibitzailea mikroglia/makrofagoen eta hainbat hantura bitartekarien adierazpena, TNFα eta IL1β besteak beste, murrizteko gai da EAE-ren fase kronikoan (Wen et al., 2015). Hala ere, hau frogatu zuten laborategi bereko kideek WWL70-a, ABHD6-arekin zer ikusirik ez duen mekanismo baten bitartez, mikroglietan prostaglandinen sintesia murrizteko gai dela erakutsi dute. Honen arabera, mekanismo hau WWL70-ak *in vivo* dituen onurekin erlazionatuta egon liteke (Tanaka et al., 2017). Esan beharra dago lan horretan KT182-ak ez zuela mikroglietan prostaglandinen sintesia murrizteko gaitasunik erakutsi (Tanaka et al., 2017), inhibitzaile honen erabileraren onurak mekanismo alternatibo honekin erlazionaturik ez daudela iradokituz.

Jarraian, ABHD6-a farmakologikoki inhibitzeak EAE-an hantura murrizteko gaitasunik duen aztertu genuen KT182 eta KT203 inhibitzaileekin tratatutako saguetan. Esperimentuaren azken egunean (30 dpi) sakrifikatutako animalien bizkar muinean egindako analisi histologian, KT182 bidezko tratamenduak hantura-lesio (**9. Irudia A** eta **B**) eta $CD11b^+$ mikroglia/makrofago (**9. Irudia C** eta **D**) kopuruan adierazgarria ez zen jaitsiera bat eragin zuela ikusi genuen. Tendentzia hau ez zen errepikatu KT203-arekin tratatutako saguetan. Beraz, aurkikuntza hauek gaixotasunaren fase kronikoan desagertzen den KT182 inhibitzailearen eraginkortasun txikiarekin bat datoz (**8. Irudia A** eta **C**).

Ondoren, hanturarekin erlazionatutako hainbat markatzaileren adierazpen mailak neurtu genituen KT182 eta KT203 inhibitzaileekin tratatutako EAE saguen garun eta bizkar-muinean. Esperimentuaren amaieran lortutako ehunetan eginiko RT-qPCR analisien arabera, EAE-ren indukzioak zenbait hantura markatzaileren adierazpen mailen igoera eragin zuen, besteak beste *Iba-1*, *COX-2*, *TNFα* eta *IL1β*-enak, bai bizkar muinean zein gorputz ildaskatu eta hipokanpoan (**9. Irudia E**). KT182 eta KT203 inhibitzaileen bidezko tratamenduak, ordea, ez ziren gai izan hantura markatzaileen igoera hau murrizteko (**9. Irudia E**). Guztira, emaitza hauek ABHD6-aren inhibizioa EAE-ren fase kronikoko hantura modulatzeko gai ez dela erakusten dute.

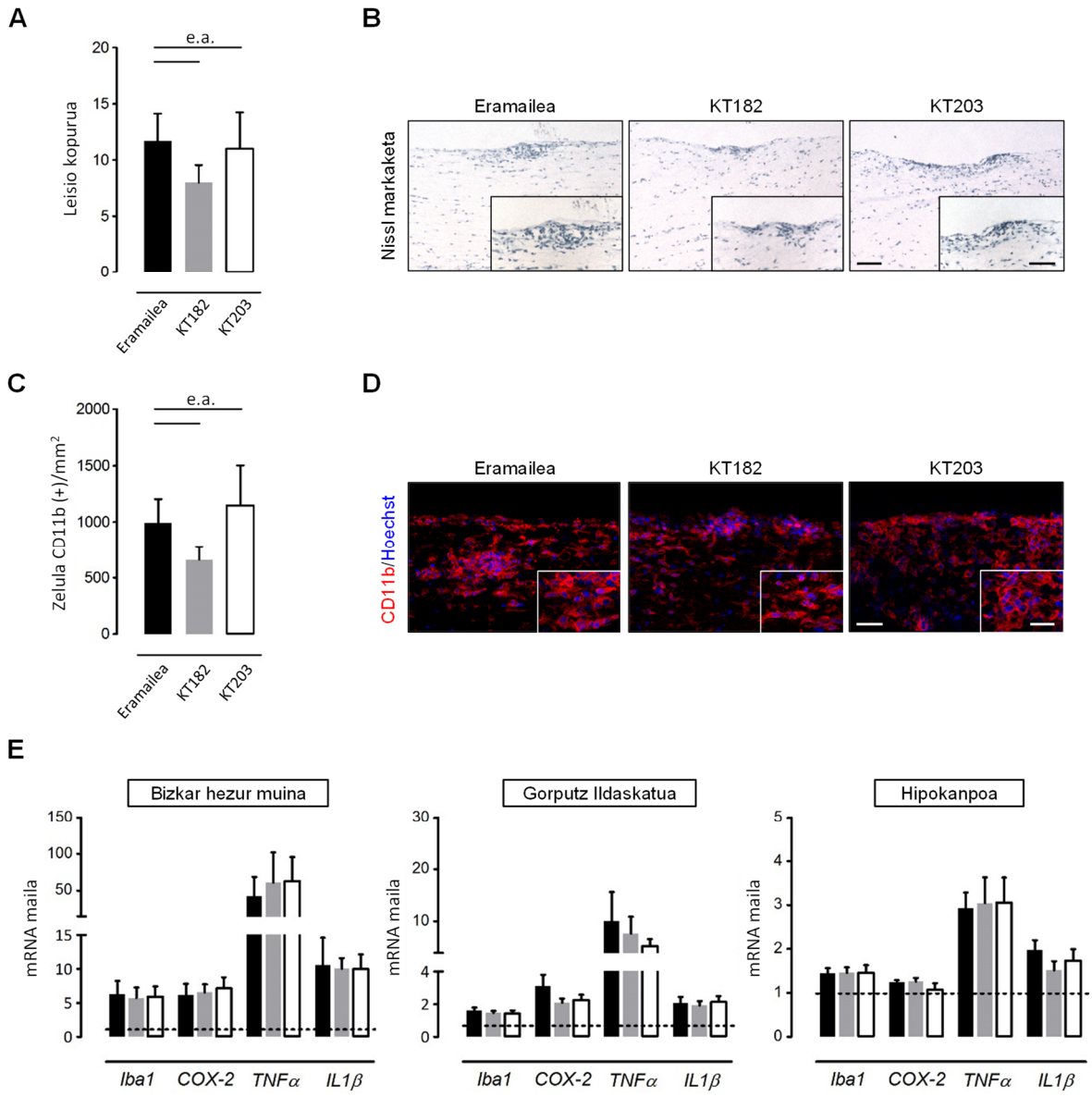

9. Irudia. EAE-aren fase kronikoan, ABHD6-aren inhibizioa ez da gai hantura murrizteko. Hantura lesioen (**A**) eta mikroglia/makrofagoen (**C**) kuantifikazioa EAE zuten saguen bizkar muinean. ABHD6 entzimaren inhibitzaileak ez ziren gai izan EAE-ren indukzioak eragindako hanturazko erantzuna murrizteko (*n* = 6-8 sagu). KT182 eta KT203 inhibitzaileekin tratatutako EAE saguen bizkar muinean burututako Nissl markaketa (**B**) eta CD11b immunomarkaketa (**D**) adierazten dituzten irudi esanguratsuak ikus ditzakegu. Eskala barrak: **B**: 100 µm eta 50 µm (intsertoa); **D**: 50 µm eta 25 µm (intsertoa). (**E**) RT-qPCR bidez neurtutako *Iba1*, *COX-2*, *TNFα*, *iNOS* eta *IL1β* markatzaileen adierazpen maila. ABHD6 entzimaren inhibitzaileak ez dira gai bizkar muinean hanturarekin erlazionatutako markatzaile hauen adierazpen maila murrizteko. Emaitzak *Gapdh* eta *Hprt1* mailekin normalizatuta daude eta immunizatu gabeko sagu kontroletan lortutako balioen arabera irudikatuta. Entsegu bakoitzeko sagu kopurua honakoa izan zen: bizkar muina *n* = 7-10, gorputz ildaskatua *n* = 12-17 eta hipokanpoa *n* = 11-16.

3.4. ABHD6-ren adierazpena ez da altuagoa EAE animali ereduan

Egoera fisiologikoetan, ABHD6-ak 2-AG-ren proportzio txiki bat besterik ez du hidrolizatzen. Beraz, ABHD6-a inhibitzeak hanturazko prozesuetan dakartzan onurak entzima honen adierazpen mailaren igoerekin erlazionaturik egon daitezkeela uste da (Blankman et al., 2007; Wen et al., 2015). Horregatik, ABHD6 entzimak EAE ereduan duen betebeharra hobeto ulertzeko asmotan, entzima honen adierazpena aztertu genuen EAE zuten saguen bizkar-muin eta garunean. 30 dpi-an eginiko RT-qPCR analisien arabera, gaixotasunaren garapenak ez zuen ABHD6-aren adierazpen maila aldatu aztertutako ehunetan, hauek sagu kontrolen adierazpenekin konparatuz gero (**10. Irudia A**). Emaitza hauek western-blot bitartez konfirmatu genituen, entzima adierazten ez duten saguetan frogatutako antigorputz espezifiko bat erabiliz (Thomas et al., 2013) (**10. Irudia A**). Emaitza hauek, beraz, gure baldintza esperimentaletan ABHD6-ak 2-AG-ren hidrolisian duen betebeharra aldatzen ez dela adierazten dute.

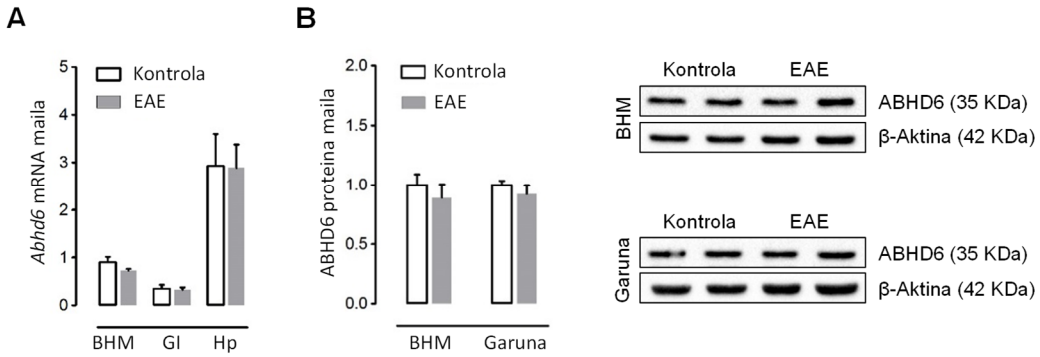

10. Irudia. ABHD6-aren adierazpena EAE kronikoan. (**A**) ABHD6 gene adierazpena EAE-a zuten saguen bizkar-muin (BM; *n* = 5-10 sagu), gorputz ildaskatu (Gi; *n* = 9-17 sagu) eta hipokanpoan (Hp; *n* = 8-16 sagu) RT-qPCR bitartez neurtu zen 30 dpi-an. Emaitzak *Gapdh* eta *Hprt1* geneen adierazpenaren arabera normalizatu ziren. (**B**) Western-blot bitartez neurtutako ABHD6 proteinaren adierazpena eta honi dagozkion irudi esanguratsuak. ABHD6 proteinaren adierazpen mailak β-aktinaren adierazpen mailaren balioekin normalizatu eta sagu kontrolen balioen arabera irudikatu ziren. Datuak batezbesteko ± S.E.M eran irudikatuta daude.

3.5. ABHD6-a kronikoki inhibitzeak garuneko CB_1 hartzaileen desentsibilizazioa eragiten du

KT182-ak EAE-ren fase kronikoan animaliak babesteko gaitasuna galtzea ABHD6-aren inhibizioak eragindako tolerantzia funtzionalarekin erlazionatuta egon zitekeela pentsatu genuen. Jakina da 2-AG kontzentrazio altuak denbora luzez mantetzeak CB_1 hartzaile bidezko seinalizazioren moldatze farmakologikoak eragiten dituela. Honek endokannbinoideak degradatzen dituzten entzimen inhibitzaileen eraginkortasun terapeutikoa murriztu egiten du (Schlosburg et al., 2010; Bernal-Chico et al., 2015). Ikerketa lan honetan, EAE animalietan ABHD6-a kronikoki inhibitzeak CB_1 hartzaileen funtzionalitatea alda dezakeen aztertu genuen [^{35}S]GTPγS eta [^{3}H]CP55,950 autorradiografia entseguen bitartez. 30 egunez KT182 inhibitzailearekin tratatu ziren saguek agonista kannabinoide bidez estimulatutako [^{35}S]GTPγS-a lotzeko gaitasunean murrizketa erakutsi zuten (desentsibilizazioa), gorputz ildaskatuan eta zerebeloan batik bat (**11. Irudia A** eta **C**). Alderantziz, KT203-aren administrazio kronikoak ez zuen eraginik izan CB_1 hartzaileen [^{35}S]GTPγS lotzeko gaitasunean .

CB_1 hartzailearen adierazpenari dagokionez, [^{3}H]CP55,950 lotura entseguen emaitzen arabera, kronikoki administratutako ABHD6 entzimaren inhibitzaileek ez zuten CB_1 hartzailearen dentsitatea aldatu EAE saguen garunean (**11. Irudia B** eta **C**). Emaitza hauen arabera, KT182 konposatuak eragindako CB_1 hartzaileen desentsibilizazioa ez dago proteina hauen internalizazioarekin erlazionatuta.

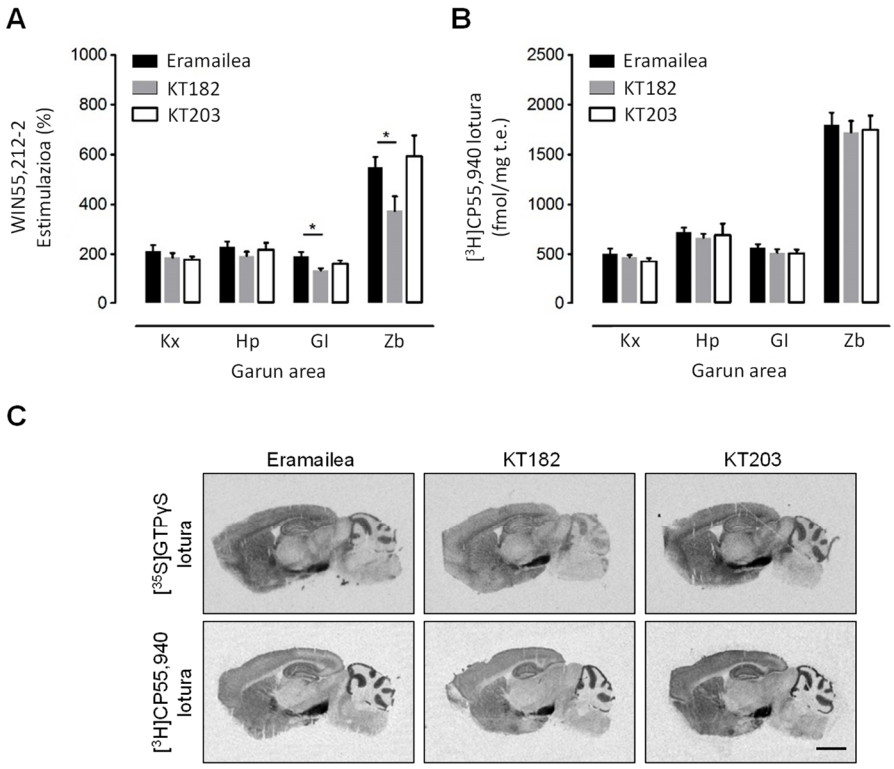

11. Irudia. ABHD6 entzima kronikoki inhibitzeak CB_1 hartzaileen funtzionalitatea murrizten du EAE animali ereduan. (**A**) Kannabinoide agonisten bidez estimulatutako [^{35}S]GTPγS-ren lotura ABHD6 inhibitzaileekin kronikoki tratatutako EAE saguen garunean. KT182 konposatuarekin tratatutako EAE saguen gorputz ildaskatuan eta zerebeloan WIN55,212-2 agonistak [^{35}S]GTPγS-aren lotura estimulatzeko duen gaitasuna eramailearekin tratatuko saguenean dutena baino baxuagoa dela ikus daiteke. (**B**) [^{3}H]CP55,940 autorradiografia bitartez neurtutako CB_1 hartzaileen adierazpen mailak EAE saguen garunetan. (**C**) WIN55,212- 2-ak estimulatutako [^{35}S]GTPγS-aren lotura eta [^{3}H]CP55,940 lotura erakusten dituzten irudi esanguratsuak. Bertan eramailearekin edo ABHD6-aren bi inhibitzaileekin tratatutako animalien garunen ebaketa sagitalak ikus daitezke. (*n* = 7-10 sagu). Kx, kortexa; Hp, hipokanpoa; Gi, gorputz ildaskatua; eta Zb, zerebeloa. Eskala barra: 2 mm. **p* < 0.05, Studenten t-testa. Datuak batezbesteko ± S.E.M eran irudikatuta daude.

4. **ABHD6 inhibitzaileen eragina NMDA-k eragindako neuronen exzitotoxizitatean**

4.1. KT182-ak NMDA-k eragindako heriotza murrizten du

KT182 inhibitzailea era kronikoan administratzeak CB_1 hartzaileen funtzio galera eragiten duela ikusteak, ABHD6-a inhibitzeak EAE-an sortzen dituen eragin onuragarriak hartzaile hauen aktibazioaren eraginez gerta daitezkeela iradokitzen du. Jakina da neuronetako CB_1 hartzaileak

aktibatzeak, zelula hauen exzitotoxizitatea murriztuz, EAE animali ereduarekin erlazionatutako sintomak kontrolatzeko gaitasuna duela (Pryce et al., 2003; Maresz et al., 2007). Beraz, gure hurrengo helburua ABHD6 entzima inhibitzeak kultibatutako neuronak NMDA-ak eragindako heriotzetik (Ruiz et al., 2014) babesteko gaitasuna duen ikustea izan zen. Lehendabizi, q-PCR bitartez, gure neuronek, *in vitro*, ABHD6-a adierazten zutela ziurtatu genuen (**12. Irudia A**). NMDA-a aplikatu baino 30 min lehenago zelulak 1 μM KT182-rekin tratatzeak LDH-ren liberazioa ∼25%-ean murriztu zuela ikusi genuen (**12. Irudia B**). Erabilitako konposaturen kontzentrazio baxuagoak, aldiz, ez ziren gai izan heriotza hori murrizteko. Kontuan izan behar da neuronak NMDA-ak eragindako heriotzetik babesteko KT182 inhibitzailearen EC_{50} eraginkorra ∼0.2 μM-koa izan zela. ABHD6 endogenoa inhibitzeko behar den EC_{50}, ordea, ∼1 nM-koa da (Hsu et al., 2013). Probatutako kontzentrazio guztiek neuronetako ABHD6 entzima inhibitzen zutela frogatzeko asmotan, ABPP entsegu bat burutu genuen. Horretarako, neuronak KT182-aren kontzentrazio desberdinekin tratatu ziren 30 minutuz eta ondoren proteomak FP-Rh sondarekin inkubatu ziren. Hsu eta kideen (2013) aurretiko datuekin bat eginez, KT182-aren kontzentrazio guztiek (10 nM-1 μM) erakutsi zuten neuronen ABHD6-a inhibitzeko ahalmena (**12. Irudia D**). Emaitza hauek ABHD6 entzimarentzat espezifikoa den HT-01 sondarekin (Hsu et al., 2013) berretsi genituen. Nahiz eta ABHD6-a inhibitzeko gai izan, KT182 kontzentrazio baxuek neuronak babesteko ahalmenik ez izateak konposatu honen kontzentrazio altuek eragindako babesa ABHD6-arekin zerikusirik ez duen mekanismo baten bitartez gertatzen dela iradokitzen dute. Hau egiaztatzeko, neuronak ABHD6-aren beste inhibitzaile batzuekin tratatu genituen. Neuronetako ABHD6-a blokeatzeko ahalmena erakutsi zuten KT203, WWL70 eta KT195-en probatutako kontzentrazioek (1-2 μM) (Marrs et al., 2010; Hsu et al., 2013) (**12. Irudia D**) ez ziren KT182-aren eragin babesgarriak imitatzeko gai izan (**12. Irudia C**). Datu hauek KT182-ak NMDA-ren aurrean neuronei eragindako babesa ABHD6-aren bitartez gertatzen ez dela frogatzen dute.

Azkenik, KT182-aren eragin babesgarrien atzean FAAH-ren inhibizioa egon zitekeen aztertu genuen. Horretarako, neuronak FAAH entzimaren bi inhibitzaileekin tratatu genituen, URB597 eta PF750 (1 μM). Bi inhibitzaile hauetako bat bera ere ez zen gai izan neuronak NMDA bidezko heriotzetik babesteko (**12. Irudia C**), KT182-aren babesa FAAH-ren inhibizioarekin erlazionatuta egon daitekeelaren ideia baztertuz.

4.2. KT182-a NMDA-k eragindako mitokondrietako kaltzio mailen igoera murrizteko gai da

Gure baldintza esperimentaletan, NMDA kontzentrazio altuek kalpainarekin erlazionatutako nekrosiaren bidezko heriotza eragiten diete neuronei (Ruiz et al., 2014). Deskribatu denaren arabera, 1,2,3-triazol urea (TU) ABHD6 inhibitzaile KT195-a, mitokondrietako kaltzio mailen igoera murriztu eta trantsizio poroaren formakuntza inhibituz, fibroblastoak nekrosi bidezko heriotzetik babesteko gai da (Yun et al., 2014). KT182-a KT195-etik optimizatutako TU inhibitzailea denez (Hsu et al., 2013), jarraian, inhibitzaile honek ere NMDA-k eragindako mitokondrietako kaltzio igoera murrizteko gaitasuna duen aztertu genuen. Horretarako, neuronak mitokondrien 2mtD4cpv adierazlearekin transfektatu ziren. NMDA-k mitokondrietako kaltzio mailen igoera bultzatu eta KT182-a igoera hau %10-ean murrizteko gai zela frogatu genuen (**12. Irudia E-F**). ABHD6-aren beste inhibitzaile guztiak (KT203, KT195 eta WWL70) eta FAAH-ren inhibitzaileak (URB597 eta PF750), ordea, ez zuten mitokondrietako kaltzio igoera murrizteko ahamenik erakutsi (**12. Irudia F**). Emaitza heuek KT182 konposatuak neuronak NMDA-ak eragindako heriotzetik babesteko duen gaitasunak mitokondrietako kaltzio igoera saihesteko duen ahalmenarekin erlazioa izan dezakeela iradokitzen dute.

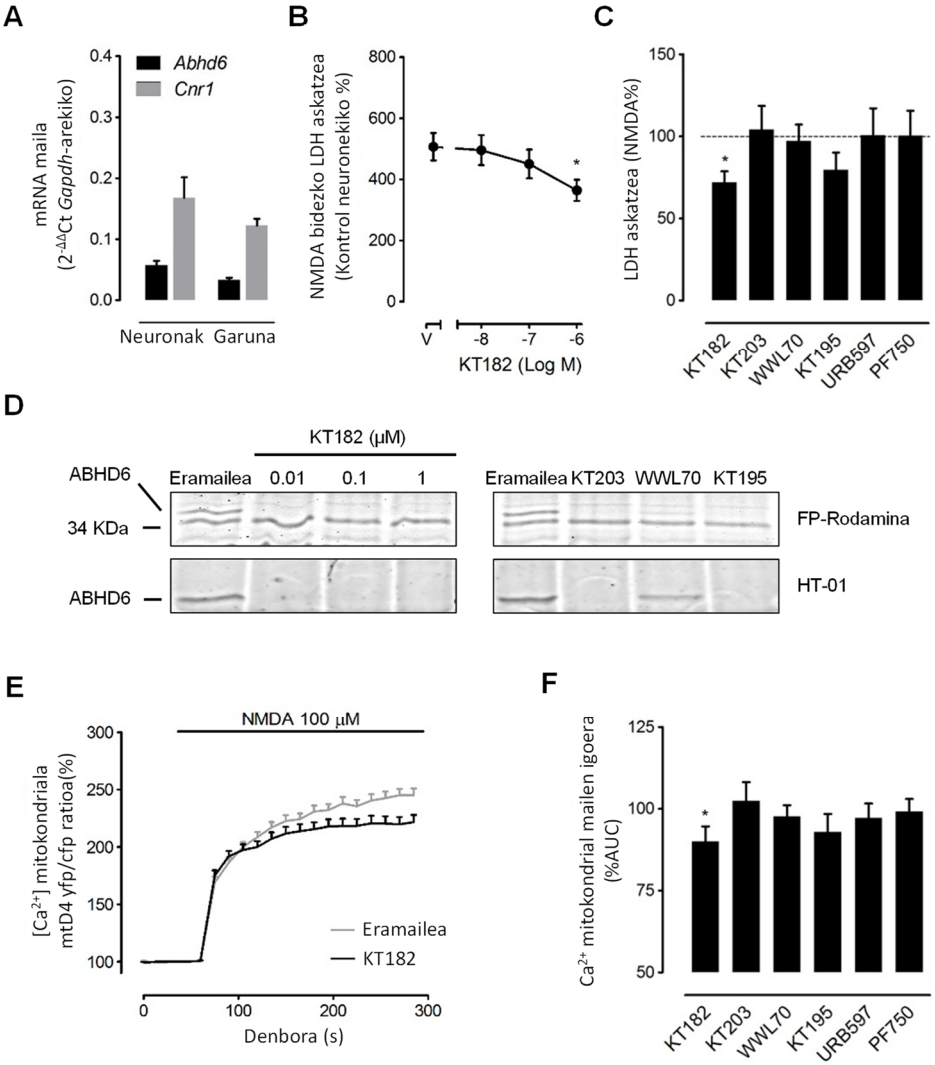

12. Irudia. KT182-a NMDA-ak eragindako heriotza eta mitokondrietako kaltzio mailen igoera murritzeko gai da. (**A**) *Abhd6* eta *Cnr1* geneen adierazpen maila RT-qPCR bitartez neurtu zen kultibatutako neurona kortikaletan (*n* = 3 zelula hazkuntza). Bi gene hauen garuneko adierazpena errefentzi gisa irudikatzen da (*n* = 7 sagu). Emaitzak *Gapdh* genearen adierazpen mailekiko irudikatuta agertzen dira. (**B**) KT182 inhibitzailearen eragin babesgarriak ezagutzeko, neuronak konposatu honekin tratatu ziren 30 minutuz. Jarraian, NMDA aplikatu zitzaien (100 μM, 15 min). (**C**) ABHD6-ak ez du NMDA bidezko exzitotoxizitatea erregulatzen. Probatutako beste ABHD6-aren inhibitzaile guztiak, KT203 (1 μM), KT195 (2 μM) etaWWL70 (1 μM), ez dira KT182-aren efektu babesgarriak antzeratzeko gai. Ezta FAAH entzimaren inhibitzaile URB597 (1 μM) eta PF750 (1 μM) ere (*n* = 10-16 zelula hazkuntza). (**D**) Inhibitzaileek ABHD6 entzima lotzeko duten ahalmena ABPP entsegu bitartez aztertu zen, proteomak lortu eta FP-Rh sondarekin inkubatu aurretik neuronak 30 minutuz inhibitzaileekin tratatuz. 2-3 entsegu desberdinen irudi esanguratsua irudikatuta ikus daiteke. (**E**, **F**) KT182-a NMDA-ak eragindako mitokondrien kaltzio mailen igoera murrizteko gai da. (**E**) Denbora kurtsoak, eramailearekin edo K182-arekin (1 μM) tratatu ondoren, NMDA-ak (100 μM) 2mtD4cpv markatzailearekin transfektatutako neuronetan eragindako yfp/cfp ratioen igoera irudikatzen du (*n* = 62-80 zelula). (**F**) Kurba azpiko areen (AUC) arteko konparaketaren arabera, KT182 konposatua NMDA-k eragindako kaltzio mailen igoera murrizteko gai da. ABHD6-aren gainontzeko inhibitzaileak (KT203, KT195, WWL70) eta FAAH-ren inhibitzaileak (URB597, PF750), ordea, ez dute babes hau eskaintzeko ahalmenik (*n* = 61-78 zelula). Datuak gutxienez 3 zelula hazkuntza desberdinen batezbesteko ± S.E.M arabera irudikatuta daude. **p* < 0.05, Studenten *t*-testa edo Mann-Whitney *U*-testa.

Eztabaida

Lan honen lehengo zatian endokannabinoideen arloan orain arte erantzun gabeko galdera baten inguruan egin dugu lan, oligodendrozito zeluletako CB_1 hartzaileen lokalizazio anatomikoari dagokiona hain zuzen ere. Mikroskopio elektronikoko teknikak eta sortu berri diren sagu transgenikoak erabiliz, hipokanpoko OPC-ek eta gorputz kailukarako oligodendrozitoek, *in situ*, CB_1 hartzaileen dentsitate baxuak adierazten dituztela ikusi dugu. Bestalde, lehen aldiz, CB_1 hartzailerik adierazten ez duten saguek mielinaren ultraegituran aldaketak dituzten aztertu dugu mielinizazio prozesuaren puntu gorenean. Mielinaren lodierari dagozkion aldaketarik ikusi ez dugun arren, CB_1 hartzailea adierazten ez duten saguek gorputz kailukara kaudalean mielinizatutako axoi kopuru altuagoa dutela deskribatu dugu. Horrek, CB_1 hartzaileek, nolabait, mielinizazio prozesuan parte hartu dezaketela iradokitzen du.

Azken bi hamarkadetan, immunohistokimia analisi konbentzionalak, mikroskopia elektronikoa eta teknika elektrofisiologikoak erabiliz, CB_1 hartzaileen lokalizazio zelular eta subzelularra sakonki aztertu da (Katona and Freund 2012). Ikerketa hauek garunean CB_1 hartzaileak era heterogeneoan adierazten direla erakutsi dute, hipokanpoko sinapsi inhibitorioetako proportzio eta dentsitatea kitzikatzailetakoa baino altuagoa izanik (Katona et al. 2006; Kawamura et al. 2006). Berriki, CB_1 hartzailea zelula mota espezifikoetan adierazten ez duten animaliak (cell-specific CB_1 knockout mice) sortu izanak, CB_1 hartzailea dentsitate baxuan adierazten duten zelula eta konpartimentu zelularretan proteina honen lokalizazioa deskribatzea ahalbidetu du, besteak beste bukaera sinaptiko glutamatergikoetan (Gutiérrez-Rodríguez et al. 2017) eta astrozitoetan (Gutiérrez-Rodríguez et al. 2018; Han et al. 2012). Aldi berean, tresna genetikoak eta mikroskopio elektronikoko lanak konbinatuz, mitokondriek beraien mintzetan CB_1 hartzailea adierazten dutela ere ikusi da (Hebert-Chatelain et al. 2016). Oligodendrozitoei dagokionez, OPC eta OL-etako CB_1 hartzaileen adierazpen funtzionala ondo aztertu da urteetan zehar (Bernal-Chico et al. 2015; Gomez et al. 2015; Mato et al. 2009; Molina-Holgado et al. 2002). Hala ere, immunohistokimia analisi arrunten bitartez ez da posible izan saguen garuneko zelula hauek CB_1 hartzailea adierazten dutela era fidagarrian frogatzea. Zoritxarrez, oraindik ez da CB_1 hartzailea espezifikoki oligodendrozitoetan falta duten sagu transgenikorik sortu, ezta *in vivo* CB_1 hartzailea oligodendrozitoetatik desagertarazteko estrategia biralik ere. Hori horrela izanda, ikerketa lan honetan bereizmen altuko mikroskopio elektronikoko teknikak erabili ditugu sagu helduen garuneko OPC eta oligodendrozito mielinizatzaileek CB_1 hartzailea adierazten duten aztertzeko. Hain zuzen ere, teknika horiek sagu basati eta $CB_1^{-/-}$ globalen garuneko ehunei aplikatuz.

OPC-etako CB_1 hartzaileen lokalizazioa aztertu ahal izateko, sagu transgeniko bikoitzak sortu genituen, CB_1 hartzailea ez adierazteaz gain*, NG2* genearen promotorearen menpe EYFP proteina adierazten dutenak. Animalia hauetan, OPC zelulen prozesuak immunoperoxidasa metodoak utzitako DAB depositoen bitartez identifikatu ziren, CB_1 hartzaileak, berriz, zilarrez anplifikatutako urre partikulen bitartez. CB_1 hartzailearekiko immunoerreaktibitate handia adierazten duen zona dela, eta bertan CB_1 hartzailearen lokalizazio lan ugari burutu direla kontuan hartuz (Gutiérrez-Rodríguez et al. 2018; Gutiérrez-Rodríguez et al. 2017; Han et al. 2012; Katona et al. 2006; Kawamura et al. 2006), azterketa hau hipokanpoan burutu genuen. Horrela, NG2-$EYFP^{+/-}$-$CB_1^{+/+}$ eta NG2-$EYFP^{+/-}$-$CB_1^{-/-}$ saguen garun ehunei markaketa bikoitza aplikatu eta hipokanpoko *stratum radiatum* geruzako OPC-en %6-ak CB_1 hartzailea adierazten dutela ikusi dugu, dentsitatea 0.2 partikula/µm-koa izanik.

Ohargarriki, NG2-EYFP$^{+/-}$-$CB_1^{+/+}$ saguen hipokanpoko bukaera sinpatiko inhibitzaile eta kitzikikatzaileetan aurkitutako CB_1 hartzaileen dentsitateak aurretik sagu basatietan deskribatutakoekin bat datozte (Gutiérrez-Rodríguez et al. 2017; Kawamura et al. 2006). Aurretiko mikroskopio elektroniko bidezko azterketa hauen arabera, CA1-eko *stratum radiatum* geruzako sinapsi inhibitzaileen %80-ak eta kitzikatzaileen %20-ak adierazten dituzte CB_1 hartzaileak euren mintzean (Gutiérrez-Rodríguez et al. 2017). Dentsitateei dagokionez, garun area berdinean, sinapsi GABAergikoek 4-5 partikula/µm-ko eta glutamatergikoek 0.3-0.4 partikula/µm-ko azaltzen dituztela deskribatu da. Ikerketa lan honetan, sinapsi GABA-ergikoetan 5.9 partikula/ µm-ko eta glutamatergikoetan 0.7 partikula/µm-ko zenbatu ditugu, gure prozedura immunohistokimikoak espezifikoak eta sentsibilitate handikoak direla frogatuz. Gure lanak, beraz, sagu helduen hipokanpoko OPC-ek CB_1 hartzailea bukaera kitzikatzaile glutamatergikoek baino dentsitate baxuagoan adierazten dutela iradokitzen du. Esan beharra dago, OPC-tan aurkitu dugun CB_1 hartzailearen dentsitatea lehenago beste zelula glialetan deskribatutako dentsitateekin bat datorrela. Ildo honetan, arestiko ikerketa batek, sagu basatien *stratum radiatum* geruzako astrozitoen %40-ak CB_1 hartzailea 0.1-0.15 partikula/µm-ko dentsitatean adierazten dutela deskribatu du (Gutiérrez-Rodríguez et al. 2018).

Bestalde, oligodendrozito helduetan CB_1 hartzailearen lokalizazioa aztertzeko, zilarrez anplifikatatuko urrezko partikuletan oinarritutako markaketa metodoa aplikatu genien sagu basati eta $CB_1^{-/-}$ globalen garun ehunei. Kasu honetan, analisia burutzeko gorputz kailukara aukeratu genuen, bertan oligodendrozitoak ugariak direlako eta beraien ezaugarriei esker oso erraz identifikatu daitezkeelako. Urre partikulen identifikazioak gorputz kailukarako oligodendrozitoen %27-ak beraien somako mintz plasmatikoan CB_1 hartzailea adierazten dutela erakusten du. Aurkikuntza hauen arabera, CB_1 hartzailearentzat positibo diren oligodendrozito kopurua handiagoa da OPC-en prozesu positibo kopurua baino. Kontu izan behar da emaitza hauek interpretatzerako orduan, bi zelula motetako CB_1 hartzaileen lokalizazio azterketak ez baitira animali berdinen ehunetan burutu. Gainera, azpimarratu beharra dago, gorputz kailukaran DAB-arentzat positibo ziren profilen kopuru txikiaren ondorioz, ez garela bertako OPC eta oligodendrozito helduen arteko konparaketa burutzeko gai izan.

Aurretiko lanen testuinguruan, OPC profilen eta oligodendrozito mielinizatzaileen CB_1 hartzailearen adierazpenak baxua dirudi, bai proportzioari eta bai dentsitateari dagokionez. Hala ere, kannabinoideen inguruko ikerketek argi utzi dute CB_1 hartzaileen garrantzia funtzionala ez datorrela beti proteina honen adierazpen mailarekin lotuta. Horrela, jakina da kannabinoideek dituzten hainbat eragin neurona glutamatergikoetako CB_1 hartzaileen aktibazio bitartez gertatzen direla. Esaterako, neurona glutamatergikoetan CB_1 hartzailea adierazten ez duten saguetan eginiko ikerketek hartzaile populazio espezifiko honek neuronen babesean (Monory et al. 2006), desgaitasun motoretan eta hipotermian (Monory et al. 2007), beldur oroitzapenen kontrolean (Metna-Laurent et al. 2012), stress-ak eragindako alterazio sozialetan (Dubreucq et al. 2012) eta antsietatearen kontrolean (Rey et al. 2012) duen betebeharra ezinbestekoa dela erakutsi dute. Bestalde, hipokanpoko astrozitoetako CB_1 hartzaileek plastizitate sinaptikoan eta memoriaren formakuntzan eginbehar garrantzitsua betetzen dutela ikusi da (Han et al. 2012; Navarrete and Araque 2010; Robin et al. 2018), nahiz eta zelula hauek aurkezten duten CB_1 hartzaileen dentsitatea neurona glumatergikoena baino ere baxuagoa izan. Azkenik, mitokondrietako CB_1 hartzaileek, organulu honen arnasketan duten parte hartzearen bitartez, aktibitate neuronala kontrolatzen dutela ere ezagutzen da, prozesu hau memoriaren formakuntzarekin erlazionatu delarik (Hebert-Chatelain et al. 2016). Ebidentzia hauetan oinarrituta, pentsa daiteke, nahiz eta dentsitatea oso

baxuan adierazten diren, oligodendrozitoetako CB_1 hartzaileek zeregin garrantzitsuak bete ditzaketela, besteak beste mielinaren formakuntza eta mantenuan.

Guztira, burututako lan honek sagu helduen garuneko OPC eta oligodendrozitoek CB_1 hartzailea adierazten dutela frogatzen du, esklerosi anizkoitzaren arloan, kannabinoideetan oinarritutako medikamentuen itu izan daitezkeela iradokituz. Hala ere, oraindik ez dakigu gehiegi oligodendrozitoetako CB_1 hartzaileen distribuzio patroiari buruz. Horretarako lagungarria litzateke gai zuriko OPC-ekin konparaketa bat egitea, CB_1 hartzaile populazio desberdinekin erlazionatutako ezaugarri espezifikoak dauden aztertzeko. Baita analisi berbera garapeneko fase desberdinetan burutzea ere, denboran zehar CB_1 hartzailearen adierazpena aldatzen den aztertuz, proteina hauek mielinaren formakuntzan, plastizitatean eta konponketan izan dezaketen eginbeharra errazago interpretatu ahal izateko.

In vitro egin diren hainbat ikerketaren arabera, zelula oligodendroglialetako CB_1 hartzaileek mielinizazio prozesuareren hainbat puntutan hartzen dute parte, besteak beste, OPC-en migrazioan (Sanchez-Rodriguez et al. 2018), proliferazioan (Gomez et al. 2015) eta diferentziazioan (Gomez et al. 2010; Gomez et al. 2011). Aurkikuntza hauek, bai OPC-ek bai oligodendrozito helduek CB_1 hartzailea *in situ* adierazten duten gure frogekin batera, zelula hauetan adierazten diren CB_1 hartzaileek mielinizazio prozesua nolabait erregulatu dezaketela iradokitzen dute. Egia da, CB_1 hartzailea konstitutiboki adierazten ez duten saguak ikerkuntza lan ugaritan erabili diren arren, sekula ez dela deskribatu animalia hauek mielina arraroa aurkezten dutenik. Hala ere, kontuan izan behar da, CB_1 hartzailea adierazten ez duten saguetan mielinaren formakuntzaren dinamika ez dela sekula sakonki aztertu.

CB_1 hartzaileek mielinizazio prozesuan izan dezaketen zeregina ulertzeko, lehen hurbilketa gisa, mielinaren ultraegitura aztertu dugu modu globalean CB_1 hartzailea adierazten ez duten saguen gorputz kailukaran. Horretarako, mielinizazioaren punturik gorenean (P30), bai sagu basati eta bai CB_1 hartzailea adierazten ez zutenetan, bi parametro hartu genituen kontutan: 1) Mielinaren lodiera, *g*- ratio balioen bitartez kalkulatua, eta 2) mielinizatutako axoi kopurua. Mikroskopio elektroniko bidez lortutako irudietan kalkulatutako *g*-ratioen arabera, CB_1 hartzailea ez adierazteak ez du mielinaren lodieran aldaketarik sortzen. CB_1 hartzailea adierazten ez duten saguek mielina mailan alterazio nabarmenik ez aurkezteak hainbat azalpen izan ditzake. Alde batetik, baliteke CB_1 hartzaileek mielinizazio prozesuan betebehar garrantzitsurik ez izatea. Hala ere, denborarekin CB_1 hartzailearen falta beste hainbat faktoreren akzioaren bitartez konpentsatua izatea ere gerta liteke. Zalantza honi erantzuna emateko, mielinaren analisi berbera garapeneko etapa goiztiarragoetan egitea estrategia aproposa izan liteke.

Harrigarriki, CB_1 hartzailea adierazten ez zuten saguen gorputz kailukara kaudalean mielinizatutako axoi kopuru haundiagoa zenbatu dugu sagu basatietan baino. Aurkikuntza honek *in vitro* deskribatu diren CB_1 hartzailearen akzio pro-mielinizatzaileekin kontrastatzen du, CB_1 hartzailearen faltak mielinizazio osatugabe edo berantiarra eragingo zuela pentsarazi zigutenak hain zuzen ere. Hala ere, CB_1 hartzailearen eginkizun biologikoak aztertzeko egin diren *in vitro* entseguetan, agonista kontzentrazio altuak erabili izan dira. Hori horrela izanda, ez da argi geratzen deskribatutako akzio pro-mielinizatzaile horiek CB_1 hartzailearen aktibazioaren ondorioz edo gehiegizko aktibazioak eragindako proteinaren funtzio galera baten ondorioz gerta daitezkeen. Bestalde, azpimarratu beharra dago, mielinaren analisi hau CB_1 hartzailea era globalean adierazten ez duten saguetan burutu zela, beraz, mielinizazio prozesuan zehar zelula espezifiko bakoitzeko CB_1 hartzaileen betebeharra zein izan daitekeen ezin dugula jakin. Esan bezala, mielinizazioa oso prozesu konplexua da, hainbat eta hainbat faktoreren bitartez erregulatzen dena, horien artean

axoiekin erlazionatutako faktoreak eta baita astrozito eta mikrogliekin erlazionatutako molekulak. Garunean CB_1 hartzaileek duten adierazpen zabala ezagututa, posible da pentsatzea zelula desberdinek adierazitako CB_1 hartzaile populazioek mielinizazio prozesua era koordinatu batean, baita kontrako efektuak eraginda ere, erregula dezaketela. Beraz, CB_1 hartzailea espezifikoki zelula oligodendroglialetan adieratzten ez duten saguen garapena izan liteke OPC eta oligodendrozito helduek adierazitako CB_1 hartzaileen funtzio biologikoa ezagutzeko estrategiarik abantailatsuena. Gainera, sagu transgeniko hauek oligodendrozitoetako CB_1 hartzaileak EA tratatzeko itu izan daitezkeen ulertzen lagunduko lukete.

Ikerketa lan honen bigarren zatian, *in vivo* eta *in vitro* estrategiak erabiliz, EA-ren testuinguruan ABHD6 entzima inhibitzeak izan dezakeen baliagarritasun terapeutikoa berraztertzen saiatu gara. Barrera hematoentzefalikoa zeharkatzeko gai den KT182 inhibitzailea kuprizonak eragindako mielinaren galera eta hanturazko erantzuna murrizteko gai dela ikusi dugu. Hala ere, konposatu hau ez da gai kuprizonaren administrazio osteko bermielinizazio prozesua bizkortzeko. *In vitro*, KT182-a ez da gai oligodendrozitoak exitotoxizitaterik babesteko, ezta OPC-ak OL heldu bihurtzeko diferentziazio prozesua bultatzeko ere. Bestalde, profilaktikoki administratuz gero, KT182 inhibitzaileak EAE animali ereduarekin erlazionatutako desgaitasun neurologikoak arinki murrizteko ahalmena daukala deskribatu dugu. Periferiara mugatutako KT203 inhibitzailea, ordea, ez da KT182 inhibitzaileak EAE-an dituen onura berdinak eragiteko gai, gaixotasunaren lehen faseetan NSZ-ko ABHD6 entzima inhibitzearen beharra iradokituz. Azpimarragarriki, KT182 inhibitzailea kronikoki administratzeak garuneko zona batzuetako CB_1 hartzaileen desentsibilizazioa eragiten du. Azkenik, *in vitro* neuronetan eginiko entseguen arabera, KT182-ak, ABHD6-arekin erlaziorik ez duen mekanismo baten bidez, zelula hauek NMDA-ak eragindako heriotzetik babesteko gai da. Aurkikuntza hauen arabera, ABHD6 entzima inhibitzeak gai zuriaren kaltean eragin onuragarri apalak besterik ez ditu eragiten.

Glutamatoak eragindako exzitotoxizitatea EA gaixotasunean gertatzen den mekanismo patogeniko garrantzitsua da (Matute et al. 2001). Testuinguru honetan, ABHD6 entzima inhibitzeak OPC-en heriotz exzitotoxikoa murrizteko gaitasuna duen aztertu dugu, hau, desmielinizazio prozesuetan, mekanismo babeslea izan daitekeela pentsatuz. Gure *in vitro* entseguen arabera, KT182 inhibitzailea ez da gai kultibatutako oligodendrozitoak AMPA-k eragindako heriotzetik babesteko. Emaitza hauek gure laborategiko aurretiko emaitzekin kontrastatu egiten dute. Haien arabera, MAGL entzimaren inhibizio farmakologikoak eragindako 2-AG kontzentrazioen gorakadak, CB_1 hartzaileen aktibazio bitartez, oligodendrozitoak heriotz exzitotoxikotik babesten ditu (Bernal-Chico et al. 2015). Gainera, kultibatutako oligodendrozitoek *Abhd6* genearen adierazpen maila altuagoak dituztela ikusi dugu *Magl* genearenak baino. Itxurazko desadostasun honen arrazoia, oligodendrozitoetan, proteinaren adierazpen mailak 2-AG-a hidrolizatzeko gaitasunarekin bat ez egitea izan daiteke, hain zuzen ere, jakina delako NSZ-ean ABHD6-ak 2-AG-ren hidrolisian duen betebeharra MAGL entzimarena baino askoz txikiagoa dela (Blankman et al. 2007).

OPC-en diferentziazioa bultzatzea estrategia terapeutiko itxaropentsua kontsideratzen da gaixotasun desmielinizatzaileetan, bereziki EA-ren kasuan (Kremer et al. 2015). Horregatik, ikerketa lan honetan, ABHD6-aren KT182 inhibitzaileak kultibatutako OPC-en diferentziazio prozesua bizkortzeko gaitasuna duen aztertu dugu. MBP-aren adierazpena heltze fasearen markatzaile kontsideratuz, ABHD6 entzima inhibitzeak OPC-en diferentziazioa bultzatzen ez duela ikusi genuen. Emaitza honek ere MAGL entzima inhibitzearen eraginekin kontrastatzen du, lan honetan konfirmatu dugun bezala, JZL184 inhibitzaileak OPC-en heltzea bultzatzeko gaitasuna baitu (Gomez et al. 2010). JZL184-aren eragin positibo hauek, gure baldintza esperimentaletan,

oligodendrozitoek 2-AG-aren produkzio eta seinalizazio makinaria adierazten dutela bermatzen dute. Beraz, emaitza hauen arabera, OPC eta oligodendrozitoetako ABHD6 entzima inhibitzea ez da nahikoa 2-AG mailak igo eta hartzaile kannabinoideen aktibazio bitartez efektu onuragarriak eragiteko.

Kuprizonaren EA animali ereduan ABHD6 entzima inhibitzearen eraginak aztertzean, KT182 inhibitzailea 3 astez administratzeak mielinaren galera murrizten duela antzeman genuen. Aurkikuntza hau MAGL entzimaren inhibizioak kuprizona, EAE eta TMEV ereduetan dituen eragin babesleekin bat dator (Bernal-Chico et al. 2015; Feliú et al. 2017; Hernández-Torres et al. 2014). Emaitza hauek guztiek desmielinizazio prozesuetan 2-AG-aren hidrolisia blokeatzea estrategia erabilgarria izan daitekeela proposatzen dute. Aipatu beharra dago, gure baldintzetan, kuprizonaren administrazioa ABHD6 entzimaren adierazpen mailen igoerarekin erlazionatuta dagoela. Beraz, ABHD6 inhibitzearen onurak entzima honek animali eredu honetan 2-AG totalaren proportzio altuago bat hidrolizatzeko izan dezakeen gaitasunarekin erlazionatuta egon litezke, hantura prozesuetan lehenago deskribatu izan den bezala (Poursharifi et al. 2017). ABHD6-ak animalia eredu honetan, egoera fisiologikoekin konparatuz, 2-AG-ren metabolismoan parte hartze handiagoa izan dezakeen arren, kuprizonak eragindako desmielinizazioan entzima hau inhibitzeak eragiten dituen efektu babesgarriak MAGL entzima inhibitzerenak baino apalagoak izaten jarraitzen dute (Bernal-Chico et al. 2015).

OPC-en errekrutamendua eta hauen proliferazioa modulatzeko gaitasunari dagokienez, gure eskuetan, ABHD6-a KT182 bidez inhibitzeak ez du desmielinizatutako gorputz kailukarako OPC kopuruan aldaketarik eragiten. Emaitza honi eta *in vitro* eginiko aurkikuntzei erreparatuz gero, ez dirudi ABHD6-aren inhibitzaileak mielina babesteko duen gaitasuna oligodendrozitoen babes zuzenarekin edo hauek diferentziarazteko ahamenarekin erlazionatuta dagoenik. Aitzitik, KT182-aren bidezko tratamenduak hanturazko erantzuna murrizten zuela ikusi genuen, desmielinizatutako gorputz kailukaran mikroglia eta astrozito gutxiago zenbatu baitgenituen. Emaitza honek KT182-ak eskainitako mielinaren babesa 2-AG mailen igoerak zelula hauek modulatzeko izan dezakeen ahalmenaren ondorio izan daitekeela iradokitzen du. Badira aukera hau babesten duten hainbat aurkikuntza, kannabinoideek mikroglia eta astrozito zelulak modulatzearen bitartez nerbio sistemako hantura murrizteko gaitasuna dutela deskribatzen dutenak. Hain zuzen ere, molekula hauek, hartzaile kannabinoideen aktibazio bitartez, hantura eragiten duten zitokinen (TNFα, IL-1β, IL-6 eta IL-12, besteak beste) eta beste hainbat hantura eragileren (horien artean oxido nitrikoa) adierazpena murrizteko gaitasuna dutela ikusi da (Eljaschewitsch et al. 2006; Ortega-Gutiérrez et al. 2005; Stella 2010). Hala eta guztiz ere, KT182-ak eragindako mikroglia eta astrozito zelulen erreaktibitatearen arintzea era autonomoan gertatzen den edo beste zeluletan ABHD6-a inhibitzeak eragindako 2-AG mailen igoeragatik gertatzen den ez dago argi. Azpimarragarria da, astrozitoetan MAGL entzimaren eginbeharra oso garrantzitsua dela desbribatu den arren (Viader et al. 2015), ABHD6-a inhibitzeak astrogliosia modulatzeko ahalmen handiagoa duela MAGL-a inhibitzeak baino (Bernal-Chico et al. 2015). Emaitza hauen arabera, desmielinizazio prozesuetan ere, 2-AG-a hidrolizatzen duten entzimek endokannabinoideen seinalizazioaren kontrol diferentziala izan dezakete zelula motaren arabera (Poursharifi et al. 2017). Gainera, aurkikuntza honek, mielinaren kaltea eragiten duten prozesuetan, ABHD6-ak astrozito zelulen funtzioen erregulazioan kontrol handia izan dezakeela iradokitzen du.

MAGL entzimaren inhibitzaileek, *in vivo*, mielinaren birsortzea bultzatzeko gaitasuna dutela ikusteak (Feliú et al. 2017), ABHD6-a inhibitzeak kuprizonaren animali ereduan eragin berdinak izan ditzakeen aztertzera eraman ginduen. Espero bezala (Skripuletz et al. 2011), kuprizona dietatik

kentzeak berezko bermielinizazio partziala eragin zuen gorputz kailukaran. Horrela, ABHD6-aren KT182 inhibitzailea prozesu hori bultzatu edo bizkortzeko gai ez dela ikusi genuen. Aurkikuntza honek baieztatu egiten du, beraz, ABHD6-aren inhibitzaileek, *in vivo*, ez dutela zelula oligodendroglialak modulatzeko gaitasunik. Bestalde, aipatu beharra dago KT182-a, hobetze fasean era terapeutikoan administratuta, ez zela desmielinizatutako gorputz kailukarako hantura murrizteko gain izan. Honek KT182-ak, era profilaktikoan administratuz gero, eragiten duen hanturaren murrizketarekin kontrastatu egiten du, mielina babestu ahal izateko ABHD6-aren inhibizio goiztiarra beharrezkoa dela iradokituz. Emaitza guzti hauen arabera, ABHD6 entzima hanturazko ingurune batean inhibitzeak ez luke mielinaren birsortzea bultzatzeko ahalmenik izango.

Lan honen hurrengo helburua sistema periferikoan eta NSZ-ean adierazitako ABHD6 entzimek EAE animali eredu kronikoan duten betebeharra aztertzea izan da. KT182 inhibitzailearen bidezko tratamendu profilaktikoa EAE-ari lotutako desgaitasun neurologikoak era apalean murrizteko gai dela ikusi genuen. Aldiz, periferiara murriztutako KT203 inhibitzailea ez da KT182-aren efektu babesgarri berdinak eragiteko gai. Aurkikuntza honen arabera, NSZ-ko ABHD6 entzimaren inhibizioa gaixotasunaren fase goiztiarretan beharrezkoa da inhibitzaileek efektu babesgarriak sortu ahal izateko. Bestalde, KT203-aren eraginkortasun faltan oinarrituta, ez dirudi inhibitzaileek hantura auto-immunean izan ditzaketen onurak periferiako ABHD6-a inhibitzearekin lotuta daudenik. Nabarmenki, ABHD6 entzimaren inhibitzaileek EAE-ren fase kronikoan hanturazko erantzuna murrizteko gaitasunik ez dutela erakutsi dute. Kasu honetan, konposatu hauek entzima era egokian ez inhibitu izanaren ideia ABPP entsegu bitartez baztertu genuen. EAE saguen garuna eta bizkar-muina aztertzean, gaixotasunak ABHD6-aren adierazpen mailetan aldaketak sortzen ez dituela frogatu ahal izan dugu, kuprizona ereduan gertatzen zenaren alderantziz. Honen arabera, desmielinizazio auto-immunean zehar ABHD6-ak 2-AG hidrolisatzeko duen gaitasuna egoera fisiologikoan duenaren antzekoa da, beraz, hori entzima hau inhibitzeak efikazia terapeutiko murritza izatearen arrazoi bat izan daiteke. Emaitza hauek, kuprizona ereduan gertatzen den bezela, desmielinizazio auto-immnunearen testuinguruan ere, MAGL entzima inhibitzea ABHD6 inhibitzea baino estrategia hobeagoa dela erakusten dute.

Guk EAE ereduan lortutako emaitzek duela gutxi argitaraturiko lan batekin guztiz kontrastatzen dute. Aurkikuntza haien arabera, ABHD6-aren WWL70 inhibitzaileak, era terapeutikoan administratuta, hanturen aurkako efektu eta eragin babesle esanguratsuak ditu EAE-ren fase kronikoan (Wen et al. 2015). Gure datuen eta Wen eta kideen emaitzen arteko desakordio hau, alde batetik, EAE-ren indukzioa eta drogen administrazioa era desberdinean burutu izanaren ondorio izan daiteke, prozedura hauek gaixotasunaren larritasunari eragin baitiezaiokete, ABHD6-aren eraginkortasuna modulatuz. Honi dagokionez, aipatu beharra dago KT182-aren administrazio kronikoak, gure baldintza metodologikoetan, gorputz ildaskatu eta zerebeloko CB_1 hartzaileen desentsibilizazioa eragiten duela. Beraz, baliteke CB_1 hartzaileen funtzionalitatearen galera partzialak ABHD6 inhibitzaileen eraginkortasuna murriztea (Maresz et al. 2007; Pryce et al. 2003). Hala ere, hipotesi hau ez da fase kronikoan KT203-ren inhibizioaren eragin onuragarrien falta azaltzeko gai. Beste arrazoi bat WWL70 inhibitzaileak EAE kronikoan dituen efektuak, partzialki bada ere, ABHD6 entzimarekin zer ikusirik ez duen mekanismo baten bitartez eragitea izan liteke, adibidez, WWL70-ak mikroglietan prostaglandinen produkzioa murrizteko duen ahalmenaren bitartez , laborategi berdinean eginiko *in vitro* lanek proposatzen duten bezala (Tanaka et al. 2017).

Ikerketa lan honetan erabilitako inhibitzaileen espezifikotasunari dagokionez, buruturiko ABPP entseguen arabera, KT182 inhibitzaileak FAAH entzimaren inhibizio partziala eragiten du. Hala ere,

KT182-ak EAE-an dituen eragin onuragarriak FAAH-ren inhibizioari lotuta egoteak ez dirudi azalpenik logikoena. Esan bezela, KT182-ak eragindako FAAH-ren inhibizioa partziala besterik ez da, beraz, inhibizio hori AEA mailak EAE-an efektu babesleak eragiteraino igotzeko nahikoa litzatekeen da sortutako zalantza. Honen inguruan, jakina da FAAH entzima adierazten ez duten saguek ($FAAH^{-/-}$), nahiz eta sagu basatiek baino 15 aldiz AEA maila altuagoak izan (Cravatt et al., 2001), EAE-ren fase akutuan ez dutela hobekuntzarik aurkezten (Webb et al. 2008). $FAAH^{-/-}$ sagu hauen profilak beraz KT182-ak gure eskuetan aurkeztutako eragin babesleekin kontrastatzen du. Gainera, FAAH adierazten ez duten saguek CB_1 hartzailearen adierazpen eta funtzio normala erakusten dute (Cravatt et al. 2001; Falenski et al. 2010), eta honek, berriro ere, KT182-ak eragindako CB_1 hartzaileen desentsibilizazioarekin kontrastatzen du. Aurkikuntza hauek, beraz, KT182-ak EAE-an aurkezten duen eragin onuragarria ABHD6 entzimaren inhibizioaren bitartez gertatzen dela iradokitzen dute.

Agonista kannabinoideak era kronikoan administratzeak CB_1 hartzaileen erregulazio negatiboa (downregulation) bultzatzen dute, kannabinoideen efektuekiko tolerantzia funtzionala eraginez (Blair et al. 2009; Sim et al. 1996). MAGL entzima kronikoki inhibitzeak ere CB_1 hartzaileen adaptazio farmakologikoak eragiten ditu, inhibitzaileen potentzial terapeutikoa murriztuz (Bernal-Chico et al. 2015; Schlosburg et al. 2010). ABHD6-ari dagokionez, gure emaitzek entzima hau kronikoki inhibitzeak garuneko zenbait zonetako CB_1 hartzaileen desentsibilizazio partziala eragiten duela erakusten dute, proteinaren galerari lotuta agertzen ez dena. KT182-ak eragindako CB_1 hartzaileen funtzionalitate galera hau gai zuri asko erakusten duten garun areatara mugatzen dela ikusi dugu, hain zuzen ere, gorputz ildaskatu eta zerebelora, hauek EAE ereduan hanturazko patologia handia erakusten duten zonak direlarik (Mandolesi et al. 2015). Hori horrela izanda, hipotesi nagusia hanturazko egoeratan ABHD6-a inhibitzeak, 2-AG mailen igoera lokalak eraginez, CB_1 hartzaileen (eta ziurrenik CB_2 hartzaileena ere) bidezko seinalizazioa martxan jartzen duela izango litzateke, azkenean hartzaile horien funtzionalitatearen galera partziala eraginez.

Kannabinoide eta endokannabinoideek EAE-an eta beste hainbat kondizio neurologikoetan aurkezten dituzten sintomen kontrolaren mekanismo nagusienetako bat, CB_1 hartzaileen aktibazioaren bitartez, neuronen exzitotoxizitatea murriztea da (Maresz et al. 2007; Marsicano et al. 2003; Pryce et al. 2003). Ebidentzia hauetan oinarrituta, ABHD6 entzima inhibitzeak neuronak babesteko gaitasunik duen aztertzea izan da gure azken helburua. Kultibatutako neuronetan eginiko esperimentuetan, KT182-ak NMDA-ak zelula hauei eragindako heriotza zelularra eta mitokondrietako kaltzio mailen igoera murrizteko gaitasuna duela ikusi genuen. ABHD6-aren beste hainbat inhibitzailek, ordea, ez zuten erakutsi KT182 –aren efektu babesgarriak imitatzeko ahalmenik, nahiz eta entzima era egokian inhibitzeko gai direla frogatu ABPP entsegu bidez. Emaitza hauek, beraz, KT182-ak neuronak NMDA-ak eragindako heriotzetik babesteko duen gaitasuna ABHD6 entzimarekin zer ikusirik ez duen eta, nolabait, mitokondrietako kaltzio barneratzearekin erlazionatuta dagoen mekanismo bati esker gertatzen dela iradokitzen dute. Aurkikuntza hauek berriki deskribatutako lan bat gogorarazten dute. Bertan, serin hidrolasen KT195 inhibitzaileak mitokondrietako kaltzioaren gorakada murrizten duela deskribatzen da, gibeleko fibroblastoak nekrositik babestuz (Yun et al. 204). Lan honen egileen arabera, KT195-aren eragin horiek ez daude kaltzio uniporterreko (MCU) serina hondarrekin erlazionatuta, MCU-aren bidezko kaltzio barneratzea kontrolatzen duen mekanismo berri batekin baizik. KT182 konposatua ABHD6-arekiko potentzia eta selektibitate handiagoa erakusten duen KT195 etik eratorritako inhibitzailea da (Hsu et al. 2013). Ildo honetan, gure *in vitro* eginiko esperimentuetan, KT195-ak NMDAK eragindako heriotza eta kaltzio mitokondrialaren igoera murrizteko ahalmen txikiagoa erakutsi du KT182-ak baino. Hala ere, estruktura kimikoan dituzten antzekotasunek mekanismo berdinak aktibatzeko

joera izan dezaketela iradokitzen dute. Gainera MCU-a mitokondrien kaltzio harreraren eta heriotza exzitotoxikoaren kontrolarekin zuzenki erlazionatu da (Qiu et al. 2013). Nahiz eta lan honetan ez dugun aurkeztu KT182-ak MCU-aren erregulazioan parte hartzen duela erakusten duen behin betiko ebidentziarik, posible da konposatu honek identifikatu gabeko serin hidrolasa baten bitartez, exzitotoxizitate neuronalean, mitokondrietako kaltzioaren harrera erregulatzeko gaitasuna izatea.

Mitokondrien kaltea, horrek eragiten duen gutxiegitasun energetikoaren bitartez, EAE-an gertatzen den desgaitasun neurologikoaren eragile nagusienetarikoa kontsideratzen da, eta baita EA-ren mekanismo patogeniko bat ere. Hala ere, bai gizaki eta bai animali ereduetan, mitokondrien disfuntzioa zerrek eragiten duen ez dago gustiz argi (Nikić et al. 2011; Sadeghian et al. 2016; Witte et al. 2014). *In vitro* ikusitakoaren arabera, KT182-ak EAE-an duen eragin onuragarria konposatu honek mitokondriak babesteko duen gaitasunarekin erlazionatuta egon liteke. Hala ere, KT182-ak *in vivo* dituen efektuen eragile bakarra mitokondrien babesa izateak ez dirudi azalpenik logikoena, konposatu honek eragindako CB_1 hartzaileen desentsibilizazioa edo ABHD6-a inhibitzeak hanturazko eta neuroendekapenezko testuinguruetan eragin onuragarriak aurkezten dituela azaltzen duten ebidentziak (Alhouayek et al. 2013; Naydenov et al. 2014) kontuan hartzen baditugu. Ikerketa honen ondorio bezala, EAE animali ereduan ABHD6 entzima inhibitzeak hanturaren kontrako efektu edo eragin neuro-babesle nabariak aurkezten ez dituela esan daiteke.

.

Ondorioak

Urteetan zehar burututako ikerketek endokannabinoide sistemak EA-rekin erlazionatutako sintomatologia arintzeko potentziala eskaintzen duela frogatu dute. Gaur egun, sistema honen erabilera mugatzen duen arrazioetako bat kannabinoideetan oinarritutako sendagaiek OPC eta OL-en biologia nola modulatzen duten ongi ez ezagutzea da. Testuinguru honetan, NSZ-ko ehunetan oligodendrozito leinuko zelulek CB_1 hartzailea ze mailatan adierazten duten erantzunik gabeko galdera da endokannabinoideen arloan. Bestalde, EA-an ABHD6 entzima inhibitzeak eskaini dezakeen potentzial terapeutikoa ez da sakonki aztertu.

Doktorego Tesi honen **ondorioak** honakoak dira:

I. Ikerketa lan honen lehen zatiak sagu helduen OPC-ek eta oligodendrozito mielinizatzaileek, dentsitate baxuan, beraien mintzean CB_1 hartzailea adierazten dutela frogatzen du. Bestalde, CB_1 hartzailea ez adierazteak mielinaren ultraegituran aldaketa arinak eragiten dituela erakusten du. Guztira, emaitza hauek zelula oligodendroglialetako CB_1 hartzaileek mielinizazio prozesuaren erregulazio finean partu hartu dezaketela proposatzen dute. Gainera, aurkikuntza hauek oinarri anatomikoa eskaintzen diete EA-ean mielinaren babesa eta birsortzea eragiten duten kannabinoideen efektuei.

II. ABHD6 entzimaren inhibizioak efektu onuragarri apalak bakarrik eskaintzen ditu desmielinizazio primario eta sistema immunearen menpeko desmielinizazioan. Bestalde, ez da gai kultibatutako oligodendrozito eta neuronei babesa eskaintzeko, ezta OPC-en diferentziazioa bultzatzeko ere. Aurreko aurkikuntzen testuinguruan, EA-n endokannabinoide bidezko efektu babesleak eragiteko, ABHD6 entzima MAGL entzima baino etorkizun txikiagoa duen itua dela iradokitzen dute emaitza hauek.

Guztira, aurkikuntza hauek endokannabinoide sistemak EA-ean duen potentzial terapeutikoaren ulermena zabaltzen dute eta kannabinoideetan oinarritutako konposatuen onura eta arriskuaren arteko ratioa hobetzen saiatuko diren etorkizuneko ikerkuntzei bidea zabaltzen diete.

Bibliografia

Aguirre A, Dupree JL, Mangin JM, Gallo V. 2007. A functional role for EGFR signaling in myelination and remyelination. Nat Neurosci 10:990-1002.

Ahrendsen JT, Macklin W. 2013. Signaling mechanisms regulating myelination in the central nervous system. Neurosci Bull 29:199-215.

Alhouayek M, Masquelier J, Cani PD, Lambert DM, Muccioli GG. 2013. Implication of the anti-inflammatory bioactive lipid prostaglandin D2-glycerol ester in the control of macrophage activation and inflammation by ABHD6. Proc Natl Acad Sci U S A 110:17558-63.

Alhouayek M, Masquelier J, Muccioli GG. 2014. Controlling 2-arachidonoylglycerol metabolism as an anti-inflammatory strategy. Drug Discov Today 19:295-304.

Almeida RG, Czopka T, Ffrench-Constant C, Lyons DA. 2011. Individual axons regulate the myelinating potential of single oligodendrocytes in vivo. Development 138:4443-50.

André A, Gonthier MP. 2010, The endocannabinoid system: its roles in energy balance and potential as a target for obesity treatment. Int J Biochem Cell Biol 42:1788-801.

Arévalo-Martín A, Vela JM, Molina-Holgado E, Borrell J, Guaza C. 2003. Therapeutic action of cannabinoids in a murine model of multiple sclerosis. J Neurosci 23:2511-6.

Atwood BK, Mackie K. 2010. CB2: a cannabinoid receptor with an identity crisis. Br J Pharmacol 160:467-79.

Baggelaar MP, van Esbroeck AC, van Rooden EJ, Florea BI, Overkleeft HS, Marsicano G, Chaouloff F, van der Stelt M. 2017. Chemical Proteomics Maps Brain Region Specific Activity of Endocannabinoid Hydrolases. ACS Chem Biol 12:852-861.

Baker D, Pryce G, Croxford JL, Brown P, Pertwee RG, Makriyannis A, Khanolkar A, Layward L, Fezza F, Bisogno T and others. 2001. Endocannabinoids control spasticity in a multiple sclerosis model. FASEB J 15:300-2.

Baker D, Pryce G, Jackson SJ, Bolton C, Giovannoni G. 2012. The biology that underpins the therapeutic potential of cannabis-based medicines for the control of spasticity in multiple sclerosis. Multiple Sclerosis and Related Disorders 1:11.

Barca-Mayo O, Lu QR. 2012. Fine-Tuning Oligodendrocyte Development by microRNAs. Front Neurosci 6:13.

Barnett MH, Prineas JW. 2004. Relapsing and remitting multiple sclerosis: pathology of the newly forming lesion. Ann Neurol 55:458-68.

Baumann N, Pham-Dinh D. 2001. Biology of oligodendrocyte and myelin in the mammalian central nervous system. Physiol Rev 81:871-927.

Bengtsson SL, Nagy Z, Skare S, Forsman L, Forssberg H, Ullén F. 2005. Extensive piano practicing has regionally specific effects on white matter development. Nat Neurosci 8:1148-50.

Benito C, Romero JP, Tolón RM, Clemente D, Docagne F, Hillard CJ, Guaza C, Romero J. 2007. Cannabinoid CB1 and CB2 receptors and fatty acid amide hydrolase are specific markers of plaque cell subtypes in human multiple sclerosis. J Neurosci 27:2396-402.

Berdyshev EV. 2000. Cannabinoid receptors and the regulation of immune response. Chem Phys Lipids 108:169-90.

Bernal-Chico A, Canedo M, Manterola A, Victoria Sánchez-Gómez M, Pérez-Samartín A, Rodríguez-Puertas R, Matute C, Mato S. 2015. Blockade of monoacylglycerol lipase inhibits oligodendrocyte excitotoxicity and prevents demyelination in vivo. Glia 63:163-76.

Berrendero F, Sánchez A, Cabranes A, Puerta C, Ramos JA, García-Merino A, Fernández-Ruiz J. 2001. Changes in cannabinoid CB(1) receptors in striatal and cortical regions of rats with experimental allergic encephalomyelitis, an animal model of multiple sclerosis. Synapse 41:195-202.

Bisogno T. 2008. Endogenous cannabinoids: structure and metabolism. J Neuroendocrinol 20 Suppl 1:1-9.

Bisogno T, Howell F, Williams G, Minassi A, Cascio MG, Ligresti A, Matias I, Schiano-Moriello A, Paul P, Williams EJ and others. 2003. Cloning of the first sn1-DAG lipases points to the spatial and temporal regulation of endocannabinoid signaling in the brain. J Cell Biol 163:463-8.

Bitsch A, Schuchardt J, Bunkowski S, Kuhlmann T, Brück W. 2000. Acute axonal injury in multiple sclerosis. Correlation with demyelination and inflammation. Brain 123 (Pt 6):1174-83.

Blair RE, Deshpande LS, Sombati S, Elphick MR, Martin BR, DeLorenzo RJ. 2009. Prolonged exposure to WIN55,212-2 causes downregulation of the CB1 receptor and the development of tolerance to its anticonvulsant effects in the hippocampal neuronal culture model of acquired epilepsy. Neuropharmacology 57:208-18.

Blankman JL, Long JZ, Trauger SA, Siuzdak G, Cravatt BF. 2013. ABHD12 controls brain lysophosphatidylserine pathways that are deregulated in a murine model of the neurodegenerative disease PHARC. Proc Natl Acad Sci U S A 110:1500-5.

Blankman JL, Simon GM, Cravatt BF. 2007. A comprehensive profile of brain enzymes that hydrolyze the endocannabinoid 2-arachidonoylglycerol. Chem Biol 14:1347-56.

Bolton C, Paul C. 1997. MK-801 limits neurovascular dysfunction during experimental allergic encephalomyelitis. J Pharmacol Exp Ther 282:397-402.

Bouaboula M, Poinot-Chazel C, Bourrié B, Canat X, Calandra B, Rinaldi-Carmona M, Le Fur G, Casellas P. 1995. Activation of mitogen-activated protein kinases by stimulation of the central cannabinoid receptor CB1. Biochem J 312 (Pt 2):637-41.

Browne P, Chandraratna D, Angood C, Tremlett H, Baker C, Taylor BV, Thompson AJ. 2014. Atlas of Multiple Sclerosis 2013: A growing global problem with widespread inequity. Neurology 83:1022-4.

Busquets-Garcia A, Puighermanal E, Pastor A, de la Torre R, Maldonado R, Ozaita A. 2011. Differential role of anandamide and 2-arachidonoylglycerol in memory and anxiety-like responses. Biol Psychiatry 70:479-86.

Bénard G, Massa F, Puente N, Lourenço J, Bellocchio L, Soria-Gómez E, Matias I, Delamarre A, Metna-Laurent M, Cannich A and others. 2012. Mitochondrial CB_1 receptors regulate neuronal energy metabolism. Nat Neurosci 15:558-64.

Cabranes A, Pryce G, Baker D, Fernández-Ruiz J. 2006. Changes in CB1 receptors in motor-related brain structures of chronic relapsing experimental allergic encephalomyelitis mice. Brain Res 1107:199-205.

Cabranes A, Venderova K, de Lago E, Fezza F, Sánchez A, Mestre L, Valenti M, García-Merino A, Ramos JA, Di Marzo V and others. 2005. Decreased endocannabinoid levels in the brain and beneficial effects of agents activating cannabinoid and/or vanilloid receptors in a rat model of multiple sclerosis. Neurobiol Dis 20:207-17.

Cadas H, Gaillet S, Beltramo M, Venance L, Piomelli D. 1996. Biosynthesis of an endogenous cannabinoid precursor in neurons and its control by calcium and cAMP. J Neurosci 16:3934-42.

Castillo PE, Younts TJ, Chávez AE, Hashimotodani Y. 2012. Endocannabinoid signaling and synaptic function. Neuron 76:70-81.

Centonze D, Bari M, Rossi S, Prosperetti C, Furlan R, Fezza F, De Chiara V, Battistini L, Bernardi G, Bernardini S and others. 2007. The endocannabinoid system is dysregulated in multiple sclerosis and in experimental autoimmune encephalomyelitis. Brain 130:2543-53.

Centonze D, Muzio L, Rossi S, Cavasinni F, De Chiara V, Bergami A, Musella A, D'Amelio M, Cavallucci V, Martorana A and others. 2009. Inflammation triggers synaptic alteration and degeneration in experimental autoimmune encephalomyelitis. J Neurosci 29:3442-52.

Chakrabarti A, Onaivi ES, Chaudhuri G. 1995. Cloning and sequencing of a cDNA encoding the mouse brain-type cannabinoid receptor protein. DNA Seq 5:385-8.

Chang A, Staugaitis SM, Dutta R, Batt CE, Easley KE, Chomyk AM, Yong VW, Fox RJ, Kidd GJ, Trapp BD. 2012. Cortical remyelination: a new target for repair therapies in multiple sclerosis. Ann Neurol 72:918-26.

Charles P, Hernandez MP, Stankoff B, Aigrot MS, Colin C, Rougon G, Zalc B, Lubetzki C. 2000. Negative regulation of central nervous system myelination by polysialylated-neural cell adhesion molecule. Proc Natl Acad Sci U S A 97:7585-90.

Chen DH, Naydenov A, Blankman JL, Mefford HC, Davis M, Sul Y, Barloon AS, Bonkowski E, Wolff J, Matsushita M and others. 2013. Two novel mutations in ABHD12: expansion of the mutation spectrum in PHARC and assessment of their functional effects. Hum Mutat 34:1672-8.

Chen Y, Liu X, Vickstrom CR, Liu MJ, Zhao L, Viader A, Cravatt BF, Liu QS. 2016. Neuronal and Astrocytic Monoacylglycerol Lipase Limit the Spread of Endocannabinoid Signaling in the Cerebellum. eNeuro 3.

Chew LJ, Coley W, Cheng Y, Gallo V. 2010. Mechanisms of regulation of oligodendrocyte development by p38 mitogen-activated protein kinase. J Neurosci 30:11011-27.

Chiarlone A, Bellocchio L, Blázquez C, Resel E, Soria-Gómez E, Cannich A, Ferrero JJ, Sagredo O, Benito C, Romero J and others. 2014. A restricted population of CB1 cannabinoid receptors with neuroprotective activity. Proc Natl Acad Sci U S A 111:8257-62.

Choi DW. 1988. Glutamate neurotoxicity and diseases of the nervous system. Neuron 1:623-34.

Colognato H, Tzvetanova ID. 2011. Glia unglued: how signals from the extracellular matrix regulate the development of myelinating glia. Dev Neurobiol 71:924-55.

Compston A, Coles A. 2008. Multiple sclerosis. Lancet 372:1502-17.

Consroe P, Musty R, Rein J, Tillery W, Pertwee R. 1997. The perceived effects of smoked cannabis on patients with multiple sclerosis. Eur Neurol 38:44-8.

Cravatt BF, Demarest K, Patricelli MP, Bracey MH, Giang DK, Martin BR, Lichtman AH. 2001. Supersensitivity to anandamide and enhanced endogenous cannabinoid signaling in mice lacking fatty acid amide hydrolase. Proc Natl Acad Sci U S A 98:9371-6.

Cravatt BF, Giang DK, Mayfield SP, Boger DL, Lerner RA, Gilula NB. 1996. Molecular characterization of an enzyme that degrades neuromodulatory fatty-acid amides. Nature 384:83-7.

Croxford JL, Pryce G, Jackson SJ, Ledent C, Giovannoni G, Pertwee RG, Yamamura T, Baker D. 2008. Cannabinoid-mediated neuroprotection, not immunosuppression, may be more relevant to multiple sclerosis. J Neuroimmunol 193:120-9.

Dendrou CA, Fugger L, Friese MA. 2015. Immunopathology of multiple sclerosis. Nat Rev Immunol 15:545-58.

DePaula-Silva AB, Hanak TJ, Libbey JE, Fujinami RS. 2017. Theiler's murine encephalomyelitis virus infection of SJL/J and C57BL/6J mice: Models for multiple sclerosis and epilepsy. J Neuroimmunol 308:30-42.

Devane WA, Hanus L, Breuer A, Pertwee RG, Stevenson LA, Griffin G, Gibson D, Mandelbaum A, Etinger A, Mechoulam R. 1992. Isolation and structure of a brain constituent that binds to the cannabinoid receptor. Science 258:1946-9.

Di Filippo M, Pini LA, Pelliccioli GP, Calabresi P, Sarchielli P. 2008. Abnormalities in the cerebrospinal fluid levels of endocannabinoids in multiple sclerosis. J Neurol Neurosurg Psychiatry 79:1224-9.

Di Marzo V, De Petrocellis L. 2010. Endocannabinoids as regulators of transient receptor potential (TRP) channels: A further opportunity to develop new endocannabinoid-based therapeutic drugs. Curr Med Chem 17:1430-49.

Dinh TP, Freund TF, Piomelli D. 2002. A role for monoglyceride lipase in 2-arachidonoylglycerol inactivation. Chem Phys Lipids 121:149-58.

Dubreucq S, Matias I, Cardinal P, Häring M, Lutz B, Marsicano G, Chaouloff F. 2012. Genetic dissection of the role of cannabinoid type-1 receptors in the emotional consequences of repeated social stress in mice. Neuropsychopharmacology 37:1885-900.

Eljaschewitsch E, Witting A, Mawrin C, Lee T, Schmidt PM, Wolf S, Hoertnagl H, Raine CS, Schneider-Stock R, Nitsch R and others. 2006. The endocannabinoid anandamide protects neurons during CNS inflammation by induction of MKP-1 in microglial cells. Neuron 49:67-79.

Falenski KW, Thorpe AJ, Schlosburg JE, Cravatt BF, Abdullah RA, Smith TH, Selley DE, Lichtman AH, Sim-Selley LJ. 2010. FAAH-/- mice display differential tolerance, dependence, and cannabinoid receptor adaptation after delta 9-tetrahydrocannabinol and anandamide administration. Neuropsychopharmacology 35:1775-87.

Fancy SP, Baranzini SE, Zhao C, Yuk DI, Irvine KA, Kaing S, Sanai N, Franklin RJ, Rowitch DH. 2009. Dysregulation of the Wnt pathway inhibits timely myelination and remyelination in the mammalian CNS. Genes Dev 23:1571-85.

Feliú A, Bonilla Del Río I, Carrillo-Salinas FJ, Hernández-Torres G, Mestre L, Puente N, Ortega-Gutiérrez S, López-Rodríguez ML, Grandes P, Mecha M and others. 2017. 2-Arachidonoylglycerol Reduces Proteoglycans and Enhances Remyelination in a Progressive Model of Demyelination. J Neurosci 37:8385-98.

Fernández-Ruiz J. 2009. The endocannabinoid system as a target for the treatment of motor dysfunction. Br J Pharmacol 156:1029-40.

Fernández-Ruiz J, García C, Sagredo O, Gómez-Ruiz M, de Lago E. 2010. The endocannabinoid system as a target for the treatment of neuronal damage. Expert Opin Ther Targets 14:387-404.

Fernández-Ruiz J, Pazos MR, García-Arencibia M, Sagredo O, Ramos JA. 2008. Role of CB2 receptors in neuroprotective effects of cannabinoids. Mol Cell Endocrinol 286:S91-6.

Fiskerstrand T, H'mida-Ben Brahim D, Johansson S, M'zahem A, Haukanes BI, Drouot N, Zimmermann J, Cole AJ, Vedeler C, Bredrup C and others. 2010. Mutations in ABHD12 cause the neurodegenerative disease PHARC: An inborn error of endocannabinoid metabolism. Am J Hum Genet 87:410-7.

Flores AI, Narayanan SP, Morse EN, Shick HE, Yin X, Kidd G, Avila RL, Kirschner DA, Macklin WB. 2008. Constitutively active Akt induces enhanced myelination in the CNS. J Neurosci 28:7174-83.

Follett PL, Rosenberg PA, Volpe JJ, Jensen FE. 2000. NBQX attenuates excitotoxic injury in developing white matter. J Neurosci 20:9235-41.

Forrest AD, Beggs HE, Reichardt LF, Dupree JL, Colello RJ, Fuss B. 2009. Focal adhesion kinase (FAK): A regulator of CNS myelination. J Neurosci Res 87:3456-64.

Franklin RJ. 2002. Why does remyelination fail in multiple sclerosis? Nat Rev Neurosci 3:705-14.

Franklin RJM, Ffrench-Constant C. 2017. Regenerating CNS myelin - from mechanisms to experimental medicines. Nat Rev Neurosci 18:753-69.

Freeman SA, Desmazières A, Simonnet J, Gatta M, Pfeiffer F, Aigrot MS, Rappeneau Q, Guerreiro S, Michel PP, Yanagawa Y and others. 2015. Acceleration of conduction velocity linked to clustering of nodal components precedes myelination. Proc Natl Acad Sci U S A 112:E321-8.

Furusho M, Dupree JL, Nave KA, Bansal R. 2012. Fibroblast growth factor receptor signaling in oligodendrocytes regulates myelin sheath thickness. J Neurosci 32:6631-41.

Fünfschilling U, Supplie LM, Mahad D, Boretius S, Saab AS, Edgar J, Brinkmann BG, Kassmann CM, Tzvetanova ID, Möbius W and others. 2012. Glycolytic oligodendrocytes maintain myelin and long-term axonal integrity. Nature 485:517-21.

Galabova-Kovacs G, Catalanotti F, Matzen D, Reyes GX, Zezula J, Herbst R, Silva A, Walter I, Baccarini M. 2008. Essential role of B-Raf in oligodendrocyte maturation and myelination during postnatal central nervous system development. J Cell Biol 180:947-55.

Galve-Roperh I, Rueda D, Gómez del Pulgar T, Velasco G, Guzmán M. 2002. Mechanism of extracellular signal-regulated kinase activation by the CB(1) cannabinoid receptor. Mol Pharmacol 62:1385-92.

Galve-Roperh I, Sánchez C, Cortés ML, Gómez del Pulgar T, Izquierdo M, Guzmán M. 2000. Anti-tumoral action of cannabinoids: involvement of sustained ceramide accumulation and extracellular signal-regulated kinase activation. Nat Med 6:313-9.

Gao Y, Vasilyev DV, Goncalves MB, Howell FV, Hobbs C, Reisenberg M, Shen R, Zhang MY, Strassle BW, Lu P and others. 2010. Loss of retrograde endocannabinoid signaling and reduced adult neurogenesis in diacylglycerol lipase knock-out mice. J Neurosci 30:2017-24.

Gérard CM, Mollereau C, Vassart G, Parmentier M. 1991. Molecular cloning of a human cannabinoid receptor which is also expressed in testis. Biochem J 279 (Pt 1):129-34.

Giera S, Deng Y, Luo R, Ackerman SD, Mogha A, Monk KR, Ying Y, Jeong SJ, Makinodan M, Bialas AR and others. 2015. The adhesion G protein-coupled receptor GPR56 is a cell-autonomous regulator of oligodendrocyte development. Nat Commun 6:6121.

Gómez del Pulgar T, Velasco G, Guzmán M. 2000. The CB1 cannabinoid receptor is coupled to the activation of protein kinase B/Akt. Biochem J 347:369-73.

Gomez O, Arevalo-Martin A, Garcia-Ovejero D, Ortega-Gutierrez S, Cisneros JA, Almazan G, Sánchez-Rodriguez MA, Molina-Holgado F, Molina-Holgado E. 2010. The constitutive production of the endocannabinoid 2-arachidonoylglycerol participates in oligodendrocyte differentiation. Glia 58:1913-27.

Gomez O, Sanchez-Rodriguez A, Le M, Sanchez-Caro C, Molina-Holgado F, Molina-Holgado E. 2011. Cannabinoid receptor agonists modulate oligodendrocyte differentiation by activating PI3K/Akt and the mammalian target of rapamycin (mTOR) pathways. Br J Pharmacol 163:1520-32.

Gomez O, Sanchez-Rodriguez MA, Ortega-Gutierrez S, Vazquez-Villa H, Guaza C, Molina-Holgado F, Molina-Holgado E. 2015. A Basal Tone of 2-Arachidonoylglycerol Contributes to Early Oligodendrocyte Progenitor Proliferation by Activating Phosphatidylinositol 3-Kinase (PI3K)/AKT and the Mammalian Target of Rapamycin (MTOR) Pathways. J Neuroimmune Pharmacol 10:309-17.

Gorzkiewicz A, Szemraj J. 2018. Brain endocannabinoid signaling exhibits remarkable complexity. Brain Res Bull 142:33-46.

Grigoriadis N, van Pesch V, Group P. 2015. A basic overview of multiple sclerosis immunopathology. Eur J Neurol 22 Suppl 2:3-13.

Gulyas AI, Cravatt BF, Bracey MH, Dinh TP, Piomelli D, Boscia F, Freund TF. 2004. Segregation of two endocannabinoid-hydrolyzing enzymes into pre- and postsynaptic compartments in the rat hippocampus, cerebellum and amygdala. Eur J Neurosci 20:441-58.

Gutiérrez-Rodríguez A, Bonilla-Del Río I, Puente N, Gómez-Urquijo SM, Fontaine CJ, Egaña-Huguet J, Elezgarai I, Ruehle S, Lutz B, Robin LM and others. 2018. Localization of the cannabinoid type-1 receptor in subcellular astrocyte compartments of mutant mouse hippocampus. Glia 525:1417-31.

Gutiérrez-Rodríguez A, Puente N, Elezgarai I, Ruehle S, Lutz B, Reguero L, Gerrikagoitia I, Marsicano G, Grandes P. 2017. Anatomical characterization of the cannabinoid CB1 receptor in cell-type-specific mutant mouse rescue models. J Comp Neurol 525:302-318.

Hájos N, Katona I, Naiem SS, MacKie K, Ledent C, Mody I, Freund TF. 2000. Cannabinoids inhibit hippocampal GABAergic transmission and network oscillations. Eur J Neurosci 12:3239-49.

Han J, Kesner P, Metna-Laurent M, Duan T, Xu L, Georges F, Koehl M, Abrous DN, Mendizabal-Zubiaga J, Grandes P and others. 2012. Acute cannabinoids impair working memory through astroglial CB1 receptor modulation of hippocampal LTD. Cell 148:1039-50.

Harrington EP, Zhao C, Fancy SP, Kaing S, Franklin RJ, Rowitch DH. 2010. Oligodendrocyte PTEN is required for myelin and axonal integrity, not remyelination. Ann Neurol 68:703-16.

Hashimotodani Y, Ohno-Shosaku T, Tsubokawa H, Ogata H, Emoto K, Maejima T, Araishi K, Shin HS, Kano M. 2005. Phospholipase Cbeta serves as a coincidence detector through its Ca2+ dependency for triggering retrograde endocannabinoid signal. Neuron 45:257-68.

Hebert-Chatelain E, Desprez T, Serrat R, Bellocchio L, Soria-Gomez E, Busquets-Garcia A, Pagano Zottola AC, Delamarre A, Cannich A, Vincent P and others. 2016. A cannabinoid link between mitochondria and memory. Nature 539:555-59.

Herkenham M, Lynn AB, Johnson MR, Melvin LS, de Costa BR, Rice KC. 1991. Characterization and localization of cannabinoid receptors in rat brain: a quantitative in vitro autoradiographic study. J Neurosci 11:563-83.

Herkenham M, Lynn AB, Little MD, Johnson MR, Melvin LS, de Costa BR, Rice KC. 1990. Cannabinoid receptor localization in brain. Proc Natl Acad Sci U S A 87:1932-6.

Hernandez M, Casaccia P. 2015. Interplay between transcriptional control and chromatin regulation in the oligodendrocyte lineage. Glia 63:1357-75.

Hernández-Torres G, Cipriano M, Hedén E, Björklund E, Canales Á, Zian D, Feliú A, Mecha M, Guaza C, Fowler CJ and others. 2014. A reversible and selective inhibitor of monoacylglycerol lipase ameliorates multiple sclerosis. Angew Chem Int Ed Engl 53:13765-70.

Howlett AC. 2002. The cannabinoid receptors. Prostaglandins Other Lipid Mediat 68-69:619-31.

Hsu KL, Tsuboi K, Chang JW, Whitby LR, Speers AE, Pugh H, Cravatt BF. 2013. Discovery and optimization of piperidyl-1,2,3-triazole ureas as potent, selective, and in vivo-active inhibitors of α/β-hydrolase domain containing 6 (ABHD6). J Med Chem 56:8270-9.

Hua T, Vemuri K, Pu M, Qu L, Han GW, Wu Y, Zhao S, Shui W, Li S, Korde A and others. 2016. Crystal Structure of the Human Cannabinoid Receptor CB. Cell 167:750-762.e14.

Human protein Atlas.2013. www.proteinatlas.org

Ishibashi T, Dakin KA, Stevens B, Lee PR, Kozlov SV, Stewart CL, Fields RD. 2006. Astrocytes promote myelination in response to electrical impulses. Neuron 49:823-32.

Ishii A, Furusho M, Dupree JL, Bansal R. 2014. Role of ERK1/2 MAPK signaling in the maintenance of myelin and axonal integrity in the adult CNS. J Neurosci 34:16031-45.

Ishii A, Fyffe-Maricich SL, Furusho M, Miller RH, Bansal R. 2012. ERK1/ERK2 MAPK signaling is required to increase myelin thickness independent of oligodendrocyte differentiation and initiation of myelination. J Neurosci 32:8855-64.

Jean-Gilles L, Feng S, Tench CR, Chapman V, Kendall DA, Barrett DA, Constantinescu CS. 2009. Plasma endocannabinoid levels in multiple sclerosis. J Neurol Sci 287:212-5.

Kahn MA, Kumar S, Liebl D, Chang R, Parada LF, De Vellis J. 1999. Mice lacking NT-3, and its receptor TrkC, exhibit profound deficiencies in CNS glial cells. Glia 26:153-65.

Kano M, Ohno-Shosaku T, Hashimotodani Y, Uchigashima M, Watanabe M. 2009. Endocannabinoid-mediated control of synaptic transmission. Physiol Rev 89:309-80.

Karram K, Goebbels S, Schwab M, Jennissen K, Seifert G, Steinhäuser C, Nave KA, Trotter J. 2008. NG2-expressing cells in the nervous system revealed by the NG2-EYFP-knockin mouse. Genesis 46:743-57.

Katona I, Freund TF. 2008. Endocannabinoid signaling as a synaptic circuit breaker in neurological disease. Nat Med 14:923-30.

Katona I, Freund TF. 2012. Multiple functions of endocannabinoid signaling in the brain. Annu Rev Neurosci 35:529-58.

Katona I, Urbán GM, Wallace M, Ledent C, Jung KM, Piomelli D, Mackie K, Freund TF. 2006. Molecular composition of the endocannabinoid system at glutamatergic synapses. J Neurosci 26:5628-37.

Katz Sand I. 2015. Classification, diagnosis, and differential diagnosis of multiple sclerosis. Curr Opin Neurol 28:193-205.

Kawamura Y, Fukaya M, Maejima T, Yoshida T, Miura E, Watanabe M, Ohno-Shosaku T, Kano M. 2006. The CB1 cannabinoid receptor is the major cannabinoid receptor at excitatory presynaptic sites in the hippocampus and cerebellum. J Neurosci 26:2991-3001.

Keough MB, Jensen SK, Yong VW. 2015. Experimental demyelination and remyelination of murine spinal cord by focal injection of lysolecithin. J Vis Exp 26.

Kim S, Kim SH, Kim H, Chung AY, Cha YI, Kim CH, Huh TL, Park HC. 2008. Frizzled 8a function is required for oligodendrocyte development in the zebrafish spinal cord. Dev Dyn 237:3324-31.

Kinney HC, Volpe JJ. 2018. Volpe´s Neurology of the Newborn (Sixth Edition). Elsevier 176-88.

Kipp M, Nyamoya S, Hochstrasser T, Amor S. 2017. Multiple sclerosis animal models: a clinical and histopathological perspective. Brain Pathol 27:123-37.

Kirby BB, Takada N, Latimer AJ, Shin J, Carney TJ, Kelsh RN, Appel B. 2006. In vivo time-lapse imaging shows dynamic oligodendrocyte progenitor behavior during zebrafish development. Nat Neurosci 9:1506-11.

Kmietowicz Z. 2010. Cannabis based drug is licensed for spasticity in patients with MS. BMJ 340:c3363.

Koch M, Kingwell E, Rieckmann P, Tremlett H. 2009. The natural history of primary progressive multiple sclerosis. Neurology 73:1996-2002.

Kozak KR, Prusakiewicz JJ, Marnett LJ. 2004. Oxidative metabolism of endocannabinoids by COX-2. Curr Pharm Des 10:659-67.

Kremer D, Akkermann R, Küry P, Dutta R. 2018. Current advancements in promoting remyelination in multiple sclerosis. Mult Scler:1352458518800827.

Kremer D, Küry P, Dutta R. 2015. Promoting remyelination in multiple sclerosis: current drugs and future prospects. Mult Scler 21:541-9.

Lau BK, Cota D, Cristino L, Borgland SL. 2017. Endocannabinoid modulation of homeostatic and non-homeostatic feeding circuits. Neuropharmacology 124:38-51.

Lee S, Leach MK, Redmond SA, Chong SY, Mellon SH, Tuck SJ, Feng ZQ, Corey JM, Chan JR. 2012. A culture system to study oligodendrocyte myelination processes using engineered nanofibers. Nat Methods 9:917-22.

Leterrier C, Bonnard D, Carrel D, Rossier J, Lenkei Z. 2004. Constitutive endocytic cycle of the CB1 cannabinoid receptor. J Biol Chem 279:36013-21.

Li W, Blankman JL, Cravatt BF. 2007. A functional proteomic strategy to discover inhibitors for uncharacterized hydrolases. J Am Chem Soc 129:9594-5.

Ligresti A, Cascio MG, Pryce G, Kulasegram S, Beletskaya I, De Petrocellis L, Saha B, Mahadevan A, Visintin C, Wiley JL and others. 2006. New potent and selective inhibitors of anandamide reuptake with antispastic activity in a mouse model of multiple sclerosis. Br J Pharmacol 147:83-91.

Liu J, Wang L, Harvey-White J, Osei-Hyiaman D, Razdan R, Gong Q, Chan AC, Zhou Z, Huang BX, Kim HY and others. 2006. A biosynthetic pathway for anandamide. Proc Natl Acad Sci U S A 103:13345-50.

Long JZ, Li W, Booker L, Burston JJ, Kinsey SG, Schlosburg JE, Pavón FJ, Serrano AM, Selley DE, Parsons LH and others. 2009. Selective blockade of 2-arachidonoylglycerol hydrolysis produces cannabinoid behavioral effects. Nat Chem Biol 5:37-44.

Loría F, Petrosino S, Mestre L, Spagnolo A, Correa F, Hernangómez M, Guaza C, Di Marzo V, Docagne F. 2008. Study of the regulation of the endocannabinoid system in a virus model of multiple sclerosis reveals a therapeutic effect of palmitoylethanolamide. Eur J Neurosci 28:633-41.

Lublin FD. 2014. New multiple sclerosis phenotypic classification. Eur Neurol 72 Suppl 1:1-5.

Lucchinetti C, Brück W, Parisi J, Scheithauer B, Rodriguez M, Lassmann H. 2000. Heterogeneity of multiple sclerosis lesions: implications for the pathogenesis of demyelination. Ann Neurol 47:707-17.

Lundgaard I, Luzhynskaya A, Stockley JH, Wang Z, Evans KA, Swire M, Volbracht K, Gautier HO, Franklin RJ, Attwell D and others. 2013. Neuregulin and BDNF induce a switch to NMDA receptor-dependent myelination by oligodendrocytes. PLoS Biol 11:e1001743.

Lutz B, Marsicano G, Maldonado R, Hillard CJ. 2015. The endocannabinoid system in guarding against fear, anxiety and stress. Nat Rev Neurosci 16:705-18.

Mandolesi G, Gentile A, Musella A, Fresegna D, De Vito F, Bullitta S, Sepman H, Marfia GA, Centonze D. 2015. Synaptopathy connects inflammation and neurodegeneration in multiple sclerosis. Nat Rev Neurol 11:711-24.

Mangin JM, Li P, Scafidi J, Gallo V. 2012. Experience-dependent regulation of NG2 progenitors in the developing barrel cortex. Nat Neurosci 15:1192-4.

Manterola A, Bernal-Chico A, Cipriani R, Canedo-Antelo M, Moreno-García Á, Martín-Fontecha M, Pérez-Cerdá F, Sánchez-Gómez MV, Ortega-Gutiérrez S, Brown JM and others. 2018. Deregulation of the endocannabinoid system and therapeutic potential of ABHD6 blockade in the cuprizone model of demyelination. Biochem Pharmacol 157:189-201.

Maresz K, Pryce G, Ponomarev ED, Marsicano G, Croxford JL, Shriver LP, Ledent C, Cheng X, Carrier EJ, Mann MK and others. 2007. Direct suppression of CNS autoimmune inflammation via the cannabinoid receptor CB1 on neurons and CB2 on autoreactive T cells. Nat Med 13:492-7.

Marinelli S, Pacioni S, Bisogno T, Di Marzo V, Prince DA, Huguenard JR, Bacci A. 2008. The endocannabinoid 2-arachidonoylglycerol is responsible for the slow self-inhibition in neocortical interneurons. J Neurosci 28:13532-41.

Maroso M, Szabo GG, Kim HK, Alexander A, Bui AD, Lee SH, Lutz B, Soltesz I. 2016. Cannabinoid Control of Learning and Memory through HCN Channels. Neuron 89:1059-73.

Marques S, Zeisel A, Codeluppi S, van Bruggen D, Mendanha Falcão A, Xiao L, Li H, Häring M, Hochgerner H, Romanov RA and others. 2016. Oligodendrocyte heterogeneity in the mouse juvenile and adult central nervous system. Science 352:1326-9.

Marrs WR, Blankman JL, Horne EA, Thomazeau A, Lin YH, Coy J, Bodor AL, Muccioli GG, Hu SS, Woodruff G and others. 2010. The serine hydrolase ABHD6 controls the accumulation and efficacy of 2-AG at cannabinoid receptors. Nat Neurosci 13:951-7.

Marsicano G, Goodenough S, Monory K, Hermann H, Eder M, Cannich A, Azad SC, Cascio MG, Gutiérrez SO, van der Stelt M and others. 2003. CB1 cannabinoid receptors and on-demand defense against excitotoxicity. Science 302:84-8.

Marsicano G, Lafenêtre P. 2009. Roles of the endocannabinoid system in learning and memory. Curr Top Behav Neurosci 1:201-30.

Marsicano G, Lutz B. 1999. Expression of the cannabinoid receptor CB1 in distinct neuronal subpopulations in the adult mouse forebrain. Eur J Neurosci 11:4213-25.

Marsicano G, Wotjak CT, Azad SC, Bisogno T, Rammes G, Cascio MG, Hermann H, Tang J, Hofmann C, Zieglgänsberger W and others. 2002. The endogenous cannabinoid system controls extinction of aversive memories. Nature 418:530-4.

Martin-Fernandez M, Jamison S, Robin LM, Zhao Z, Martin ED, Aguilar J, Benneyworth MA, Marsicano G, Araque A. 2017. Synapse-specific astrocyte gating of amygdala-related behavior. Nat Neurosci 20:1540-48.

Mato S, Alberdi E, Ledent C, Watanabe M, Matute C. 2009. CB1 cannabinoid receptor-dependent and -independent inhibition of depolarization-induced calcium influx in oligodendrocytes. Glia 57:295-306.

Matsuda LA, Lolait SJ, Brownstein MJ, Young AC, Bonner TI. 1990. Structure of a cannabinoid receptor and functional expression of the cloned cDNA. Nature 346:561-4.

Matute C, Alberdi E, Domercq M, Pérez-Cerdá F, Pérez-Samartín A, Sánchez-Gómez MV. 2001. The link between excitotoxic oligodendroglial death and demyelinating diseases. Trends Neurosci 24:224-30.

Matute C, Sánchez-Gómez MV, Martínez-Millán L, Miledi R. 1997. Glutamate receptor-mediated toxicity in optic nerve oligodendrocytes. Proc Natl Acad Sci U S A 94:8830-5.

McCarthy KD, de Vellis J. 1980. Preparation of separate astroglial and oligodendroglial cell cultures from rat cerebral tissue. J Cell Biol 85:890-902.

McDonald JW, Althomsons SP, Hyrc KL, Choi DW, Goldberg MP. 1998. Oligodendrocytes from forebrain are highly vulnerable to AMPA/kainate receptor-mediated excitotoxicity. Nat Med 4:291-7.

McKenzie IA, Ohayon D, Li H, de Faria JP, Emery B, Tohyama K, Richardson WD. 2014. Motor skill learning requires active central myelination. Science 346:318-22.

Mecha M, Carrillo-Salinas FJ, Feliú A, Mestre L, Guaza C. 2016. Microglia activation states and cannabinoid system: Therapeutic implications. Pharmacol Ther 166:40-55.

Mecha M, Feliú A, Machín I, Cordero C, Carrillo-Salinas F, Mestre L, Hernández-Torres G, Ortega-Gutiérrez S, López-Rodríguez ML, de Castro F and others. 2018. 2-AG limits Theiler's virus induced acute neuroinflammation by modulating microglia and promoting MDSCs. Glia 66:1447-63.

Mechoulam R. 1970. Marihuana chemistry. Science 168:1159-66.

Metna-Laurent M, Marsicano G. 2015. Rising stars: modulation of brain functions by astroglial type-1 cannabinoid receptors. Glia 63:353-64.

Metna-Laurent M, Soria-Gómez E, Verrier D, Conforzi M, Jégo P, Lafenêtre P, Marsicano G. 2012. Bimodal control of fear-coping strategies by CB_1 cannabinoid receptors. J Neurosci 32:7109-18.

Mi S, Miller RH, Lee X, Scott ML, Shulag-Morskaya S, Shao Z, Chang J, Thill G, Levesque M, Zhang M and others. 2005. LINGO-1 negatively regulates myelination by oligodendrocytes. Nat Neurosci 8:745-51.

Möbius W. 2010. Electron Microscopy of the Mouse Central Nervous System. Methods in Cell Biology (Volume 96). Elsevier Inc. Academic Press, p. 475.

Mogha A, D'Rozario M, Monk KR. 2016. G Protein-Coupled Receptors in Myelinating Glia. Trends Pharmacol Sci 37:977-87.

Molina-Holgado E, Vela JM, Arévalo-Martín A, Almazán G, Molina-Holgado F, Borrell J, Guaza C. 2002. Cannabinoids promote oligodendrocyte progenitor survival: involvement of cannabinoid receptors and phosphatidylinositol-3 kinase/Akt signaling. J Neurosci 22:9742-53.

Monory K, Blaudzun H, Massa F, Kaiser N, Lemberger T, Schütz G, Wotjak CT, Lutz B, Marsicano G. 2007. Genetic dissection of behavioural and autonomic effects of Delta(9)-tetrahydrocannabinol in mice. PLoS Biol 5:e269.

Monory K, Massa F, Egertová M, Eder M, Blaudzun H, Westenbroek R, Kelsch W, Jacob W, Marsch R, Ekker M and others. 2006. The endocannabinoid system controls key epileptogenic circuits in the hippocampus. Neuron 51:455-66.

Morales P, Reggio PH. 2017. An Update on Non-CB. Cannabis Cannabinoid Res 2:265-273.

Munro S, Thomas KL, Abu-Shaar M. 1993. Molecular characterization of a peripheral receptor for cannabinoids. Nature 365:61-5.

Murray TJ. 2009. The history of multiple sclerosis: the changing frame of the disease over the centuries. J Neurol Sci 277 Suppl 1:S3-8.

Narayanan SP, Flores AI, Wang F, Macklin WB. 2009. Akt signals through the mammalian target of rapamycin pathway to regulate CNS myelination. J Neurosci 29:6860-70.

Naruse M, Ishizaki Y, Ikenaka K, Tanaka A, Hitoshi S. 2017. Origin of oligodendrocytes in mammalian forebrains: a revised perspective. J Physiol Sci 67:63-70.

Navarrete M, Araque A. 2008. Endocannabinoids mediate neuron-astrocyte communication. Neuron 57:883-93.

Navarrete M, Araque A. 2010. Endocannabinoids potentiate synaptic transmission through stimulation of astrocytes. Neuron 68:113-26.

Navarro G, Morales P, Rodríguez-Cueto C, Fernández-Ruiz J, Jagerovic N, Franco R. 2016. Targeting Cannabinoid CB2 Receptors in the Central Nervous System. Medicinal Chemistry Approaches with Focus on Neurodegenerative Disorders. Front Neurosci 10:406.

Nave KA, Ehrenreich H. 2014. Myelination and Oligodendrocyte Functions in Psychiatric Diseases. JAMA Psychiatry 71:582-4.

Nave KA, Werner HB. 2014. Myelination of the nervous system: mechanisms and functions. Annu Rev Cell Dev Biol 30:503-33.

Navia-Paldanius D, Savinainen JR, Laitinen JT. 2012. Biochemical and pharmacological characterization of human α/β-hydrolase domain containing 6 (ABHD6) and 12 (ABHD12). J Lipid Res 53:2413-24.

Naydenov AV, Horne EA, Cheah CS, Swinney K, Hsu KL, Cao JK, Marrs WR, Blankman JL, Tu S, Cherry AE and others. 2014. ABHD6 blockade exerts antiepileptic activity in PTZ-induced seizures and in spontaneous seizures in R6/2 mice. Neuron 83:361-71.

Nikić I, Merkler D, Sorbara C, Brinkoetter M, Kreutzfeldt M, Bareyre FM, Brück W, Bishop D, Misgeld T, Kerschensteiner M. 2011. A reversible form of axon damage in experimental autoimmune encephalomyelitis and multiple sclerosis. Nat Med 17:495-9.

Nomura DK, Morrison BE, Blankman JL, Long JZ, Kinsey SG, Marcondes MC, Ward AM, Hahn YK, Lichtman AH, Conti B and others. 2011. Endocannabinoid hydrolysis generates brain prostaglandins that promote neuroinflammation. Science 334:809-13.

Okamoto Y, Morishita J, Tsuboi K, Tonai T, Ueda N. 2004. Molecular characterization of a phospholipase D generating anandamide and its congeners. J Biol Chem 279:5298-305.

Oliveira da Cruz JF, Robin LM, Drago F, Marsicano G, Metna-Laurent M. 2016. Astroglial type-1 cannabinoid receptor (CB1): A new player in the tripartite synapse. Neuroscience 323:35-42.

Ortega-Gutiérrez S, Molina-Holgado E, Arévalo-Martín A, Correa F, Viso A, López-Rodríguez ML, Di Marzo V, Guaza C. 2005. Activation of the endocannabinoid system as therapeutic approach in a murine model of multiple sclerosis. FASEB J 19:1338-40.

Palazuelos J, Davoust N, Julien B, Hatterer E, Aguado T, Mechoulam R, Benito C, Romero J, Silva A, Guzmán M and others. 2008. The CB(2) cannabinoid receptor controls myeloid progenitor trafficking: involvement in the pathogenesis of an animal model of multiple sclerosis. J Biol Chem 283:13320-9.

Palmer AE, Giacomello M, Kortemme T, Hires SA, Lev-Ram V, Baker D, Tsien RY. 2006. Ca2+ indicators based on computationally redesigned calmodulin-peptide pairs. Chem Biol 13:521-30.

Pasquali L, Lucchesi C, Pecori C, Metelli MR, Pellegrini S, Iudice A, Bonuccelli U. 2015. A clinical and laboratory study evaluating the profile of cytokine levels in relapsing remitting and secondary progressive multiple sclerosis. J Neuroimmunol 278:53-9.

Patricelli MP, Giang DK, Stamp LM, Burbaum JJ. 2001. Direct visualization of serine hydrolase activities in complex proteomes using fluorescent active site-directed probes. Proteomics 1:1067-71.

Paxinos G, Franklin K. 2012. Paxinos and Franklin´s the Mouse Brain in Stereotaxic Coordinates (4th Edition). Elsevier Inc. Academic Press.p.360.

Pertwee RG, Howlett AC, Abood ME, Alexander SP, Di Marzo V, Elphick MR, Greasley PJ, Hansen HS, Kunos G, Mackie K and others. 2010. International Union of Basic and Clinical Pharmacology. LXXIX. Cannabinoid receptors and their ligands: beyond CB_1 and CB_2. Pharmacol Rev 62:588-631.

Peters A, Folger C. 2013. A website entitled "The fine structure of the aging brain". J Comp Neurol 521:1203-6.

Pfeiffer SE, Warrington AE, Bansal R. 1993. The oligodendrocyte and its many cellular processes. Trends Cell Biol 3:191-7.

Piomelli D. 2003. The molecular logic of endocannabinoid signalling. Nat Rev Neurosci 4:873-84.

Piro JR, Benjamin DI, Duerr JM, Pi Y, Gonzales C, Wood KM, Schwartz JW, Nomura DK, Samad TA. 2012. A dysregulated endocannabinoid-eicosanoid network supports pathogenesis in a mouse model of Alzheimer's disease. Cell Rep 1:617-23.

Pitt D, Werner P, Raine CS. 2000. Glutamate excitotoxicity in a model of multiple sclerosis. Nat Med 6:67-70.

Polman CH, Reingold SC, Banwell B, Clanet M, Cohen JA, Filippi M, Fujihara K, Havrdova E, Hutchinson M, Kappos L and others. 2011. Diagnostic criteria for multiple sclerosis: 2010 revisions to the McDonald criteria. Ann Neurol 69:292-302.

Poursharifi P, Madiraju SRM, Prentki M. 2017. Monoacylglycerol signalling and ABHD6 in health and disease. Diabetes Obes Metab 19 Suppl 1:76-89.

Procaccini C, De Rosa V, Pucino V, Formisano L, Matarese G. 2015. Animal models of Multiple Sclerosis. Eur J Pharmacol 759:182-91.

Pryce G, Ahmed Z, Hankey DJ, Jackson SJ, Croxford JL, Pocock JM, Ledent C, Petzold A, Thompson AJ, Giovannoni G and others. 2003. Cannabinoids inhibit neurodegeneration in models of multiple sclerosis. Brain 126:2191-202.

Pryce G, Cabranes A, Fernández-Ruiz J, Bisogno T, Di Marzo V, Long JZ, Cravatt BF, Giovannoni G, Baker D. 2013. Control of experimental spasticity by targeting the degradation of endocannabinoids using selective fatty acid amide hydrolase inhibitors. Mult Scler 19:1896-904.

Puighermanal E, Marsicano G, Busquets-Garcia A, Lutz B, Maldonado R, Ozaita A. 2009. Cannabinoid modulation of hippocampal long-term memory is mediated by mTOR signaling. Nat Neurosci 12:1152-8.

Qiu J, Tan YW, Hagenston AM, Martel MA, Kneisel N, Skehel PA, Wyllie DJ, Bading H, Hardingham GE. 2013. Mitochondrial calcium uniporter Mcu controls excitotoxicity and is transcriptionally repressed by neuroprotective nuclear calcium signals. Nat Commun 4:2034.

Reich DS, Lucchinetti CF, Calabresi PA. 2018. Multiple Sclerosis. N Engl J Med 378:169-80.

Rey AA, Purrio M, Viveros MP, Lutz B. 2012. Biphasic effects of cannabinoids in anxiety responses: CB1 and GABA(B) receptors in the balance of GABAergic and glutamatergic neurotransmission. Neuropsychopharmacology 37:2624-34.

Richardson WD, Young KM, Tripathi RB, McKenzie I. 2011. NG2-glia as multipotent neural stem cells: fact or fantasy? Neuron 70:661-73.

Rivers LE, Young KM, Rizzi M, Jamen F, Psachoulia K, Wade A, Kessaris N, Richardson WD. 2008. PDGFRA/NG2 glia generate myelinating oligodendrocytes and piriform projection neurons in adult mice. Nat Neurosci 11:1392-401.

Robin LM, Oliveira da Cruz JF, Langlais VC, Martin-Fernandez M, Metna-Laurent M, Busquets-Garcia A, Bellocchio L, Soria-Gomez E, Papouin T, Varilh M and others. 2018. Astroglial CB1 Receptors Determine Synaptic D-Serine Availability to Enable Recognition Memory. Neuron 98:935-944.

Rodriguez JJ, Mackie K, Pickel VM. 2001. Ultrastructural localization of the CB1 cannabinoid receptor in mu-opioid receptor patches of the rat Caudate putamen nucleus. J Neurosci 21:823-33.

Rosenberg SS, Kelland EE, Tokar E, De la Torre AR, Chan JR. 2008. The geometric and spatial constraints of the microenvironment induce oligodendrocyte differentiation. Proc Natl Acad Sci U S A 105:14662-7.

Rueda D, Galve-Roperh I, Haro A, Guzmán M. 2000. The CB(1) cannabinoid receptor is coupled to the activation of c-Jun N-terminal kinase. Mol Pharmacol 58:814-20.

Ruiz A, Alberdi E, Matute C. 2014. CGP37157, an inhibitor of the mitochondrial Na+/Ca2+ exchanger, protects neurons from excitotoxicity by blocking voltage-gated Ca2+ channels. Cell Death Dis 5:e1156.

Sadeghian M, Mastrolia V, Rezaei Haddad A, Mosley A, Mullali G, Schiza D, Sajic M, Hargreaves I, Heales S, Duchen MR and others. 2016. Mitochondrial dysfunction is an important cause of neurological deficits in an inflammatory model of multiple sclerosis. Sci Rep 6:33249.

Sampaio-Baptista C, Khrapitchev AA, Foxley S, Schlagheck T, Scholz J, Jbabdi S, DeLuca GC, Miller KL, Taylor A, Thomas N and others. 2013. Motor skill learning induces changes in white matter microstructure and myelination. J Neurosci 33:19499-503.

Sanchez-Rodriguez MA, Gomez O, Esteban PF, Garcia-Ovejero D, Molina-Holgado E. 2018. The endocannabinoid 2-arachidonoylglycerol regulates oligodendrocyte progenitor cell migration. Biochem Pharmacol 157:180-88.

Savinainen JR, Saario SM, Laitinen JT. 2012. The serine hydrolases MAGL, ABHD6 and ABHD12 as guardians of 2-arachidonoylglycerol signalling through cannabinoid receptors. Acta Physiol (Oxf) 204:267-76.

Schlosburg JE, Blankman JL, Long JZ, Nomura DK, Pan B, Kinsey SG, Nguyen PT, Ramesh D, Booker L, Burston JJ and others. 2010. Chronic monoacylglycerol lipase blockade causes functional antagonism of the endocannabinoid system. Nat Neurosci 13:1113-9.

Scholz J, Klein MC, Behrens TE, Johansen-Berg H. 2009. Training induces changes in white-matter architecture. Nat Neurosci 12:1370-1.

Seehusen F, Baumgärtner W. 2010. Axonal pathology and loss precede demyelination and accompany chronic lesions in a spontaneously occurring animal model of multiple sclerosis. Brain Pathol 20:551-9.

Serafini B, Rosicarelli B, Magliozzi R, Stigliano E, Capello E, Mancardi GL, Aloisi F. 2006. Dendritic cells in multiple sclerosis lesions: maturation stage, myelin uptake, and interaction with proliferating T cells. J Neuropathol Exp Neurol 65:124-41.

Shao Z, Yin J, Chapman K, Grzemska M, Clark L, Wang J, Rosenbaum DM. 2016. High-resolution crystal structure of the human CB1 cannabinoid receptor. Nature.

Shin D, Lin ST, Fu YH, Ptácek LJ. 2013. Very large G protein-coupled receptor 1 regulates myelin-associated glycoprotein via Gαs/Gαq-mediated protein kinases A/C. Proc Natl Acad Sci U S A 110:19101-6.

Shire D, Calandra B, Rinaldi-Carmona M, Oustric D, Pessègue B, Bonnin-Cabanne O, Le Fur G, Caput D, Ferrara P. 1996. Molecular cloning, expression and function of the murine CB2 peripheral cannabinoid receptor. Biochim Biophys Acta 1307:132-6.

Sieber SA, Cravatt BF. 2006. Analytical platforms for activity-based protein profiling--exploiting the versatility of chemistry for functional proteomics. Chem Commun (Camb):2311-9.

Sim FJ, Lang JK, Waldau B, Roy NS, Schwartz TE, Pilcher WH, Chandross KJ, Natesan S, Merrill JE, Goldman SA and others. 2006. Complementary patterns of gene expression by human oligodendrocyte progenitors and their environment predict determinants of progenitor maintenance and differentiation. Ann Neurol 59:763-79.

Sim LJ, Hampson RE, Deadwyler SA, Childers SR. 1996. Effects of chronic treatment with delta9-tetrahydrocannabinol on cannabinoid-stimulated [35S]GTPgammaS autoradiography in rat brain. J Neurosci 16:8057-66.

Simons M, Nave KA. 2015. Oligodendrocytes: Myelination and Axonal Support. Cold Spring Harb Perspect Biol 8:a020479.

Skripuletz T, Gudi V, Hackstette D, Stangel M. 2011. De- and remyelination in the CNS white and grey matter induced by cuprizone: the old, the new, and the unexpected. Histol Histopathol 26:1585-97.

Snaidero N, Simons M. 2014. Myelination at a glance. J Cell Sci 127:2999-3004.

Soliven B. 2001. Calcium signalling in cells of oligodendroglial lineage. Microsc Res Tech 52:672-9.

Sperber BR, McMorris FA. 2001. Fyn tyrosine kinase regulates oligodendroglial cell development but is not required for morphological differentiation of oligodendrocytes. J Neurosci Res 63:303-12.

Spitzer S, Volbracht K, Lundgaard I, Káradóttir RT. 2016. Glutamate signalling: A multifaceted modulator of oligodendrocyte lineage cells in health and disease. Neuropharmacology 110:574-85.

Stankoff B, Aigrot MS, Noël F, Wattilliaux A, Zalc B, Lubetzki C. 2002. Ciliary neurotrophic factor (CNTF) enhances myelin formation: a novel role for CNTF and CNTF-related molecules. J Neurosci 22:9221-7.

Stella N. 2010. Cannabinoid and cannabinoid-like receptors in microglia, astrocytes, and astrocytomas. Glia 58:1017-30.

Stevens B, Porta S, Haak LL, Gallo V, Fields RD. 2002. Adenosine: a neuron-glial transmitter promoting myelination in the CNS in response to action potentials. Neuron 36:855-68.

Stover JF, Lowitzsch K, Kempski OS. 1997. Cerebrospinal fluid hypoxanthine, xanthine and uric acid levels may reflect glutamate-mediated excitotoxicity in different neurological diseases. Neurosci Lett 238:25-8.

Strachan-Whaley M, Rivest S, Yong VW. 2014. Interactions between microglia and T cells in multiple sclerosis pathobiology. J Interferon Cytokine Res 34:615-22.

Sugiura T, Kobayashi Y, Oka S, Waku K. 2002. Biosynthesis and degradation of anandamide and 2-arachidonoylglycerol and their possible physiological significance. Prostaglandins Leukot Essent Fatty Acids 66:173-92.

Sugiura T, Kondo S, Sukagawa A, Nakane S, Shinoda A, Itoh K, Yamashita A, Waku K. 1995. 2-Arachidonoylglycerol: a possible endogenous cannabinoid receptor ligand in brain. Biochem Biophys Res Commun 215:89-97.

Tanaka M, Moran S, Wen J, Affram K, Chen T, Symes AJ, Zhang Y. 2017. WWL70 attenuates PGE2 production derived from 2-arachidonoylglycerol in microglia by ABHD6-independent mechanism. J Neuroinflammation 14:7.

Tanimura A, Yamazaki M, Hashimotodani Y, Uchigashima M, Kawata S, Abe M, Kita Y, Hashimoto K, Shimizu T, Watanabe M and others. 2010. The endocannabinoid 2-arachidonoylglycerol

produced by diacylglycerol lipase alpha mediates retrograde suppression of synaptic transmission. Neuron 65:320-7.

Thomas G, Betters JL, Lord CC, Brown AL, Marshall S, Ferguson D, Sawyer J, Davis MA, Melchior JT, Blume LC and others. 2013. The serine hydrolase ABHD6 Is a critical regulator of the metabolic syndrome. Cell Rep 5:508-20.

Thompson AJ, Baranzini SE, Geurts J, Hemmer B, Ciccarelli O. 2018. Multiple sclerosis. Lancet 391:1622-36.

Tsai HH, Niu J, Munji R, Davalos D, Chang J, Zhang H, Tien AC, Kuo CJ, Chan JR, Daneman R and others. 2016. Oligodendrocyte precursors migrate along vasculature in the developing nervous system. Science 351:379-84.

Vercellino M, Masera S, Lorenzatti M, Condello C, Merola A, Mattioda A, Tribolo A, Capello E, Mancardi GL, Mutani R and others. 2009. Demyelination, inflammation, and neurodegeneration in multiple sclerosis deep gray matter. J Neuropathol Exp Neurol 68:489-502.

Viader A, Blankman JL, Zhong P, Liu X, Schlosburg JE, Joslyn CM, Liu QS, Tomarchio AJ, Lichtman AH, Selley DE and others. 2015. Metabolic Interplay between Astrocytes and Neurons Regulates Endocannabinoid Action. Cell Rep 12:798-808.

Walter L, Dinh T, Stella N. 2004. ATP induces a rapid and pronounced increase in 2-arachidonoylglycerol production by astrocytes, a response limited by monoacylglycerol lipase. J Neurosci 24:8068-74.

Wang S, Sdrulla AD, diSibio G, Bush G, Nofziger D, Hicks C, Weinmaster G, Barres BA. 1998. Notch receptor activation inhibits oligodendrocyte differentiation. Neuron 21:63-75.

Webb M, Luo L, Ma JY, Tham CS. 2008. Genetic deletion of Fatty Acid Amide Hydrolase results in improved long-term outcome in chronic autoimmune encephalitis. Neurosci Lett 439:106-10.

Weiner HL. 2004. Multiple sclerosis is an inflammatory T-cell-mediated autoimmune disease. Arch Neurol 61:1613-5.

Weissert R. 2013. The immune pathogenesis of multiple sclerosis. J Neuroimmune Pharmacol 8:857-66.

Wen J, Ribeiro R, Tanaka M, Zhang Y. 2015. Activation of CB2 receptor is required for the therapeutic effect of ABHD6 inhibition in experimental autoimmune encephalomyelitis. Neuropharmacology 99:196-209.

White R, Gonsior C, Bauer NM, Krämer-Albers EM, Luhmann HJ, Trotter J. 2012. Heterogeneous nuclear ribonucleoprotein (hnRNP) F is a novel component of oligodendroglial RNA transport granules contributing to regulation of myelin basic protein (MBP) synthesis. J Biol Chem 287:1742-54.

Wingerchuk DM, Carter JL. 2014. Multiple sclerosis: current and emerging disease-modifying therapies and treatment strategies. Mayo Clin Proc 89:225-40.

Witte ME, Mahad DJ, Lassmann H, van Horssen J. 2014. Mitochondrial dysfunction contributes to neurodegeneration in multiple sclerosis. Trends Mol Med 20:179-87.

Witting A, Chen L, Cudaback E, Straiker A, Walter L, Rickman B, Möller T, Brosnan C, Stella N. 2006. Experimental autoimmune encephalomyelitis disrupts endocannabinoid-mediated neuroprotection. Proc Natl Acad Sci U S A 103:6362-7.

Witting A, Walter L, Wacker J, Möller T, Stella N. 2004. P2X7 receptors control 2-arachidonoylglycerol production by microglial cells. Proc Natl Acad Sci U S A 101:3214-9.

Woodhams SG, Chapman V, Finn DP, Hohmann AG, Neugebauer V. 2017. The cannabinoid system and pain. Neuropharmacology 124:105-120.

Xiao J, Wong AW, Willingham MM, van den Buuse M, Kilpatrick TJ, Murray SS. 2010. Brain-derived neurotrophic factor promotes central nervous system myelination via a direct effect upon oligodendrocytes. Neurosignals 18:186-202.

Xiao L, Ohayon D, McKenzie IA, Sinclair-Wilson A, Wright JL, Fudge AD, Emery B, Li H, Richardson WD. 2016. Rapid production of new oligodendrocytes is required in the earliest stages of motor-skill learning. Nat Neurosci 19:1210-7.

Ye P, Carson J, D'Ercole AJ. 1995. In vivo actions of insulin-like growth factor-I (IGF-I) on brain myelination: studies of IGF-I and IGF binding protein-1 (IGFBP-1) transgenic mice. J Neurosci 15:7344-56.

Yun B, Lee H, Ghosh M, Cravatt BF, Hsu KL, Bonventre JV, Ewing H, Gelb MH, Leslie CC. 2014. Serine hydrolase inhibitors block necrotic cell death by preventing calcium overload of the mitochondria and permeability transition pore formation. J Biol Chem 289:1491-504.

Zonouzi M, Scafidi J, Li P, McEllin B, Edwards J, Dupree JL, Harvey L, Sun D, Hübner CA, Cull-Candy SG and others. 2015. GABAergic regulation of cerebellar NG2 cell development is altered in perinatal white matter injury. Nat Neurosci 18:674-82.

Zou S, Kumar U. 2018. Cannabinoid Receptors and the Endocannabinoid System: Signaling and Function in the Central Nervous System. Int J Mol Sci 19.